

# BULLETIN OF RUSSIAN STATE MEDICAL UNIVERSITY

BIOMEDICAL JOURNAL OF PIROGOV RUSSIAN NATIONAL  
RESEARCH MEDICAL UNIVERSITY

**EDITOR-IN-CHIEF** Denis Rebrikov, DSc, professor

**DEPUTY EDITOR-IN-CHIEF** Alexander Oettinger, DSc, professor

**EDITORS** Valentina Geidebrekht, Liliya Egorova

**TECHNICAL EDITOR** Nina Tyurina

**TRANSLATORS** Ekaterina Tretiyakova, Vyacheslav Vityuk

**DESIGN AND LAYOUT** Marina Doronina

## EDITORIAL BOARD

**Averin VI**, DSc, professor (Minsk, Belarus)

**Alipov NN**, DSc, professor (Moscow, Russia)

**Belousov VV**, DSc, professor (Moscow, Russia)

**Bogomilskiy MR**, corr. member of RAS, DSc, professor (Moscow, Russia)

**Bozhenko VK**, DSc, CSc, professor (Moscow, Russia)

**Bylova NA**, CSc, docent (Moscow, Russia)

**Gainetdinov RR**, CSc (Saint-Petersburg, Russia)

**Gendlin GYe**, DSc, professor (Moscow, Russia)

**Ginter EK**, member of RAS, DSc (Moscow, Russia)

**Gorbacheva LR**, DSc, professor (Moscow, Russia)

**Gordeev IG**, DSc, professor (Moscow, Russia)

**Gudkov AV**, PhD, DSc (Buffalo, USA)

**Gulyaeva NV**, DSc, professor (Moscow, Russia)

**Gusev EI**, member of RAS, DSc, professor (Moscow, Russia)

**Danilenko VN**, DSc, professor (Moscow, Russia)

**Zarubina TV**, DSc, professor (Moscow, Russia)

**Zatevakhin II**, member of RAS, DSc, professor (Moscow, Russia)

**Kagan VE**, professor (Pittsburgh, USA)

**Kzyzhkowska YuG**, DSc, professor (Heidelberg, Germany)

**Kobrinikii BA**, DSc, professor (Moscow, Russia)

**Kozlov AV**, MD PhD, (Vienna, Austria)

**Kotelevtsev YuV**, CSc (Moscow, Russia)

**Lebedev MA**, PhD (Darem, USA)

**Manturova NE**, DSc (Moscow, Russia)

**Milushkina OYu**, DSc, professor (Moscow, Russia)

**Mitupov ZB**, DSc, professor (Moscow, Russia)

**Moshkovskii SA**, DSc, professor (Moscow, Russia)

**Munblit DB**, MSc, PhD (London, Great Britain)

**Negrebetsky VV**, DSc, professor (Moscow, Russia)

**Novikov AA**, DSc (Moscow, Russia)

**Pivovarov YuP**, member of RAS, DSc, professor (Moscow, Russia)

**Polunina NV**, corr. member of RAS, DSc, professor (Moscow, Russia)

**Poryadin GV**, corr. member of RAS, DSc, professor (Moscow, Russia)

**Razumovskii AYU**, corr. member of RAS, DSc, professor (Moscow, Russia)

**Rebrova OYu**, DSc (Moscow, Russia)

**Rudoy AS**, DSc, professor (Minsk, Belarus)

**Rylova AK**, DSc, professor (Moscow, Russia)

**Savelieva GM**, member of RAS, DSc, professor (Moscow, Russia)

**Semiglazov VF**, corr. member of RAS, DSc, professor (Saint-Petersburg, Russia)

**Skoblina NA**, DSc, professor (Moscow, Russia)

**Slavyanskaya TA**, DSc, professor (Moscow, Russia)

**Smirnov VM**, DSc, professor (Moscow, Russia)

**Spallone A**, DSc, professor (Rome, Italy)

**Starodubov VI**, member of RAS, DSc, professor (Moscow, Russia)

**Stepanov VA**, corr. member of RAS, DSc, professor (Tomsk, Russia)

**Suchkov SV**, DSc, professor (Moscow, Russia)

**Takhchidi KhP**, corr. member of RAS, DSc (medicine), professor (Moscow, Russia)

**Trufanov GE**, DSc, professor (Saint-Petersburg, Russia)

**Favorova OO**, DSc, professor (Moscow, Russia)

**Filipenko ML**, CSc, leading researcher (Novosibirsk, Russia)

**Khazipov RN**, DSc (Marsel, France)

**Chundukova MA**, DSc, professor (Moscow, Russia)

**Shimanovskii NL**, corr. member of RAS, DSc, professor (Moscow, Russia)

**Shishkina LN**, DSc, senior researcher (Novosibirsk, Russia)

**Yakubovskaya RI**, DSc, professor (Moscow, Russia)

**SUBMISSION** <http://vestnikrgmu.ru/login?lang=en>

**CORRESPONDENCE** [editor@vestnikrgmu.ru](mailto:editor@vestnikrgmu.ru)

**COLLABORATION** [manager@vestnikrgmu.ru](mailto:manager@vestnikrgmu.ru)

**ADDRESS** ul. Ostrovityanova, d. 1, Moscow, Russia, 117997

Indexed in Scopus. CiteScoreTracker: 0.15

**Scopus**<sup>®</sup>

Indexed in WoS since 2018

**WEB OF SCIENCE**<sup>™</sup>

Five-year h-index is 3

**Google**  
scholar

Indexed in RSCI. IF 2017: 0.326

**НАУЧНАЯ ЭЛЕКТРОННАЯ  
БИБЛИОТЕКА  
LIBRARY.RU**

Listed in HAC 27.01.2016 (no. 1760)



**ВЫСШАЯ  
АТТЕСТАЦИОННАЯ  
КОМИССИЯ (ВАК)**

Open access to archive

**CYBERLENINKA**

Issue DOI: 10.24075/brsmu.2019-01

The mass media registration certificate no. 012769 issued on July 29, 1994

Founder and publisher is Pirogov Russian National Research Medical University (Moscow, Russia)

The journal is distributed under the terms of Creative Commons Attribution 4.0 International License [www.creativecommons.org](http://www.creativecommons.org)



Approved for print 15.03.2019  
Circulation: 100 copies. Printed by Print.Formula  
[www.print-formula.ru](http://www.print-formula.ru)

# ВЕСТНИК РОССИЙСКОГО ГОСУДАРСТВЕННОГО МЕДИЦИНСКОГО УНИВЕРСИТЕТА

НАУЧНЫЙ МЕДИЦИНСКИЙ ЖУРНАЛ РНИМУ ИМ. Н. И. ПИРОГОВА

**ГЛАВНЫЙ РЕДАКТОР** Денис Ребриков, д. б. н., профессор

**ЗАМЕСТИТЕЛЬ ГЛАВНОГО РЕДАКТОРА** Александр Эттингер, д. м. н., профессор

**РЕДАКТОРЫ** Валентина Гейдебрект, Лилия Егорова

**ТЕХНИЧЕСКИЙ РЕДАКТОР** Нина Тюрина

**ПЕРЕВОДЧИКИ** Екатерина Третьякова, Вячеслав Виток

**ДИЗАЙН И ВЕРСТКА** Марина Доронина

## РЕДАКЦИОННАЯ КОЛЛЕГИЯ

В. И. Аверин, д. м. н., профессор (Минск, Белоруссия)  
Н. Н. Алипов, д. м. н., профессор (Москва, Россия)  
В. В. Белоусов, д. б. н., профессор (Москва, Россия)  
М. Р. Богомилский, член-корр. РАН, д. м. н., профессор (Москва, Россия)  
В. К. Боженко, д. м. н., к. б. н., профессор (Москва, Россия)  
Н. А. Былова, к. м. н., доцент (Москва, Россия)  
Р. Р. Гайнетдинов, к. м. н. (Санкт-Петербург, Россия)  
Г. Е. Гендлин, д. м. н., профессор (Москва, Россия)  
Е. К. Гинтер, академик РАН, д. б. н. (Москва, Россия)  
Л. Р. Горбачева, д. б. н., профессор (Москва, Россия)  
И. Г. Гордеев, д. м. н., профессор (Москва, Россия)  
А. В. Гудков, PhD, DSc (Буффало, США)  
Н. В. Гуляева, д. б. н., профессор (Москва, Россия)  
Е. И. Гусев, академик РАН, д. м. н., профессор (Москва, Россия)  
В. Н. Даниленко, д. б. н., профессор (Москва, Россия)  
Т. В. Зарубина, д. м. н., профессор (Москва, Россия)  
И. И. Затевахин, академик РАН, д. м. н., профессор (Москва, Россия)  
В. Е. Каган, профессор (Питтсбург, США)  
Ю. Г. Кжышковска, д. б. н., профессор (Гейдельберг, Германия)  
Б. А. Кобринский, д. м. н., профессор (Москва, Россия)  
А. В. Козлов, MD PhD (Вена, Австрия)  
Ю. В. Котелевцев, к. х. н. (Москва, Россия)  
М. А. Лебедев, PhD (Дарем, США)  
Н. Е. Мантурова, д. м. н. (Москва, Россия)  
О. Ю. Милушкина, д. м. н., доцент (Москва, Россия)  
З. Б. Митупов, д. м. н., профессор (Москва, Россия)  
С. А. Мошковский, д. б. н., профессор (Москва, Россия)  
Д. Б. Мунблит, MSc, PhD (Лондон, Великобритания)

В. В. Негребецкий, д. х. н., профессор (Москва, Россия)  
А. А. Новиков, д. б. н. (Москва, Россия)  
Ю. П. Пивоваров, д. м. н., академик РАН, профессор (Москва, Россия)  
Н. В. Полунина, член-корр. РАН, д. м. н., профессор (Москва, Россия)  
Г. В. Порядин, член-корр. РАН, д. м. н., профессор (Москва, Россия)  
А. Ю. Разумовский, член-корр., профессор (Москва, Россия)  
О. Ю. Реброва, д. м. н. (Москва, Россия)  
А. С. Рудой, д. м. н., профессор (Минск, Белоруссия)  
А. К. Рылова, д. м. н., профессор (Москва, Россия)  
Г. М. Савельева, академик РАН, д. м. н., профессор (Москва, Россия)  
В. Ф. Семиглазов, член-корр. РАН, д. м. н., профессор (Санкт-Петербург, Россия)  
Н. А. Скоблина, д. м. н., профессор (Москва, Россия)  
Т. А. Славянская, д. м. н., профессор (Москва, Россия)  
В. М. Смирнов, д. б. н., профессор (Москва, Россия)  
А. Спаллоне, д. м. н., профессор (Рим, Италия)  
В. И. Стародубов, академик РАН, д. м. н., профессор (Москва, Россия)  
В. А. Степанов, член-корр. РАН, д. б. н., профессор (Томск, Россия)  
С. В. Сучков, д. м. н., профессор (Москва, Россия)  
Х. П. Тахчиди, член-корр. РАН, д. м. н., профессор (Москва, Россия)  
Г. Е. Труфанов, д. м. н., профессор (Санкт-Петербург, Россия)  
О. О. Фаворова, д. б. н., профессор (Москва, Россия)  
М. Л. Филипенко, к. б. н. (Новосибирск, Россия)  
Р. Н. Хазипов, д. м. н. (Марсель, Франция)  
М. А. Чундокова, д. м. н., профессор (Москва, Россия)  
Н. Л. Шимановский, член-корр. РАН, д. м. н., профессор (Москва, Россия)  
Л. Н. Шишкина, д. б. н. (Новосибирск, Россия)  
Р. И. Якубовская, д. б. н., профессор (Москва, Россия)

**ПОДАЧА РУКОПИСЕЙ** <http://vestnikrgmu.ru/login>

**ПЕРЕПИСКА С РЕДАКЦИЕЙ** [editor@vestnikrgmu.ru](mailto:editor@vestnikrgmu.ru)

**СОТРУДНИЧЕСТВО** [manager@vestnikrgmu.ru](mailto:manager@vestnikrgmu.ru)

**АДРЕС РЕДАКЦИИ** ул. Островитянова, д. 1, г. Москва, 117997

Журнал включен в Scopus. CiteScoreTracker: 0,15

Журнал включен в WoS с 2018 г.

Индекс Хирша (h<sup>2</sup>) журнала по оценке Google Scholar: 3

Scopus®

WEB OF SCIENCE™

Google  
scholar

Журнал включен в РИНЦ. IF 2017: 0,326

Журнал включен в Перечень 27.01.2016 (№ 1760)

Здесь находится открытый архив журнала

НАУЧНАЯ ЭЛЕКТРОННАЯ  
БИБЛИОТЕКА  
LIBRARY.RU



ВЫСШАЯ  
АТТЕСТАЦИОННАЯ  
КОМИССИЯ (ВАК)

CYBERLENINKA

DOI выпуска: 10.24075/vrgmu.2019-01

Свидетельство о регистрации средства массовой информации № 012769 от 29 июля 1994 г.

Учредитель и издатель — Российский национальный исследовательский медицинский университет имени Н. И. Пирогова (Москва, Россия)

Журнал распространяется по лицензии Creative Commons Attribution 4.0 International [www.creativecommons.org](http://www.creativecommons.org)



Подписано в печать 15.03.2019

Тираж 100 экз. Отпечатано в типографии Print.Formula  
[www.print-formula.ru](http://www.print-formula.ru)

**REVIEW**

5

**Laboratory diagnostics as a basis for 5P medicine**

Shcherbo SN, Shcherbo DS

**Лабораторная диагностика как основа медицины 5П**

С. Н. Щербо, Д. С. Щербо

**ORIGINAL RESEARCH**

13

**Assessment of diastolic function in patients with chest pain and angiographically normal coronary arteries using ECG-gated SPECT**

Khachirova EA, Samoilenko LE, Shevchenko OP

**Оценка диастолической функции миокарда у пациентов с болевым синдромом в грудной клетке и ангиографически неизменными коронарными артериями методом синхронизированной с ЭКГ однофотонной эмиссионной компьютерной томографии**

Э. А. Хачирова, Л. Е. Самоиленко, О. П. Шевченко

**ORIGINAL RESEARCH**

20

**Investigating a correlation between the levels of peripheral blood cytokines and the risk for cardiovascular complications in patients with stage II essential hypertension**

Radaeva OA, Simbirtsev AS

**Анализ корреляции содержания цитокинов периферической крови с риском развития сердечно-сосудистых осложнений у больных эссенциальной артериальной гипертензией II стадии**

О. А. Радаева, А. С. Симбирцев

**ORIGINAL RESEARCH**

27

**Combination of ribosome and phage display for fast selection of high affinity VHH antibody fragments**

Kravchenko YE, Ivanov SV, Kravchenko DS, Frolova EI, Chumakov SP

**Использование комбинации рибосомного и фагового дисплея для быстрого отбора высокоаффинных VHH-фрагментов антител альпак**

Ю. Е. Кравченко, С. В. Иванов, Д. С. Кравченко, Е. И. Фролова, С. П. Чумаков

**ORIGINAL RESEARCH**

34

**Detection of ser450leu mutation in *rpoB* gene of *Mycobacterium tuberculosis* by allele-specific loop-mediated isothermal dna amplification method**

Filipenko ML, Oskorbin IP, Khrapov EA, Shamovskaya DV, Cherednichenko AG, Shvartz YaSh

**Выявление мутации Ser450Leu в гене *rpoB* *Mycobacterium tuberculosis* методом аллель-специфичной изотермической петлевой амплификации ДНК**

М. Л. Филипенко, И. П. Оскорбин, Е. А. Храпов, Д. В. Шамова, А. Г. Чередниченко, Я. Ш. Шварц

**ORIGINAL RESEARCH**

41

**Evaluation of the ejaculate microbiota by real-time pcr and culture-based technique**

Voroshiilina ES, Zornikov DL, Panacheva EA

**Сравнительное исследование микробиоты эякулята методом количественной ПЦР и культуральным методом**

Е. С. Ворошилина, Д. Л. Зорников, Е. А. Паначева

**ORIGINAL RESEARCH**

46

**Lipid metabolic changes in rat brain during permanent cerebral ischemia**

Kostyuk AI, Kotova DA, Demidovich AD, Panova AS, Kelmanson IV, Belousov VV, Bilan DS

**Изменение ключевых параметров метаболизма липидов в тканях мозга крыс при перманентной ишемии**

А. И. Костюк, Д. А. Котова, А. Д. Демидович, А. С. Панова, И. В. Кельмансон, В. В. Белоусов, Д. С. Билан

**ORIGINAL RESEARCH**

53

**Heart injuries: main clinical symptoms**

Maslyakov VV, Krjukov EV, Barsukov VG, Kurkin KG, Dorzhiev PA, Gorbelyk VR

**Основные клинические симптомы при ранениях сердца**

В. В. Масляков, Е. В. Крюков, В. Г. Барсуков, К. Г. Куркин, П. А. Доржиев, В. Р. Горбелик

**ORIGINAL RESEARCH**

57

**Humoral response to Epstein-Barr viral infection in patients with allergies**

Svirshchevskaya EV, Simonova MA, Matushevskaya EV, Fattakhova GV, Khlgatian SV, Ryazantsev DYU, Chudakov DB, Zavriev SK

**Гуморальный ответ на вирус Эпштейна-Барр при аллергии**

Е. В. Свирищевская, М. А. Симонова, Е. В. Матушевская, Г. В. Фаттахова, С. В. Хлгатян, Д. Ю. Рязанцев, Д. Б. Чудаков, С. К. Завриев

**ORIGINAL RESEARCH**

65

**A correlation between the fluctuations of cytokine concentrations measured in the morning and evening and the circadian blood pressure rhythm in patients with stage II essential hypertension**

Radaeva OA, Simbirtsev AS, Khovryakov AV

**Связь суточных колебаний содержания цитокинов с изменением ритмов артериального давления при эссенциальной артериальной гипертензии второй стадии**

О. А. Радаева, А. С. Симбирцев, А. В. Ховряков

**ORIGINAL RESEARCH**

71

**Injectable collagen in correction of age-related skin changes: experimental and clinical parallels**

Manturova NE, Stenko AG, Petinati YaA, Chaikovskaya EA, Bolgarina AA

**Ињекционный коллаген в коррекции возрастных изменений кожи: экспериментально-клинические параллели**

Н. Е. Мантурова, А. Г. Стенько, Я. А. Петинати, Е. А. Чайковская, А. А. Болгарина

**OPINION**

78

**Glycoprotein GP as a basis for the universal vaccine against Ebola virus disease**

Dolzhikova IV, Tukhvatulin AI, Gromova AS, Grousova DM, Tukhvatulina NM, Tokarskaya EA, Logunov DY, Naroditskiy BS, Gintsburg AL

**Использование гликопротеина GP для создания универсальной вакцины против лихорадки Эбола**

И. В. Должикова, А. И. Тухватулин, А. С. Громова, Д. М. Гроусова, Н. М. Тухватулина, Е. А. Токарская, Д. Ю. Логунов, Б. С. Народицкий, А. Л. Гинцбург

**ORIGINAL RESEARCH**

86

**A genetically encoded biosensor roKate for monitoring the redox state of the glutathione pool**

Shokhina AG, Belousov VV, Bilan DS

**Генетически кодируемый биосенсор roKate для регистрации редокс-состояния пула глутатиона**

А. Г. Шохина, В. В. Белоусов, Д. С. Билан

**ORIGINAL RESEARCH**

93

**Takayasu's arteritis: the retrospective analysis of patients from the Ural population**

Borodina IE, Popov AA, Salavatova GG, Shardina LA

**Артериит Такаясу: результаты ретроспективного анализа пациентов уральской популяции**

И. Э. Бородина, А. А. Попов, Г. Г. Салаватова, Л. А. Шардина

**ORIGINAL RESEARCH**

102

**Frequency of carbohydrate metabolism disorders in day-care patients with borderline fasting blood sugar levels and at least one risk factor for diabetes mellitus**

Boeva VV, Boeva TA, Zavyalov AN

**Частота нарушений углеводного обмена у пациентов дневного стационара с пограничными значениями гликемии натощак и хотя бы одним фактором риска развития сахарного диабета**

В. В. Боева, Т. А. Боева, А. Н. Завьялов

**ERRATUM**

108

## Erratum to

**The proper structure of a biosafety system as a way of reducing the vulnerability of a society, economy or state in the face of a biogenic threat**

Gushchin VA, Manuilov VA, Makarov VV, Tkachuk AP

Published in Bulletin of RSMU (july–august 2018, 5–18).

## Исправление к статье

**Надлежащая организация системы биобезопасности как средство снижения уязвимости общества, экономики и государства перед биогенными угрозами**

В. А. Гушчин, В. А. Мануйлов, В. В. Макаров, А. П. Ткачук

Опубликована в журнале Вестник РГМУ (июль–август 2018, с. 5–18).

**ERRATUM**

109

## Erratum to

**High-performance aerosol sampler with liquid phase recirculation and pre-concentration of particles**

Akmalov AE, Kotkovskii GE, Stolyarov SV, Verdiev BI, Ovchinnikov RS, Pochtovyy AA, Tkachuk AP, Chistyakov AA

Published in Bulletin of RSMU (july–august 2018, 25–31).

## Исправление к статье

**Высокопроизводительный аэрозольный пробоотборник с рециркуляцией жидкой фазы и предварительным концентрированием**

А. Э. Акмалов, Г. Е. Котковский, С. В. Столяров, Б. И. Вердиев, Р. С. Овчинников, А. А. Почтовый, А. П. Ткачук, А. А. Чистяков

Опубликована в журнале Вестник РГМУ (июль–август 2018, с. 25–31).

**ERRATUM**

110

## Erratum to

**Performance of the original workstation for aerosol tests under controlled conditions**

Kleymenov DA, Verdiev BI, Enenko AA, Gushchin VA, Tkachuk AP

Published in Bulletin of RSMU (july–august 2018, 32–38).

## Исправление к статье

**Опыт использования аналитического стенда для проведения аэрозольных испытаний в контролируемых условиях**

Д. А. Клейменов, Б. И. Вердиев, А. А. Ененко, В. А. Гушчин, А. П. Ткачук

Опубликована в журнале Вестник РГМУ (июль–август 2018, с. 32–38).

## LABORATORY DIAGNOSTICS AS A BASIS FOR 5P MEDICINE

Shcherbo SN ✉, Shcherbo DS

Pirogov Russian National Research Medical University, Moscow, Russia

As public health systems are being modernized across the world, conventional medicine is undergoing a serious transformation and new medical models are emerging based on personalized, predictive, preventive, participatory, precision, mobile, and digital approaches. So far, there is no consensus in the literature and the medical community about the goals, objectives and applications of these models, particularly precision medicine, which is sometimes perceived as merely a fancier term for personalized medicine. The role of laboratory diagnostics in precision medicine is also a matter of intense debate. This review analyzes the currently available information about precision medicine and gives examples of how 5P approaches can be used in clinical practice.

**Keywords:** medicine 5P, clinical laboratory diagnostics, precision medicine, cancer, diabetes mellitus

✉ **Correspondence should be addressed:** Sergey N. Shcherbo  
Ostrovityanova 1, Moscow, 117997; shcherbos@mail.ru

**Received:** 30.01.2019 **Accepted:** 13.02.2019 **Published online:** 14.02.2019

**DOI:** 10.24075/brsmu.2018.095

## ЛАБОРАТОРНАЯ ДИАГНОСТИКА КАК ОСНОВА МЕДИЦИНЫ 5П

С. Н. Щербо ✉, Д. С. Щербо

Российский национальный исследовательский медицинский университет имени Н. И. Пирогова, Москва, Россия

В рамках модернизации системы здравоохранения в настоящее время происходят изменение старых и становление новых направлений современной медицины: персонализированной, предиктивной, превентивной, партисипативной, прецизионной, мобильной и цифровой. Вместе с тем, в научной литературе и медицинском сообществе имеются различные мнения о целях, области применения и задачах указанных направлений здравоохранения и роли в них лабораторной диагностики. Прежде всего это относится к прецизионной медицине, которая воспринимается только как более современное название персонализированной медицины. В обзоре проанализирована и обобщена имеющаяся на сегодняшний день информация и представлены примеры применения подходов медицины 5П в клинической практике.

**Ключевые слова:** медицина 5П, клиническая лабораторная диагностика, прецизионная медицина, онкология, сахарный диабет

✉ **Для корреспонденции:** Сергей Николаевич Щербо  
ул. Островитянова, д. 1, г. Москва, 117997; shcherbos@mail.ru

**Статья получена:** 30.01.2019 **Статья принята к печати:** 13.02.2019 **Опубликована онлайн:** 14.02.2019

**DOI:** 10.24075/vrgmu.2018.095

As the new wave of innovations driven by powerful technologies heralds a shift in the scientific paradigm expected to reach its maturity in the 2040s, we are witnessing the fast-paced evolution of nature and the human society. In these times of rapid progress, it is becoming crucial to identify major healthcare trends and to assess their potential. It is important to understand how conventional medical approaches and the medicine of the future will co-exist and interact. In 2015, the authors of this article proposed a concept of 5P medicine [1, 2] based on the analysis of the evolution of medicine and biology in the preceding 10 years. The concept was inspired by the precision medicine initiative that was intended to cover a wide range of public health aspects and to integrate genomic breakthroughs with the achievements of the communication revolution, cellular medicine and omics technologies (such as diagnostic panels of biomarkers measured at different levels of biological organization). Precision medicine approaches are mindful of the shifts in philosophical beliefs, ethical norms and the economic situation in a society. The long-reigning medical paternalism is now giving way to participatory medicine that encourages active interaction between the doctor and the patient. The concept of 5P medicine emerged in the wake of failed expectations imposed on genome-wide association studies (one of their challenges being the missing heritability problem) and reflects the current state of the medical and biological sciences. At the moment, there is some confusion about the terms describing the components of 5PM, their relationships and the directions 5PM may take. Will the medicine of the future be 4P (predictive, preventive, participatory, and personalized) or 5P, introducing precision medicine as the 5<sup>th</sup> component? Failure to understand the fundamental principles

and objectives of precision medicine may lead to it being perceived as merely a fancier term for personalized medicine [3]. Although each of the components constituting 5P medicine certainly has a value of its own, together they complement and reinforce each other (hence the term “predictive preventive medicine”). The adoption of the 5PM concept allows us to clearly delineate the goals and objectives of contemporary medicine. This is particularly important in educating and training medical staff. Previously, we showed that the evolution of laboratory medicine would take the direction determined by the goals of emerging healthcare areas. Depending on the objective, laboratory medicine can deal with different types and arrays (panels) of biomarkers at different levels of biological organization [4–6].

**Predictive medicine**

The problems of early diagnosis, prognostication and assessment of risks for developing a pathology constitute one of the most promising areas of contemporary molecular medicine that relies on laboratory diagnostics. Preventive medicine makes predictions about the probability of a certain disease based on a patient's data, including the results of omics tests. The Nobel laureate Jean Dausset (1980) who proposed the term “predictive” commented that prevention is the main goal of the medical science. He realized it after discovering associations between the alleles of the HLA genetic locus and a few multifactorial diseases (diabetes mellitus, bronchial asthma, etc.). Predictive medicine seeks to notice change in patients' general health before they develop clinical symptoms. It is a diagnostic branch of medicine that exploits laboratory

and functional tests, various imaging modalities, bioinformatics, etc. Disease prediction can be aided by genetic testing, which has been instrumental in discovering genetic predisposition to somatic and infectious diseases (TB, viral hepatitis, HIV, etc.). Preventive testing involves identification of the hallmarks of pathogenesis. For example, Michael Snyder carried out a laborious expensive experiment allowing him to catch the onset of diabetes signaled by abrupt changes in the levels of biomarkers that had never been linked to diabetes before [7]. Using omics technologies, Snyder was able to obtain a highly accurate integrative personal omics profile (iPOP) containing information about his genomic sequence, blood biochemistry, and the levels of mRNA, proteins and other biomolecules measured repeatedly (20 times) over the course of 14 months. The experiment yielded a database of 3 billion records in total. At present, exhaustive iPOP-profiling is not available for the majority of patients. However, smaller profiles built from dozens of the most informative parameters instead of hundreds of thousands can still be very useful. It's unrealistic to believe that a healthy individual will be eager to give their blood for tests every hour or pay frequent visits to a doctor's office for a checkup. Therefore, we need rapid and cost-effective methods for studying biological specimens. For example, instead of proteomic testing, which lasts for 30 to 200 minutes, one can analyze protein metabolites; the latter can be measured in as little as 30 seconds. A team of researchers has tested the ability of whole-genome sequencing to predict the risk of 24 relatively prevalent diseases. Based on the sequencing data, they were able to predict predisposition to at least one disease in the majority of patients [8]. Contemporary medicine has embraced the importance of early diagnosis, which improves treatment outcomes and reduces its costs. The use of highly sensitive and highly specific diagnostic tools is vital for early diagnosis. So are regular medical examinations and checkups.

### Preventive medicine

Preventive care (from French *préventif*) is a branch of medicine that aims to delay the onset of a disease, mitigate its severity or treat its first manifestations, such as unhealthy weight gain, decline in physical activity, etc. The National Institutes of Health (USA) describe preventive care as one of 5 prioritized areas of medicine that needs to be actively supported and developed in order to provide customized care for patients aiming to improve their quality of life and extending the life span to its natural limits.

### Participatory (patient-oriented) medicine

As the name suggests, participatory medicine encourages a patient to be involved in the medical process and actively interact with their doctor. Participatory medicine is intimately related to predicative and preventive medicine and draws on philosophy, deontology and psychology. Cooperation and sympathy have always played a crucial role in the doctor-patient relationship. A physician and writer Abu'l Faraj who lived in the 13<sup>th</sup> century appealed to his patient: "There are 3 of us here: you, the illness and myself. If you join the illness, the two of you will overpower me. If you join me instead, the illness will have no one to turn to, and together we will defeat it". However, it was not until the 16<sup>th</sup> and 17<sup>th</sup> centuries that European physicians, such as John Gregory and Thomas Percival, started to admit that a patient has a right to voice their own opinion about the medical process. The legal term "informed consent" dates back to 1957. Even today, there are situations when full informed consent cannot be obtained, as is the case with unconscious

patients. But under any circumstances, a doctor should treat their patients with respect and not look down on them. The patient has a right to ask questions and make their own choice. Unfortunately, treatment guidelines and standards of care formulated by expert organizations unintentionally become the source of medical paternalism, although it is stressed that they should not be followed blindly and individual characteristics of a patient should be taken into account. In the not so distant past, a patient had no access to their medical records made during a short physical examination, and the doctor-patient interaction was best described as silent [9]. In contrast, participatory medicine recognizes that a patient knows his/her body better than anyone else and is interested in maintaining good health; therefore, the patient should actively participate in generating the vast array of medical data related to their health. These data originate from a medical history, diagnostic images, instrumental readings, results of omics and other types of tests. Integrated medical records will soon be available to patients via cloud database services, a supercomputer or telemedically. The state-of-the-art technologies allows patients to obtain health-related information on internet forums or in expert internet communities, from mobile applications, including medication reminder apps, electronic diaries, and medical devices for self-testing. Thus, the accumulated information will be communicated between the doctor and the patient.

### Personalized medicine

The term "personalized medicine" (PM) was first used in 1998 [10]. Sometimes, PM is defined as pharmacogenomics (genomic medicine, genotype-based therapy, customized healthcare, information-based medicine, integrated healthcare, rational prescribing, etc. [2]). The Personalized Medicine Coalition (Washington, USA) stresses that PM uses "new methods of molecular analysis to better manage a patient's disease or predisposition toward a disease. It aims to achieve optimal medical outcomes by helping physicians and patients choose the disease management approaches likely to work best in the context of a patient's genetic and environmental profile" [11]. Hopes are high that personalized medicine will improve the quality of healthcare services and significantly reduce their costs. US Food and Drug Administration (FDA) sees PM as an arsenal of therapeutic techniques that "consider a patient's genetic, anatomical, and physiological characteristics" providing "the right patient with the right drug at the right dose at the right time" [12]. PM can also be regarded as a novel healthcare model that exploits diagnostic, prevention, and therapeutic tools that are economically or ethically feasible for a given patient and best cater to their needs. PM objectives include elucidating molecular mechanisms underlying a pathology, identifying its most important biomarkers, and designing personalized therapeutic drugs (TD) that can effectively modify or eliminate the targets associated with pathology [13]. PM attempts to categorize pathogenetic mechanisms associated with the development of a disease into types and subtypes (here, cancer research is a good example); it looks for effective therapeutic targets and seeks to improve patient stratification. It should be born in mind that PM is a branch of healthcare that deals with diseases that have already set in and manifested themselves through clinical symptoms and signs [6]. The UNESCO International Bioethics Committee defines personalized medicine as "the tailoring of medical interventions to the specific characteristics of each patient, realized through pharmacogenomics and genotype-based treatments". The majority of experts agree that better patient stratification will produce better outcomes in terms of

treatment efficacy and good tolerance. A team of researchers has published an analysis of 683 medical articles from PubMed containing definitions of “personalized medicine”. It turned out that this term was present in 2,457 articles (at the time of publication); 60.4% of the papers issued before 2009 and devoted to the problem of treatment customization contained a definition of this term. The authors concluded that PM seeks to improve patient stratification and healthcare timing by using data on the molecular pathways of a disease and its biomarkers [14].

The balance between standardization and personalization is very important. In a man-made environment standardization has become the cornerstone of industrialization, allowing no space for differences that did not fit into the accepted model. This principle was later applied to healthcare to establish standards for drug-based therapies, surgical intervention, etc. The post-industrial society has taken a different course of development, defying standardization. The mass media are getting demassified and focus on smaller niche audiences. This process is linked to the spread of Internet. The principle of differentiation is replacing standardization. Concentration gives way to decentralization, maximization is taken over by the principle of adequate scales, etc.

The first large-scale application of PM approaches occurred in the context of blood types discovery [15]. To date, intelligent systems for decision making have been developed to help physicians select the right medication for their patients. These systems warn the doctors of the adverse effects that may occur in patients with certain genotypes, suggest conducting a pharmacogenomic test and provide accurate clinical interpretations of its results. Preemptive pharmacogenomic testing is being actively promoted across the world. A few years back, the University of Chicago launched a project that demonstrated the feasibility of pharmacogenomic testing in the clinical setting. The physicians received alerts about patients' genotypes, which ultimately improved efficacy and safety of the prescribed treatments [16].

### Precision medicine

The birth of precision medicine (PrM) is associated with the development of medical, biological and information technologies and frustration that invaded the scientific community in 2010 when it became clear that human genome sequencing and GWAS had not lived up to the expectations [2]. In 2012, it was proposed to give up the term “personalized medicine” that did not reflect the situation in the medical science. The term “precision medicine” first appeared in the book by C. Christensen and J. Grossman *The innovator's prescription* (2009) and then was adopted in the report *Toward precision medicine* prepared by the Institute of Medicine of the National Academy of Sciences (2011). In 2015 the National Precision Medicine Initiative was launched [17]. The initiative aimed to collect medical data from a cohort of 1,000,000 Americans and arrange them into a database [18]. Such studies are resource-consuming [19] yet instrumental in elaborating effective treatment algorithms. Precision and personalized medicines have a lot in common. But although the term “personalized” has long been used to refer to precision medicine, the National Research Council (USA) advises against it. Among the short-term objectives of PrM is its application in cancer research; it is hoped that in the long run precision medicine will find its way into all areas of healthcare. Biological specimens, genetic data, information about lifestyles, the environment and general health provided by the volunteers constituting the cohort can be used to study a wide range of diseases [15, 20].

Let's take a look at the potential benefits of the PrM initiative. Note that the objectives faced by 5PM are given in brackets. Under this initiative, novel approaches will be applied to protect the privacy of study participants and ensure the confidentiality of their data (this pertains to the legal aspect of participatory medicine); novel tools will be designed to build, analyze and use the vast arrays of medical data; quality of clinical trials will improve, as well as control over drug manufacturing. New opportunities will appear facilitating cooperation between researchers with different expertise, patient communities, universities, pharmaceutical companies, etc. Millions of people will be able to make their personal contribution to scientific research (participatory medicine). Among the long-term goals of the project are extensive use of genetic and other information about biological molecules in clinical routine; accurate prediction of treatment outcomes in individual patients (predictive medicine); deeper understanding of the mechanisms underlying pathology (a challenge faced by medical and biological sciences); improving approaches to prevention, diagnostics and treatment of a wide range of diseases; deep integration of electronic medical records into clinical routine to simplify access to patients' records for medical personnel.

PM and PrM share a number of tasks: they both aim to promote the use of omics technologies and targeted TD and are supposed to account for the role of external factors in treatment. Precision medicine also faces new challenges, including promotion of electronic medical records, artificial intelligence and digital databases in healthcare facilities, as well as the use of mobile applications (24/7 health monitoring, telemedicine). The evolution of PrM will contribute to a more accurate classification of pathological conditions, help to effectively distinguish between patients' subpopulations and improve clinical outcomes. Personomics is a word that is often used when it comes to discussing the objectives of PM and PrM [21]. Genomics, proteomics, metabolomics, epigenomics, pharmacogenomics, and other omics are tools exploited by both PrM and PM [2]. Personomics can be recruited by precision medicine to describe the 5P approaches. According to the principles of personomics, differences between people are not limited to biological variability, but also comprise personal traits, attitude to healthcare, activity in social media, wealth, and other unique characteristics that have a strong impact on how and when patients will react to treatment [21]. 5P medicine is a milestone in the evolution of PM and PrM, and personomics is its missing link. In fact, transition from PM to PrM is the evolution from healthcare to health caring: “What do I need to know about you as a person to give you the best care possible?” [22].

5P medicine seeks to create diagnostic and therapeutic models in which the central focus is on the variability of symptoms determined by the individual characteristics of a patient [23]. Theranostics (therapy + diagnostics) could be a handy tool for 5P medicine. It is a diagnostic therapy that allows tailoring a treatment strategy to an individual patient in cases when standard therapeutic options cannot be used [24]. Obviously, precision medicine dictates the need for leaders with fundamental knowledge of genomic medicine and molecular diagnostic methods (NGS, interpretation of whole-genome sequencing data) who will introduce PrM approaches into conventional healthcare [24]. It is expected that electronic records and genomic studies will contribute to the spread of 5P medicine. In 2007, the eMERGE network was launched. It is essentially a consortium for genomic research and discoveries that advocates the use of biorepositories connected to the

systems of electronic medical records [25]. Development of 5PM is dependent on the efficient IT infrastructure capable of storing, maintaining and transmitting vast arrays of genomic data to facilitate their use in the treatment of individual patients and scientific research [26].

### Application of PrM and 5PM in diagnostics and therapy

At present, PrM is enjoying a somewhat limited application in public healthcare. PrM approaches are popular in oncology where they are employed to treat metastatic melanoma, breast, brain and lung malignancies, and leukemia. The most ambitious PrM project was started in Germany in 2013 (the German National Cohort or GNC). It is a nation-wide long-term study planned to last 25-30 years. Another study revealed that tumor molecular panels and personal genomic profiling had limited benefits for patients with cancer in terms of prognosis or quality of life. In a randomized controlled SHIVA study [27] samples of solid tumors were collected and subjected to molecular profiling using a special algorithm; based on the obtained profiles, targeted medication therapy was selected, and then its efficacy was assessed. SHIVA demonstrated that the median progression-free survival was almost similarly low in both groups (2.3 and 2.0 months, respectively). This does not mean, though, that PrM practices should be discontinued, especially in oncology. The negative results could be explained by the heterogeneity of tumors and the ongoing evolution of their cells [28]. Tumor cells circulating in the peripheral blood hold promise for early cancer detection and liquid biopsy (monitoring of relapse in patients with colon and lung cancers); they can be used to analyze a tumor's resistance to drugs and assist selection of adequate therapy. Tumor cells, exosomes and circulating free DNA are convenient diagnostic and prognostic markers that can be measured using minimally invasive techniques [2, 29].

Prevention, screening and diagnosis of prostate cancer still poses a medical dilemma [30]. Prostate cancer is the most prevalent malignancy in men. It is a heterogeneous group of pathologies with unique genetic and proteomic profiles. Molecular genotyping has helped to identify at least 7 molecular subtypes of prostate cancer that differ in their ability to metastasize [31]. According to some estimates, heritability of prostate cancer reaches 42% (95% CI). Genome-wide association studies have reported over 70 different SNPs that can predict the risk of this disease [32]. Genetic data, such as information about the BRCA genotype, can considerably facilitate selection of an adequate screening strategy and stop overtreatment of men at low risk for prostate cancer. Genotyping also serves to identify patients with a potentially good response to 5-alpha-reductase inhibitors, nonsteroidal anti-inflammatory drugs, selective estrogen receptor modulators, and statins [33]. PrM approaches could be beneficial for patients with benign prostatic hyperplasia [34], another heterogeneous group of diseases with unique molecular profiles, varying in their growth rate and severity [35]. So far, GWAS have detected associations between certain SNPs and the risk for/severity of benign prostatic hyperplasia. Knowledge of these associations opens new possibilities for stratifying patients based on the results of pharmacogenomic testing in groups at risk or those receiving treatment [36]. Better understanding of the mechanisms regulating the contractility of prostatic smooth muscles through  $\alpha_1$ -adrenergic receptors and androgen signaling expands the list of the available treatment options (in about 30% of men inhibition of 5AR2 methylation is associated with resistance to finasteride).

Precision diabetes mellitus (DM) is a disease manifested as a broken balance between the body's need for insulin and the actual amount of insulin produced or the resistance to this hormone in the backdrop of normal secretion. Diabetes is triggered by many factors, including obesity. There is little doubt that in the future DM will be managed using the principles of precision medicine. The current classification of diabetes into types 1 and 2 relies on the detection of antibodies against pancreatic  $\beta$ -cell antigens; more than 80% of diagnosed cases are type 2 diabetes. The latter can be broken down into a number of subtypes. For example, by 2018, a few new subtypes had been described, including latent autoimmune diabetes of adults (LADA) affecting patients over 18 years of age, maturity onset diabetes of the young (MODY) striking teenagers under 18, and some others. In 2017, Swedish researchers showed that type 3c (diabetes of the exocrine pancreas) is often mistaken for type 2 DM. Studies of glutamic acid decarboxylase antibodies (GADA) and genetic polymorphisms demonstrate that DM is very diverse, and early diagnosis and therapy are crucial for minimizing its sequelae, preventing chronic complications and reducing mortality associated with this disease. Omics technologies have been very instrumental in discovering promising diabetes biomarkers, such as microRNA. This molecule is involved in insulin secretion, the growth and differentiation of pancreatic  $\beta$ -cells, and the regulation of glucose and lipid metabolism. It is also implicated in obesity and secondary complications of diabetes. The list of microRNA types that affect production and secretion of insulin by pancreatic  $\beta$ -cells includes microRNA-375, -9, -96, and -124a. MicroRNA-375 of pancreatic  $\beta$ -cells regulates insulin secretion in response to stimulation with glucose. Specifically, its overexpression inhibits insulin secretion [2, 37].

Researchers from Lund University (Sweden) have proposed a new classification of DM in adults: instead of types 1 and 2, 5 subtypes should be distinguished. They are characterized by unique progression patterns and different risks of complications. The classification was proposed upon analyzing the data collected from 14,000 individuals. The data came from 5 different sources: the ANDIS project, which recruited more than 8,000 participants over the course of 8 years (2008–2016), the Scania Diabetes Registry, ANDIU, Baaca (DIREVA), and the Cancer Cardiovascular Arm of Malmö Diet. The researchers analyzed the results yielded by laboratory tests, patients' age at the time of diagnosis and the first manifestations, BMI, levels of GADA, glycated haemoglobin HbA1c and C-peptide, HOMA-IR, and insulin resistance. The proposed classification has a potential to become a powerful tool for tailoring treatment strategies to individual patients and for the identification of people at risk for complications. Under this classification, patients are divided into 5 clusters [38]: severe autoimmune diabetes (6–15%) with early onset, corresponding to classic type 1 DM and LADA; severe diabetes with insulin deficiency (9–20%) characterized by elevated HbA1c levels, rapid progression of retinopathy and negative GADA; severe diabetes with insulin resistance (11–17%) diagnosed in overweight patients with BMI > 25 (in this cluster nephropathy and retinopathy were the most prevalent); moderate diabetes associated with obesity (18–27%) occurring in young patients with BMI > 30–34; moderate diabetes of adults (33–47%) with moderate metabolic changes. This type occurs much later in life in comparison with other diabetes types and its course is milder. Patients with severe forms of the disease need aggressive therapy. Patients from cluster 2 are diagnosed with type 2 DM, because the disease is not autoimmune; this type is presumably caused by defective pancreatic islets and not obesity. In this case therapy must be

based on the regimens typically prescribed to patients with type 1 DM; Such patients suffer from ocular pathology more often, while patients from group 3 tend to develop a kidney disease. This must not be overlooked when deciding on the adequate screening procedure. Perhaps, there are hundreds of diabetes subtypes in the world shaped by various genetic, ethnic or environmental factors. People of South Asian origin are at a higher risk for DM. Diabetes is diagnosed in one of 6 Native Americans and Alaskan Inuit.

Although DM is not a monogenic hereditary disease, its risk increases in children born into the families where one or more relatives already have diabetes and carry predisposition genes (HLA-DR3 and HLA-DR4 haplotypes) [39]. Type 2 DM is characterized by carbohydrate metabolism disorders caused by insulin resistance or insulin deficiency. The risk of this disease is as high as 40% if one of the parents has it, and reaches 70% if both parents are affected [40]. Type 2 DM displays a considerable variability in its progression patterns, response to treatment and the risk of complications. Type 2 is believed to be a polygenic condition with up to 20 genes involved, including those coding for the structure of insulin molecules, insulin receptors, glucokinase, glycogen synthase, and mitochondrial components. There are genes accountable for insulin resistance (*PPARG*, *THADA*, *ADAMTS9*, and others),  $\beta$ -cell dysfunction (*KCNJ11*, *HNF1B*, *HNF4A*, *JAZF*, etc.), obesity (*FTO*), and defective incretin hormone secretion (*TCF7L2*). Because insulin resistance is heterogeneous, traditional drugs, such as metformin or thiazolidinedione are often ineffective in patients with type 2 DM. At present, the arsenal of anti-diabetes therapies includes 8 classes of glucose-lowering drugs that target different components pathogenic pathways implicated in type 2 DM. Another 5 novel drug classes are now undergoing preclinical studies. At the moment, we cannot accurately distinguish between diabetes subtypes based on their molecular etiology and have to rely on patients' response to treatment. The initial differentiation should be carried out using the available clinical data (sex, BMI, age at diagnosis) or biomarkers that are easy to measure. So far, this approach has been successfully used to identify female patients with positive response to thiazolidinedione (obesity) or sulphonylurea [41].

It took the medical community some time to recognize the MODY subtype. Genetic testing for DM will soon be available in most countries. In 2016, 5, 000 studies were conducted in the UK and clear diagnostic guidelines were proposed [42]. No sophisticated probability computations are required to assess the risk for MODY; the diagnosis can be established using a statistical calculator and the available clinical data. The MODY probability calculator is free and can be accessed at [www.diabetesgenes.org](http://www.diabetesgenes.org) and in the "Diabetes" application for IOS and Android [43]. It works best for patients who do not receive insulin. This popular calculator (> 6,000 downloads) has become an important step toward precision diabetology. It is a good example of how a complex diagnostic task can be solved using a simple tool that analyzes the available clinical data. Next generation sequencing has made genetic testing easier. But there has to be pre-screening to select patients with possible monogenic diabetes for the test. Modern technologies allow rapid and effective analysis of classic genes implicated in diabetes using a genetic panel [44] and are capable of identifying 25% of patients with monogenic diabetes caused by less popular genes.

Neurological diseases are a rewarding object for PrM application due to the rapid accumulation of genetic knowledge, extensive phenotypical classification, discovery of biomarkers,

and development of potentially promising treatments [45]. A good example here is Parkinson's disease [46]. Precision psychiatry (the term was coined by Vieta et al. [47]) is one of the most advanced PrM branches [48]. The pathophysiology of neurological disorders remains understudied: the symptoms of different conditions often overlap or vary significantly between patients affected by the same disease [49]. A new approach to the classification of psychiatric disorders has been proposed that relies on neurobiological research [50]. Today, we are bestowed with an unprecedented opportunity to build vast databases from large-scale biological data that can be submitted using electronic devices (smartphones). This facilitates the analysis and allows identifying specific characteristics of an individual patient [51]. Considering that none of known biomarkers is likely to signal a psychiatric disorder on its own [52], theoretical and practical approaches to data acquisition are needed to delineate complex profiles of biomarker combinations accounting for the heterogeneity of manifestations of psychiatric diseases. It is important to recruit *panomics* and employ computational modeling of biological systems that could shed light on the major biological pathways involved in the development of psychiatric pathologies. Neurobiological data can be incorporated into the corresponding behavioral profiles that can be acquired using mobile technologies [53]. We believe that in the years to come, the new precision paradigm will lead to the discovery of biomarkers that can simplify decision making about a treatment strategy and predict response to the most widely used medications, such as antidepressants and antipsychotic drugs. This is already happening: C-reactive protein is exploited as a differential predictor of a patient's response to escitalopram and nortriptyline [54].

Immunotherapy is an optimal model for PrM as it describes the symptoms, functions, and molecular etiology of the disease; it can also be tailored to the needs of an individual patient [55]. Allergen immunotherapy remains one of the best candidates for the application of PM approaches. Today we understand what major immunologic and molecular events underlie the symptoms of allergies [56]. There are sensitive diagnostic tests for the detection of IgE-mediated reactions; molecules are known participating in allergic reactions; purified and standardized products are manufactured to ensure safe and effective treatment of allergies. 5PM remains a defining aspect in the treatment of "difficult and expensive" diseases, such as COPD [57] and asthma [58].

We need computational models to predict the risk of pathology for healthy people, prognosticate disease progression and design effective treatments with minimal adverse effects [59]. The "virtual patient" is one of such models based on the integration of molecular, physiological and anatomic data of humans collected under the ITFoM initiative. ITFoM is one of 6 technologies of the future funded by the European Commission. It has attracted over 150 academic and industrial partners from 34 countries. The initiative will promote the development of functional genomics and computer technologies to create a model of a virtual patient suitable for the use in the clinical setting. Genome profiles will be integrated with proteome and metabolome data generated by powerful chromatography, mass spectrometry and nuclear magnetic resonance technologies. The model will be used to analyze the current situation and predict a patient's response to therapy, including intolerance to therapeutic drugs. Successful clinical application of laboratory tests requires identification of healthy populations whose characteristics could be used as

a reference. Organized into biorepositories, such data will play a key role in determining reference ranges needed to improve treatment outcomes.

## CONCLUSIONS

5P medicine is an evolving area of public healthcare. Many of the technologies required to accomplish its ambitious goals are still in the early stages of development or yet to be designed. Researchers have to find a way to standardize collection of clinical data, create databases for the convenient storage of vast data arrays and promote biorepositories. 5PM raises important ethical, social and legal questions. Patients' privacy and confidentiality of their medical records must be protected. Patients should be informed of the risks and

benefits associated with their participation in clinical studies and the use of modern 5PM technologies. This means that a procedure for obtaining informed consent has to be elaborated. The cost of the studies is another obstacle in the way of 5PM: DNA sequencing is fairly expensive, although recently its costs have been going down and tiny, flashcard-sized sequencers have emerged. Perhaps, targeted therapy will still be slightly more expensive than conventional treatments, and this may pose a problem of reimbursing the expenses to state agencies and insurance companies. It is vital that 5PM approaches should become a part of routine medical care. Medical staff will learn more and more about 5P medicine and its prospects over time, and a need will arise to interpret the results of genetic and omics tests in the context of treatment and prophylaxis.

## References

- Shcherbo SN, Shcherbo DS. Medicina 5P: Precizionnaja medicina. Medicinskij alfavit. Sovremennaja laboratorija. 2015; (4): 5–10.
- Shcherbo SN, Shcherbo DS. Personalizirovannaja medicina: monografija v 7 tomah. t. 1. Biologicheskie osnovy. Moskva. RUDN. 2016, 224 s.; t. 2. Laboratornye tehnologii. Moskva. RUDN. 2017, 437 s.
- Raskina KV, Martynova EJu, Perfil'ev AV, i dr. Ot personalizirovannoj k tochnoj medicine. Racional'naja farmakoterapija v kardiologii. 2017; 13 (1): 69–79.
- Shcherbo SN, Shcherbo DS. Medicina 5P: mobil'noe zdravoohranenie. Medicinskij alfavit. Sovremennaja laboratorija. 2017; 4 (28): 5–11.
- Godkov MA. Laboratornaja diagnostika v jepohu nauchno-tehnicheskoy revoljucii. Zakat ili rassvet? Laboratornaja sluzhba. 2017; 6 (3): 5–8.
- Shcherbo SN, Toguzov RT. Tendencii razvitija sovremennoj laboratornoj mediciny (lekcija). Klinicheskaja laboratornaja diagnostika. 2009; (3): 25–32.
- Snyder M. iPOP and its role in participatory medicine. Genome Med. 2014; (6): 6.
- Roberts NJ, Vogelstein JT, Parmigiani G, et al. The predictive capacity of personal genome sequencing. Sci Transl Med. 2012; 4 (133): 133ra58.
- Katz J. The silent wold of doctor and patient. Baltimore: Johns Hopkins University Press, 1983.
- Jain KK. Personalized Medicine. Waltham: Decision Resoures Inc., MA, USA; 1998.
- Personalized Medicine Coalition (PMC). The Case for Personalized Medicine. 2010.
- U.S. Food and Drug Administration (FDA) Department of Health and Human Services, Paving the Way for Personalized Medicine: FDA Role in a New Era of Medical Product Development. [accessed on 10 January 2014]; Available from: <http://www.fda.gov/downloads/ScienceResearch/SpecialTopics/PersonalizedMedicine/UCM372421.pdf>.
- Ginsburg GS, Willard HF. Genomic and Personalized Medicine. Elsevier Science. 2012; 1350 p.
- Schleidgen S, Klingler C, Bertram T, et al. What is personalized medicine: sharpening a vague term based on a systematic literature review. BMC Med Ethics. 2013; (14): 55.
- Nabipour I, Assadi M. Precision medicine, an approach for development of the future medicine technologies. ISMJ. 2016; (19): 167–84.
- O'Donnell PH, Danahey K, Jacobs M. Adoption of a clinical pharmacogenomics implementation program during outpatient care — initial results of the University of Chicago «1,200 Patients Project». Am J Med Genet C Semin Med Genet. 2014; (166C): 68–75.
- Juengst E, McGowan ML, Fishman JR, et al. From «Personalized» to «Precision» Medicine: The Ethical and Social Implications of Rhetorical Reform in Genomic Medicine. Hastings Cent Per. 2016; 46 (5): 21–33.
- Interlandi J. The Paradox of Precision Medicine. Sci Am. 2016; 314 (4): 24–25.
- Joyner MJ, Paneth N. Seven Questions for Personalized Medicine. JAMA. 2015; (55905): 2015–16.
- Collins FS, Varmus H. A New Initiative on Precision Medicine. N Engl J Med. 2015; (372): 793–95.
- Ziegelstein RC. Personomics. JAMA Intern. Med. 2015; (175): 888–89.
- Chochinov HM. Health care, health caring, and the culture of medicine. Curr Oncol. 2014; (21): e668–e669.
- Gupte AA, Hamilton DJ. Molecular Imaging and Precision Medicine. Cardiology. 2016; (133): 178–80.
- Mason-Suares H, Sweetser D, Lindeman N, et al. Training the Future Leaders in Personalized Medicine. J Pers Med. 2016; 6 (1): 1.
- Smoller J, Karlson E, Green R, et al. An eMERGE Clinical Center at Partners Personalized Medicine. J Pers Med. 2016; 6 (1): 5.
- Hricak H. Oncologic imaging: a guiding hand of personalized cancer care. Radiology. 2011; (259): 633–40.
- Le Tourneau C, Delord JP, Gonçaves A, et al. Molecularly targeted therapy based on tumour molecular profiling versus conventional therapy for advanced cancer (SHIVA): a multicentre, open-label, proof-of-concept, randomised, controlled phase 2 trial. Lancet Oncol. 2015; (16): 1324–34.
- Garraway LA, Verweij J, Ballman KV. Precision oncology: an overview. J Clin Oncol. 2013; 31 (15): 1803–05.
- Bettgowda C, Sausen M, Leary R.J, et al. Detection of circulating tumor DNA in early- and late-stage human malignancies. Sci Transl Med. 2014; (6): 224ra24.
- Malvezzi M, Bertuccio P, Levi F, et al. European cancer mortality predictions for the year 2014. Annals of Oncology. 2014; (25): 1650–56.
- Attard G, Beltran H. Prioritizing precision medicine for prostate cancer. Annals of Oncology. 2015; (26): 1041–42.
- Amin AI, Olama A, Benlloch S, et al. Risk analysis of prostate cancer in PRACTICAL, a multinational consortium, using 25 known prostate cancer susceptibility loci. Cancer Epidemiology, Biomarkers & Prevention. 2015; (24): 1121–29.
- Bancroft EK, Page EC, Castro E, et al. Targeted prostate cancer screening in BRCA1 and BRCA2 mutation carriers: Results from the initial screening round of the IMPACT study. European Urology. 2014; (66): 489–99.
- Bechis SK, Otsetov AG, Ge R, et al. Age and obesity promote methylation and suppression of 5-alpha reductase 2—Implications for personalized therapy in benign prostatic hyperplasia. Journal of Urology. 2015; (194): 1031–37.
- Prakash K, Pirozzi G, Elashoff M, et al. Symptomatic and

- asymptomatic benign prostatic hyperplasia: Molecular differentiation by using microarrays. *Proceedings of the National Academy of Sciences of the United States of America*. 2002; (99): 7598–603.
36. Helfand BT, Hu Q, Loeb S, et al. Genetic sequence variants are associated with severity of lower urinary tract symptoms and prostate cancer susceptibility. *Journal of Urology*. 2013; (189): 845–48.
  37. Tofilo MA, Egorova EN. MikroRNK, regulirujushhie adipogenez pri saharanom diabete 2-go tipa. *Zdorov'e i obrazovanie v XXI veke*. 2017; 19 (3): 108–11.
  38. Ahlqvist E, Storm P, Karajamaki A, et al. Novel subgroups of adult-onset diabetes and their association with outcomes: a data-driven cluster analysis of six variables. *The Lancet Diabetes Endocrinology*. 2018; 6 (5): 361–69.
  39. Dedov II, Titovich EV, Kuraeva TL, i dr. Vzaimosvjaz' geneticheskikh i immunologicheskikh markerov u rodstvennikov bol'nyh SD 1 tipa. *Saharnyj diabet*. 2008; (4): 46–50.
  40. Meigs JB, Cupples LA, Wilson PW. Parental transmission of type 2 diabetes: the Framingham Offspring study. *Diabetes*. 2000; (49): 2201–17.
  41. Shields BM, Longergan M, Dennis J, et al. Patient characteristics are associated with treatment response to second line glucose lowering therapy: a MASTERMIND study abstracts of 51st EASD annual meeting. *Diabetologia*. 2015; 58 (Suppl 1): S405.
  42. Chakera AJ, Steele AM, Gloyn AL, et al. Recognition and management of individuals with hyperglycemia because of a heterozygous glucokinase mutation. *Diabetes Care*. 2015; (38): 1383–92.
  43. Shields BM, McDonald TJ, Ellard S, et al. The development and validation of a clinical prediction model to determine the probability of MODY in patients with young-onset diabetes. *Diabetologia*. 2012; (55): 1265–72.
  44. Pearson ER, Pruhova S, Tack CJ, et al. Molecular genetics and phenotypic characteristics of MODY caused by hepatocyte nuclear factor 4alpha mutations in a large European collection. *Diabetologia*. 2005; (48): 878–85.
  45. Tan Lin, Jiang T, Tan Lan, et al. Toward precision medicine in neurological diseases. *Ann Transl Med*. 2016; 4. (6): 104.
  46. Bu L-L, Yang K, Xiong W.-X, et al. Toward precision medicine in Parkinson s disease. *Ann Transl Med*. 2016; 4 (2): 26.
  47. Vieta E. Personalised medicine applied to mental health: Precision psychiatry. *Rev Psiquiatr Salud Ment*. 2015; 8 (3): 117–18.
  48. Fernandes BS, Williams LM, Steiner J, et al. The new field of “precision psychiatry”. *BMC Med*. 2017; (15): 80.
  49. Stephan KE, Bach DR, Fletcher PC, et al. Charting the landscape of priority problems in psychiatry, part 1: classification and diagnosis. *Lancet Psychiatry*. 2016; 3 (1): 77–83.
  50. Insel TR. The NIMH Research Domain Criteria (RDoC) Project: precision medicine for psychiatry. *Am J Psychiatry*. 2014; 171 (4): 395–7.
  51. Andersson G, Titov N. Advantages and limitations of Internet-based interventions for common mental disorders. *World Psychiatry*. 2014; 13 (1): 4–11.
  52. Carvalho AF, Kohler CA, Brunoni AR, et al. Bias in peripheral depression biomarkers. *Psychother Psychosom*. 2016; 85 (2): 81–90.
  53. Marzano L, Bardill A, Fields B, et al. The application of mHealth to mental health: opportunities and challenges. *Lancet Psychiatry*. 2015; 2 (10): 9442–48.
  54. Uher R, Tansey KE, Dew T, et al. An inflammatory biomarker as a differential predictor of outcome of depression treatment with escitalopram and nortriptyline. *Am J Psychiatry*. 2014; 171 (12): 1278–86.
  55. Passalacqua G, Canonica GW. AIT (allergen immunotherapy): a model for the “precision medicine”. *Clin Mol Allergy*. 2015; (1): 24.
  56. Akdis CA, Akdis M. Mechanisms of allergen-specific immunotherapy and immune tolerance to allergens. *World Allergy Organ J*. 2015; 8 (1): 17.
  57. Agusti A. The path to personalised medicine in COPD. *Thorax*. 2014; (69): 857–64.
  58. Fajt ML, Wenzel SE. Asthma phenotypes and the use of biologic medications in asthma and allergic disease: the next steps toward personalized care. *J Allergy Clin Immunol*. 2015; (135): 299–310.
  59. Zazzu V, Regierer B, Kuhn A, et al. IT Future of Medicine: from molecular analysis to clinical diagnosis and improved treatment. *N Biotechnol*. 2013; 30 (4): 362–65.

## Литература

1. Щербо С. Н., Щербо Д. С. Медицина 5П: Прецизионная медицина. Медицинский алфавит. Современная лаборатория. 2015; (4): 5–10.
2. Щербо С. Н., Щербо Д. С. Персонализированная медицина: монография в 7 томах. т. 1. Биологические основы. Москва. РУДН. 2016, 224 с.; т. 2. Лабораторные технологии. Москва. РУДН. 2017, 437 с.
3. Раскина К. В., Мартынова Е. Ю., Перфильев А. В. и др. От персонализированной к точной медицине. Рациональная фармакотерапия в кардиологии. 2017; 13 (1): 69–79.
4. Щербо С. Н., Щербо Д. С. Медицина 5П: мобильное здравоохранение. Медицинский алфавит. Современная лаборатория. 2017; 4 (28): 5–11.
5. Годков М. А. Лабораторная диагностика в эпоху научно-технической революции. Закат или рассвет? Лабораторная служба. 2017; 6 (3): 5–8.
6. Щербо С. Н., Тогузов Р. Т. Тенденции развития современной лабораторной медицины (лекция). Клиническая лабораторная диагностика. 2009; (3): 25–32.
7. Snyder M. iPOP and its role in participatory medicine. *Genome Med*. 2014; (6): 6.
8. Roberts NJ, Vogelstein JT, Parmigiani G, et al. The predictive capacity of personal genome sequencing. *Sci Transl Med*. 2012; 4 (133): 133ra58.
9. Katz J. *The silent world of doctor and patient*. Baltimore: Johns Hopkins University Press, 1983.
10. Jain KK. *Personalized Medicine*. Waltham: Decision Resources Inc., MA, USA; 1998.
11. Personalized Medicine Coalition (PMC). *The Case for Personalized Medicine*. 2010.
12. U.S. Food and Drug Administration (FDA) Department of Health and Human Services, *Paving the Way for Personalized Medicine: FDA Role in a New Era of Medical Product Development*. [(accessed on 10 January 2014)]; Available from: <http://www.fda.gov/downloads/ScienceResearch/SpecialTopics/PersonalizedMedicine/UCM372421.pdf>.
13. Ginsburg GS, Willard HF. *Genomic and Personalized Medicine*. Elsevier Science. 2012; 1350 p.
14. Schleidgen S, Klingler C, Bertram T, et al. What is personalized medicine: sharpening a vague term based on a systematic literature review. *BMC Med Ethics*. 2013; (14): 55.
15. Nabipour I, Assadi M. Precision medicine, an approach for development of the future medicine technologies. *ISMJ*. 2016; (19): 167–84.
16. O'Donnell PH, Danahey K, Jacobs M. Adoption of a clinical pharmacogenomics implementation program during outpatient care — initial results of the University of Chicago «1,200 Patients Project». *Am J Med Genet C Semin Med Genet*. 2014; (166C): 68–75.
17. Juengst E, McGowan ML, Fishman JR, et al. From «Personalized» to «Precision» Medicine: The Ethical and Social Implications of Rhetorical Reform in Genomic Medicine. *Hastings Cent Per*. 2016; 46 (5): 21–33.
18. Interlandi J. *The Paradox of Precision Medicine*. *Sci Am*. 2016; 314 (4): 24–25.
19. Joyner MJ, Paneth N. *Seven Questions for Personalized Medicine*.

- JAMA. 2015; (55905): 2015–16.
20. Collins FS, Varmus H. A New Initiative on Precision Medicine. *N Engl J Med.* 2015; (372): 793–95.
  21. Ziegelstein RC. Personomics. *JAMA Intern. Med.* 2015; (175): 888–89.
  22. Chochinov HM. Health care, health caring, and the culture of medicine. *Curr Oncol.* 2014; (21): e668–e669.
  23. Gupte AA, Hamilton DJ. Molecular Imaging and Precision Medicine. *Cardiology.* 2016; (133): 178–80.
  24. Mason-Suares H, Sweetser D, Lindeman N, et al. Training the Future Leaders in Personalized Medicine. *J Pers Med.* 2016; 6 (1): 1.
  25. Smoller J, Karlson E, Green R, et al. An eMERGE Clinical Center at Partners Personalized Medicine. *J Pers Med.* 2016; 6 (1): 5.
  26. Hricak H. Oncologic imaging: a guiding hand of personalized cancer care. *Radiology.* 2011; (259): 633–40.
  27. Le Tourneau C, Delord JP, Gonçalves A, et al. Molecularly targeted therapy based on tumour molecular profiling versus conventional therapy for advanced cancer (SHIVA): a multicentre, open-label, proof-of-concept, randomised, controlled phase 2 trial. *Lancet Oncol.* 2015; (16): 1324–34.
  28. Garraway LA, Verweij J, Ballman KV. Precision oncology: an overview. *J Clin Oncol.* 2013; 31 (15): 1803–05.
  29. Bettgowda C, Sausen M, Leary R.J, et al. Detection of circulating tumor DNA in early- and late-stage human malignancies. *Sci Transl Med.* 2014; (6): 224ra24.
  30. Malvezzi M, Bertuccio P, Levi F, et al. European cancer mortality predictions for the year 2014. *Annals of Oncology.* 2014; (25): 1650–56.
  31. Attard G, Beltran H. Prioritizing precision medicine for prostate cancer. *Annals of Oncology.* 2015; (26): 1041–42.
  32. Amin AI, Olama A, Benlloch S, et al. Risk analysis of prostate cancer in PRACTICAL, a multinational consortium, using 25 known prostate cancer susceptibility loci. *Cancer Epidemiology, Biomarkers & Prevention.* 2015; (24): 1121–29.
  33. Bancroft EK, Page EC, Castro E, et al. Targeted prostate cancer screening in BRCA1 and BRCA2 mutation carriers: Results from the initial screening round of the IMPACT study. *European Urology.* 2014; (66): 489–99.
  34. Bechis SK, Otsetov AG, Ge R, et al. Age and obesity promote methylation and suppression of 5-alpha reductase 2—Implications for personalized therapy in benign prostatic hyperplasia. *Journal of Urology.* 2015; (194): 1031–37.
  35. Prakash K, Pirozzi G, Elashoff M, et al. Symptomatic and asymptomatic benign prostatic hyperplasia: Molecular differentiation by using microarrays. *Proceedings of the National Academy of Sciences of the United States of America.* 2002; (99): 7598–603.
  36. Helfand BT, Hu Q, Loeb S, et al. Genetic sequence variants are associated with severity of lower urinary tract symptoms and prostate cancer susceptibility. *Journal of Urology.* 2013; (189): 845–48.
  37. Тофило М. А., Егорова Е. Н. МикроРНК, регулирующие адипогенез при сахарном диабете 2-го типа. *Здоровье и образование в XXI веке.* 2017; 19 (3): 108–11.
  38. Ahlqvist E, Storm P, Karajamaki A, et al. Novel subgroups of adult-onset diabetes and their association with outcomes: a data-driven cluster analysis of six variables. *The Lancet Diabetes Endocrinology.* 2018; 6 (5): 361–69.
  39. Дедов И. И., Титович Е. В., Кураева Т. Л. и др. Взаимосвязь генетических и иммунологических маркеров у родственников больных СД 1 типа. *Сахарный диабет.* 2008; (4): 46–50.
  40. Meigs JB, Cupples LA, Wilson PW. Parental transmission of type 2 diabetes: the Framingham Offspring study. *Diabetes.* 2000; (49): 2201–17.
  41. Shields BM, Longergan M, Dennis J, et al. Patient characteristics are associated with treatment response to second line glucose lowering therapy: a MASTERMIND study abstracts of 51st EASD annual meeting. *Diabetologia.* 2015; 58 (Suppl 1): S405.
  42. Chakera AJ, Steele AM, Gloyn AL, et al. Recognition and management of individuals with hyperglycemia because of a heterozygous glucokinase mutation. *Diabetes Care.* 2015; (38): 1383–92.
  43. Shields BM, McDonald TJ, Ellard S, et al. The development and validation of a clinical prediction model to determine the probability of MODY in patients with young-onset diabetes. *Diabetologia.* 2012; (55): 1265–72.
  44. Pearson ER, Pruhova S, Tack CJ, et al. Molecular genetics and phenotypic characteristics of MODY caused by hepatocyte nuclear factor 4alpha mutations in a large European collection. *Diabetologia.* 2005; (48): 878–85.
  45. Tan Lin, Jiang T, Tan Lan, et al. Toward precision medicine in neurological diseases. *Ann Transl Med.* 2016; 4. (6): 104.
  46. Bu L-L, Yang K, Xiong W.-X, et al. Toward precision medicine in Parkinson s disease. *Ann Transl Med.* 2016; 4 (2): 26.
  47. Vieta E. Personalised medicine applied to mental health: Precision psychiatry. *Rev Psiquiatr Salud Ment.* 2015; 8 (3): 117–18.
  48. Fernandes BS, Williams LM, Steiner J, et al. The new field of “precision psychiatry”. *BMC Med.* 2017; (15): 80.
  49. Stephan KE, Bach DR, Fletcher PC, et al. Charting the landscape of priority problems in psychiatry, part 1: classification and diagnosis. *Lancet Psychiatry.* 2016; 3 (1): 77–83.
  50. Insel TR. The NIMH Research Domain Criteria (RDoC) Project: precision medicine for psychiatry. *Am J Psychiatry.* 2014; 171 (4): 395–7.
  51. Andersson G, Titov N. Advantages and limitations of Internet-based interventions for common mental disorders. *World Psychiatry.* 2014; 13 (1): 4–11.
  52. Carvalho AF, Kohler CA, Brunoni AR, et al. Bias in peripheral depression biomarkers. *Psychother Psychosom.* 2016; 85 (2): 81–90.
  53. Marzano L, Bardill A, Fields B, et al. The application of mHealth to mental health: opportunities and challenges. *Lancet Psychiatry.* 2015; 2 (10): 9442–48.
  54. Uher R, Tansey KE, Dew T, et al. An inflammatory biomarker as a differential predictor of outcome of depression treatment with escitalopram and nortriptyline. *Am J Psychiatry.* 2014; 171 (12): 1278–86.
  55. Passalacqua G, Canonica GW. AIT (allergen immunotherapy): a model for the “precision medicine”. *Clin Mol Allergy.* 2015; (1): 24.
  56. Akdis CA, Akdis M. Mechanisms of allergen-specific immunotherapy and immune tolerance to allergens. *World Allergy Organ J.* 2015; 8 (1): 17.
  57. Agusti A. The path to personalised medicine in COPD. *Thorax.* 2014; (69): 857–64.
  58. Fajt ML, Wenzel SE. Asthma phenotypes and the use of biologic medications in asthma and allergic disease: the next steps toward personalized care. *J Allergy Clin Immunol.* 2015; (135): 299–310.
  59. Zazzu V, Regierer B, Kuhn A, et al. IT Future of Medicine: from molecular analysis to clinical diagnosis and improved treatment. *N Biotechnol.* 2013; 30 (4): 362–65.

## ASSESSMENT OF DIASTOLIC FUNCTION IN PATIENTS WITH CHEST PAIN AND ANGIOGRAPHICALLY NORMAL CORONARY ARTERIES USING ECG-GATED SPECT

Khachirova EA<sup>1</sup> ✉, Samoylenko LE<sup>2</sup>, Shevchenko OP<sup>1</sup>

<sup>1</sup> Pirogov Russian National Research Medical University, Moscow, Russia

<sup>2</sup> Russian Medical Academy of Postgraduate Education, Moscow, Russia

The diagnosis and treatment of patients with angiographically normal or near normal coronary arteries remains a clinically relevant problem. The aim of this study was to assess diastolic function in patients with chest pain and normal/near normal coronary arteries (NECA) using ECG-gated SPECT/CT. The study recruited 49 patients presenting with chest pain, a positive cardiac stress test and normal coronary arteries, as demonstrated by coronary angiography. All patients were ordered a myocardial SPECT/CT scan, which was performed according to a two-day protocol. After the scan, the patients were divided into 3 groups. Group 1 consisted of 17 patients with microvascular angina. Group 2 was composed of 22 patients with borderline-high blood pressure or stage I hypertensive heart disease associated with secondary microvascular dysfunction. Ten seemingly healthy individuals constituted the control group. According to coronary angiography, the controls had no cardiovascular pathologies accompanied by coronary artery disorders or impaired myocardial perfusion (SPECT). The majority of patients from groups 1 and 2 were found to have impaired diastolic function. The impairments were more pronounced in group 2 tended to exacerbate with stress. The most sensitive parameter of diastolic function, MFR/3, was outside the reference range in almost all patients in groups 1 and 2. MFR/3 characterizes the mean filling rate of the left ventricle in the first third of diastole. The control group showed no symptoms of diastolic dysfunction. Thus, the patients with chest pain, a positive stress test and NECA had signs of left ventricular diastolic dysfunction exacerbated with stress. Such patients are at risk for heart failure with preserved ejection fraction.

**Keywords:** single-photon emission computed tomography, microvascular angina, diastolic function, angiographically normal or near normal epicardial coronary arteries, myocardial perfusion

**Acknowledgements:** the authors wish to thank Viktor K. Sychev for kindly allowing them to use the equipment of the Laboratory for Radioisotopes.

**Author contribution:** Khachirova EA recruited patients for the study, prepared the necessary documentation, participated in conducting the cardiac stress test and SPECT/CT, and processed the obtained data; Samoylenko LE controlled the course of the study and double-checked the obtained results; Shevchenko OP made sure inclusion and exclusion criteria were met.

**Compliance with ethical standards:** the study was approved by the Ethics Committee of Pirogov Russian Medical Research Medical University (Protocol 150 dated December 15, 2015). All patients gave informed consent to participate.

✉ **Correspondence should be addressed:** Elvira A. Khachirova  
Ostrovityanova 1, Moscow, 117997; elchik09@mail.ru

**Received:** 17.09.2018 **Accepted:** 11.11.2018 **Published online:** 23.02.2019

**DOI:** 10.24075/brsmu.2019.001

## ОЦЕНКА ДИАСТОЛИЧЕСКОЙ ФУНКЦИИ МИОКАРДА У ПАЦИЕНТОВ С БОЛЕВЫМ СИНДРОМОМ В ГРУДНОЙ КЛЕТКЕ И АНГИОГРАФИЧЕСКИ НЕИЗМЕННЫМИ КОРОНАРНЫМИ АРТЕРИЯМИ МЕТОДОМ СИНХРОНИЗИРОВАННОЙ С ЭКГ ОДНОФОТОННОЙ ЭМИССИОННОЙ КОМПЬЮТЕРНОЙ ТОМОГРАФИИ

Э. А. Хачирова<sup>1</sup> ✉, Л. Е. Самойленко<sup>2</sup>, О. П. Шевченко<sup>1</sup>

<sup>1</sup> Российский национальный исследовательский университет имени Н. И. Пирогова, Москва, Россия

<sup>2</sup> Российская медицинская академия постдипломного образования, Москва, Россия

На протяжении многих лет остается актуальной тема диагностики и тактики ведения пациентов с ангиографически неизменными или малоизменными коронарными артериями (КА). Целью исследования было оценить диастолическую функцию у пациентов с болевым синдромом в грудной клетке и неизменными/малоизменными КА (Н/МКА) по данным синхронизированной с ЭКГ однофотонной эмиссионной компьютерной томографии (С-ОЭКТ/КТ). В исследование вошли 49 пациентов с болевым синдромом в области грудной клетки, положительными результатами нагрузочного теста и Н/МКА по данным коронароангиографии (КАГ). Всем пациентам выполнили С-ОЭКТ/КТ миокарда по двухдневному протоколу. После исследования пациенты были разделены на три группы: 17 пациентов с микрососудистой стенокардией составили группу 1; 22 пациента с пограничной артериальной гипертензией (АГ), или гипертонической болезнью (ГБ) I стадии, ассоциирующейся с вторичной микрососудистой дисфункцией — группу 2. Группу контроля, или группу 3, составили 10 практически здоровых лиц, у которых при КАГ были исключены заболевания со стороны сердечно-сосудистой системы, сопровождающиеся изменениями коронарных артерий и нарушениями перфузии миокарда при проведении ОЭКТ. У большинства пациентов в группах 1 и 2 были выявлены нарушения диастолической функции, при этом в группе 2 они глубже и усугубляются при нагрузке. Наиболее чувствительный параметр диастолической функции — средняя скорость наполнения ЛЖ в первую треть диастолы (MFR/3) — изменен практически у всех пациентов групп 1 и 2. У пациентов группы контроля изменения не выявлены. Таким образом, у пациентов с болью в груди, положительным стресс-тестом и Н/МКА выявлены признаки диастолической дисфункции ЛЖ (ДДФ) и дальнейшее ее ухудшение при нагрузке. Эти пациенты могут представлять собой группу риска развития сердечной недостаточности с сохраненной фракцией выброса.

**Ключевые слова:** однофотонная эмиссионная компьютерная томография, ангиографически неизменные/малоизмененные эпикардальные коронарные сосуды, диастолическая функция, перфузионная сцинтиграфия, микрососудистая стенокардия

**Благодарности:** авторы благодарят Виктора Константиновича Сычева за возможность воспользоваться радиоизотопной лабораторией и оборудованием в процессе сбора материала.

**Информация о вкладе авторов:** Э. А. Хачирова подбирала пациентов, оформляла документацию для проведения исследования, участвовала в проведении велоэргометрии и сцинтиграфического исследования, обрабатывала полученные данные; Л. Е. Самойленко контролировала протокол исследования, проверяла полученные результаты; О. П. Шевченко контролировал соблюдение критериев включения в исследование и критериев исключения при отборе пациентов.

**Соблюдение этических стандартов:** исследование одобрено этическим комитетом РНИМУ им. Н. И. Пирогова (протокол № 150 от 15 декабря 2015 г.). Все пациенты подписали добровольное информированное согласие на проведение исследования.

✉ **Для корреспонденции:** Эльвира Азреталиевна Хачирова  
ул. Островитянова, д. 1, г. Москва, 117997; elchik09@mail.ru

**Статья получена:** 17.09.2018 **Статья принята к печати:** 11.11.2018 **Опубликована онлайн:** 23.02.2019

**DOI:** 10.24075/vrgmu.2019.001

The use of echocardiography (EchoCG) in clinical diagnostics shed light on the actual prevalence of heart failure (HF) with preserved left ventricular (LV) systolic function (ejection fraction (EF) > 45%), which turned out to be a very widespread condition. According to the Framingham Heart Study (1948–2012), the Rochester Epidemiology Project (1960–1984) and some other research studies, patients with preserved LVEF make up over one-third of all individuals with HF, and their number is growing steadily [1, 2]. Diastolic dysfunction (DD) is believed to be one of the possible causes of HF in such patients [3–5]. Isolated DD is more often diagnosed in patients with angiographically normal or near normal epicardial coronary arteries (NECA) [6].

In spite of the obvious advances in the understanding of DD in patients with NECA, there are questions about the etiology and pathogenesis of diastolic impairment that still need to be answered [7, 8]. The underlying causes of DD and DD-associated HF named in the literature include LV hypertrophy, metabolic shifts, myocardial fibrosis, and coronary microvascular dysfunction (CMD) that many authors also regard as a risk factor for adverse cardiovascular events [9, 10].

Clinical data corroborating the role of CMD in triggering DD in patients with normal epicardial coronary arteries come from limited sources. For example, there was an extensive retrospective study in which the medical histories of 376 patients with LVEF  $\geq$  50% and without signs of obstructive coronary artery disease were analyzed [11]. Cardiac PET imaging revealed that all patients with HF, preserved LVEF and signs of DD had reduced coronary flow reserve, which, according to the authors of the study, may have indicated an association between a microvascular pathology, DD and HF. Myocardial hypertrophy (MH) is another possible reason of DD in patients with NECA. A transesophageal Doppler study assessing diastolic function in 30 patients with left ventricular hypertrophy (LVH) found that 16 participants had symptoms of ischemia and angiographically normal CA whereas in 14 patients LVH was asymptomatic. Signs of DD were present in both groups, but tended to be more pronounced in group 1 [12].

Ectopic fat deposition referred to as myocardial steatosis may also increase the risk of DD. A team of researchers measured myocardial triglyceride content and assessed diastolic function in 13 women with intact CA using proton magnetic resonance spectroscopy and magnetic resonance tissue tagging [6]. Five women were shown to have signs of CMD and subclinical DD correlated with high triglyceride content in the myocardium. The authors concluded that myocardial steatosis has a distinct association with diastolic dysfunction in the studied cohort of patients.

At the same time, there are reports that such patients do not develop DD. For example, ECG revealed no significant impairment of diastolic function in 99 patients with syndrome X confirmed by a stress test [13].

Given that the literature reports are controversial, research into DD should be continued in order to work out criteria for this condition and to prevent diastolic heart failure in patients with angiographically normal or near normal epicardial coronary arteries. Today, echocardiography remains the most available and popular method for the assessment of systolic and diastolic myocardial function. However, its reproducibility is quite low and depends largely on the operator who performs the scan. In contrast, cardiac radionuclide imaging is characterized by higher reproducibility and high accuracy, and its results only slightly depend on the operator's skills.

Considering the abovesaid, the aim of this study was to measure the left ventricular function in patients with chest pain and normal or near normal epicardial coronary arteries

using cardiac single-photon emission computed tomography (C-SPECT).

## METHODS

The study recruited 49 participants (24 men and 25 women) aged 43 to 77 years (the mean age was  $62.6 \pm 8.9$  years) with chest pain (CP) and a positive stress test. All patients were examined and received treatment at the facilities of the Department of Cardiology, Pirogov Russian Medical Research Medical University.

The following exclusion criteria were applied: hypertension (systolic blood pressure  $\geq$  180 mmHg and diastolic blood pressure  $\geq$  110 mmHg), cardiac lesions, LVH, hypertrophic and dilated cardiomyopathies, acute myocardial infarction within 6 months preceding our study, LVEF < 45%, persistent flutter and atrial fibrillation, arrhythmias, impaired conductivity, valvular/endocrine/neurological/ disorders, kidney or liver failure, and other diseases leading to impaired myocardial perfusion or affecting systolic and diastolic functions of the myocardium.

A detailed medical history was taken from all participants; a full blood count and a blood biochemistry test were also performed. The patients underwent a physical examination, a standard 12-lead ECG, Holter monitoring, a cardiac stress test on a stationary bicycle (CST), coronary angiography, and a C-SPECT/CT scan at rest and with stress. Angiography identified 37 patients with intact coronary arteries and 12 patients with stenosis (<40%) in one artery and normal systolic function (as assessed by EchoCG). Twenty-two participants had borderline-high blood pressure or stage I hypertensive heart disease with a LV mass index of  $132 \pm 21$ ; the blood pressure was lowered to an average of 125/80 mmHg by the prescribed medication therapy. Seventeen patients had no comorbidities (the LV mass index was  $128 \pm 27$ ). Twenty-one patient had hypercholesterinemia: total cholesterol levels were  $5.4 \pm 1.68$  mmol/l, concentrations of low-density lipoproteins were  $3.3 \pm 1.0$  mmol/l. Ten participants who did not have any cardiovascular disorders constituted the control group. Clinical characteristics of the patients are given in Table 1.

All patients underwent a myocardial SPECT/CT scan at the Department of Radionuclide Diagnostics. The scans were ordered to assess the systolic and diastolic functions of the heart. Antianginal therapy was temporarily discontinued before the scan for the period of > 5 elimination half-lives of the used drug.

A 2-day C-SPECT/CT protocol was applied. On the first day, the scan was performed at rest; on the second day, stress images were obtained following the exercise ECG test. During the test on the Ergoline bicycle ergometer, the blood pressure was monitored. The test was conducted according to the standard protocol. The initial workload was 25 W; it was increased by 25 W every 3 minutes. Once the maximal workload was achieved, the patients received an intravenous injection of a radiopharmaceutical and then continued exercising for another minute.

The radiopharmaceutical selected for our study was Technetium ( $^{99m}\text{Tc}$ ) sestamibi (Russia). It was administered intravenously via a 444–555 MBq bolus injection. Images were recorded using a gamma camera. Stress images were obtained 45–60 min after the injection administered during the exercise test, whereas rest images were obtained 60–90 min after the injection at rest.

ECG-gated SPECT/CT imaging was assisted by the dual-detector gamma camera Symbia T-16 (Siemens; Germany) connected to a low-dose scanner for computed tomography

equipped with a SMARTZOOM collimator for cardiac studies. Image acquisition was triggered by the R wave. During the scan, the patients were lying in the supine position. The detectors were positioned at 90° to each other and were rotating 180° around the patient's body. In total, 32 projections (16 per detector) were obtained for each patient.

Myocardial perfusion and diastolic function were analyzed in QPS\QGS, AutoSPECT (Quark Inc., version 8.5) using a 17-segment model of the left ventricle. The following systolic and diastolic parameters were assessed.

1. Systole:

- EF  $\geq$  50% at rest and with stress;
- PER (the peak ejection rate of the LV, expressed as end-systolic volume per second, the normal range is from 2 to 3) at rest and with stress.

2. Diastole:

- PFR (the peak filling rate of the LV, expressed as end-diastolic volume per second, the normal range is from 2 to 3); characterizes myocardial diastolic function;
- MFR<sub>3</sub> (the mean filling rate of the LV during the first-third of diastole, expressed as end-diastolic volume per second, the reference range is from 1.5 to 2);
- PFR2 (secondary peak filling rate, not observed in healthy patients); in patients with two or more filling peaks, the peak filling rate during the second peak was calculated;
- TTPF (time from end systole to peak filling, the normal range is 100–150 ms).

If at least parameter of diastolic function fell outside the reference range, DD was presumed [10].

The obtained data were processed in Statistica 6.0 (StatSoft; version 6.0) and are presented in this work as M  $\pm$  SD (mean  $\pm$  standard deviation). Qualitative parameters were compared using the Pearson's chi square test. If the number of observations in one of the compared groups was less than 11, the Yates correction was applied. If the number of observations was below 5, the two-sided Fisher's test was used.

Quantitative data were compared using nonparametric tests, including the Mann Whitney U for 2 independent variables and the Kruskal-Wallis for 3 or more independent variables.

## RESULTS

The study participants were examined and divided into 3 groups. Group 1 consisted of 17 patients with microvascular angina (MA) who complained of chest pain but had no comorbidities that could lead to impaired myocardial perfusion; their coronary arteries appeared intact during the coronary angiography, and C-SPECT/CT verified transient myocardial ischemia. Group 2 was composed of 22 patients with borderline-high blood pressure or stage I hypertensive heart disease confirmed by the results of 24-h blood pressure monitoring. The patients in group 2 had no LVH (LV mass index was  $132 \pm 21$ ) and no cardiac lesions; their blood pressure was lowered to the desired values, and C-SPECT/CT verified transient myocardial ischemia associated with secondary CMD. The control group included 10 seemingly healthy individuals with no cardiovascular conditions, intact coronary arteries and normal myocardial perfusion. In each group, the patients were comparable in terms of age, BMI, heart rate (HR) and blood pressure measured at rest. No significant differences were observed between the groups regarding heart rate, blood pressure, ESD, and EDD (measured by echocardiography) determined at rest (Table 1). In the controls, the systolic and diastolic parameters of the left ventricle fell within the normal reference range both at rest and after exercise.

No significant differences were found in the parameters characterizing the systolic function of the LV between the patients with NECA. EF and peak ejection rate at rest and after the stress test did not differ significantly between groups 1 and 2. At rest, EF was  $58.5 \pm 6.6$  and  $59.5 \pm 6.8$  ( $p > 0.05$ ) in groups 1 and 2, respectively, whereas after the stress test, it reached  $65.6 \pm 7.8$  and  $66.4 \pm 8.8$  ( $p > 0.05$ ), respectively. In

**Table 1.** Clinical characteristics of the study participants

Parameter	Group 1 (MVA), <i>n</i> = 17	Group 2 (CMD), <i>n</i> = 22	Group 3 controls, <i>n</i> = 10
Age	62.7 $\pm$ 7.8 (50–77)	60.6 $\pm$ 8.1 (44–75)	63.2 (43–74)
Sex, male/female	6/11	12/10	6/4
BMI (kg/m <sup>2</sup> )	25.8 $\pm$ 3.6	26.7 $\pm$ 3.2	25.7 $\pm$ 3.47
Duration of disease, years	3.4 $\pm$ 2	3.8 $\pm$ 1.9	3.2 $\pm$ 1.7
Systolic blood pressure (mmHg)	122 $\pm$ 9.2	130 $\pm$ 6.8	126 $\pm$ 6.4
Diastolic blood pressure (mmHg)	73 $\pm$ 5.8	74 $\pm$ 4.0	72 $\pm$ 6.0
LV mass index	128 $\pm$ 27	132 $\pm$ 21	127 $\pm$ 18
Resting heart rate	67 $\pm$ 8	72 $\pm$ 6	66 $\pm$ 8
Pain type:			
Nonanginal (localized, lasting for several hours or more, not relieved by nitroglycerin)	5	7	10
Anginal	12	15	0
Holter monitoring results:			
NORM	6	11	10
ST depression $\geq$ 2.0 mm	4	5	0
ST depression $\leq$ 2.0 mm	7	6	0
EchoCG of LV:			
EF (biplane Simpson's method), %	64.5 $\pm$ 9.5	60.7 $\pm$ 4.0	67.4 $\pm$ 10.2
ESD, cm	3.5 $\pm$ 0.3	3.6 $\pm$ 0.3	2.77 $\pm$ 0.5
EDD, cm	4.8 $\pm$ 0.3	4.9 $\pm$ 0.4	4.65 $\pm$ 0.2
PWT, cm	1.0 $\pm$ 0.06	1.04 $\pm$ 0.08	0.98 $\pm$ 0.15

**Note:** MVA stands for microvascular angina; ESD is end-systolic dimension; EDD is end-diastolic dimension; PWT is posterior wall thickness; HR is heart rate.

group 1, PER at rest was  $2.5 \pm 0.2$ , increasing up to  $2.7 \pm 0.3$  after the stress test. In group 2, PER was  $2.4 \pm 0.3$  and  $2.7 \pm 0.4$  ( $p > 0.05$ ) at rest and after the stress test, respectively.

Left ventricular systolic function was normal in both groups.

Diastolic abnormalities were detected in the majority of the patients with NECA both at rest and with stress. At least one measured parameter fell outside the normal range in all patients from group 1 and 17 patients from group 2, indicating DD. MFR/3 was aberrant almost in all participants. However, deviations from the norm were more often observed for more than one measured parameter. At rest, 5 patients from group 1 had abnormal MFR/3 only; 6 patients had abnormal MFR/3+another parameter; in another 5 patients 3 parameters fell outside the reference range; and in 1 patient 4 measured parameters deviated from the norm. After the stress test, deviations from the normal range affecting only 1 parameter were observed in 3 patients; 2 parameters, in 4 patients; 3 parameters, in 7 patients; and 4 parameters, in 2 patients. To sum up, after the stress test the majority of the patients had abnormal values of 3 to 4 parameters characterizing myocardial function, as compared to the same parameters measured at rest.

In group 2, one parameter measured at rest fell outside the normal range in 2 patients; 2 parameters, in 7 patients; 3, in 5 patients; and 4, in 3 patients. In another 5 patients all studied parameters were perfectly normal. However, after the stress test, only one patient still had only one abnormality in the measured parameters; 2 abnormal parameters were detected in 7 patients; 3, in 6 patients; and 4, in 4 patients.

Mean values characterizing myocardial function in patients with normal or near normal epicardial coronary arteries and healthy controls are presented in Table 2.

There were significant differences between groups 1 and 2 in the values of PFRrest, MFR/3stress, TTPFrest, and PFR2stress. At rest, secondary filling peaks were detected in 3 (17%) patients from group 1 and 5 patients (23%) from group 2; after the stress test, secondary filling peaks were present in 4 (23%) and 7 (32%) patients from groups 1 and 2, respectively. No significant difference in MFR/3 at rest and with stress was observed between groups 1 and 2. Perhaps, this is because in both groups this parameter was initially abnormal both at rest and with stress.

When comparing groups 1 and 2 with the controls, we discovered significant differences in all parameters except for PFRrest in group 1. Importantly, EchoCG identified DD signs in 11 (65%) patients from group 1 and 14 (82%) patients from group 2. Echocardiographic criteria for DD include a decline

in peak early-diastolic velocity  $e'$  ( $e' < 9$  cm/s on average), an increased ratio of early to late diastolic annular velocities ( $> 15$ ), and a combination of a few other parameters [12]. All cases of diastolic dysfunction suggested by EchoCG were confirmed by C-SPECT.

Below we describe a clinical case of a female patient aged 69 who presented with chest pain and shortness of breath lasting for up to 25 min that appeared following emotional stress and could not be relieved by nitroglycerin. The coronary arteries were intact. The established diagnose was class II effort angina. The patient had had this condition for about 2 years, with almost daily episodes of pain. The patient had no history of familial cardiovascular diseases or addictions.

The patient was in a satisfactory condition at admission. BMI was 20. Blood count and biochemistry, as well as thyroid hormone levels, were within the reference range. ECG revealed normal sinus rhythm and HR of 68 beats/min. EchoCG findings: EDD = 4.6 cm, ESD = 3.2 cm, PWT = 1.0 cm. EF was  $> 60\%$ , local contractility was without abnormalities. The stress test revealed episodes of ST depression of up to 1.5 mm. Coronary angiography showed that the coronary arteries were intact.

According to C-SPECT scans (Fig. 1, 2) performed at rest (1) and with stress (2), left ventricular systolic function was intact: EF was 67% at rest and 76% after the exercise test. No LV wall motion abnormalities were observed; LV PER was 2.7 at rest and 2.94 after the stress test.

LV PFR was within the reference range: 2.71 at rest and 3.04 after the stress test; MFR/3 was 0.77 at rest and 0.91 after the stress test. LV TTPF was impaired (286 at rest and 287 after the stress test). Additional LV filling peaks were not detected.

The patient exhibited signs of diastolic dysfunction suggested by abnormal MFR/3 and TTPF. Perfusion myocardial SPECT registered signs of transient myocardial ischemia in the upper and medial regions of the anterior wall.

## DISCUSSION

It was established that the majority of patients with NECA participating in our study had diastolic dysfunction. What factors can contribute to the impairment of the diastolic cycle in such patients? One of the causes named in the literature is myocardial fibrosis accompanied by changes in cardiac contractility [3, 6]. All patients recruited in our study did not have problems with their left ventricular systolic function; EF and PER measured at rest and after the cardiac test were within

**Table 2.** Quantitative parameters of diastolic function in the studied groups of patients

Parameters	Parameters of diastolic function				Difference between the groups ( $p$ -value)			
	Groups 1 and 2, $n = 39$	Group 1, $n = 17$	Group 2, $n = 22$	Group 3 (controls), $n = 10$	Columns 1 and 4	Columns 2 and 3	Columns 2 and 4	Columns 3 and 4
	1	2	3	4				
PFRstress, EDV/s	$1.89 \pm 0.21$	$1.93 \pm 0.17$	$1.86 \pm 0.24$	$2.75 \pm 0.31$	<b>0.000001</b>	0.5	<b>0.00002</b>	<b>0.000009</b>
PFRrest, EDV/s	$1.97 \pm 0.27$	$2.12 \pm 0.28$	$1.86 \pm 0.20$	$2.32 \pm 0.32$	<b>0.002</b>	<b>0.003</b>	0.14	<b>0.0001</b>
MFR/3stress, EDV/s	$1.12 \pm 0.22$	$1.01 \pm 0.23$	$1.20 \pm 0.17$	$1.77 \pm 0.14$	<b>0.000001</b>	<b>0.009</b>	<b>0.00002</b>	<b>0.000009</b>
MFR/3rest, EDV/s	$1.26 \pm 0.24$	$1.26 \pm 0.24$	$1.26 \pm 0.25$	$1.60 \pm 0.15$	<b>0.0003</b>	0.9	<b>0.0008</b>	<b>0.001</b>
TTPFrest, ms	$164.1 \pm 18.1$	$156.0 \pm 13.1$	$170.4 \pm 19.2$	$138.4 \pm 9.5$	<b>0.000047</b>	<b>0.015</b>	<b>0.001</b>	<b>0.00005</b>
TTPFstress, ms	$172.3 \pm 24.9$	$166.3 \pm 13.5$	$176.9 \pm 30.5$	$153.0 \pm 6.8$	<b>0.01</b>	0.3	<b>0.009</b>	<b>0.04</b>
PFR2stress, number of patients, abs. number, %	14 (35.9%)	3 (17.6%)	11 (50.0%)	0	–	<b>0.049</b>	–	–
PFR2rest, number of patients, abs. number, %	8 (20.5%)	1 (5.9%)	7 (31.8%)	0	–	0.1	–	–

**Note:** significant differences are shown in bold; stress stands for the measurements done after the stress test; rest stands for the measurements at rest.

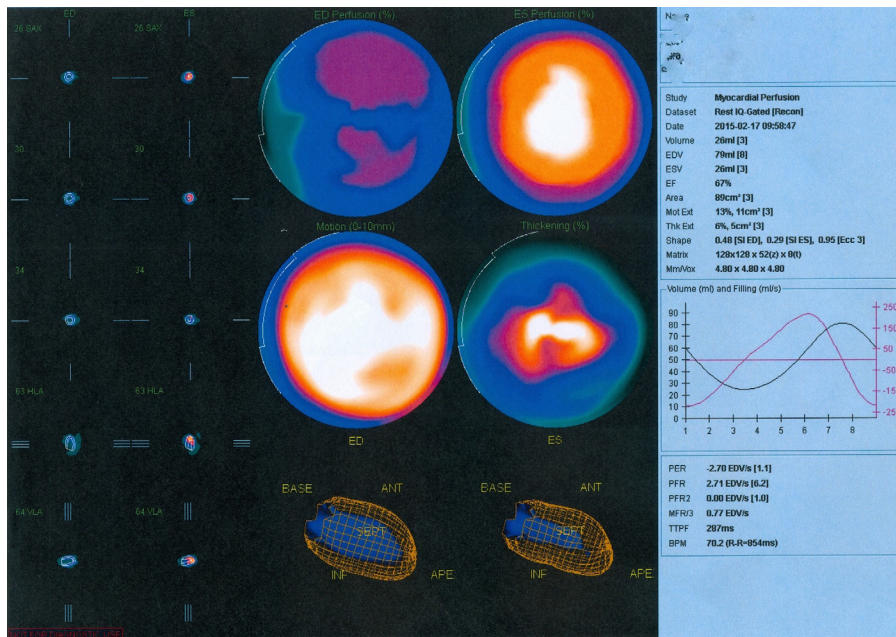


Fig. 1. A resting C-SPECT scan of a female patient aged 69 who presented with chest pain and intact coronary arteries (class II effort angina)

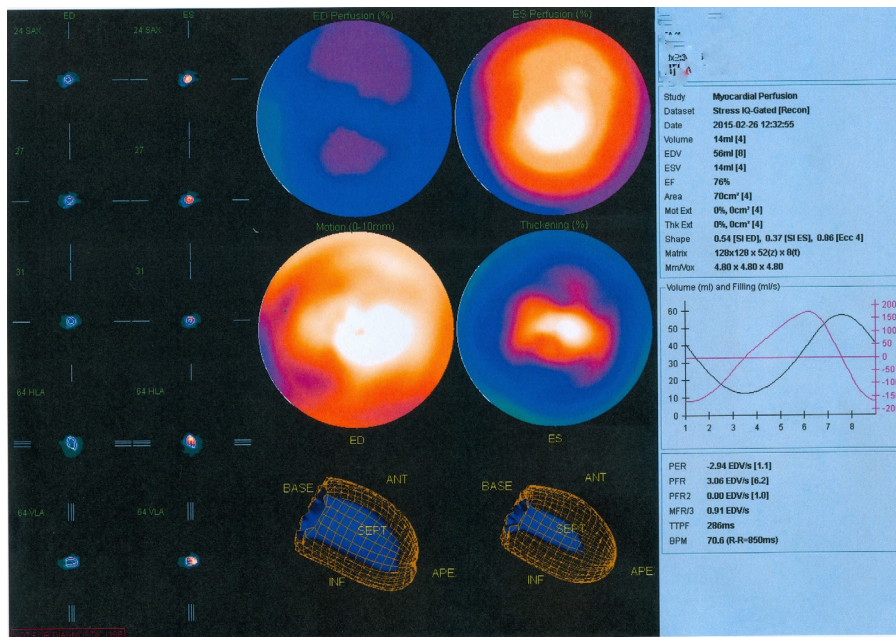


Fig. 2. A stress C-SPECT scan of a female patient aged 69 who presented with chest pain and intact coronary arteries

the normal reference range. No local impairment of LV wall motion was observed. Therefore, we conclude that diastolic dysfunction in our patients is not associated with impaired contractility (myocardial fibrosis).

LV hypertrophy is another possible cause underlying DD. Patients with myocardial hypertrophy were not included in the present study. LV mass index was within the reference range in all patients, reaching  $128 \pm 27$ ,  $132 \pm 21$  and  $127 \pm 18$  in groups 1 and 2 and the controls, respectively.

Metabolic shifts can also be regarded as a factor contributing to DD. However, our study did not include patients suffering from the conditions associated with metabolic shifts, except for those accompanying transient myocardial ischemia.

The most probable cause of DD in the studied cohort of patients is microvascular dysfunction. Although coronary arteries were intact in all examined patients, C-SPECT/

CT verified the diagnosis of transient ischemia in groups 1 and 2.

Patients from group 2 had abnormal left ventricular PFR and TTPF. Those deviations from the norm were more noticeable in group 2 than in patients from group 1 who did not have hypertension. MFR/3, the most sensitive parameter of diastolic function, was abnormal at rest in groups 1 and 2, as compared with the controls, but did not differ significantly between the groups. The abnormalities became more pronounced after the stress test in the absence of any LV wall motion pathology. This could be explained by reduced myocardial perfusion and transient myocardial ischemia.

Besides, a secondary filling peak was detected in some patients from both groups at rest; the number of peaks increased in response to physical exercise.

Our findings are consistent with other studies of diastolic function in patients with intact coronary arteries. For example, an

echocardiographic Doppler study demonstrated that diastolic function was impaired in female patients with microvascular angina [14]. In another study, diastolic function was assessed using C-SPECT, EchoCG and heart MRI [15]. Importantly, those C-SPECT findings are consistent with the results of the present study. In [15] EchoCG suggested DD in more than 60% of patients with DD detected by C-SPECT, which also concurs with our findings (65% and 82% in groups 1 and 2, respectively). According to Y.W. Wu et al, C-SPECT is less sensitive to DD than Doppler echocardiography. At the same time, the authors point to high sensitivity of 64-slice computed tomography in the assessment of DF [15].

In conclusion, we would like to stress that all studies listed above, including our own, were performed on a small sample, meaning they have serious limitations. Therefore, research into the causes of diastolic dysfunction should be continued.

## CONCLUSIONS

The present study has demonstrated that diastolic function is impaired in patients with intact coronary arteries and chest pain. Given that the literature on the subject is scarce and controversial, we believe that research into the causes of diastolic dysfunction should be continued.

## References

- Hogg K, Swedberg K, McMurray J. Heart Failure with preserved left ventricular systolic function. Epidemiology, Clinical Characteristics, and Prognosis. *J Am Coll Cardiol*. 2004; 43 (3): 317–27.
- Fomin IV, Belenkov JuN, Mareev Vju, et al. Rasprostranennost' hronicheskoy serdechnoj nedostatochnosti v Evropejskoj chasti RF (dannye issledovaniya «JePOHA – HSN»). *ZhSN*. 2006; 3 (7): 112–5.
- Paulus WJ, Tschope C. A novel paradigm for heart failure with preserved ejection fraction: comorbidities drive myocardial dysfunction and remodeling through coronary microvascular endothelial inflammation. *J Am Coll Cardiol*. 2013; 62: 263–71.
- Taqueti VR, Ridker PM. Inflammation, coronary flow reserve, and microvascular dysfunction: moving beyond cardiac syndrome X. *JACC Cardiovasc Imaging*. 2013; (6): 668–71.
- Crea F, Merz CNB, Beltrame JF, et al. Coronary Vasomotion Disorders International Study Group. The parallel tales of microvascular angina and heart failure with preserved ejection fraction: a paradigm shift. *Eur Heart J*. 2017; (38): 473–77.
- Wei J, Nelson MD, Szczepaniak EW, et al. Myocardial steatosis as a possible mechanistic link between diastolic dysfunction and coronary microvascular dysfunction in women *Am J Physiol Heart Circ Physiol*. 2016; 310 (1): H14–H11.
- Ponikowski P, Voors AA, Anker SD, et al. 2016 ESC Guidelines for the diagnosis and treatment of acute and chronic heart failure: the task force for the diagnosis and treatment of acute and chronic heart failure of the European Society of Cardiology (ESC) developed with the special contribution of the Heart Failure Association (HFA) of the ESC. *Eur Heart J*. 2016; (37): 2129–200.
- Redfield MM. Heart failure with preserved ejection fraction. *N Engl J Med*. 2016; (375): 1868–77.
- Van Kraijl DJ, van Pol PE, Ruiters AW, et al. Diagnosing diastolic heart failure. *Eur J Heart Fail*. 2002; 4 (4): 419–30.
- Kato S, Saito N, Kirigaya H, et al. Impairment of coronary flow reserve evaluated by phase contrast cine-magnetic resonance imaging in patients with heart failure with preserved ejection fraction. *J Am Heart Assoc*. 2016; (5): e002649.
- Srivaratharajah K, Coutinho T, Liu P, et al. Reduced myocardial flow in heart failure patients with preserved ejection fraction. *Circ Heart Fail*. 2016; 9 (7): e002562.
- Isaaz K, Bruntz JF, Paris D, et al. Abnormal coronary flow velocity pattern in patients with left ventricular hypertrophy, angina pectoris, and normal coronary arteries: A transesophageal Doppler echocardiographic study. *American Heart Journal*. 1994; 128 (3): 500–10.
- Kaski JC, Rosano GMC, Collins P, et al. Cardiac syndrome X: clinical characteristics and left ventricular function. *Journal of the American College of Cardiology*. 1995; (25): 807–14.
- Nelson MD, Szczepaniak LS, Weiet J, al. Diastolic Dysfunction in Women With Signs and Symptoms of Ischemia in the Absence of Obstructive Coronary Artery Disease A Hypothesis-Generating Study. *Circ Cardiovasc Imaging*. 2014; (7): 510–6.
- Wu Y, Tadamura E, Yamamuro M, et al. Estimation of global and regional cardiac function using 64-slice computed tomography: a comparison study with echocardiography, gated-SPECT and cardiovascular magnetic resonance. *Int J Cardiol*. 2008; 128 (1): 69–76.

## Литература

- Hogg K, Swedberg K, McMurray J. Heart Failure with preserved left ventricular systolic function. Epidemiology, Clinical Characteristics, and Prognosis. *J Am Coll Cardiol*. 2004; 43 (3): 317–27.
- Фомин И. В., Беленков Ю. Н., Мареев В. Ю. и др. Распространенность хронической сердечной недостаточности в Европейской части РФ (данные исследования «ЭПОХА — ХСН»). *ЖСН*, 2006; 3 (7): 112–15.
- Paulus WJ, Tschope C. A novel paradigm for heart failure with preserved ejection fraction: comorbidities drive myocardial dysfunction and remodeling through coronary microvascular endothelial inflammation. *J Am Coll Cardiol*. 2013; 62: 263–71.
- Taqueti VR, Ridker PM. Inflammation, coronary flow reserve, and microvascular dysfunction: moving beyond cardiac syndrome X. *JACC Cardiovasc Imaging*. 2013; (6): 668–71.
- Crea F, Merz CNB, Beltrame JF, et al. Coronary Vasomotion Disorders International Study Group. The parallel tales of microvascular angina and heart failure with preserved ejection fraction: a paradigm shift. *Eur Heart J*. 2017; (38): 473–77.
- Wei J, Nelson MD, Szczepaniak EW, et al. Myocardial steatosis as a possible mechanistic link between diastolic dysfunction and coronary microvascular dysfunction in women *Am J Physiol Heart Circ Physiol*. 2016; 310 (1): H14–H11.
- Ponikowski P, Voors AA, Anker SD, et al. 2016 ESC Guidelines for the diagnosis and treatment of acute and chronic heart failure: the task force for the diagnosis and treatment of acute and chronic heart failure of the European Society of Cardiology (ESC) developed with the special contribution of the Heart Failure Association (HFA) of the ESC. *Eur Heart J*. 2016; (37): 2129–200.
- Redfield MM. Heart failure with preserved ejection fraction. *N Engl J Med*. 2016; (375): 1868–77.
- Van Kraijl DJ, van Pol PE, Ruiters AW, et al. Diagnosing diastolic heart failure. *Eur J Heart Fail*. 2002; 4 (4): 419–30.
- Kato S, Saito N, Kirigaya H, et al. Impairment of coronary flow reserve evaluated by phase contrast cine-magnetic resonance imaging in patients with heart failure with preserved ejection

- fraction. *J Am Heart Assoc.* 2016; (5): e002649.
11. Srivaratharajah K, Coutinho T, Liu P, et al. Reduced myocardial flow in heart failure patients with preserved ejection fraction. *Circ Heart Fail.* 2016; 9 (7): e002562.
  12. Isaz K, Bruntz JF, Paris D, et al. Abnormal coronary flow velocity pattern in patients with left ventricular hypertrophy, angina pectoris, and normal coronary arteries: A transesophageal Doppler echocardiographic study. *American Heart Journal.* 1994; 128 (3): 500–10.
  13. Kaski JC, Rosano GMC, Collins P, et al. Cardiac syndrome X: clinical characteristics and left ventricular function. *Journal of the American College of Cardiology.* 1995; (25): 807–14.
  14. Nelson MD, Szczepaniak LS, Weiet J, al. Diastolic Dysfunction in Women With Signs and Symptoms of Ischemia in the Absence of Obstructive Coronary Artery Disease A Hypothesis-Generating Study. *Circ Cardiovasc Imaging.* 2014; (7): 510–6.
  15. Wu Y, Tadamura E, Yamamuro M, et al. Estimation of global and regional cardiac function using 64-slice computed tomography: a comparison study with echocardiography, gated-SPECT and cardiovascular magnetic resonance. *Int J Cardiol.* 2008; 128 (1): 69–76.

## INVESTIGATING A CORRELATION BETWEEN THE LEVELS OF PERIPHERAL BLOOD CYTOKINES AND THE RISK FOR CARDIOVASCULAR COMPLICATIONS IN PATIENTS WITH STAGE II ESSENTIAL HYPERTENSION

Radaeva OA<sup>1</sup>✉, Simbirtsev AS<sup>2</sup>

<sup>1</sup> National Research Mordovia State University, Saransk, Russia

<sup>2</sup> State Research Institute of Highly Pure Biopreparations, FMBA, St. Petersburg, Russia

Essential hypertension (EH) is one of the most common modifiable risk factors for cardiovascular diseases and death. The aim of this study was to investigate a correlation between the levels of some cytokines (interleukins, adhesion molecules, tumor necrosis and growth factors, etc.) in the peripheral blood of patients with stage II EH and the rate of complications (myocardial infarction, acute cerebrovascular events, and transient ischemic attacks) occurring in a 5-year follow-up period. Twenty-eight cytokines were measured using ELISA, including IL1 $\beta$ , IL1 $\alpha$ , IL1ra, IL18, IL18BP, IL37, IL6, sIL6r, LIF, sLIFr, IGF-1, IGFBP-1, TNF $\alpha$ , sTNF-R1, sVCAM-1, IL17, IL2, IL4, IL10, TGF- $\beta$ 1, IL8, CX3CL1, CXCL10, INF $\gamma$ , M-CSF, IL34, VEGF-A, and erythropoietin, and a few vasoactive peptides, including NO, iNOS, eNOS, ADMA, SDMA, Nt-proCNP, and Nt-proBNP, in the peripheral blood samples of 200 patients with stage II EH who had been suffering from this condition for 10 to 14 years and were receiving comparable therapies to bring their blood pressure down. The patients were followed up for 5 years to keep track of complications. The retrospective analysis revealed that the group of patients who developed complications during the 5-year follow-up period exhibited a decline in the levels of IL1ra ( $p < 0.001$ ) and IL10 ( $p < 0.001$ ) and a rise in IL1 $\beta$  ( $p < 0.001$ ), TNF $\alpha$  ( $p < 0.001$ ) and M-CSF ( $p < 0.001$ ) in comparison with the group of those who did not develop any complications. The multivariate Cox regression analysis was applied to the following parameters: IL1 $\beta$  > 18.8 pg/ml; IL1ra < 511 pg/ml; IL6 > 23.8 pg/ml; IL10 < 26.3 pg/ml; 389 pg/ml < M-CSF < 453 pg/ml; ADMA > 0.86  $\mu$ mol/L; total cholesterol > 4.9 mmol/L; LDL > 3.0 mmol/L; HDL in men < 1.0 mmol/L; HDL in women < 1.2 mmol/L. The analysis revealed that M-CSF in the range from 389 to 453 pg/ml ( $p < 0.001$ ) and LDL above 3.0 mmol/L ( $p < 0.01$ ) correlated with an increase in the risk for end-organ damage in stage II EH. Changes in the cytokine levels can be regarded as a predictor of myocardial and cerebral damage in patients with stage II EH. Measurement of peripheral blood M-CSF can be included into the classic risk assessment schemes for the cardiovascular complications in the studied cohort of patients.

**Keywords:** cytokines, essential hypertension, myocardial infarction, stroke, M-CSF

**Author contribution:** Radaeva OA recruited patients, collected blood samples for the study took medical histories, interpreted the study results, and wrote the manuscript. Simbirtsev AS conceived and planned the study, analyzed the obtained data and revised the manuscript.

**Compliance with ethical standards:** the study was approved by the Ethics Committee of Ogariov Mordovian State University (Protocol 12 dated December 12, 2008). All patients gave their informed consent to participate. Blood samples were collected in full compliance with the Declaration of Helsinki (2000) and the Protocol of the Convention on Human Rights and Biomedicine of the Council of Europe (1999).

✉ **Correspondence should be addressed:** Olga A. Radaeva  
Ulianova 26/a, Saransk, 430030; vtlbwbyf\_79@mail.ru

**Received:** 16.07.2018 **Accepted:** 27.02.2019 **Published online:** 06.03.2019

**DOI:** 10.24075/brsmu.2019.006

## АНАЛИЗ КОРРЕЛЯЦИИ СОДЕРЖАНИЯ ЦИТОКИНОВ ПЕРИФЕРИЧЕСКОЙ КРОВИ С РИСКОМ РАЗВИТИЯ СЕРДЕЧНО-СОСУДИСТЫХ ОСЛОЖНЕНИЙ У БОЛЬНЫХ ЭССЕНЦИАЛЬНОЙ АРТЕРИАЛЬНОЙ ГИПЕРТЕНЗИЕЙ II СТАДИИ

О. А. Радаева<sup>1</sup>✉, А. С. Симбирцев<sup>2</sup>

<sup>1</sup> Мордовский государственный университет имени Н. П. Огарева, Саранск, Россия

<sup>2</sup> Государственный научно-исследовательский институт особо чистых биопрепаратов Федерального медико-биологического агентства, Санкт-Петербург, Россия

Эссенциальная артериальная гипертензия (ЭАГ) остается наиболее распространенным модифицируемым фактором риска сердечно-сосудистых заболеваний и смерти. Целью исследования было выявить корреляцию содержания цитокинов (интерлейкинов, молекул адгезии, факторов некроза опухоли, роста и др.) в сыворотке периферической крови и частоты осложнений (инфаркта миокарда, острого нарушения мозгового кровообращения) в последующие 5 лет у больных ЭАГ II стадии. У 200 пациентов с ЭАГ II стадии с длительностью заболевания 10–14 лет, получавших сопоставимую гипотензивную терапию и показавших целевые уровни АД, с помощью ИФА в сыворотке периферической крови определяли содержание 28 цитокинов (IL1 $\beta$ , IL1 $\alpha$ , IL1ra, IL18, IL18BP, IL37, IL6, sIL6r, LIF, sLIFr, IGF-1, IGFBP-1, TNF $\alpha$ , sTNF-R1, sVCAM-1, IL17, IL2, IL4, IL10, TGF- $\beta$ 1, IL8, CX3CL1, CXCL10, INF $\gamma$ , M-CSF, IL34, VEGF-A, эритропоэтина) и vasoактивных пептидов (NO, iNOS, eNOS, ADMA, SDMA, Nt-proCNP, Nt-proBNP). В течение последующих 5 лет фиксировали случаи развития осложнений. Ретроспективный анализ показал, что для группы с развитием осложнений в последующие 5 лет характерно предварительное снижение уровней IL1ra ( $p < 0,001$ ) и IL10 ( $p < 0,001$ ) на фоне повышения содержания IL1 $\beta$  ( $p < 0,001$ ), TNF $\alpha$  ( $p < 0,001$ ) и M-CSF ( $p < 0,001$ ) в сыворотке крови при сравнении с группой без осложнений. Многофакторный анализ с включением в регрессионную модель Кокса ряда показателей: IL1 $\beta$  > 18,8 пг/мл; IL1ra < 511 пг/мл; IL6 > 23,8 пг/мл; IL10 < 26,3 пг/мл; 389 пг/мл < M-CSF < 453 пг/мл; ADMA > 0,86 ммоль/л; общий холестерин > 4,9 ммоль/л; ЛПНП > 3,0 ммоль/л; ЛПВП у мужчин < 1,0 ммоль/л; у женщин < 1,2 ммоль/л выявил независимый характер «влияния» на повышение частоты повреждения органов-мишеней при ЭАГ II стадии следующих показателей: содержания M-CSF в диапазоне 389–453 пг/мл ( $p < 0,001$ ), а также уровня ЛПНП более 3,0 ммоль/л ( $p < 0,01$ ). Изменение уровня цитокинов является патогенетически обоснованным предиктором повреждения миокарда и головного мозга у больных ЭАГ II стадии, а определение уровня M-CSF в крови может дополнить классические схемы расчета риска развития сердечно-сосудистых осложнений у данной категории больных.

**Ключевые слова:** цитокины, эссенциальная артериальная гипертензия, инфаркт миокарда, острое нарушение мозгового кровообращения, колониестимулирующий фактор макрофагов M-CSF

**Информация о вкладе авторов:** О. А. Радаева — набор группы пациентов, забор материала для исследования, сбор данных, интерпретация результатов исследования, написание и компьютерная подготовка рукописи; А. С. Симбирцев — планирование и разработка методологии исследования, анализ данных, редактирование текста.

**Соблюдение этических стандартов:** исследование одобрено этическим комитетом МГУ им. Н. П. Огарева (протокол № 12 от 14 декабря 2008); все пациенты подписали добровольное информированное согласие; получение биологического материала для исследования (кровь) производили с учетом положений Хельсинкской декларации ВМА (2000) и протокола Конвенции Совета Европы о правах человека и биомедицине (1999).

✉ **Для корреспонденции:** Ольга Александровна Радаева  
ул. Ульянова, д. 26а, г. Саранск, 430030; vtlbwbyf\_79@mail.ru

**Статья получена:** 16.07.2018 **Статья принята к печати:** 27.02.2019 **Опубликована онлайн:** 06.03.2019

**DOI:** 10.24075/vrgmu.2019.006

Essential hypertension (EH) is one of the most common modifiable risk factors for cardiovascular diseases and death. According to some estimates, more than 1 billion adults suffer from EH. Their number is expected to have reached 1.5 billion in 2025 [1]. It was long thought that end-organ damage resulted from the increased hydrostatic pressure against blood vessel walls. However, recently a few research studies have been conducted [2–10] into the cytokine pathways in EH complications, including myocardial infarction (MI), acute cerebrovascular events (ACVE), and transient ischemic attacks (TIA), that pose a significant risk of death and morbidity to the working-age population. It is hardly disputable that end-organ damage is the ultimate sequela of chronic inflammation in the presence of elevated blood pressure and atherosclerosis. However, it is still unclear whether certain cytokines have a prognostic potential in the assessment of long-term risks for cardiovascular disorders in patients with stage II EH. The aim of this study was to investigate a correlation between peripheral blood concentrations of some cytokines in patients with stage II EH and the rate of cardiovascular complications (MI, ACVE, TIA) developed during the 5-year observation period.

## METHODS

The study was carried out at the facilities of the Regional Vascular Center of Mordovian Republican Clinical Hospital No. 4, Mordovian Republican Clinical Hospital No. 3 and the Department of Immunology, Microbiology and Virology of Ogariov Mordovian State University in 2013 through 2018. The study recruited 490 participants with stage II EH. Of them, 200 patients were prescribed comparable antihypertensive therapies and then followed up for 5 years. Among them were 100 females and 100 males with the mean age of  $57.5 \pm 1.2$  years at the beginning of the study.

The following inclusion criteria were applied: stage II EH lasting for 10–14 years; working age (females under 60, males under 65); comparable treatment regimens prescribed (monotherapy with ACE inhibitors or ACEIs+ diuretics); informed consent to participate. Patients with comorbidities, type I diabetes mellitus, metabolic syndrome, allergies, autoimmune conditions, secondary hypertension, infections or mental health problems 1 month before the study, alcoholism/drug abuse, and those who refused to participate were excluded from the study. The following cytokines were measured in the peripheral blood samples of 100 female and 100 male patients with stage II EH in order to assess their potential in predicting long-term cardiovascular complications (MI and ACVE): IL1 $\beta$ , IL1 $\alpha$ , IL1ra, IL18, IL18BP, IL37, IL6, sIL6r, LIF, sLIFr, IGF-1, IGFBP-1, TNF $\alpha$ , sTNF-RI, sVCAM-1, IL17, IL2, IL4, IL10, TGF- $\beta$ 1, IL8, CX3CL1, CXCL10, INF $\gamma$ , M-CSF, IL34, VEGF-A, erythropoietin, and a group of vasoactive peptides including NO, iNOS, eNOS, ADMA, SDMA, Nt-proCNP, and Nt-proBNP. These proteins were selected because they are either synthesized by vascular cells or the end organs have receptors recognizing the listed cytokines. Their concentrations were determined using immunoassays. In the 5-year follow-up period, the patients were surveyed on the phone using the original questionnaire; complications (MY, ACVE, TIA) were noted down and later correlated to the patients' medical records.

The obtained data were processed in *Statistica* 8.0 (*StatSoft*; ver 8.0). Normality of data distribution was tested using the one-sample Kolmogorov-Smirnoff test. In this article, the data are presented as an arithmetic mean (M), a standard deviation (SD) and 95% confidence interval for the mean (95% CI) for normal distribution. Student's t-test was used to

compare the main groups. Absolute and relative risks of end-organ damage (MI, ACVE, TIA) were computed, as well as 95% CI for sensitivity (Se) and specificity (Sp). Uni- and multivariate Cox regressions were calculated.

## RESULTS

We correlated the levels of IL1 $\beta$ , IL1 $\alpha$ , IL1ra, IL37, IL18, IL18BP, IL6, sIL6r, LIF, sLIFr, TNF $\alpha$ , sTNF-RI, sVCAM, IL2, IL8, IL4, IL10, INF $\gamma$ , IGF-1, IGFBP-1, M-CSF, IL34, VEGF-A, CX3CL1, CXCL10, TGF $\beta$ 1, IL17A, and erythropoietin in the peripheral blood of 200 patients in treatment for stage II EH who had been suffering from the condition for 10–14 years to the development of cardiovascular complications during the 5-year follow-up period. The retrospective analysis revealed a decline in IL1ra ( $p < 0.001$ ) and IL10 ( $p < 0.001$ ) concentrations and a rise in IL1 $\beta$  ( $p < 0.001$ ), TNF $\alpha$  ( $p < 0.001$ ), and M-CSF ( $p < 0.001$ ) levels in the group of 47 patients who developed cardiovascular complications in the follow-up period, including MI (20 patients), ACVE (14 patients) and TIA (13 patients), as compared to the group of patients who did not develop any long-term complications during the study (Table 1). No significant differences were observed in the average values of other parameters between the groups of patients with and without complications ( $p > 0.05$ ).

Further analysis of interquartile ranges for the patients with EH who developed complications after 6–10 years of observation demonstrated (Table 2) that at IL1ra  $< 513$  pg/ml, the rate of complications over those 5 years increased 2.24 times ( $p < 0.05$ ) reaching 45% (Sp was 83%, Se was 41.7%),  $\chi^2 = 5.25$  ( $p < 0.05$ ),  $C = 0.33$  (a moderate correlation); at IL10  $< 26.3$  pg/ml the risk grew 1.94 times ( $p < 0.05$ ), reaching 31% (Sp 54.9%, Se 66%),  $\chi^2 = 6.26$  ( $p < 0.05$ ),  $C = 0.17$  (a weak correlation); at IL1 $\beta$   $> 18.7$  pg/ml the risk increased 2.37 times ( $p < 0.05$ ) reaching 38% (Sp 59%, Se 80%),  $\chi^2 = 7.59$  ( $p < 0.05$ ),  $C = 0.22$  (a moderate correlation); at IL6  $> 23.8$  the risk grew 1.76 times ( $p < 0.05$ ) reaching 30% (Sp 54%, Se 63.8%),  $\chi^2 = 6.45$  ( $p < 0.05$ ),  $C = 0.17$  (a weak correlation). At M-CSF concentrations in the blood serum ranging from 389 to 453 pg/ml the risk of cardiovascular complications in year 5 and in the next 5 years grew 3.87-fold ( $p < 0.001$ ), as compared to M-CSF concentrations  $< 389$  pg/ml and  $> 453$  pg/ml, reaching 62% (Sp 81.6%, Se 66%),  $\chi^2 = 32.5$  ( $p < 0.001$ ),  $C = 0.6$  (a relatively strong correlation). M-CSF was the most significant risk predictor in comparison with other cytokines. The analysis of interquartile ranges for the patients who developed cardiovascular complications in years 6–10 of the observation did not reveal any significant correlations between TNF $\alpha$  concentrations measured in year 5 and the analyzed risks.

The univariate Cox regression analysis confirmed a reliable correlation between the changes in the peripheral blood cytokine concentrations in patients with stage II EH (IL1 $\beta$   $> 18.8$  pg/ml; IL1ra  $< 511$  pg/ml; IL6  $> 23.8$  pg/ml; IL10  $< 26.3$  pg/ml; 389 pg/ml  $<$  M-CSF  $<$  453 pg/ml) and the risk of cardiovascular disorders during the observation period (Table 3).

The analysis of relationships between all studied parameters and vasoactive peptides (Tables 4, 5) demonstrated that cytokines that could be regarded as potential long-term predictors of cardiovascular complications in patients with stage II EH, namely IL1ra, IL10, IL1 $\beta$ , TNF $\alpha$ , and M-CSF, correlate with the serum levels of asymmetric dimethylarginine (ADMA), a vasoactive peptide. Therefore, when building the pathogenic model, we added ADMA to the list of variables subjected to the multivariate regression analysis to assess the independence of

the revealed risk factors. This has a pathogenic significance and affects the diagnostic and clinical value of the recorded changes. M-CSF concentrations in the blood serum of patients with stage II EH have the strongest correlation with ADMA. The model subjected to the multivariate analysis also included classic risk factors as recommended by the international and Russian guidelines for the risk assessment of complications in patients with hypertension. Based on the results yielded by the multivariate analysis, increased rates of end-organ damage in patients with stage II EH reported during the 5-year observation period correlated with M-CSF levels in the range between 389 and 453 pg/ml ( $p < 0.001$ ) regardless of patients' sex, as well as with the classic risk factor: LDP  $> 3.0$  mmol/L ( $p < 0.01$ ) (Table 6).

## DISCUSSION

Significant correlations have been reported between EH complications, including ACVE and MI, and the peripheral blood concentrations of IL17, IFN $\gamma$ , TNF $\alpha$ , IL6 [2, 11], sTNF-

RI [9], IL1 [12, 13], CXC chemokines [6], LIF [14], IL12 [15], and other cytokines. However, there have been few longitudinal studies of this problem, and only a small range of cytokines has been analyzed. Considering that the literature on the role of cytokines in the pathogenesis of EH is scarce, it is important to study the dynamics of these immunoregulatory factors in patients who develop EH complications and to identify factors that maintain their statistical and pathogenic significance when other cytokines or classic risk factors are introduced into the pathogenic model. We have found that changes in IL1ra, IL10, IL1 $\beta$ , IL6, and M-CSF levels correlate with the development of complications (MI, ACVE, TIA) during a 5-year period. In our study, the increase in the concentrations of anti-inflammatory IL1ra and IL10 correlated with a lower number of complications. Correlations between other analyzed cytokines and the risk for EH complications were not observed. Our findings are not fully consistent with the literature reporting correlations between LIF, IL1 $\alpha$ , etc. and the risk for developing EH complications [10, 14]. This could be due to different inclusion criteria applied in different studies (the sex ratio, age, antihypertensive

**Table 1.** Cytokine levels in patients in treatment for stage II EH who developed cardiovascular complications during the 5-year follow-up period and those who did not have any complications. M ( $\sigma$ )

Cytokine levels (pg/ml)	Patients without complications <i>n</i> = 153	Patients with EH and complications <i>n</i> = 47
IL1 $\beta$	14.2 (4.42)	21.3 (3.32)*no complications
IL1 $\alpha$ (f)	12.6 (3.21)	13.2 (2.91)
IL1ra	650 (112)	496 (93)*no complications
IL18	360 (64)	393 (87)
IL18BP	6790 (1170)	6440(1620)
IL6	21.7 (4.94)	24.9 (4.41) <sup>^</sup> no complications
sIL6r	1889 (323)	1733 (312)
TNF $\alpha$	20.2 (4.47)	26.6 (4.5)*no complications
sTNF-RI	2598 (680)	2873 (699)
sVCAM-1	577 (101)	591 (90)
IL2	10.6 (3.16)	10.9 (3.02)
IL8	28.7 (6.74)	30.6 (7.16)
IL4	19.8 (4.11)	20.8 (4.05)
IL10	29.3 (6.99)	23.8 (7.17)*no complications
IFN $\gamma$	18.4 (4.18)	18.1 (4.39)
IL37	93.2 (26.9)	90.1 (24.2)
IL17A	2.5 (0.56)	2.46 (0.49)
LIF (females)	7.28 (2.78)	7.76 (2.63)
sLIFr (females)	40500 (1120)	42100 (1600)
IGF-1	116000 (32300)	122000 (30800)
M-CSF	352 (88)	456 (69)*no complications
IL34	133 (40)	137 (36)
VEGF-A	339 (101)	344 (95)
CX3CL1	510 (105)	542 (120)
CXCL10	17.8 (4.33)	18.9 (3.92)
TGF $\beta$ 1	21.8 (4.57)	22.1 (4.24)
Neopterin	8.81 (3.19)	8.23 (2.8)
Erythropoietin	11.4 (3.64)	16.6 (3.12)*no complications

**Note:** <sup>^</sup> —  $p < 0.01$ ; \* —  $p < 0.001$  in comparison with patients without complications reported in the 5-year follow-up period.

treatment, normalized blood pressure, etc) and indicates the high significance of the observational group homogeneity, which affects the pathogenic significance of the obtained data. Importantly, our study shows that only cytokines correlating with ADMA levels can be regarded as potential predictors of end-organ damage in patients undergoing treatment against stage II EH and suffering from the pathology for 10–14 years. ADMA is a methylated analog of L-arginine (a substrate for NO

synthesis) that competitively inhibits the functional activity of eNOS [16], curbing the NO synthesis and leading to its poor availability for vasorelaxation and vasoprotection [17]. This pathogenic pathway is important: the role of ADMA and SDMA in pathology is currently in the focus of scientific research. This study established that M-CSF was the only independent criterium (from the entire spectrum of the analyzed parameters) that had a high predictive value (even when compared to

**Table 2.** The relationship between changes in IL1ra, IL1β, IL6, TNFα, M-CSF, and IL10 concentrations measured at the beginning of the study AND the rate of complications (95% CI) during the 5-year follow-up period in patients in treatment for long-settled EH

	Quartile I <i>n</i> = 50	Quartile II <i>n</i> = 50	Quartile III <i>n</i> = 50	Quartile VI <i>n</i> = 50
IL1ra	(330–511)	(512–575)	(574–633)	(634–820)
Complications (number of patients)	18	9	10	10
Absolute risk (%)	36 [22.7–49.3]	18 [7.35–28.6]	20 [8.91–31]	20 [8.91–31]
Risk ratio	36 [22.7–49.3] 19.3 [13–25.6]			
Risk ratio	Quartiles I / II + III + IV: 1.86 [1.13–3.05]*			
IL1β	(2.95–14.8)	(14.9–8.7)	(18.8–22.5)	(22.6–34.4)
Complications (number of patients)	1	8	18	20
Absolute risk (%)	2 [2.43–4.43]	16 [5.84–26.2]	36 [22.7–49.3]	40 [26.4–53.6]
Risk ratio	38 [28.5–47.5]			
Risk ratio	Quartiles II / III + IV: 2.37 [1.2 – 4.7]*			
Risk ratio	Quartiles I / II + III + IV: 1.86 [1.13–3.05]*			
IL6	(12.5–20.8)	(20.9–23.7)	(23.8–27.5)	(27.6–36.4)
Complications (number of patients)	8	9	14	16
Absolute risk (%)	16 [5.8–26]	18 [7.35–28.6]	28 [15.6–40]	32 [19–45]
Risk ratio	17 [8–22.1] 30 [21–39]			
Risk ratio	Quartiles I + II / III + IV: 1.76 [1.04 – 2.99]*			
TNFα	(10.3–18.3)	(18.6–23.7)	(21.4–24)	(24.1–32.4)
Complications (number of patients)	10	13	12	12
Absolute risk (%)	20 [8.9–31]	26 [13.8–38]	24 [12.2–35.8]	24 [12.2–35.8]
Risk ratio	Quartiles I / II: 1.3 [0.63–2.69]		Quartiles II / III + IV: 0.92 [1.04–1.65]	
M-CSF	(138–319)	(320–388)	(389–453)	(454–640)
Complications (number of patients)	0	7	31	9
Absolute risk (%)	0	14 [4.42–23.6]	62 [48.5–55.4]	18 [7.55–28.6]
Risk ratio	Quartiles II + IV / III: 3.87 [2.35–6.38]* Quartiles II/IV = 1.28 [0.52–3.18]			
IL10	(5.1–19.9)	(20–26.2)	(26.3–31.5)	(31.6–47.5)
Complications (number of patients)	15	16	8	8
Absolute risk (%)	30 [19–45]	32 [15.6–40]	16 [5.84–26.2]	16 [5.84–26.2]
Risk ratio	31 [22–40] 16 [5.84–26.2]			
Risk ratio	Quartiles I + II / III + IV: 1.94 [1.13–3.31]*			

Note: \* — *p* < 0.05 for the comparison of absolute risks if the interval does not include 1.

**Table 3.** Correlations between IL1β, IL1ra, IL6, IL10, and M-CSF concentrations AND the rate of cardiovascular complications (95% CI) during the 5-year observation period in patients with stage II EH. The univariate Cox regression

Variables	Beta	Standard	t-value	Exponent Beta	<i>p</i>
IL1β (> 18.8 pg/ml)	1.99	0.35	5.68	2.37	0.006
IL1ra (< 511 pg/ml)	1.24	0.28	4.43	2.06	0.009
IL6 (> 23.8 pg/ml)	1.27	0.35	3.62	1.89	0.042
IL10 (< 26.3 pg/ml)	1.22	0.27	4.52	1.91	0.007
M-CSF (389–453) pg/ml	2.44	0.25	9.76	3.89	0.0004

Note: in our Cox regression models, Beta is a regression coefficient; Standard is a standard error of the regression coefficient; t-value is the t-statistic; Exponent Beta is the value of the relative risk indicating a connection with the range of changes in the analyzed factor; *p* shows statistical significance.

ADMA and classic risk factors) in the assessment of risks for developing ACVE, MI and TIA in patients undergoing treatment for stage II EH who had been suffering from this condition for 10 to 14 years. This confirms the priority of the cytokine in the M-CSF-ADMA correlational pathogenic model with a subsequent cascade of reactions causing progression of the pathology. Earlier, we published an article demonstrating a direct correlation between M-CSF concentrations > 453 pg/ml and the levels of VEGF-A in the peripheral blood, which was consistent with a significant increase in the myocardial collateral blood flow (coronary angiography) and might explain a low rate of MI in the studied cohort of patients [18], affecting the total risk for cardiovascular complications. M-CSF can activate MAP-kinases via the M-CSFR-1 receptor; the kinases

play a key role in the production of VEGF-A by activating ERK, increasing the p38 and JNK promoter activity and stabilizing VEGF-A mRNA in a dose-dependent pattern [19].

CONCLUSIONS

The data yielded by this study prove that changes in the cytokine concentrations (IL1β > 18.8 pg/ml, IL1ra < 511 pg/ml, IL6 > 23.8 pg/ml, IL10 < 26.3 pg/ml) measured in the peripheral blood of patients suffering from stage II EH for 10 to 14 years and undergoing antihypertensive treatment correlate with a 5-year rate of cardiovascular complications (MI, ACVE, TIA). Only M-CSF at concentrations between 389 and 453 pg/ml can be regarded as a predictor of cardiac and cerebrovascular

**Table 4.** A correlation matrix for the cytokines in the peripheral blood of patients in treatment for stage II EH and the vasoactive peptides measured in the same patients

	IL37	LIF	sLIFr	IGF-1	IGFBP-1	M-CSF	IL34	VEGF-A	CX3CL1	CXCL10	TGFB1	IL17A	Erythropoietin
AT II	-0.28 <i>p</i> > 0.05	0.51 <i>p</i> < 0.05	-0.36 <i>p</i> > 0.05	0.23 <i>p</i> > 0.05	0.23 <i>p</i> > 0.05	0.34 <i>p</i> > 0.05	0.24 <i>p</i> > 0.05	0.29 <i>p</i> > 0.05	0.12 <i>p</i> > 0.05	0.31 <i>p</i> > 0.05	0.23 <i>p</i> > 0.05	0.21 <i>p</i> > 0.05	0.23 <i>p</i> > 0.05
ET-1	-0.41 <i>p</i> > 0.05	0.31 <i>p</i> > 0.05	0.28 <i>p</i> > 0.05	0.21 <i>p</i> > 0.05	0.22 <i>p</i> > 0.05	0.43 <i>p</i> > 0.05	0.21 <i>p</i> > 0.05	0.42 <i>p</i> > 0.05	0.27 <i>p</i> > 0.05	0.35 <i>p</i> > 0.05	0.31 <i>p</i> > 0.05	0.23 <i>p</i> > 0.05	0.32 <i>p</i> > 0.05
NO	0.69 <i>p</i> < 0.05	0.42 <i>p</i> > 0.05	0.41 <i>p</i> > 0.05	0.23 <i>p</i> > 0.05	0.18 <i>p</i> > 0.05	0.32 <i>p</i> > 0.05	0.31 <i>p</i> > 0.05	0.34 <i>p</i> > 0.05	0.31 <i>p</i> > 0.05	0.39 <i>p</i> > 0.05	0.48 <i>p</i> > 0.05	0.21 <i>p</i> > 0.05	0.23 <i>p</i> > 0.05
ADMA	-0.32 <i>p</i> > 0.05	0.33 <i>p</i> > 0.05	0.49 <i>p</i> > 0.05	0.28 <i>p</i> > 0.05	0.45 <i>p</i> > 0.05	0.58 <i>p</i> < 0.05	0.24 <i>p</i> > 0.05	0.28 <i>p</i> > 0.05	0.22 <i>p</i> > 0.05	0.15 <i>p</i> > 0.05	0.34 <i>p</i> > 0.05	0.31 <i>p</i> > 0.05	0.32 <i>p</i> > 0.05
SDMA	-0.78 <i>p</i> < 0.001	0.28 <i>p</i> > 0.05	0.45 <i>p</i> > 0.05	0.38 <i>p</i> > 0.05	0.27 <i>p</i> > 0.05	0.52 <i>p</i> < 0.05	0.41 <i>p</i> > 0.05	0.31 <i>p</i> > 0.05	0.52 <i>p</i> < 0.05	0.5 <i>p</i> < 0.05	0.26 <i>p</i> > 0.05	0.31 <i>p</i> > 0.05	0.21 <i>p</i> > 0.05
eNOS	0.32 <i>p</i> > 0.05	0.38 <i>p</i> > 0.05	-0.39 <i>p</i> > 0.05	0.21 <i>p</i> > 0.05	0.34 <i>p</i> > 0.05	0.31 <i>p</i> > 0.05	0.24 <i>p</i> > 0.05	0.11 <i>p</i> > 0.05	-0.18 <i>p</i> > 0.05	-0.31 <i>p</i> > 0.05	0.23 <i>p</i> > 0.05	0.32 <i>p</i> > 0.05	0.34 <i>p</i> > 0.05
iNOS	-0.41 <i>p</i> > 0.05	0.28 <i>p</i> > 0.05	0.45 <i>p</i> > 0.05	0.34 <i>p</i> > 0.05	0.38 <i>p</i> > 0.05	0.17 <i>p</i> > 0.05	0.21 <i>p</i> > 0.05	0.21 <i>p</i> > 0.05	0.69 <i>p</i> < 0.01	0.71 <i>p</i> < 0.01	0.34 <i>p</i> > 0.05	0.21 <i>p</i> > 0.05	0.21 <i>p</i> > 0.05
NT-proCNP	-0.27 <i>p</i> > 0.05	0.41 <i>p</i> > 0.05	-0.28 <i>p</i> > 0.05	0.27 <i>p</i> > 0.05	0.37 <i>p</i> > 0.05	0.41 <i>p</i> > 0.05	0.25 <i>p</i> > 0.05	0.32 <i>p</i> > 0.05	-0.31 <i>p</i> > 0.05	-0.27 <i>p</i> > 0.05	0.52 <i>p</i> < 0.05	0.23 <i>p</i> > 0.05	0.24 <i>p</i> > 0.05
NT-proBNP	-0.78 <i>p</i> < 0.01	-0.65 <i>p</i> < 0.05	0.31 <i>p</i> > 0.05	0.31 <i>p</i> > 0.05	0.24 <i>p</i> > 0.05	0.45 <i>p</i> > 0.05	0.18 <i>p</i> > 0.05	0.34 <i>p</i> > 0.05	0.21 <i>p</i> > 0.05	0.2 <i>p</i> > 0.05	0.33 <i>p</i> > 0.05	0.27 <i>p</i> > 0.05	0.12 <i>p</i> > 0.05

**Note:** the data are presented as a coefficient of multiple correlation; the minus symbol indicates that the established correlation is negative; *p* shows the significance of differences.

**Table 5.** A correlation matrix for the cytokines in the peripheral blood of patients in treatment for stage II EH and the vasoactive peptides measured in the same patients

	IL1β	IL1α	IL1ra	IL18	IL18BP	IL6	sIL6r	TNFα	sTNF-RI	sVCAM-1	IL2	IL8	IL4	IL10	IFNy
AT II	0.41 <i>p</i> > 0.05	0.34 <i>p</i> > 0.05	-0.19 <i>p</i> > 0.05	0.41 <i>p</i> > 0.05	-0.23 <i>p</i> > 0.05	0.43 <i>p</i> > 0.05	0.33 <i>p</i> > 0.05	0.41 <i>p</i> > 0.05	0.22 <i>p</i> > 0.05	0.21 <i>p</i> > 0.05	0.18 <i>p</i> > 0.05	0.37 <i>p</i> > 0.05	0.22 <i>p</i> > 0.05	-0.62 <i>p</i> < 0.05	0.16 <i>p</i> > 0.05
ET-1	0.68 <i>p</i> < 0.05	0.65 <i>p</i> < 0.05	-0.62 <i>p</i> < 0.05	0.34 <i>p</i> > 0.05	-0.36 <i>p</i> > 0.05	0.27 <i>p</i> > 0.05	0.41 <i>p</i> > 0.05	0.36 <i>p</i> > 0.05	0.24 <i>p</i> > 0.05	0.31 <i>p</i> > 0.05	0.25 <i>p</i> > 0.05	0.69 <i>p</i> < 0.01	0.24 <i>p</i> > 0.05	-0.36 <i>p</i> > 0.05	0.18 <i>p</i> > 0.05
NO	0.64 <i>p</i> < 0.05	0.46 <i>p</i> > 0.05	0.49 <i>p</i> < 0.05	-0.27 <i>p</i> > 0.05	0.64 <i>p</i> < 0.05	0.49 <i>p</i> > 0.05	0.33 <i>p</i> > 0.05	0.44 <i>p</i> > 0.05	-0.38 <i>p</i> > 0.05	0.25 <i>p</i> > 0.05	0.37 <i>p</i> > 0.05	-0.41 <i>p</i> > 0.05	-0.38 <i>p</i> > 0.05	0.33 <i>p</i> > 0.05	0.41 <i>p</i> > 0.05
ADMA	0.52 <i>p</i> < 0.05	0.4 <i>p</i> > 0.05	-0.58 <i>p</i> < 0.05	0.36 <i>p</i> > 0.05	-0.41 <i>p</i> > 0.05	0.57 <i>p</i> < 0.05	0.25 <i>p</i> > 0.05	0.38 <i>p</i> > 0.05	0.31 <i>p</i> > 0.05	0.38 <i>p</i> > 0.05	0.33 <i>p</i> > 0.05	0.27 <i>p</i> > 0.05	0.31 <i>p</i> > 0.05	-0.55 <i>p</i> < 0.05	0.24 <i>p</i> > 0.05
SDMA	0.34 <i>p</i> > 0.05	0.29 <i>p</i> > 0.05	-0.16 <i>p</i> > 0.05	0.48 <i>p</i> > 0.05	-0.71 <i>p</i> < 0.01	0.29 <i>p</i> > 0.05	0.23 <i>p</i> > 0.05	0.26 <i>p</i> > 0.05	0.25 <i>p</i> > 0.05	0.43 <i>p</i> > 0.05	0.72 <i>p</i> < 0.01	0.53 <i>p</i> < 0.05	0.25 <i>p</i> > 0.05	-0.23 <i>p</i> > 0.05	0.58 <i>p</i> < 0.05
eNOS	-0.62 <i>p</i> < 0.05	-0.67 <i>p</i> < 0.05	0.51 <i>p</i> < 0.05	0.22 <i>p</i> > 0.05	0.37 <i>p</i> > 0.05	-0.22 <i>p</i> > 0.05	-0.35 <i>p</i> > 0.05	0.4 <i>p</i> > 0.05	0.27 <i>p</i> > 0.05	0.31 <i>p</i> > 0.05	-0.13 <i>p</i> > 0.05	-0.31 <i>p</i> > 0.05	0.27 <i>p</i> > 0.05	0.46 <i>p</i> > 0.05	-0.19 <i>p</i> > 0.05
iNOS	0.78 <i>p</i> < 0.01	0.49 <i>p</i> > 0.05	-0.12 <i>p</i> > 0.05	0.36 <i>p</i> > 0.05	-0.39 <i>p</i> > 0.05	0.68 <i>p</i> < 0.05	0.56 <i>p</i> < 0.05	0.42 <i>p</i> > 0.05	0.41 <i>p</i> > 0.05	0.41 <i>p</i> > 0.05	0.62 <i>p</i> < 0.05	0.42 <i>p</i> > 0.05	0.41 <i>p</i> > 0.05	-0.4 <i>p</i> > 0.05	0.52 <i>p</i> < 0.05
NT-proCNP	-0.58 <i>p</i> < 0.05	0.68 <i>p</i> < 0.05	0.13 <i>p</i> > 0.05	0.31 <i>p</i> > 0.05	-0.37 <i>p</i> > 0.05	-0.61 <i>p</i> < 0.05	0.24 <i>p</i> > 0.05	0.52 <i>p</i> < 0.05	0.39 <i>p</i> > 0.05	0.24 <i>p</i> > 0.05	-0.74 <i>p</i> < 0.01	-0.37 <i>p</i> > 0.05	0.39 <i>p</i> > 0.05	0.29 <i>p</i> > 0.05	-0.64 <i>p</i> < 0.05
NT-proBNP	0.47 <i>p</i> > 0.05	0.29 <i>p</i> > 0.05	-0.31 <i>p</i> > 0.05	0.14 <i>p</i> > 0.05	-0.73 <i>p</i> < 0.01	0.17 <i>p</i> > 0.05	-0.12 <i>p</i> > 0.05	0.51 <i>p</i> < 0.05	0.24 <i>p</i> > 0.05	0.32 <i>p</i> > 0.05	0.32 <i>p</i> > 0.05	0.21 <i>p</i> > 0.05	0.24 <i>p</i> > 0.05	-0.22 <i>p</i> > 0.05	0.32 <i>p</i> > 0.05

**Note:** the data are presented as a coefficient of multiple correlation; the minus symbol indicates that the established correlation is negative; *p* shows the significance of differences.

**Table 6.** Correlations between IL1 $\beta$ , IL1ra, IL6, IL10, M-CSF, ADMA concentrations and classic risk factors AND the rate of cardiovascular complications (95% CI) in a 5-year observation period in patients with stage II EH; the table shows the Cox regression model; the multivariate analysis was applied

Variables	Beta	Standard	t-value	Exponent Beta	p
IL1 $\beta$ (> 18.8 pg/ml)	1.19	0.73	1.63	2.05	0.058
IL1ra (< 511 pg/ml)	1.04	0.62	1.67	1.34	0.067
IL6 (> 23.8 pg/ml)	1.07	0.63	1.69	2.17	0.062
IL10 (< 26.3 pg/ml)	1.06	0.66	1.61	1.32	0.072
M-CSF (389–453) pg/ml	2.17	0.34	6.38	2.53	0.0007
ADMA (> 0.86 $\mu$ mol/l)	1.49	0.77	1.93	2.09	0.068
Total cholesterol > 4.9 mmol/l	1.18	0.73	1.62	1.63	0.062
LDL > 3.0 mmol/l	1.88	0.43	4.37	2.28	0.004
HDL in men < 1.0 mmol/l. in women < 1.2 mmol/l	1.12/1.19	0.71/0.68	1.58	1.38/1.32	0.071/0.069

**Note:** in our Cox regression models, Beta is a regression coefficient; Standard is a standard error of the regression coefficient; t-value is the t-statistic; Exponent Beta is the value of the relative risk indicating a connection with the range of changes in the analyzed factor; p shows statistical significance.

complications. Although the obtained data have a theoretical significance, M-CSF concentrations in the range from 389 to 453 pg/ml are a highly specific (81%) but lowly sensitive (66%) parameter in terms of predicting MI, ACVE and TIA in the studied cohort of patients. This means that an additional criterium should

be added to the model to improve the diagnostic (prognostic) value of this cytokine. The role of patients' individual characteristics, such as genetic components including CSF1R TC/CA rs386693509: TC/CA variants in the established correlations should be further studied in patients with the prodigious disease.

## References

- Wenzel U, Turner JE, Krebs C, et al. Immune Mechanisms in Arterial Hypertension. *J Am Soc Nephrol.* 2016; 27 (3): 677–86.
- McMaster WG, Kirabo A, Madhur MS, Harrison DG. Inflammation, immunity, and hypertensive end organ damage. *Circ Res.* 2015; 116 (6): 1022–33.
- Bennardo M, Alibhai F, Tsimakouridze E, et al. Day-night dependence of gene expression and inflammatory responses in the remodeling murine heart post-myocardial. *Am J Physiol Regul Integr Comp Physiol.* 2016; 311 (6): 1243–54.
- Ji Q, Cheng G, Ma N, et al. Circulating Th1, Th2, and Th17 Levels in Hypertensive Patients. *Dis Markers* 2017; (2017): 7146290. Available from: <https://www.hindawi.com/journals/dm/2017/7146290>. PubMed PMID: 28757677.
- Nosalski R, McGinnigle E, Siedlinski M, Guzik TJ. Novel Immune Mechanisms in Hypertension and Cardiovascular Risk. *Current Cardiovascular Risk Reports.* 2017; 11 (4): 12. Available from: [https://www.researchgate.net/publication/314274524\\_Novel\\_Immune\\_Mechanisms\\_in\\_Hypertension\\_and\\_Cardiovascular\\_Risk](https://www.researchgate.net/publication/314274524_Novel_Immune_Mechanisms_in_Hypertension_and_Cardiovascular_Risk).
- Rudemiller NP, Crowley SD. The role of chemokines in hypertension and consequent target organ damage. *Pharmacological research.* 2017; (119): 404–11.
- Schwanekamp JA, Lorts A, Sargent MA, et al. TGFBI functions similar to periostin but is uniquely dispensable during cardiac injury. *PLoS ONE.* 2017; 12 (7). Available from: <https://journals.plos.org/plosone/article?id=10.1371/journal.pone.0181945>.
- Wang P, He Q, Liu C, et al. Functional polymorphism rs3783553 in the 3'-untranslated region of IL-1A increased the risk of ischemic stroke: A case-control study. *Medicine.* 2016; 96 (46). Available from: [https://www.researchgate.net/publication/320348816\\_4-bp\\_insertiondeletion\\_rs3783553\\_polymorphism\\_within\\_the\\_3aposUTR\\_of\\_IL1A\\_contributes\\_to\\_the\\_risk\\_of\\_prostate\\_cancer\\_in\\_a\\_sample\\_of\\_Iranian\\_Population](https://www.researchgate.net/publication/320348816_4-bp_insertiondeletion_rs3783553_polymorphism_within_the_3aposUTR_of_IL1A_contributes_to_the_risk_of_prostate_cancer_in_a_sample_of_Iranian_Population).
- Carlsson AC, Jansson JH, Söderberg S, et al. Levels of soluble tumor necrosis factor receptor 1 and 2, gender, and risk of myocardial infarction in Northern Sweden. *Atherosclerosis.* 2018; (272): 41–6.
- Huang S, Frangogiannis NG. Anti-inflammatory therapies in myocardial infarction: failures, hopes and challenges. *Br J Pharmacol.* 2018; 175 (9): 1377–400.
- Itani HA, Harrison DG. Memories that last in hypertension. *Am J Physiol Renal Physiol.* 2015; 308 (11): F1197–F1199. DOI: 10.1152/ajprenal.00633.2014.
- Rucker JA, Crowley SD. The role of macrophages in hypertension and its complications. *Pflugers Arch.* 2017; 469 (3–4): 419–30.
- Hartman MHT, Groot HE, et al. Translational overview of cytokine inhibition in acute myocardial infarction and chronic heart failure. *Trends Cardiovasc Med.* 2018; 28 (6). DOI: 10.1016/j.tcm.2018.02.003. Available from: [https://www.researchgate.net/publication/260757993\\_Heart\\_Failure](https://www.researchgate.net/publication/260757993_Heart_Failure).
- Jia D, Cai M, XiY, et al. Interval exercise training increases LIF expression and prevents myocardial infarction-induced skeletal muscle atrophy in rats. *Life Sci.* 2018; (193): 77–86.
- Van der Heijden T, Bot I, Kuiper J. The IL-12 cytokine family in cardiovascular diseases. *Cytokine.* 2017; S1043-4666(17)30315-0. DOI: 10.1016/j.cyto.2017.10.010.
- Papageorgiou N, Androulakis E, Papaioannou S, et al. Homoarginine in the shadow of asymmetric dimethylarginine: from nitric oxide to cardiovascular disease. *Amino Acids.* 2015; 47 (9): 1741–50.
- Shin S, Thapa SK, Fung H-L. Cellular interactions between L-arginine and asymmetric dimethylarginine: Transport and metabolism. *PLoS One.* 2017; 12 (5): e0178710. DOI: 10.1371/journal.pone.0178710.
- Radaeva OA, Simbirtsev AS. M-CSF, IL-34, VEGF-A kak faktory riska razvitiya infarkta miokarda, ostrogo narusheniya mozgovogo krovoobrashheniya u bol'nyh jessencial'noj arterial'noj gipertenziej. *Rossiiskij immunologicheskij zhurnal.* 2015; 9 (1): 93–101.
- Lee S, Shi XQ, Fan A et al. Targeting macrophage and microglia activation with colony stimulating factor 1 receptor inhibitor is an effective strategy to treat injury-triggered neuropathic pain. *Mol Pain.* 2018; (14): 1744806918764979. DOI: 10.1177/1744806918764979.

## Литература

- Wenzel U, Turner JE, Krebs C, et al. Immune Mechanisms in Arterial Hypertension. *J Am Soc Nephrol.* 2016; 27 (3): 677–86.
- McMaster WG, Kirabo A, Madhur MS, Harrison DG. Inflammation, immunity, and hypertensive end organ damage. *Circ Res.* 2015;

- 116 (6): 1022–33.
3. Bennardo M, Alibhai F, Tsimakouridze E, et al. Day-night dependence of gene expression and inflammatory responses in the remodeling murine heart post-myocardial. *Am J Physiol Regul Integr Comp Physiol.* 2016; 311 (6): 1243–54.
  4. Ji Q, Cheng G, Ma N, et al. Circulating Th1, Th2, and Th17 Levels in Hypertensive Patients. *Dis Markers* 2017; (2017): 7146290. Available from: <https://www.hindawi.com/journals/dm/2017/7146290>. PubMed PMID: 28757677.
  5. Nosalski R, McGinnigle E, Siedlinski M, Guzik TJ. Novel Immune Mechanisms in Hypertension and Cardiovascular Risk. *Current Cardiovascular Risk Reports.* 2017; 11 (4): 12. Available from: [https://www.researchgate.net/publication/314274524\\_Novel\\_Immune\\_Mechanisms\\_in\\_Hypertension\\_and\\_Cardiovascular\\_Risk](https://www.researchgate.net/publication/314274524_Novel_Immune_Mechanisms_in_Hypertension_and_Cardiovascular_Risk).
  6. Rudemiller NP, Crowley SD. The role of chemokines in hypertension and consequent target organ damage. *Pharmacological research.* 2017; (119): 404–11.
  7. Schwanekamp JA, Lorts A, Sargent MA, et al. TGFBI functions similar to periostin but is uniquely dispensable during cardiac injury. *PLoS ONE.* 2017; 12 (7). Available from: <https://journals.plos.org/plosone/article?id=10.1371/journal.pone.0181945>.
  8. Wang P, He Q, Liu C, et al. Functional polymorphism rs3783553 in the 3'-untranslated region of IL-1A increased the risk of ischemic stroke: A case-control study. *Medicine.* 2016; 96 (46). Available from: [https://www.researchgate.net/publication/320348816\\_4-bp\\_insertiondeletion\\_rs3783553\\_polymorphism\\_within\\_the\\_3aposUTR\\_of\\_IL1A\\_contributes\\_to\\_the\\_risk\\_of\\_prostate\\_cancer\\_in\\_a\\_sample\\_of\\_Iranian\\_Population](https://www.researchgate.net/publication/320348816_4-bp_insertiondeletion_rs3783553_polymorphism_within_the_3aposUTR_of_IL1A_contributes_to_the_risk_of_prostate_cancer_in_a_sample_of_Iranian_Population).
  9. Carlsson AC, Jansson JH, Söderberg S, et al. Levels of soluble tumor necrosis factor receptor 1 and 2, gender, and risk of myocardial infarction in Northern Sweden. *Atherosclerosis.* 2018; (272): 41–6.
  10. Huang S, Frangogiannis NG. Anti-inflammatory therapies in myocardial infarction: failures, hopes and challenges. *Br J Pharmacol.* 2018; 175 (9): 1377–400.
  11. Itani HA, Harrison DG. Memories that last in hypertension. *Am J Physiol Renal Physiol.* 2015; 308 (11): F1197–F1199. DOI: 10.1152/ajprenal.00633.2014.
  12. Rucker JA, Crowley SD. The role of macrophages in hypertension and its complications *Pflugers Arch.* 2017; 469 (3–4): 419–30.
  13. Hartman MHT, Groot HE, et al. Translational overview of cytokine inhibition in acute myocardial infarction and chronic heart failure. *Trends Cardiovasc Med.* 2018; 28 (6). DOI: 10.1016/j.tcm.2018.02.003. Available from: [https://www.researchgate.net/publication/260757993\\_Heart\\_Failure](https://www.researchgate.net/publication/260757993_Heart_Failure).
  14. Jia D, Cai M, XiY, et al. Interval exercise training increases LIF expression and prevents myocardial infarction-induced skeletal muscle atrophy in rats. *Life Sci.* 2018; (193): 77–86.
  15. Van der Heijden T, Bot I, Kuiper J. The IL-12 cytokine family in cardiovascular diseases. *Cytokine.* 2017; S1043-4666(17)30315-0. DOI: 10.1016/j.cyto.2017.10.010.
  16. Papageorgiou N, Androulakis E, Papaioannou S, et al. Homoarginine in the shadow of asymmetric dimethylarginine: from nitric oxide to cardiovascular disease. *Amino Acids.* 2015; 47 (9): 1741–50.
  17. Shin S, Thapa SK, Fung H-L. Cellular interactions between L-arginine and asymmetric dimethylarginine: Transport and metabolism. *PLoS One.* 2017; 12 (5): e0178710. DOI: 10.1371/journal.pone.0178710.
  18. Радаева О. А., Симбирцев А. С. М-CSF, IL-34, VEGF-A как факторы риска развития инфаркта миокарда, острого нарушения мозгового кровообращения у больных эссенциальной артериальной гипертензией. *Российский иммунологический журнал.* 2015; 9 (1): 93–101.
  19. Lee S, Shi XQ, Fan A et al. Targeting macrophage and microglia activation with colony stimulating factor 1 receptor inhibitor is an effective strategy to treat injury-triggered neuropathic pain. *Mol Pain.* 2018; (14): 1744806918764979. DOI: 10.1177/1744806918764979.

## COMBINATION OF RIBOSOME AND PHAGE DISPLAY FOR FAST SELECTION OF HIGH AFFINITY VHH ANTIBODY FRAGMENTS

Kravchenko YE, Ivanov SV, Kravchenko DS, Frolova EI, Chumakov SP ✉

Shemyakin-Ovchinnikov Institute of Bioorganic Chemistry, Moscow, Russia

Selection of antibodies using phage display involves the preliminary cloning of the repertoire of sequences encoding antigen-binding domains into phagemid, which is considered the bottleneck of the method, limiting the resulting diversity of libraries and leading to the loss of poorly represented variants before the start of the selection procedure. Selection in cell-free conditions using a ribosomal display is devoid of this drawback, however is highly sensitive to PCR artifacts and the RNase contamination. The aim of the study was to test the efficiency of a combination of both methods, including pre-selection in a cell-free system to enrich the source library, followed by cloning and final selection using phage display. This approach may eliminate the shortcomings of each method and increase the efficiency of selection. For selection, alpaca VHH antibody sequences suitable for building an immune library were used due to the lack of VL domains. Analysis of immune libraries from the genes of the VH3, VHH3 and VH4 families showed that the VHH antibodies share in the VH3 and VH4 gene groups is insignificant, and selection from the combined library is less effective than from the VHH3 family of sequences. We found that the combination of ribosomal and phage displays leads to a higher enrichment of high-affinity fragments and avoids the loss of the original diversity during cloning. The combined method allowed us to obtain a greater number of different high-affinity sequences, and all the tested VHH fragments were able to specifically recognize the target, including the total protein extracts of cell cultures.

**Keywords:** nanobodies, VHH antibodies, ribosome display, phage display, biopanning, PDLIM4

**Funding:** the work was funded by MESR, project code RFMEFI60716X0156.

**Author contribution:** Kravchenko YuE — Alpaca blood collection and processing, RNA extraction, ELISA; Ivanov SV — construction of libraries of VHH-fragments of antibodies, selection by phage display; Kravchenko DS — protein purification, experiments with eucaryotic cell cultures; Frolova EI — research planning, animal immunization, manuscript editing; Chumakov SP — research planning, selection by ribosome display, analysis of the results, writing a manuscript.

**Compliance with ethical standards:** the work with animals was carried out in accordance with the principles and requirements of the International Animal Care Laboratory and the Council of Europe Directive (86/609 / EEC) of November 24, 1986.

✉ **Correspondence should be addressed:** Stepan P. Chumakov  
Miklukho-Maklaya, 16/10, Moscow, 117997; hathkul@gmail.com

**Received:** 08.12.2018 **Accepted:** 22.12.2018 **Published online:** 24.02.2019

**DOI:** 10.24075/brsmu.2019.002

## ИСПОЛЬЗОВАНИЕ КОМБИНАЦИИ РИБОСОМНОГО И ФАГОВОГО ДИСПЛЕЕВ ДЛЯ БЫСТРОГО ОТБОРА ВЫСОКОАФФИННЫХ VHH-ФРАГМЕНТОВ АНТИТЕЛ АЛЬПАК

Ю. Е. Кравченко, С. В. Иванов, Д. С. Кравченко, Е. И. Фролова, С. П. Чумаков ✉

Институт биоорганической химии имени М. М. Шемякина и Ю. А. Овчинникова, Москва, Россия

Селекция антител с помощью фагового дисплея предполагает предварительное клонирование репертуара последовательностей, кодирующих антигенсвязывающие участки, в фагмиду, что считается «бутылочным горлышком» метода, ограничивающим итоговое разнообразие библиотек и ведущим к потере слабо представленных вариантов еще до начала процедуры селекции. Отбор в бесклеточных условиях при помощи рибосомного дисплея лишен этого недостатка, однако отличается высокой чувствительностью к артефактам ПЦР и присутствию РНКаз. Целью работы было исследование эффективности сочетания двух методов: проведения предварительной селекции в бесклеточной системе для обогащения исходной библиотеки с последующим клонированием и заключительной селекцией при помощи фагового дисплея. Предполагалось, что такой режим селекции позволит устранить недостатки каждого из методов и повысить эффективность отбора. Для селекции использовали последовательности VHH-антител альпаки, удобные для построения иммунной библиотеки из-за отсутствия VL-доменов. Анализ иммунных библиотек из генов семейств VH3, VHH3 и VH4 показал, что в группах генов VH3 и VH4 доля VHH-антител незначительна, и селекция из комбинированной библиотеки менее эффективна, чем из библиотеки последовательностей семейства VHH3. Мы установили, что комбинация рибосомного и фагового дисплея приводит к более высокому обогащению высокоаффинными фрагментами и позволяет избежать потери исходного разнообразия при клонировании. Комбинированный метод позволил получить большее количество различных высокоаффинных последовательностей, а все протестированные VHH-фрагменты оказались способными специфично распознавать мишень, в том числе в тотальных белковых экстрактах клеточных культур.

**Ключевые слова:** наноантитела, VHH-антитела, рибосомный дисплей, фаговый дисплей, биопаннинг, PDLIM4

**Финансирование:** работа выполнена при финансовой поддержке Министерства образования и науки РФ, уникальный код проекта RFMEFI60716X0156.

**Информация о вкладе авторов:** Ю. Е. Кравченко выделяла генетический материал альпак, готовила РНК, проводила ИФА; С. В. Иванов конструировал библиотеки VHH-фрагментов антител, проводил селекцию методом фагового дисплея; Д. С. Кравченко нарабатывал белковые препараты, работал с эукариотическими клеточными культурами; Е. И. Фролова планировала исследование, проводила иммунизацию животных, редактировала рукопись; С. П. Чумаков планировал исследование, проводил селекцию методом рибосомного дисплея, анализировал результаты, писал рукопись.

**Соблюдение этических стандартов:** работу с животными проводили в соответствии с принципами и требованиями Международной лаборатории по уходу за животными и Директивой совета европейских сообществ (86/609/EEC) от 24 ноября 1986 г.

✉ **Для корреспонденции:** Степан Петрович Чумаков  
ул. Миклухо-Маклая, 16/10, г. Москва, 117997; hathkul@gmail.com

**Статья получена:** 08.12.2018 **Статья принята к печати:** 22.12.2018 **Опубликована онлайн:** 24.02.2019

**DOI:** 10.24075/vrgmu.2019.002

Monoclonal antibodies, as well as their antigen-binding fragments, are one of the most important tools in biological research, diagnostic applications, and disease therapy. The traditional method of antibody identification by testing of individual clones of hybridomas is laborious and inefficient. More advanced approaches, including *in vitro* selection from libraries of antigen-binding fragments of antibodies, simplify the production of antibodies, and allow to select antibodies that have certain properties, for example, the ability to block specific interactions between a receptor and its ligand. Among the methods of selection *in vitro*, phage display technology has become the most widely used, as it allows to create libraries of antigen-binding fragments relatively quickly and with high reliability. This method is based on production of genetically modified phage particles exposing antigen-binding sites of antibodies on their surface. Selection involves incubating a mixture of phage particles with an immobilized antigen. After washing and elution, bound variants of phage particles are propagated in permissive bacteria, followed by the selection of individual variants that are most abundant in the mixture [1]. One of the drawbacks of the method is the requirement to clone the repertoire of fragments encoding the antigen-binding fragments into a special phagemid and then to obtain a pool of transformed cells to produce libraries of phage particles. This stage is considered to be the bottleneck of the method, limiting the diversity of the resulting libraries. As a result, rare variants of antibody fragments may be lost before the beginning of the selection process [2]. Another disadvantage follows from the very structure of traditional antibodies, in which the binding of the antigen is carried out by the interaction of antigen-binding sites located on two separate polypeptide chains. When creating clonal libraries, the probability that the antigen-binding regions of the heavy and light chains of a certain immunoglobulin will be joined in one single-chain scFv antigen-binding fragment is extremely low due to the randomness of the combinatorial process. As a result, the final mixture contains mostly inactive combinations of sections of heavy and light chains, which significantly complicates the selection of scFvs with the desired properties.

To overcome the drawback associated with the need to transform bacteria, there have been developed several modifications of the method, that are based on selection in cell-free conditions, in particular, a ribosome display. This method is based on a coupled cell-free transcription and translation system, where complexes consisting of transcripts (mRNA), ribosomes, and growing protein chains corresponding to the repertoire of antigen-binding regions of antibodies are subjected to affinity selection on the immobilized antigen. Bound variants are amplified by RT-PCR, resulting in an enrichment of the desired variants [3]. Although the initial diversity of the repertoire when using this method is much higher, selection is often biased towards variants of antigen-binding sites that are most easily amplified in PCR [4]. It can be assumed that by combining the methods of ribosome and phage display it will be possible to overcome the weak spots of both methods and to increase the overall efficiency of selection. In this case, it would be possible to preliminarily select variants in a cell-free system, achieving enrichment with high-affinity variants, and then clone the resulting repertoire of fragments into a phagemid and carry out the final selection using phage display.

Animals of the camelid family possess, in addition to antibodies of the traditional structure, antibodies consisting only of heavy chains of immunoglobulins (variable heavy-heavy, VHH antibodies) [5]. This type of antibodies was formed as a result of a mutation in the hinge region of the heavy chain,

which resulted in the deletion of the heavy and light chain binding site. To compensate for the absence of the antigen-recognizing region of the light chain, the VH domains of such antibodies have longer CDR3 regions, which ensures high affinity and specificity for the recognition of antigens. Antibodies of this structure make it possible to obtain compact antigen-recognition sites. The process of *in vitro* selection of VHH antibodies is more efficient due to the lacking stage of random joining of two polypeptide chains, as the resulting libraries are devoid of inactive combinations. VHH antibodies are already widely used for *in vitro* selection by phage display, and several products were already created on their basis for diagnostic applications and disease treatment [6].

The aim of this work was to select for VHH antibodies to the tumor marker PDLIM4 from the immune library of alpaca antibodies with different selection methods. We wanted to test whether the combination of ribosomal and phage displays allows for more efficient selection of sequences of antigen-binding fragments with high affinity and specificity.

## METHODS

### Animal immunization

The source of biological material (blood) was the alpaca (*Vicugna pacos*) of the camelid family. 700 µg of purified PDLIM4 protein was dissolved in complete (for primary immunization) or incomplete (for repeated immunizations) Freund's adjuvant (Pierce; USA) according to the manufacturer's protocol. Immunization of alpaca was carried out in three stages (primary and two boosts, with an interval of 3 weeks) by intramuscular injection into the thigh of the hind leg of the animal. 4 weeks after the last boost, 100 ml of heparinized blood was collected. Peripheral blood mononuclear cells (PBMC) were isolated by centrifuging with a 1.077 Ficoll solution (PanEco; Russia) according to a standard protocol.

### RNA isolation, cDNA synthesis and PCR

Total RNA was extracted from PBMC cells using ExtractRNA reagent (Evrogen; Russia)

in accordance with the manufacturer's recommendations. The mRNA molecules encoding VHH fragments were used to prepare the cDNA with the *CH2-IgG-sp rev* primer (Table) using the ProtoScript cDNA kit (NEB; USA). Further amplification was carried out using high-precision polymerase Tersus (Evrogen; Russia) and primers AlpVHH3 uni fwd, AlpVH4 uni fwd, AlpVH3 uni fwd, AlpVHH-R1 and AlpVHH-R2 for creating libraries containing collections genes VH3, VHH3 and VH4, or with primers AlpVHH3 uni fwd, AlpVHH-R1 and AlpVHH-R2 to create a library containing only genes from the VHH3 family (Table).

### Construction of expression cassettes for selection by ribosome display

Linear expression cassettes were prepared by performing bridge-PCR with Ck gene fragment, which was amplified with primers Flag-Ck (CGGATCCGGATTACAAGGAC GACGACGATAAGACTGTGGCTGCACC) and Ck/for 4 (AACACTCTCCCCTGTTGAAGCT); and a set of VHH fragment sequences. Bridge-PCR was performed with primers RD1x (GGATCCTAATACGACTCACTATAGGGAACAGACCACCATGT CTAG) and Ck/for 4. Resulting DNA fragments were isolated from agarose gel using the Cleanup standard (Evrogen; Russia) reagent kit and used for ribosome display selection.

**Preparation of phagemid libraries for phage display selection**

Phagemid libraries were prepared by cloning the amplified VHH sequences into a modified pHEN2-XB phagemid containing the restriction sites XbaI and BamHI between the sequences of the periplasmic localization signal PelB and c-Myc epitope at the indicated restriction sites, using XbaI and BamHI-HF restriction endonucleases (NEB; USA) и T4 DNA Ligase (NEB, USA). Phagemid libraries were transduced into TG-1 electrocompetent cells using the GenePulser (Bio-Rad; USA) electroporator.

**Selection with ribosome display**

Selection was carried out according to the method described elsewhere [7]. Briefly, the TNT T7 Quick for PCR (Promega; USA) *in vitro* transcription-translation kit was used, 20 µl of the mixture and 100 ng of expression constructs were taken for the reaction. The target (PDLIM4 fragment, amino acids 111–224, corresponding to the linker region between the LIM and PDZ domains) was immobilized by the C-terminal biotin on hydrophilic streptavidin magnetic microspheres conjugated to streptavidin (NEB; USA) in an amount of 100 ng per 5 µl of microspheres; microspheres treated with biotin were used for counter-selection. Restoration of a full-size cassettes after each selection round was performed with OneTaq Onestep RT-PCR kit (NEB; USA) and HSTaq polymerase (Evrogen; Russia) using primers RD1x, RT1 (ACTTCGCAGGCGTAGAC) and Kc/for 9 (AACACTCTCCCCTGTTGAAGCTCTTTGTGAC

GGGCGAGCTCAGGCCCTGATGGGTGACTTCGCAGGCGTAGACTTTG). Selected constructs were cloned directly after reverse transcription step using XbaI and BamHI-HF restriction endonucleases (NEB; USA).

**Phage display selection**

Selection was carried out according to the published protocol [8] using an antigen immobilized in accordance with the description given above, without the counter-selection step.

**Production of soluble forms of VHH fragments**

Individual clones of TG-1 cells identified after selection were used to obtain bacteriophage preparations, which were then transduced to HB-2151 cells cultured in M9 medium. Transduced cells were cultured on solid medium in the presence of ampicillin, after which individual colonies were used to obtain soluble protein in a liquid medium in accordance with the protocol [9]. Purification was performed using Ni-NTA magbeads (Cube Biotech; Germany) as recommended by the manufacturer.

**Evaluation of library enrichment during ribosome and phage displays**

For phage display, the assessment was carried out in accordance with the published protocol [8]. Wells of an immunological plate with sorbed PDLIM4 (111–224 aa) or

**Table 1.** Primer sequences used for amplification of VHH fragments

AlpVHH3 uni fwd	GAACAGACCACCATGTCTAGASAGKTGCAGSTSGTRGAGTCTGKGGGAGG
AlpVH4 uni fwd	GAACAGACCACCATGTCTAGASAGTGCAGSKGCAGGAGTCGGGCCAGGC
AlpVH3 uni fwd	GAACAGACCACCATGTCTAGASARKTGCRSTSGTRGAGWCYKGGGRRGG
AlpVHH-R2	CCTTGTAAATCCGGATCCGGTTGTGTTTTGGTGTCTTGGG
AlpVHH-R1	CCTTGTAAATCCGGATCCGGGGGTCTTCGCTGTGGTGCG
CH2-IgG-sp rev	GGTACGTGCTGTTGAACTGTTCC

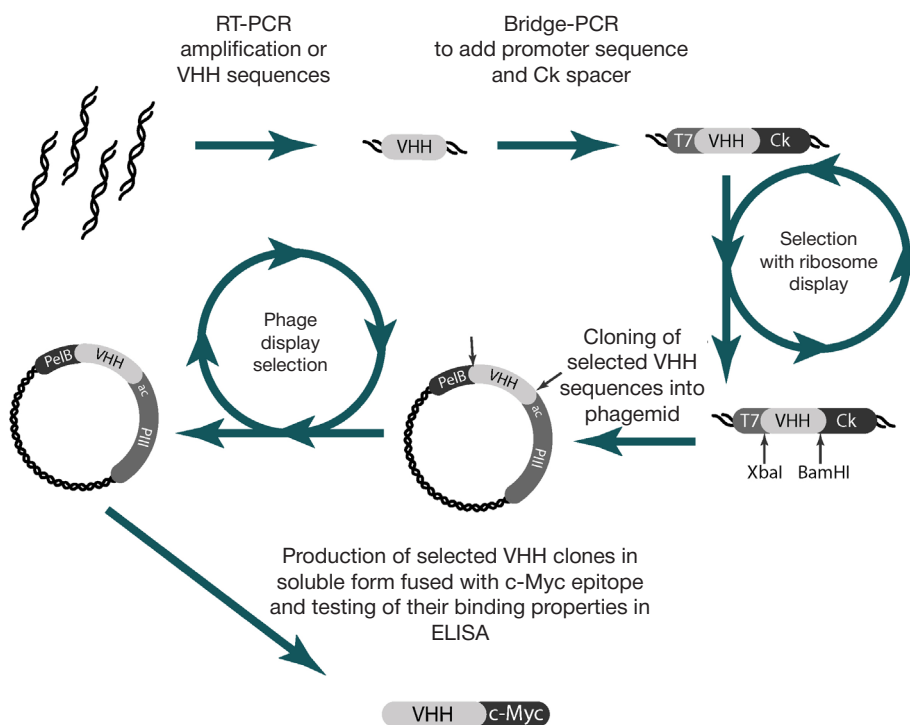


**Fig. 1.** Schematic representation of selection process combining ribosome and phage display

bovine serum albumin (control) were treated with preparations of phage particles displaying VHH fragments, obtained after each round of selection. Detection was performed using horseradish peroxidase-labeled antibodies to phage M13 (Sino Biological; China; cat. 11973-MM05T-H). For selection using the ribosome display, instead of phage particles, mixtures of mRNA–ribosome–protein complexes were obtained using *in vitro* transcription-translation kit TNT T7 Quick for PCR (Promega; USA). Detection was performed using antibodies to the Flag epitope labeled with horseradish peroxidase (Proteintech; USA; cat. HRP-66008).

### Evaluation of the binding capability of individual variants of VHH fragments

The wells of immunological plate were coated either with PDLIM4, or with total protein extracts obtained from MBA-MB-231 and T47D cell lines in accordance with standard protocols, in an amount of 10 µg of cell extract per well. Next, wells were treated with preparations of purified VHH fragments, obtained according to the procedure described above; detection was performed using biotinylated antibodies to the Myc epitope (SciStoreLab; Russia; cat. PSM003BN-100) and streptavidin conjugated with horseradish peroxidase (R&D Systems; USA; cat. DY998). To obtain statistically reliable results, each reaction was reproduced in three independent replications.

### RESULTS

Many studies on the selection of VHH fragments for various targets are based on the use of a single primer set developed over 15 years ago for amplifying VHH sequences [10]. Since then, the alpaca and llama VHH3 genome locus has been

studied using deep sequencing and the sequences of all of its genes have been determined [11]. In addition, it has been reported that some genes of the VH4 and VH3 loci can also participate in formation of mature VHH antibodies. We collected all known sequences of the VH3, VHH3 and VH4 genes, and made a set of primers for amplifying all members of each of the gene families (Table). For reverse primers, we used well-proven sequences corresponding to unique hinge regions of VHH antibodies. Each primer variant was tested in PCR on alpaca cDNA generated using a primer on the CH2 region of the immunoglobulin heavy chain, which is common to VHH antibodies and antibodies of traditional structure. Sequencing of individual clones showed that each of the primer variants specifically amplifies the sequence variants belonging to the corresponding family.

Each additional stage of amplification of the library of VHH fragments leads to a change in the representation of the variants and the leaching of rare sequences from it. To avoid reducing the quality of libraries when combining ribosome and phage displays, we modified the pHEN2 phagemid and introduced restriction sites into primers to create ribosome display constructs, which allowed us to directly clone the VHH fragments into the phagemid library (Fig. 1).

In order to check whether the combination of two selection methods can lead to an increase in its efficiency, two libraries of VHH fragments were constructed from a common initial alpaca cDNA: library 1 consisted solely of sequences belonging to the VHH3 family, library 2 consisted of sequences included in the VH3, VHH3 and VH4 families. Each library was cloned into a phagemid, and also used to generate a linear construct for selection in a cell-free system. Phage libraries were subjected to three rounds of selection, and libraries of linear constructs after the first round of selection by ribosome display were

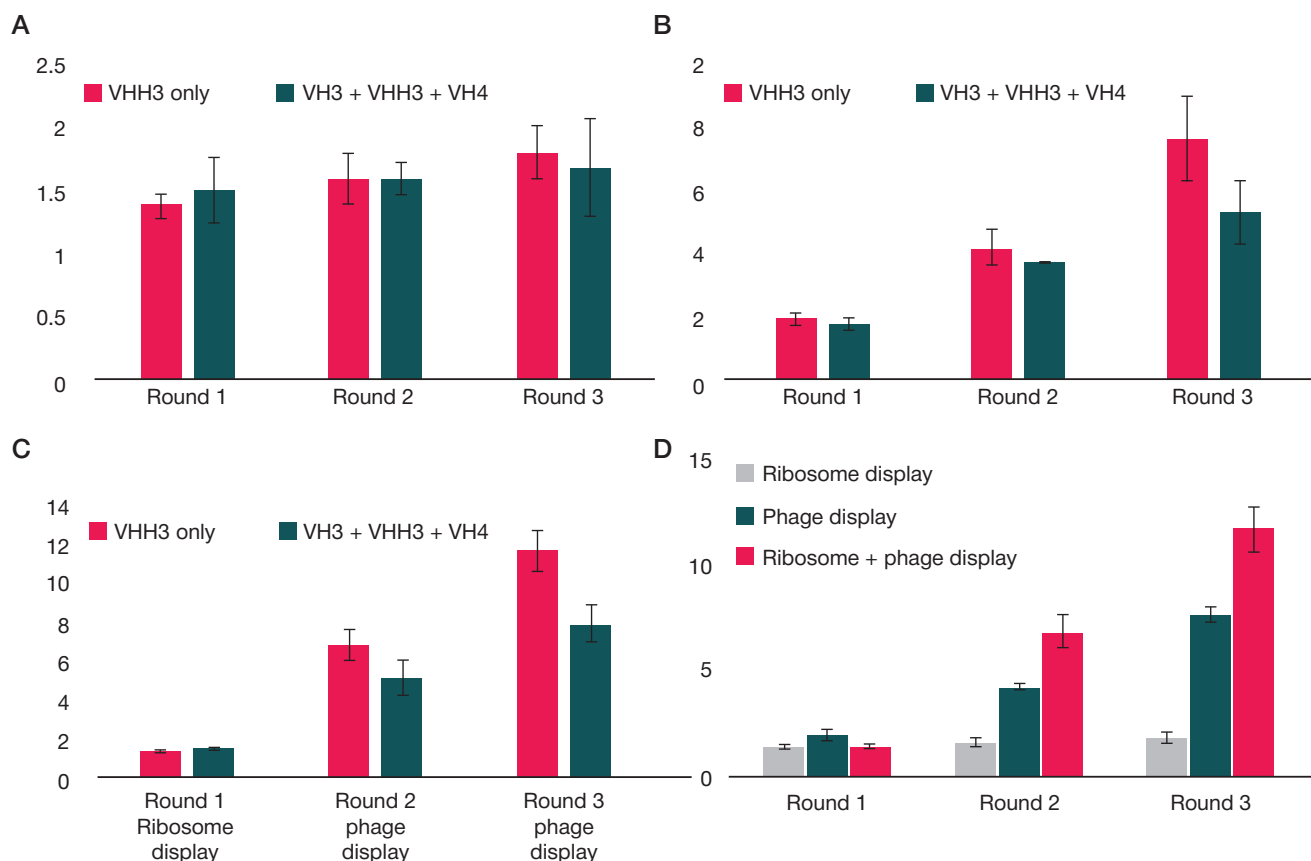
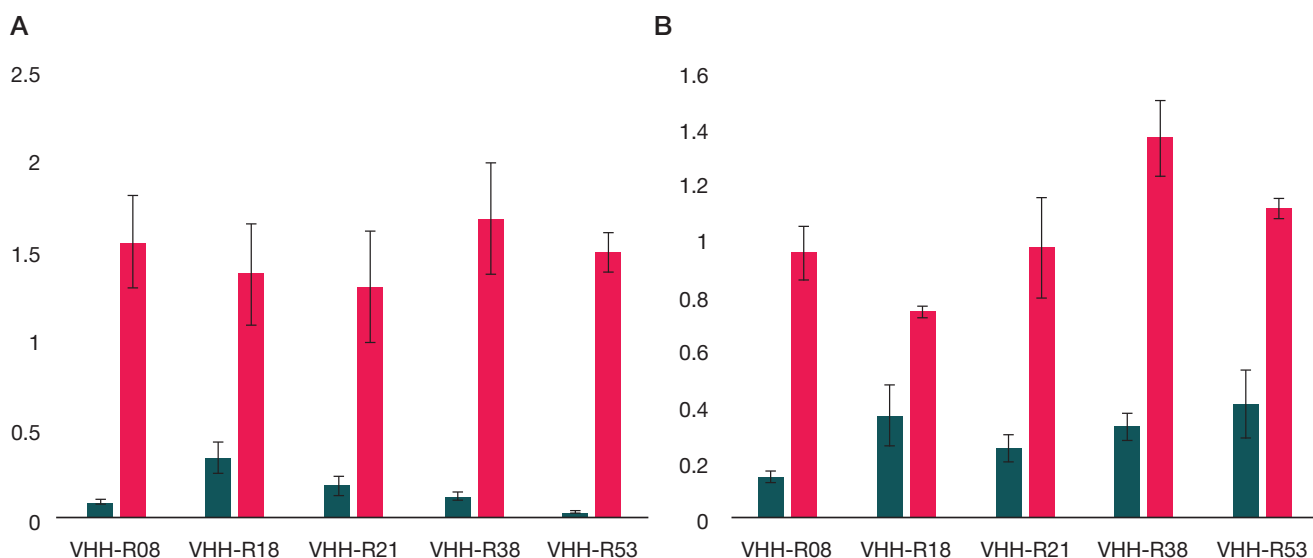


Fig. 2. Enrichment of libraries of VHH fragments during selection: with ribosome display (A); with phage display (B); with combination of ribosome and phage display (C). Comparison of enrichment by all methods for VHH3 library (D)



**Fig. 3.** Comparison of binding properties of five selected VHH fragments in ELISA

divided into two parts: one was subjected to two more rounds of selection, and the second was cloned into phagemid and selected by phage display. After each round, the level of enrichment of affinity fragments was estimated for each library using direct ELISA against negative control (BSA) and the target (PDLIM4 protein linker region). The ratios of signals obtained in the reactions vs control were used to assess the presence of desired VHH sequences in the library (Fig. 2).

The results showed that the library, consisting solely of sequences of the VHH3 family, demonstrated high rates of enrichment with affine variants in all three selection modes. Based on this, we can conclude that the VH3 and VH4 families do not make a significant contribution to the formation of a variety of single-chain VHH antibodies, and their inclusion in the resulting library is impractical. If we compare the efficiency of selection with different methods from the library of sequences of the VHH3 family, the selection in the ribosomal display was much less effective than in the phage display. On average, enrichment from round to round was 26.45% for ribosomal and 220.4% for phage displays. At the same time, the use of a combination of selection methods made it possible to increase the average enrichment to 355%.

After three rounds of selection using the phage display and the combined method, 35 individual clones were isolated and analyzed from the final enriched libraries. Contrary to expectations, the variety of sequences in the final library after combined selection was higher than after selection using the phage display method — 18 different types of sequences were found, while in phage selection there were only 11.

To assess specificity and affinity of interactions between selected VHH fragments and the target, five most represented variants obtained after the combined selection were expressed as monomers in strain HB-2151; purified using affinity chromatography and tested by ELISA. The target was either the PDLIM4 antigen preparation (the central part of the protein, unique to this member of the PDLIM family), or the total protein extracts of the MDA-MB-231 and T47D cell lines characterized by the normal and knockout status of the PDLIM4 gene [12], respectively (Fig. 3).

The experimental results showed that all five variants of VHH fragments are capable to specifically bind the PDLIM4 protein. Variant VHH-R53 possess the maximum specificity in the experiment with purified PDLIM4 protein, but at the same time, it intensely stained a PDLIM4-negative sample of the

protein extract from T47D cells. VHH-R08 had a slightly worse specificity when tested on the purified protein preparation, but showed the greatest difference in signals in experiments with total protein extracts.

#### DISCUSSION

Regardless of the method of selection used, we observed differences in the dynamics of the enrichment of functionally active VHH fragments. It can be assumed that the proportion of VHH antibodies for the VH3 and VH4 gene families is insignificant, and that the combined library may contain a large number of defective variants of VH fragments that could specifically bind the antigen only in conjunction with the VL fragment and make selection difficult. Perhaps some tasks may require the use of such a combination of VHH and VH fragments. For example, since the framework structure of antibodies of the VH4 family of alpaca is very similar in structure to human antibodies, such antibodies are well suited for further humanization [13]. However, for routine selections, it is preferable to use a library containing only members of the VHH3 family.

The relatively low selection efficiency when using a ribosome display can be attributed to two factors: the use of too mild washing conditions that prevent the removal of low-affinity sequences, or the systematic cross-contamination of libraries with DNA fragments that are not completely removed at the stage of preparation of functional units of the library. At the same time, it should be noted that the use of more stringent conditions for the selection and DNA removal can lead to the destruction of the target complexes of mRNA–ribosome–protein. It seems that further optimization of the conditions of this selection method can increase the efficiency of selection, but it is unlikely to improve the result qualitatively. Interestingly, although in the combined selection method, the efficiency of the first round, which used the ribosome display, was relatively low (37% enrichment versus 97% in the first round of phage display), the final efficiency of the combined selection was improved dramatically. Probably, this combination made it possible to increase the representation of most capable variants of VHH fragments at the library cloning stage into a phagemid, while the “parasitic” sequences that persisted from round to round when selected in the ribosome display were removed during the subsequent round of phage display. As a result, the combined selection method led to the elimination of the

bottleneck which is characteristic of the phage display method. This is also supported by the greater variety of different VHH fragments found as a result of combined selection.

The selected variants of VHH fragments demonstrated high specificity for the PDLIM4 protein in *in vitro* experiments. However, in experiments with total protein extracts of cells, some variants, apparently, were able to bind to other proteins of the PDLIM family. For purpose of detection of the status of intracellular PDLIM4, the most promising is the selected variant VHH-R08, for which non-specific binding was minimal.

It can be concluded that the developed for combined selection method makes it possible to achieve better results, without increasing labor costs and selection time, without the requirement to introduce additional amplification stages when constructing phagemid libraries.

## CONCLUSIONS

A new primer system has been successfully tested for amplifying all members of the VHH3 family and creating libraries of VHH antibody fragments for combined selection using the ribosome and phage display methods. Comparison of the efficiency of selection showed that the combined method allows to achieve greater enrichment of the library with high-affinity fragments, and to reduce the loss of the initial diversity of the repertoire during cloning into a phagemid vector. By selecting using the combined method, it was possible to obtain a greater number of variants of high-affinity sequences, and all the VHH fragments subjected to individual testing were able to specifically recognize the target (PDLIM4 protein fragment) both in reactions with a purified protein preparation and in reactions with total protein extracts of cells.

## References

- Carmen S, Jermutus L. Concepts in antibody phage display. *Brief Funct Genomic Proteomic*. 2002; 1 (2): 189–203. PubMed PMID: 15239904.
- Vaughan TJ, Williams AJ, Pritchard K, Osbourn JK, Pope AR, Earnshaw JC, et al. Human antibodies with sub-nanomolar affinities isolated from a large non-immunized phage display library. *Nat Biotechnol*. 1996; 14 (3): 309–14. DOI: 10.1038/nbt0396-309. PubMed PMID: 9630891.
- He M, Khan F. Ribosome display: next-generation display technologies for production of antibodies *in vitro*. *Expert Rev Proteomics*. 2005; 2 (3): 421–30. Epub 2005/07/08. DOI: 10.1586/14789450.2.3.421. PubMed PMID: 16000087.
- Ponsel D, Neugebauer J, Ladetzki-Baehs K, Tissot K. High affinity, developability and functional size: the holy grail of combinatorial antibody library generation. *Molecules*. 2011; 16 (5): 3675–700. Epub 2011/05/05. DOI: 10.3390/molecules16053675 [pii]. PubMed PMID: 21540796.
- Maass DR, Sepulveda J, Pernthaner A, Shoemaker CB. Alpaca (*Lama pacos*) as a convenient source of recombinant camelid heavy chain antibodies (VHHs). *J Immunol Methods*. 2007; 324 (1–2): 13–25. Epub 2007/06/15. DOI: S0022-1759(07)00119-6 [pii]. 10.1016/j.jim.2007.04.008. PubMed PMID: 17568607.
- Van Bockstaele F, Holz JB, Revets H. The development of nanobodies for therapeutic applications. *Curr Opin Investig Drugs*. 2009; 10 (11): 1212–24. Epub 2009/10/31. PubMed PMID: 19876789.
- He M, Taussig MJ. Eukaryotic ribosome display with *in situ* DNA recovery. *Nat Methods*. 2007; 4 (3): 281–8. DOI: 10.1038/nmeth1001. PubMed PMID: 17327849.
- Benhar I, Reiter Y. Phage display of single-chain antibody constructs. *Curr Protoc Immunol*. 2002; Chapter 10: Unit 10 9B. DOI: 10.1002/0471142735.im1019bs48. PubMed PMID: 18432867.
- Studier FW. Protein production by auto-induction in high density shaking cultures. *Protein Expr Purif*. 2005; 41 (1): 207–34. PubMed PMID: 15915565.
- Harmsen MM, Ruuls RC, Nijman IJ, Niewold TA, Frenken LG, de Geus B. Llama heavy-chain V regions consist of at least four distinct subfamilies revealing novel sequence features. *Mol Immunol*. 2000; 37 (10): 579–90. PubMed PMID: 11163394.
- Avila F, Baily MP, Perelman P, Das PJ, Pontius J, Chowdhary R, et al. A comprehensive whole-genome integrated cytogenetic map for the alpaca (*Lama pacos*). *Cytogenet Genome Res*. 2014; 144 (3): 196–207. DOI: 10.1159/000370329. PubMed PMID: 25662411.
- Grigoriadis A, Mackay A, Noel E, Wu PJ, Natrajan R, Frankum J, et al. Molecular characterisation of cell line models for triple-negative breast cancers. *BMC Genomics*. 2012; 13 (13): 619. DOI: 10.1186/1471-2164-13-619. PubMed PMID: 23151021.
- Deschacht N, De Groeve K, Vincke C, Raes G, De Baetselier P, Muyldermans S. A novel promiscuous class of camelid single-domain antibody contributes to the antigen-binding repertoire. *J Immunol*. 2010; 184 (10): 5696–704. DOI: 10.4049/jimmunol.0903722. PubMed PMID: 20404276.

## Литература

- Carmen S, Jermutus L. Concepts in antibody phage display. *Brief Funct Genomic Proteomic*. 2002; 1 (2): 189–203. PubMed PMID: 15239904.
- Vaughan TJ, Williams AJ, Pritchard K, Osbourn JK, Pope AR, Earnshaw JC, et al. Human antibodies with sub-nanomolar affinities isolated from a large non-immunized phage display library. *Nat Biotechnol*. 1996; 14 (3): 309–14. DOI: 10.1038/nbt0396-309. PubMed PMID: 9630891.
- He M, Khan F. Ribosome display: next-generation display technologies for production of antibodies *in vitro*. *Expert Rev Proteomics*. 2005; 2 (3): 421–30. Epub 2005/07/08. DOI: 10.1586/14789450.2.3.421. PubMed PMID: 16000087.
- Ponsel D, Neugebauer J, Ladetzki-Baehs K, Tissot K. High affinity, developability and functional size: the holy grail of combinatorial antibody library generation. *Molecules*. 2011; 16 (5): 3675–700. Epub 2011/05/05. DOI: 10.3390/molecules16053675 [pii]. PubMed PMID: 21540796.
- Maass DR, Sepulveda J, Pernthaner A, Shoemaker CB. Alpaca (*Lama pacos*) as a convenient source of recombinant camelid heavy chain antibodies (VHHs). *J Immunol Methods*. 2007; 324 (1–2): 13–25. Epub 2007/06/15. DOI: S0022-1759(07)00119-6 [pii]. 10.1016/j.jim.2007.04.008. PubMed PMID: 17568607.
- Van Bockstaele F, Holz JB, Revets H. The development of nanobodies for therapeutic applications. *Curr Opin Investig Drugs*. 2009; 10 (11): 1212–24. Epub 2009/10/31. PubMed PMID: 19876789.
- He M, Taussig MJ. Eukaryotic ribosome display with *in situ* DNA recovery. *Nat Methods*. 2007; 4 (3): 281–8. DOI: 10.1038/nmeth1001. PubMed PMID: 17327849.
- Benhar I, Reiter Y. Phage display of single-chain antibody constructs. *Curr Protoc Immunol*. 2002; Chapter 10: Unit 10 9B. DOI: 10.1002/0471142735.im1019bs48. PubMed PMID: 18432867.

- 18432867.
9. Studier FW. Protein production by auto-induction in high density shaking cultures. *Protein Expr Purif.* 2005; 41 (1): 207–34. PubMed PMID: 15915565.
  10. Harmsen MM, Ruuls RC, Nijman IJ, Niewold TA, Frenken LG, de Geus B. Llama heavy-chain V regions consist of at least four distinct subfamilies revealing novel sequence features. *Mol Immunol.* 2000; 37 (10): 579–90. PubMed PMID: 11163394.
  11. Avila F, Baily MP, Perelman P, Das PJ, Pontius J, Chowdhary R, et al. A comprehensive whole-genome integrated cytogenetic map for the alpaca (*Lama pacos*). *Cytogenet Genome Res.* 2014; 144 (3): 196–207. DOI: 10.1159/000370329. PubMed PMID: 25662411.
  12. Grigoriadis A, Mackay A, Noel E, Wu PJ, Natrajan R, Frankum J, et al. Molecular characterisation of cell line models for triple-negative breast cancers. *BMC Genomics.* 2012; (13): 619. DOI: 10.1186/1471-2164-13-619. PubMed PMID: 23151021.
  13. Deschacht N, De Groeve K, Vincke C, Raes G, De Baetselier P, Muyldermans S. A novel promiscuous class of camelid single-domain antibody contributes to the antigen-binding repertoire. *J Immunol.* 2010; 184 (10): 5696–704. DOI: 10.4049/jimmunol.0903722. PubMed PMID: 20404276.

## DETECTION OF SER450LEU MUTATION IN *RPOB* GENE OF *MYCOBACTERIUM TUBERCULOSIS* BY ALLELE-SPECIFIC LOOP-MEDIATED ISOTHERMAL DNA AMPLIFICATION METHOD

Filipenko ML<sup>1</sup>✉, Oscorbin IP<sup>1</sup>, Khrapov EA<sup>1</sup>, Shamovskaya DV<sup>1</sup>, Cherednichenko AG<sup>2</sup>, Shvartz YaSh<sup>2</sup>

<sup>1</sup> Institute of Chemical Biology and Fundamental Medicine, Novosibirsk, Russia

<sup>2</sup> Novosibirsk Tuberculosis Research Institute, Novosibirsk, Russia

To identify genetic mutations a rather time-consuming and expensive method of polymerase chain reaction (PCR) is widely used. The aim of the present work was to evaluate the possibility of using the two schemes of the method of allele-specific isothermal loop amplification (LAMP) to detect the TCG/TTG (S450L) mutation in the *rpoB* gene of *Mycobacterium tuberculosis*. 48 clinical isolates of *M. tuberculosis* and 11 samples of sputum were used, randomized and obtained in the microbiological laboratory of the city of Novosibirsk from incident patients. It is shown that the use of an analysis scheme using the allele-specific primer FIP compared to F3 has the best resolution: the difference between the amplification time of the mutation and the wild type allele was  $22 \pm 2,4$  versus  $13 \pm 4,1$  minutes ( $p = 0,0011$ ). When using 100 DNA genomic equivalents a true positive signal (amplification of the *rpoB* gene with a mutation using the corresponding allele-specific primer) was detected after  $29,4 \pm 3,4$  minutes. A positive signal was visualized after adding SYBR Green I to the reaction, both when illuminated with daylight and when using a UV transilluminator. Using the developed method the DNA sample of 20 RIF<sup>R</sup> isolates from *M. tuberculosis* was analyzed containing the Ser450Leu mutation in the *rpoB* gene, 10 RIF<sup>R</sup> isolates containing other mutations in the *rpoB* gene and 18 RIF<sup>S</sup> isolates without any mutations; the presence of mutations in the samples was determined using classical Sanger sequencing. The sensitivity and specificity of LAMP for detecting a Ser450Leu mutation in the *rpoB* gene was 100%. This approach allows the use of crude lysates of mycobacteria as DNA, which reduces the total analysis time to 1,5 hour.

**Keywords:** *Mycobacterium tuberculosis*, drug resistance, rifampicin, *rpoB* gene, isothermal loop amplification, LAMP

**Funding:** the study was done with the financial support of the basic budgetary financing project № VI.62.1.5 «Synthetic biology: development of tools for the genetic material manipulation and creation of promising drugs for therapy and diagnostics» (0309-2018-0003).

**Author contribution:** Filipenko ML created a general concept of the study, planned experiments, analyzed the results and participated in the writing of this article; Oscorbin IP participated in the writing of this article; Khrapov EA conducted experiments; Shamovskaya DV conducted experiments; Cherednichenko AG analyzed the experiments results; Shvartz YaSh was involved in planning and analyzed the experiments results.

**Compliance with ethical standards:** the study was approved by the Ethics Committee of Institute of Chemical Biology and Fundamental Medicine (Protocol 4 dated April 09, 2009). All patients signed a voluntary informed consent to participate in the study.

✉ **Correspondence should be addressed:** Maxim L. Filipenko  
Lavrentyev Prospect 8/2, Novosibirsk, 630090; mfilipenko@gmail.com

**Received:** 07.12.2018 **Accepted:** 25.02.2019 **Published online:** 09.03.2019

**DOI:** 10.24075/brsmu.2019.007

## ВЫЯВЛЕНИЕ МУТАЦИИ SER450LEU В ГЕНЕ *RPOB* *MYCOBACTERIUM TUBERCULOSIS* МЕТОДОМ АЛЛЕЛЬ-СПЕЦИФИЧНОЙ ИЗОТЕРМИЧЕСКОЙ ПЕТЛЕВОЙ АМПЛИФИКАЦИИ ДНК

М. Л. Филипенко<sup>1</sup>✉, И. П. Оскорбин<sup>1</sup>, Е. А. Храпов<sup>1</sup>, Д. В. Шамо́вская<sup>1</sup>, А. Г. Чередниченко<sup>2</sup>, Я. Ш. Шварц<sup>2</sup>

<sup>1</sup> Институт химической биологии и фундаментальной медицины СО РАН, Новосибирск, Россия

<sup>2</sup> Новосибирский научно-исследовательский институт туберкулеза, Новосибирск, Россия

Для выявления генетических мутаций широко используют достаточно трудоемкий и дорогостоящий метод полимеразной цепной реакции (ПЦР). Целью работы было оценить возможность применения двух схем метода аллель-специфичной изотермической петлевой амплификации (loop-mediated isothermal amplification, LAMP) для выявления мутации TCG/TTG (S450L) в гене *rpoB* *Mycobacterium tuberculosis*. Использовали 48 клинических изолятов *M. tuberculosis* и 11 образцов мокроты, выбранных случайным образом и полученных в микробиологической лаборатории г. Новосибирска от пациентов с впервые выявленным заболеванием. Показано, что применение схемы анализа с использованием аллель-специфичного праймера FIP по сравнению с F3 имеет лучшую разрешающую способность: разница между временем амплификации мутации и аллеля дикого типа составила  $22 \pm 2,4$  против  $13 \pm 4,1$  мин ( $p = 0,0011$ ). При использовании 100 геном-эквивалентов ДНК истинно положительный сигнал (амплификация гена *rpoB* с мутацией при использовании соответствующего аллель-специфического праймера) детектировался после  $29,4 \pm 3,4$  мин. Положительный сигнал визуализировался после добавления в реакцию SYBR Green I, как при освещении дневным светом, так и при использовании трансиллюминатора с УФ-излучением. С помощью разработанного нами метода была проанализирована выборка ДНК 20 RIF<sup>R</sup> изолятов *M. tuberculosis*, несущих мутацию Ser450Leu в гене *rpoB*, 10 RIF<sup>R</sup> изолятов, несущих другие мутации в гене *rpoB*, а также 18 RIF<sup>S</sup> изолятов без мутаций; наличие мутаций в образцах было определено с помощью классического секвенирования по Сенгеру. Чувствительность и специфичность LAMP для выявления мутации Ser450Leu в гене *rpoB* составили 100%. Данный подход позволяет использовать в качестве ДНК грубые лизаты микобактерий, что сокращает общее время анализа до 1,5 ч.

**Ключевые слова:** *Mycobacterium tuberculosis*, лекарственная устойчивость, мутации, рифампицин, ген *rpoB*, изотермическая петлевая амплификация, LAMP

**Финансирование:** работа выполнена при финансовой поддержке проекта базового бюджетного финансирования № VI.62.1.5 «Синтетическая биология: разработка средств манипуляции генетическим материалом и создание перспективных препаратов для терапии и диагностики» (0309-2018-0003).

**Информация о вкладе авторов:** М. Л. Филипенко — общий замысел работы, планирование экспериментов, анализ результатов экспериментов, написание статьи; И. П. Оскорбин — написание статьи; Е. А. Храпов — проведение экспериментов; Д. В. Шамо́вская — проведение экспериментов; А. Г. Чередниченко — анализ результатов экспериментов; Я. Ш. Шварц — планирование и анализ результатов экспериментов.

**Соблюдение этических стандартов:** исследование одобрено комитетом по медицинской этике Института химической биологии и фундаментальной медицины СО РАН (№ 4 от 9 апреля 2009 г.). Все пациенты подписали добровольное информированное согласие на участие в исследовании.

✉ **Для корреспонденции:** Максим Леонидович Филипенко  
пр. академика Лаврентьева, д. 8/2, г. Новосибирск, 630090; mfilipenko@gmail.com

**Статья получена:** 07.12.2018 **Статья принята к печати:** 25.02.2019 **Опубликована онлайн:** 09.03.2019

**DOI:** 10.24075/vrgmu.2019.007

Through many centuries tuberculosis is among the most difficult in treatment infectious diseases with high mortality. Now drug-resistant (DR) isolates of *M. tuberculosis* are a threat to public health: they complicate conservative treatment, lead to patient disability, and the growth and spread of DR-strains among healthy populations is observed. This determines the necessity of the development of effective and possibly simple methods for detecting drug resistance of mycobacteria. One of the widely used first-line anti-TB drugs in the treatment of tuberculosis is rifampicin. Resistance to rifampicin is often considered as a surrogate marker of multidrug resistance (MDR) of the tuberculosis mycobacterium complex [1]. Rifampicin was introduced into the phthisiatricians clinical practice in 1972. It is highly effective against *Mycobacterium tuberculosis*, the minimal inhibiting concentration (MIC) of rifampicin is 0,1–0,2 µg/ml [2]. In combination with isoniazid and pyrazinamide rifampicin is the base of pharmacotherapy of the tuberculosis infection.

The cell target of rifampicin is the DNA-dependent RNA polymerase enzyme, which is extremely conservative among bacteria and archaea. The overwhelming majority of mutations responsible for rifampicin resistance are localized in three regions of the *rpoB* gene, encoding the beta subunit of the RNA polymerase: cluster I (encodes 512–534 amino acid positions), cluster II (563–574), and cluster III (687). In 95% of cases, mutations affect cluster I or the so-called rifampicin-resistance determining region (RRDR) consisting of 81 base pairs. This region corresponds to codons 426–452 in *Mycobacterium tuberculosis* and 507–533 in *Escherichia coli*. Traditionally designated by the *E. coli* nomenclature mutations in codons 521, 526, 531 and 533 (positions 440, 445, 450 and 452 in the *rpoB* gene of *Mycobacterium tuberculosis*) are the most common for rifampicin-resistant *Mycobacterium tuberculosis* [3].

Amino acid substitutions at positions 526 and 531 lead to resistance to high doses of rifampicin. Amino acid substitution Ser450Leu (S450L, nomenclature of the *Mycobacterium tuberculosis* gene, which will be used in the present article) dominates among all other substitutions, determining resistance in 30–70% of rifampicin-resistant (RIF<sup>r</sup>) isolates (the median is about 60%) [3]. This makes the S450L mutation (TCG/TTG) the most significant candidate for the validation of a wide variety of genetic screening methods for detection of *Mycobacterium tuberculosis* resistance to rifampicin [4, 5].

Today, the most commonly used method for detecting genetic mutations is the polymerase chain reaction (PCR). This method is simple to perform, and demonstrates enough reliability. PCR modifications using monitoring of specific amplicons by detecting accumulation of a fluorescent signal (real time PCR) make the analysis homogeneous and allow to avoid additional manipulations with the amplicon extra vitro. However, PCR is performed using rather complicated and expensive instruments. This was the reason for the development of alternative methods of nucleic acids amplifying, primarily feasible under isothermal conditions [6].

In 2000 the loop-mediated isothermal amplification (LAMP) method was developed. Initially, the method assumed the use of two pairs of primers (outer and inner) and DNA polymerase with chain-displacing activity [7]. Later, the developers introduced an additional pair of primers to improve the amplification kinetics.

In specificity and sensitivity LAMP (the limit of sensitivity is around several DNA molecules) is comparable to PCR, and in some cases takes precedence over it. The increased resistance of LAMP to the PCR inhibitors was also noted [8]. For the detection of LAMP results, approaches based on different principles can be used. First of all it is the measurement of optical density due to magnesium pyrophosphate formed

during DNA synthesis [9], or the fluorescence measurement in response to introduction of the intercalating dyes [9], primer modification [10] or the introduction of fluorescently-labeled probes [11], as well as colorimetric detection of metal-sensitive dyes due to the binding of magnesium ions by pyrophosphate [12].

To date, a significant amount of research has been done on the development of test systems for detecting *Mycobacterium tuberculosis* using LAMP [13]. The Loopamp MTBC Detection Kit (Eiken Chemical Company Ltd; Japan) based on the LAMP method has been noted by WHO as a possible replacement for microscopic examination for the diagnosis of tuberculosis [14]. It was also recommended as an additional to microscopy test in the diagnosis of adults with clinical symptoms of tuberculosis, including the diagnosis of negative according to the results of microscopy patients. However, the use of LAMP for detection of mutations of *Mycobacterium tuberculosis* causing drug resistance has not yet been described.

The aim of our work was to develop a method for detecting TCG/TTG mutation (S450L) in the *rpoB* gene of *Mycobacterium tuberculosis* for detection of rifampicin resistance without using expensive equipment, and also to evaluate the effectiveness of two types of the allele-specific isothermal loop amplification (AS-LAMP) design, and to determine the optimal system's analytical characteristics on a representative DNA sample of *Mycobacterium tuberculosis* isolates.

## METHODS

### Clinical isolates

Clinical isolates from *M. tuberculosis* (48 isolates) as well as 11 sputum samples were selected randomly and obtained in the microbiological laboratory of the Novosibirsk Tuberculosis Research Institute, Novosibirsk, from the patients living in the city of Novosibirsk and the Novosibirsk region, who were examined in 2009–2011. The taking and processing of sputum was carried out in accordance with the MOH order № 109 of 21.03.2003 (edition of 29.10.2009). Criteria for inclusion of patients in the study: males and females of any age; incident patients; rifampicin resistance presence. Exclusion criteria: not a newly diagnosed disease; rifampicin resistance absence. Rifampicin resistance (40 µg/ml) was determined according to the absolute concentrations method on a Lowenstein-Jensen medium. Isolate resistance to rifampicin was determined in the BACTEC MGIT 960 fluorometric system (Becton-Dickinson; USA). Crude lysates as well as DNA from bacterial colonies of isolates were obtained by heating in 300 µl of buffer containing 10 mmol of sodium tetraborate (pH 9.5) and 1% 2-methoxyethanol during 10 minutes at 98 °C followed by centrifugation to precipitate cellular debris.

### Sequencing of *rpoB* gene

For amplification of the 322 nucleotide pairs *rpoB* gene fragment the *rpoB*1 5'-AACCGCCGCCTGCGTACGGT-3' and *rpoB*2 5'-GGCCGTAGTGCACGGGTGCA-3' primers were used. The reaction mixture of 25 µl contained 65 mmol of Tris-HCl (pH 8,9), 16 mmol of (NH<sub>4</sub>)<sub>2</sub>SO<sub>4</sub>, 3 mmol of MgCl<sub>2</sub>, 0,05% Tween-20, 0,2 mmol of dNTP, one unit of *Taq*-polymerase (Fermentas; Lithuania), 0,3 µmol of mentioned above oligonucleotide primers and 1–10 ng of genome DNA from *M. tuberculosis*. Amplification was performed in the PTC-200 amplifier (BioRad; USA) using the following program: 96 °C — 3 minutes, then 35 cycles at 95 °C — 10 seconds, 64 °C — 10 seconds and 72 °C — 20 seconds with final elongation at

72 °C — 3 minutes. The presence of amplification product of the required size was checked by electrophoresis in 6% polyacrylamide gel with visualization of DNA fragments with ethidium bromide using the UV irradiation. The sequence of the PCR products was determined at the SB RAS Genomics Core Facility using the sequencing reagents from the Big Dye Terminator v3.1 Cycle Sequencing Kit (Life Technologies; USA) and the capillary electrophoresis unit ABI 3130xl Genetic Analyzer (Life Technologies; USA) according to manufacturer's instructions. Mutations were detected by comparing the obtained nucleotide sequences with the *rpoB* gene of *M. tuberculosis* (H37Rv) using the Unipro UGENE software 1.11.3 (Unipro; Russia).

### Obtaining of standard plasmid samples carrying frequent mutations

The 505 nucleotide pairs DNA fragment was obtained using amplification with oligonucleotide primers cl-rpobU and cl-rpobR (Table 1) in the following conditions: the PCR reaction mixture of 50 µl contained the buffer for Taq polymerase (65 mmol TrisHCl; pH 8,9; 16 mmol (NH<sub>4</sub>)<sub>2</sub>SO<sub>4</sub>; 0,05% Tween-20; 3,5 mmol MgCl<sub>2</sub>), 0,2 mmol of dNTP, 10 ng of genome DNA from *Mycobacterium tuberculosis* H37 Rv or DNA isolate with a TCG/TTG (S450L) mutation in the *rpoB* gene, one activity unit of Taq-polymerase (Biosan; Russia). Amplification was performed in the Tercyc amplifier (DNA-Technology; Russia) according to the following program: 3 minutes at 95 °C for initial denaturation, then 34 cycles: 10 seconds at 95 °C for denaturation, 10 seconds at 60 °C for primer hybridization, 20 seconds at 72 °C for elongation. Amplification products were hydrolyzed with restriction endonucleases Hind III and BamHI (Sibenzyme; Russia) ligated with the pBluescript II SK

(+) vector that was hydrolyzed with the same endonucleases, during 8 hours with 100 activity units of T4 DNA-ligase (Biosan; Russia). Using the ligase mixture competent cells from *E. coli* of the XL1Blue strain (Stratagene; USA) were transformed. In plasmid clones selected from the results of restriction analysis, to confirm the structure, the nucleotide sequence of the insert was determined by Sanger sequencing. Sequencing was performed in the ABI 3130XL GeneticAnalyzer automatic sequencer (Applied Biosystems; USA) using the BigDye 3.1 kit (SB RAS Genomics Core Facility; Russia). Plasmid recombinant DNA pRPOB-M and pRPOB-W were isolated from 50 ml of night culture in LB medium using the QIAGEN Plasmid Midi Kit (QIAGEN; Germany) according to manufacturer's instructions.

The concentration of the obtained standard plasmid DNA was determined by spectrophotometry and fluorometry using the Qubit™ BR kit (Invitrogen; USA). Then 2 µg of DNA were subjected to hydrolysis by HindIII restriction endonuclease for linearization. The resulting linear standards were diluted to concentration of 105 and further to concentration of 5 × 10<sup>2</sup> plasmid DNA copies for 1 µl in sterile buffer, containing 10 mmol of Tris HCl (pH 7,6) and 5 ng/µl of lambda phage DNA.

The DNA concentration in the obtained standards was refined using digital PCR in the QX100™ Droplet Digital™ PCR System (Bio-Rad; USA) according to manufacturer's instructions. To do this, 20 µl of PCR mixture containing the test DNA (about 10<sup>3</sup> per 20 µl), 1 × PCR mixture (Bio-Rad; USA), 300 nmol oligonucleotide primers Bla-U, Bla-R and 100 nmol TaqMan Bla-P probe for beta-lactamase gene amplifying (Table 1) were prepared. To obtain microdroplets, 20 µl of the prepared PCR mixture and 70 µl of oil needed to generate droplets were placed in the corresponding wells of the DG8 cartridge. Then, 40 µl of the obtained microdroplets were transferred to a 96-well PCR plate, sealed with foil and placed in an amplifier.

**Table 1.** List of oligonucleotide primers and fluorescently labeled probes used in present study

	Name	Nucleotide sequence
AS-FIP design		
1	450-F3	5'-CCAGAACAACCCGCTGTCG-3'
2	450-B3	5'-TGACCCGCACGTACACCGACA-3'
3	450a-FIP-M	5'-GGACCTCCAGCCCGGCACACCCACAAGCGCCGACTGCT-3'
4	450a-FIP-W	5'-GGACCTCCAGCCCGGCACACCCACAAGCGCCGACTGGC-3'
5	450a-FIP-rpoB	5'-GGACCTCCAGCCCGGCACACCCACAAGCGCCGACTG-3'
6	450a-BIP	5'-TGCACCCGTGCACTACGGGCCGATCAGACCGATGTTGG-3'
7	450a-LF	5'-CCGATCGAAACCCCTGAGG-3'
8	450a-LB	5'-CACGTGACAGACCGCCG-3'
AS-F3 design		
9	450b-F3m	5'-CCACAAGCGCCGACTGCT-3'
10	450b-F3w	5'-CCACAAGCGCCGACTGGC-3'
11	450b-FIP	5'-CACGTGCGGACCTCCAG-GCGCTGGGGCCCGGC-3'
12	450b-BIP	5'-ACCGTTCGCACTACGGC-GATCAGACCGATGTTGGGC-3'
13	450b-B3	5'-CGTACACCGACAGCGAGC-3'
14	450b-531-LF	5'-CCGATCGAAACCCCTGAGG-3'
15	450b-LB	5'-CCCGGCACGCTCACGT-3'
16	cl-rpobU	5'-GAAGGATCCACCATCGAATATCTGGTC-3'
17	cl-rpobR	5'-AAGCTTCTCCTCGTCGGCGGTCAGGT-3'
18	Bla-U	5'-CGTCGTTTGGTATGGCTTCATTC-3'
19	Bla-R	5'-AGGACCGAAGGAGCTAACCG-3'
20	Bla-P	5'-HEX-CGGTTCCTCAACGATCAAGGCAG-BHQ2-3'

The following amplification program was used: 96 °C — 10 minutes, then 50 cycles 96 °C — 15 seconds, 60 °C — 40 seconds, with final warming up during 10 minutes at 98 °C. After that, the droplets were read using the Droplet Reader unit, the obtained data was processed using the QuantaSoft software (Bio-Rad; USA).

### Loop-mediated isothermal amplification

The reaction mixture with a volume of 20  $\mu$ l contained 1 $\times$  reaction buffer (pH 8,0) for Bst-polymerase (New England Biolabs; USA), 0,2  $\mu$ mol of each outer primer (F3/B3), 0,4  $\mu$ mol of each loop primer (LF/BF), 1,2  $\mu$ mol of each inner primer (FIP/BIP), sequences of which are represented in Table 1, DNA matrix (1000 plasmid copies or 0,5–2 ng of mycobacterial DNA isolate for one reaction mixture), 2 activity units of Gss-polymerase from *Geobacillus* sp. 777 [15]. In the case of using LAMP in the real time mode the SYTO-9 intercalating dye bringing concentration to 2  $\mu$ mol was added [16]. The reaction was carried out in the CFX 96 amplifier (Bio-Rad; USA). The program included the following stages: primer annealing and elongation at 60 °C for 80 minutes with recording of the fluorescence signal once a minute on the FAM channel; determination of the melting point of amplification products in the range of 75–95 °C after amplification for specificity analysis. To evaluate the isothermal amplification results the Tt (time-to-threshold — time needed by the accumulation curve of the amplification product to intersect the threshold value) parameter was used. All LAMP reactions were performed in three iterations, the table shows the mean values together with standard deviations for them.

### RESULTS

We used two previously described [17, 18] schemes for the design of allele-specific isothermal loop amplification (AS-LAMP) (Fig. 1). According to the first scheme, the detection of a mutation or a wild type allele is carried out using two allele-specific FIP primers. In the second scheme, allele-specific LAMP is initiated from a mutation-specific F3 primer. At the initial stage, we used plasmids with a cloned wild type *rpoB* fragment and a fragment containing the mutation as a matrix for working out the conditions. To optimize the reaction pS450L-M or pS450L-W with a concentration of 1000 copies per reaction served as a matrix for AS-LAMP. All optimization reactions were performed together with monitoring the accumulation of isothermal amplification products in real time using the SYTO9 intercalating dye. As the main parameter for optimization, the mutation discrimination index was used, which was defined as the difference in Tt for wild-type DNA and for mutant DNA when using the set of primers, including the allele-specific primer (AS-FIP or AS-F3), for amplification.

In model experiments with the plasmid DNA, we have shown that the use of an analysis scheme using the allele-specific primer FIP compared to F3 has the best mutation discrimination index: the difference between the amplification time of the mutation and the wild type allele was  $22 \pm 2,4$  versus  $13 \pm 4,1$  minutes (Fig. 2). Use of non-parametric U-test (Mann–Whitney U-test) showed that the resulting discrimination indexes demonstrate the statistically significant difference ( $p = 0,0011$ ). When using 100 DNA genomic equivalents a true positive signal (amplification of the *rpoB* gene with a mutation

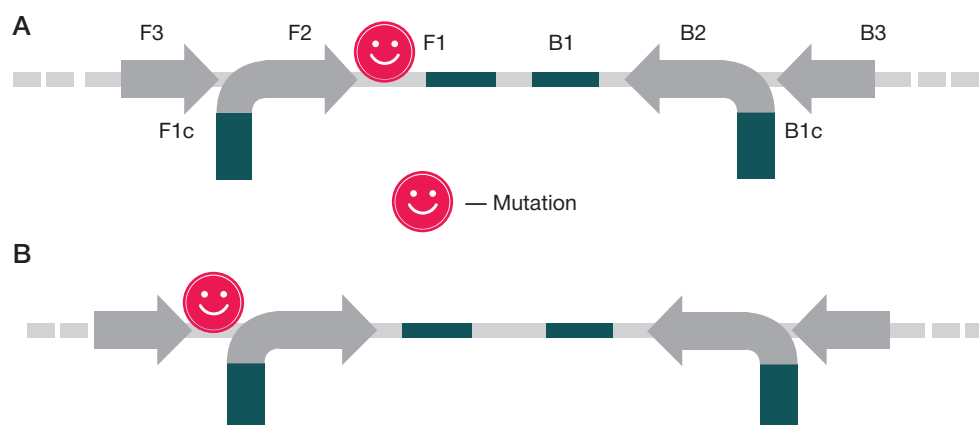


Fig. 1. Schematic illustration of the different principles of allele-specific isothermal loop amplification (AS-LAMP): allele-specific primer FIP (A), allele-specific primer F3 (B)

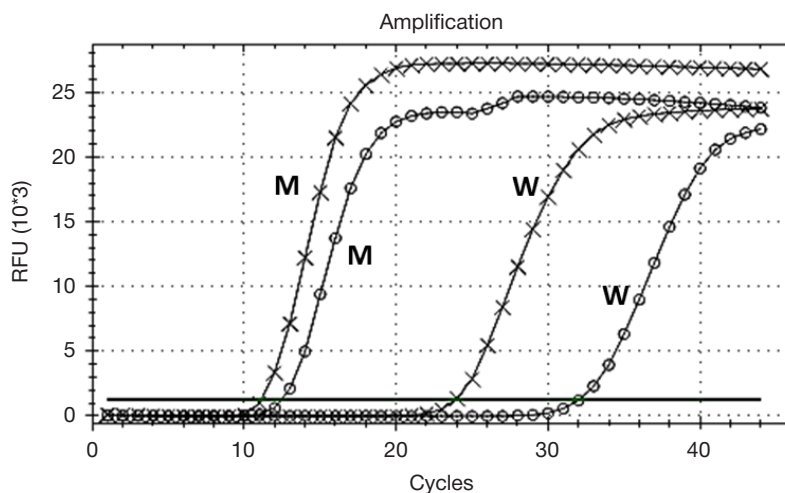
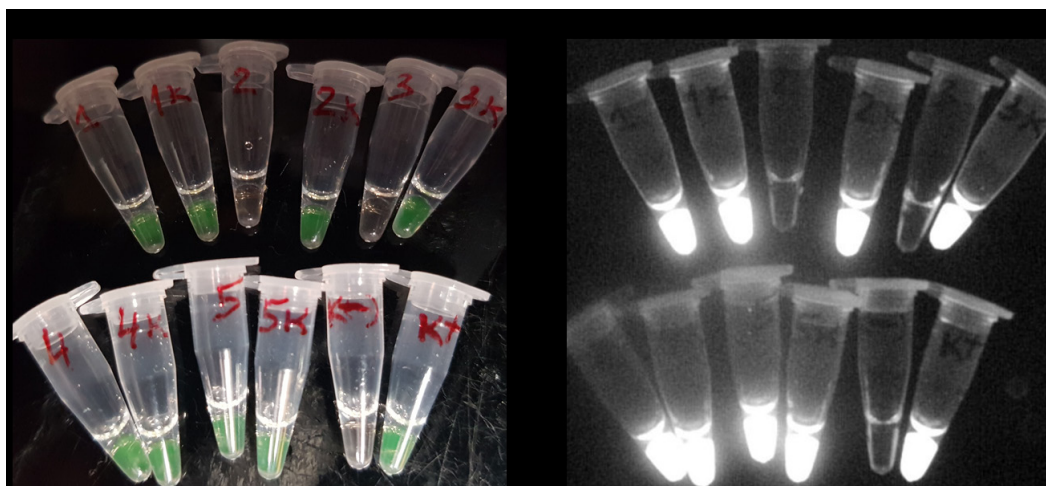


Fig. 2. Fluorescence accumulation curves for AS-LAMP products. Curves marked by circles correspond to FIP-AS-LAMP, marked by crosses — to F3-AS-LAMP



**Fig. 3.** Detection of TCG/TTG (S450L) mutation of the *rpoB* gene by AS-LAMP method with visualization of amplification products by adding the SYBR Green I intercalating dye in natural light (A) and with the 280 nm UV illumination (B). Samples 1, 4, 5 contain a mutation, 2 and 3 — contain no mutation, they were amplified with mutation-specific primer, tubes marked with «K» were amplified with norm-specific primer

**Table 2.** The range of *rpoB* gene mutations of the *Mycobacterium tuberculosis* isolates detected by Sanger sequencing and the results of a TCG/TTG (S450L) mutation detection using AS-LAMP

No	Mutation	Sequencing	AS-LAMP
1	No mutation	18	18
2	Ser450Leu (TCG->TTG)	20	20
3	His445Leu (CAC->CTC)	4	0
4	His445Gln (CAC->CAA)	1	0
5	Asp440Val (GAC->GTC)	3	0
6	Asp440Asn (GAC->AAC)	1	0
7	Asp440His (GAC->CAC)	1	0

when using the corresponding allele-specific primer) was detected after  $29,4 \pm 3,4$  minutes.

We also made an attempt to improve the mutation discrimination index by changing the concentration of betaine, as well as by adding dimethylsulfoxide (DMSO) which has the ability to increase the standard PCR specificity [19]. The optimal betaine concentration was 0,75 mol, adding DMSO did not improve the discrimination and even slightly increased the overall response time.

A positive signal was reliably visualized after adding SYBR Green I (at a concentration of 1: 1000 of commercial dye) to the reaction, both when illuminated with daylight and when using a UV transilluminator (Fig. 3). For further diagnostic validation, two reactions were performed for each test sample: the first one was AS-LAMP using the 531-FIP-M primer for mutation detection, the other one was using the 531-FIP-*rpoB* primer for *Mycobacterium tuberculosis* DNA detection. Reactions were performed either in a thermostat at 65 °C for 40 minutes with visualization of the reaction result using SYBR Green I or in real time (see the “Methods” chapter).

Using the developed method the DNA sample of 20 RIF<sup>R</sup> isolates from *Mycobacterium tuberculosis* was analyzed containing the Ser450Leu mutation in the *rpoB* gene, 10 RIF<sup>R</sup> isolates containing other mutations in the *rpoB* gene (especially in His445 and Asp440 codons) as well as 18 RIF<sup>S</sup> isolates without any mutations; the presence of mutations in the samples was determined using Sanger sequencing (Table 2). All tested samples were identified correctly, sensitivity and specificity of LAMP for detecting a Ser450Leu mutation in the *rpoB* gene was 100%.

The use of AS-LAMP on a small sample of 11 DNA samples from the sputum of patients with active bacteria excretion

showed complete concordance with the Sanger sequencing results (4 samples containing a mutation and 7 samples with no mutation).

Using human DNA as a matrix did not produce a significant signal.

It has been shown that analysis can be performed on crude lysates of bacterial cells. In this case, the total time of the analysis, starting from a biological sample, may not exceed 1,5 hour, given the fact that obtaining of crude mycobacterial lysates takes no more than 15–30 minutes.

## DISCUSSION

In the past few years, several approaches have been proposed to identify single nucleotide DNA replacements using the LAMP method. All of them use allele-specific hybridization with amplification products [20, 21], allele-specific primers [22, 23] as well as the oligonucleotides selectively blocking the amplification of the studied structural variants [24].

Allele-specific polymerase chain reaction (AS-PCR) is one of the most widely used methods for DNA mutations detection [25]. Classical AS-PCR variant implies the use of two allele-specific primers, in which the 3'-terminal nucleotide is complementary to the polymorphic nucleotide, and the third common primer. The method is based on the difference in the efficiency of paired and unpaired 3'-nucleotide elongation by DNA polymerase. Under ideal conditions (with complete elongation inhibition), this should lead to the absence of the amplification product in reaction with the primer to a mutation on the wild type DNA matrix.

To improve discrimination of products with “mutant” and “normal” DNA, the use of additional unpaired nucleotides at the

3'-end of the primer (at the -2, -3 or -4 position) is widely used for further destabilization of the duplex in order to reduce the efficiency of DNA polymerase elongation. We suggested that when elongating allele-specific primers with a chain-displacing DNA polymerase, a similar principle can be used. For the design of allele-specific primers, we chose the approach that was described in 2004. [26]. The authors proposed to increase the discrimination of the mutant allele by introduction of the second unpaired nucleotide at the -2 position of the allele-specific primer, as well as a simple set of rules for choosing the type of this base to achieve the maximum effect. Using these recommendations, we synthesized two fundamentally different sets of AS primers for isothermal loop amplification: the first one corresponds to FIP primer, the other one — to F3 primer.

Optimization of the detection of the TCG/TTG mutation (S450L) in the *rpoB* gene of *Mycobacterium tuberculosis* using the plasmid control DNA showed the preference of AS-FIP. Using it, we were able to classify all analyzed DNA samples of *Mycobacterium tuberculosis* isolates correctly, including the negative for TCG/TTG replacement (S450L) DNA samples carrying mutations in codons 445 and 440, by visual analysis of the results of isothermal amplification in a standard thermostat that maintains temperature of 65 °C. AS-LAMP was also effective in detecting the Ser450Leu mutation of the *rpoB* gene in DNA from sputum of patients with known *rpoB* gene mutation status. We managed to classify 4 samples with the Ser450Leu mutation and 7 samples without this mutation correctly. The proposed approach showed high specificity and sensitivity to identify the most common *Mycobacterium tuberculosis*

mutation causing resistance to rifampicin. Nevertheless, for a meaningful determination of the mentioned above parameters, it is necessary to test the method on a sample of a much larger scope.

Despite the fact that the overwhelming number of works on LAMP describes the qualitative detection of the presence of an infectious agent, this method also has a high potential for determining the structural polymorphism of the analyzed DNA. For example, it has been shown that it is possible to identify isolates of the Beijing *Mycobacterium tuberculosis* family using region RD207 and the Rv0679c gene as a target [27]. Our work contributes to the development of methods for identifying point mutations using LAMP and also increases the research potential of this method.

The limitations and disadvantages of the method proposed in this work include the need for additional validation of the method of extracting DNA and the associated amount of bacteria due to the dependence of the choice of the optimal analysis time, in which the positive signal of the mutation-specific system is not yet determined, on the mycobacterial DNA concentration.

## CONCLUSIONS

We have demonstrated the fundamental possibility of determining mutations TCG/TTG (S450L) in the *rpoB* gene from *Mycobacterium tuberculosis* by allele-specific loop-mediated isothermal amplification method with high reliability without the use of expensive equipment. The total time required to test a clinical DNA sample may not exceed 1,5 hour.

## References

1. Drobniowski FA, Wilson SM. The rapid diagnosis of isoniazid and rifampicin resistance in *Mycobacterium tuberculosis* — a molecular story. *J Med Microbiol*. 1998; 47 (3): 189–96.
2. Heifets LB. Antimycobacterial drugs. *Semin Respir Infect*. 1994; 9 (2): 84–103.
3. TB Drug Resistance Mutation Database. Available from: <https://tbdreamdb.ki.se/Data/MutationDetail.aspx?Areald=RIF&GeneID=Rv0667>.
4. Mokrousov I, Otten T, Vyshnevskiy B, Narvskaya O. Allele-specific *rpoB* PCR assays for detection of rifampin-resistant *Mycobacterium tuberculosis* in sputum smears. *Antimicrob Agents Chemother*. 2003; 47 (7): 2231–5.
5. Filipenko ML, Dymova MA, Hrapov EA, Bojarskih, UA, Petrenko TI, Cherednichenko AG i dr. Sposob vyjavlenija ustojchivyh k rifampicinu izolatov. *Vestnik NGU*. 2012; 10 (2): 101–6.
6. Gill P, Ghaemi A. Nucleic acid isothermal amplification technologies: a review. *Nucleosides Nucleotides Nucleic Acids*. 2008; 27 (3): 224–43.
7. Notomi T, Okayama H, Masubuchi H, Yonekawa T, Watanabe K, Amino N et al. Loop-mediated isothermal amplification of DNA. *Nucleic Acids Res*. 2000; 28 (12): E63.
8. Francois P, Tangomo M, Hibbs J, Bonetti E-J, Boehme CC, Notomi T et. al. Robustness of a loop-mediated isothermal amplification reaction for diagnostic applications. *FEMS Immunol Med Microbiol*. 2011; 62 (1): 41–8.
9. Mori Y, Nagamine K, Tomita N, Notomi T. Detection of loop-mediated isothermal amplification reaction by turbidity derived from magnesium pyrophosphate formation. *Biochem Biophys Res Commun*. 2001; 289 (1): 150–4.
10. Kouguchi Y, Fujiwara T, Teramoto M, Kuramoto M. Homogenous, real-time duplex loop-mediated isothermal amplification using a single fluorophore-labeled primer and an intercalator dye: Its application to the simultaneous detection of Shiga toxin genes 1 and 2 in Shiga toxigenic *Escherichia coli* isolates. *Mol Cell Probes*. 2010; 24 (4): 190–5.
11. Liu W, Huang S, Liu N, Dong D, Yang Z, Tang Y et al. Establishment of an accurate and fast detection method using molecular beacons in loop-mediated isothermal amplification assay. *Sci Rep*. 2017; (7): 40125.
12. Goto M, Honda E, Ogura A, Nomoto A, Hanaki K-I. Colorimetric detection of loop-mediated isothermal amplification reaction by using hydroxy naphthol blue. *Biotechniques*. 2009; 46 (3): 167–72.
13. Nagai K, Horita N, Yamamoto M, Tsukahara T, Nagakura H, Tashiro K et al. Diagnostic test accuracy of loop-mediated isothermal amplification assay for *Mycobacterium tuberculosis*: systematic review and meta-analysis. *Sci Rep*. 2016; (6): 39090.
14. World Health Organization, editors. Global Tuberculosis Programme The use of loop-mediated isothermal amplification (TB-LAMP) for the diagnosis of pulmonary tuberculosis: policy guidance. 2016.
15. Ostorbin IP, Boyarskikh UA, Filipenko ML. Large fragment of DNA polymerase I from *Geobacillus* sp. 777: cloning and comparison with DNA polymerases I in practical applications. *Mol Biotechnol*. 2015; 57 (10): 947–59.
16. Ostorbin IP, Belousova EA, Zakabunin AI, Boyarskikh UA, Filipenko ML. Comparison of fluorescent intercalating dyes for quantitative loop-mediated isothermal amplification (qLAMP). *Biotechniques*. 2016; 61 (1): 20–5.
17. Badolo A, Bando H, Traoré A, Ko-ketsu M, Guelbeogo WM, Kanuka H et al. Detection of G119S ace-1 R mutation in field-collected *Anopheles gambiae* mosquitoes using allele-specific loop-mediated isothermal amplification (AS-LAMP) method. *Malar J*. 2015; (14): 477.
18. Carlos FF, Veigas B, Matias AS, Doria G, Flores O, Baptista PV. Allele specific LAMP-gold nanoparticle for characterization of single nucleotide polymorphisms. *Biotechnol Reports*. 2017; (16): 21–5.
19. Chakrabarti R, Schutt CE. The enhancement of PCR amplification by low molecular-weight sulfones. *Gene*. 2001; 274 (1–2): 293–8.
20. Jiang YS, Bhadra S, Li B, Wu YR, Milligan JN, Ellington AD. Robust strand exchange reactions for the sequence-specific,

- real-time detection of nucleic acid amplicons. *Anal Chem.* 87 (6): 3314–20.
21. Nakamura N, Ito K, Takahashi M, Hashimoto K, Kawamoto M, Yamanaka M et al. Detection of six single-nucleotide polymorphisms associated with rheumatoid arthritis by a loop-mediated isothermal amplification method and an electrochemical DNA chip. *Anal Chem.* 2007; 79 (12): 9484–93.
  22. Yongkiettrakul S, Kampeera J, Chareanchim W, Rattanajak R, Pornthanakasem W, Kiatpathomchai W et al. Simple detection of single nucleotide polymorphism in *Plasmodium falciparum* by SNP-LAMP assay combined with lateral flow dipstick. *Parasitol Int.* 2017; 66 (1): 964–71.
  23. Zhang L, Zhang Y, Wang C, Feng Q, Fan F, Zhang G, et al. Integrated microcapillary for sample-to-answer nucleic acid pretreatment, amplification, and detection. *Anal Chem.* 2014; 86 (20): 10461–6.
  24. Itonaga M, Matsuzaki I, Warigaya K, Tamura T, Shimizu Y, Fujimoto M, et al. Novel methodology for rapid detection of KRAS mutation using PNA-LNA mediated loop-mediated isothermal amplification. *PLoS One.* 2016; (11): e0151654.
  25. Newton CR, Graham A, Heptinstall LE, Powell SJ, Summers C, Kalsheker N, et al. Analysis of any point mutation in DNA. The amplification refractory mutation system (ARMS). *Nucleic Acids Res.* 1989; 17 (7): 2503–16.
  26. Li B, Kadura I, Fu D-J, Watson DE. Genotyping with TaqMAMA. *Genomics.* 2004; 83 (2): 311–20.
  27. Nagai Y, Iwade Y, Nakano M, Akachi S, Kobayashi T, Nishinaka T. Rapid and simple identification of Beijing genotype strain of *Mycobacterium tuberculosis* using a loop-mediated isothermal amplification assay. *Microbiol Immunol.* 2016; 60 (7): 459–67.

## Литература

1. Drobniowski FA, Wilson SM. The rapid diagnosis of isoniazid and rifampicin resistance in *Mycobacterium tuberculosis* — a molecular story. *J Med Microbiol.* 1998; 47 (3): 189–96.
2. Heifets LB. Antimycobacterial drugs. *Semin Respir Infect.* 1994; 9 (2): 84–103.
3. TB Drug Resistance Mutation Database. Доступно по ссылке: <https://tbdreamdb.ki.se/Data/MutationDetail.aspx?Areald=RIF&GeneID=Rv0667>.
4. Mokrousov I, Otten T, Vyshnevskiy B, Narvskaya O. Allele-specific rpoB PCR assays for detection of rifampin-resistant *Mycobacterium tuberculosis* in sputum smears. *Antimicrob Agents Chemother.* 2003; 47 (7): 2231–5.
5. Филипенко М. Л., Дымова М. А., Храпов Е. А., Боярских, У. А., Петренко Т. И., Чередииченко А. Г. и др. Способ выявления устойчивых к рифампицину изолятов. *Вестник НГУ.* 2012; 10 (2): 101–6.
6. Gill P, Ghaemi A. Nucleic acid isothermal amplification technologies: a review. *Nucleosides Nucleotides Nucleic Acids.* 2008; 27 (3): 224–43.
7. Notomi T, Okayama H, Masubuchi H, Yonekawa T, Watanabe K, Amino N et al. Loop-mediated isothermal amplification of DNA. *Nucleic Acids Res.* 2000; 28 (12): E63.
8. Francois P, Tangomo M, Hibbs J, Bonetti E-J, Boehme CC, Notomi T et al. Robustness of a loop-mediated isothermal amplification reaction for diagnostic applications. *FEMS Immunol Med Microbiol.* 2011; 62 (1): 41–8.
9. Mori Y, Nagamine K, Tomita N, Notomi T. Detection of loop-mediated isothermal amplification reaction by turbidity derived from magnesium pyrophosphate formation. *Biochem Biophys Res Commun.* 2001; 289 (1): 150–4.
10. Kouguchi Y, Fujiwara T, Teramoto M, Kuramoto M. Homogenous, real-time duplex loop-mediated isothermal amplification using a single fluorophore-labeled primer and an intercalator dye: Its application to the simultaneous detection of Shiga toxin genes 1 and 2 in Shiga toxinigenic *Escherichia coli* isolates. *Mol Cell Probes.* 2010; 24 (4): 190–5.
11. Liu W, Huang S, Liu N, Dong D, Yang Z, Tang Y et al. Establishment of an accurate and fast detection method using molecular beacons in loop-mediated isothermal amplification assay. *Sci Rep.* 2017; (7): 40125.
12. Goto M, Honda E, Ogura A, Nomoto A, Hanaki K-I. Colorimetric detection of loop-mediated isothermal amplification reaction by using hydroxy naphthol blue. *Biotechniques.* 2009; 46 (3): 167–72.
13. Nagai K, Horita N, Yamamoto M, Tsukahara T, Nagakura H, Tashiro K et al. Diagnostic test accuracy of loop-mediated isothermal amplification assay for *Mycobacterium tuberculosis*: systematic review and meta-analysis. *Sci Rep.* 2016; (6): 39090.
14. World Health Organization, editors. Global Tuberculosis Programme The use of loop-mediated isothermal amplification (TB-LAMP) for the diagnosis of pulmonary tuberculosis: policy guidance. 2016.
15. Ostorbin IP, Boyarskikh UA, Filipenko ML. Large fragment of DNA polymerase I from *Geobacillus* sp. 777: cloning and comparison with DNA polymerases I in practical applications. *Mol Biotechnol.* 2015; 57 (10): 947–59.
16. Ostorbin IP, Belousova EA, Zakabunin AI, Boyarskikh UA, Filipenko ML. Comparison of fluorescent intercalating dyes for quantitative loop-mediated isothermal amplification (qLAMP). *Biotechniques.* 2016; 61 (1): 20–5.
17. Badolo A, Bando H, Traoré A, Ko-ketsu M, Guelbeogo WM, Kanuka H et al. Detection of G119S ace-1 R mutation in field-collected *Anopheles gambiae* mosquitoes using allele-specific loop-mediated isothermal amplification (AS-LAMP) method. *Malar J.* 2015; (14): 477.
18. Carlos FF, Veigas B, Matias AS, Doria G, Flores O, Baptista PV. Allele specific LAMP-gold nanoparticle for characterization of single nucleotide polymorphisms. *Biotechnol Reports.* 2017; (16): 21–5.
19. Chakrabarti R, Schutt CE. The enhancement of PCR amplification by low molecular-weight sulfones. *Gene.* 2001; 274 (1–2): 293–8.
20. Jiang YS, Bhadra S, Li B, Wu YR, Milligan JN, Ellington AD. Robust strand exchange reactions for the sequence-specific, real-time detection of nucleic acid amplicons. *Anal Chem.* 87 (6): 3314–20.
21. Nakamura N, Ito K, Takahashi M, Hashimoto K, Kawamoto M, Yamanaka M et al. Detection of six single-nucleotide polymorphisms associated with rheumatoid arthritis by a loop-mediated isothermal amplification method and an electrochemical DNA chip. *Anal Chem.* 2007; 79 (12): 9484–93.
22. Yongkiettrakul S, Kampeera J, Chareanchim W, Rattanajak R, Pornthanakasem W, Kiatpathomchai W et al. Simple detection of single nucleotide polymorphism in *Plasmodium falciparum* by SNP-LAMP assay combined with lateral flow dipstick. *Parasitol Int.* 2017; 66 (1): 964–71.
23. Zhang L, Zhang Y, Wang C, Feng Q, Fan F, Zhang G, et al. Integrated microcapillary for sample-to-answer nucleic acid pretreatment, amplification, and detection. *Anal Chem.* 2014; 86 (20): 10461–6.
24. Itonaga M, Matsuzaki I, Warigaya K, Tamura T, Shimizu Y, Fujimoto M, et al. Novel methodology for rapid detection of KRAS mutation using PNA-LNA mediated loop-mediated isothermal amplification. *PLoS One.* 2016; (11): e0151654.
25. Newton CR, Graham A, Heptinstall LE, Powell SJ, Summers C, Kalsheker N, et al. Analysis of any point mutation in DNA. The amplification refractory mutation system (ARMS). *Nucleic Acids Res.* 1989; 17 (7): 2503–16.
26. Li B, Kadura I, Fu D-J, Watson DE. Genotyping with TaqMAMA. *Genomics.* 2004; 83 (2): 311–20.
27. Nagai Y, Iwade Y, Nakano M, Akachi S, Kobayashi T, Nishinaka T. Rapid and simple identification of Beijing genotype strain of *Mycobacterium tuberculosis* using a loop-mediated isothermal amplification assay. *Microbiol Immunol.* 2016; 60 (7): 459–67.

## EVALUATION OF THE EJACULATE MICROBIOTA BY REAL-TIME PCR AND CULTURE-BASED TECHNIQUE

Voroshilina ES<sup>1,2</sup>✉, Zornikov DL<sup>1</sup>, Panacheva EA<sup>1,2</sup><sup>1</sup> Ural State Medical University of the Ministry of health, Yekaterinburg, Russia<sup>2</sup> Medical Center "Garmonia", Yekaterinburg, Russia

Among other things male sterility can be caused by inflammatory diseases of the urogenital tract, often associated with opportunistic microorganisms. Thus, it is necessary to implement modern methods for the detection and identification of opportunistic microorganisms in the urogenital tract. The aim of the work was to conduct comparative analysis of the ejaculate microbiota from men of the reproductive age and studied using quantitative polymerase chain reaction (PCR) and culture method. 86 samples of ejaculate collected from men aged 18–57 years after observing sexual abstinence for 3–5 days were examined. With culture study in 50% of samples we observed growth of gram positive facultative anaerobic bacteria in the amount less than  $10^3$  CFU/ml; in 16.3% of samples — the growth of bacteria was not observed. With real-time PCR in each sample 8–15 groups of microorganisms were detected (including the prevailing groups) in the amount of  $10^2$ – $10^6$  GE/ml. In all 86 samples obligate anaerobes that cannot not be cultured *in vitro* were detected. The predominant groups of microorganisms, as determined by real-time PCR, were detected by the culture method only in 24.4% of cases.

**Keywords:** ejaculate microbiota, real-time PCR, culture-based technique

**Acknowledgments:** the authors would like to thank V. N. Khayutin, director of Garmonia Medical Center, for allowing to conduct the study in the clinic's laboratory department.

**Author contribution:** Voroshilina ES — organization of the study, conducting tests, data analysis, article authoring; Zornikov DL — data analysis, statistical processing, article authoring; Panacheva EA — literature review, clinical data collection, statistical analysis, article authoring.

**Compliance with ethical standards:** the study was approved by the Ethics Committee of Ural State Medical University, Federal State Budget Educational Institution of Higher Education under the Ministry of Health of the Russian Federation (Minutes № 4 of October 18, 2017). All patients signed the informed written consent to participation in the study.

✉ **Correspondence should be addressed:** Ekaterina S. Voroshilina  
Furmanova 30, Yekaterinburg, 620142; voroshilina@gmail.com

**Received:** 11.02.2019 **Accepted:** 28.02.2019 **Published online:** 11.03.2019

**DOI:** 10.24075/brsmu.2019.009

## СРАВНИТЕЛЬНОЕ ИССЛЕДОВАНИЕ МИКРОБИОТЫ ЭЯКУЛЯТА МЕТОДОМ КОЛИЧЕСТВЕННОЙ ПЦР И КУЛЬТУРАЛЬНЫМ МЕТОДОМ

Е. С. Ворошилина<sup>1,2</sup> ✉, Д. Л. Зорников<sup>1</sup>, Е. А. Паначева<sup>1,2</sup><sup>1</sup> Уральский государственный медицинский университет, Екатеринбург, Россия<sup>2</sup> Медицинский центр «Гармония», Екатеринбург, Россия

Одной из причин мужского бесплодия могут быть воспалительные заболевания уrogenитального тракта, развитие которых в ряде случаев ассоциировано с условно-патогенными микроорганизмами (УПМ). В связи с этим актуальна проблема внедрения современных методов выявления и идентификации УПМ в уrogenитальном тракте. Целью работы было провести сравнительный анализ результатов исследования микробиоты эякулята мужчин репродуктивного возраста с помощью количественной полимеразной цепной реакции (ПЦР) (тест Андрофлор) и культурального метода. Исследовали 86 образцов эякулята, собранных у мужчин в возрасте 18–57 лет после соблюдения полового воздержания в течение 3–5 суток. При культуральном исследовании в 50% образцов наблюдали рост грамположительных факультативно анаэробных бактерий в количестве менее  $10^3$  КОЕ/мл; в 16,3% образцов — роста бактерий отмечено не было. При использовании ПЦР в реальном времени (ПЦР-РВ) в каждом образце выявляли 8–15 групп микроорганизмов (в том числе определяли преобладающую) в количестве  $10^2$ – $10^6$  ГЭ/мл. Во всех 86 образцах были обнаружены облигатные анаэробы, которые не культивируются *in vitro*. Преобладающие группы микроорганизмов, определяемые в ПЦР-РВ, были выявлены культуральным методом только в 24,4% случаев.

**Ключевые слова:** микробиота эякулята, ПЦР-РВ, культуральный метод

**Благодарности:** авторы благодарят директора Медицинского центра «Гармония» В. Н. Хаютина за предоставленную возможность проведения исследования на базе лабораторного отделения клиники.

**Информация о вкладе авторов:** Е. С. Ворошилина — организация исследования, выполнение ПЦР-РВ, анализ данных, написание статьи; Д. Л. Зорников — анализ данных, статистическая обработка, написание статьи; Е. А. Паначева — обзор литературы, сбор клинических данных, статистический анализ, написание статьи.

**Соблюдение этических стандартов:** исследование одобрено этическим комитетом при ФГБОУ ВО УГМУ МЗ РФ (протокол № 4 от 18 октября 2017 г.). Все пациенты подписали информированное письменное согласие на участие в исследовании.

✉ **Для корреспонденции:** Екатерина Сергеевна Ворошилина  
ул. Фурманова, 30, г. Екатеринбург, 620142; voroshilina@gmail.com

**Статья получена:** 11.02.2019 **Статья принята к печати:** 28.02.2019 **Опубликована онлайн:** 11.03.2019

**DOI:** 10.24075/vrgmu.2019.009

The idea of the sterility of some biotopes, urine and bladder in particular, has changed in a decade due to new data about human microbiome composition. Urine of healthy men contains a number of opportunistic microorganisms (OM) of genus *Lactobacillus*, *Sneathia*, *Veillonella*, *Corynebacterium*, *Prevotella*, *Streptococcus* and *Ureaplasma* [1]. Earlier, it was shown that bacteria inhabit only the urethra and coronal

sulcus of the healthy men's urogenital tract (UGT) [2, 3, 4]. Later, bacteria were found in the upper sections of the UGT of clinically healthy men, prostate tissue in particular [5].

Semen microbiota originates from different parts of the UGT, and it is dominated with urethral bacteria in healthy men. In patients with symptoms of urogenital inflammation bacteria from the upper parts of the UGT could be detected in semen [2].

Composition of semen microbiota in patients with infertility and prostatitis is of great interest for practical medicine. Recently, a number of differences were discovered between the composition of semen microbiota of healthy men and those suffering from prostatitis: the former had more *Lactobacillus iners* therein, while the semen of the latter generally had a greater number and diversity of microorganisms, including *Proteobacteria* phylum [6].

Male UGT infections are the cause of male infertility in 6–10% of cases [7]. However, etiology of prostatitis remains unclear; moreover, an appropriate treatment could not be prescribed to symptomatic patients with negative semen cultures [8]. Contribution of specific OM to the development of the UGT inflammatory processes is debatable. In the absence of obligate pathogens, opportunistic bacteria, like *Escherichia coli*, *Klebsiella spp.*, *Proteus spp.*, *Enterococcus spp.*, *Staphylococcus spp.*, *Ureaplasma spp.*, *Mycoplasma hominis* etc. could trigger an inflammation [7].

Asymptomatic and subclinical forms of male urogenital infections have been frequently detected in the last decades. Evaluation of local inflammatory response and of the UGT microbiota composition helps us to establish a diagnosis in these cases. The use of highly informative laboratory tests is of great significance in the UGT's microbiota studies.

A number of methods are used for the semen microbiota composition evaluation. The real-time PCR (Androflor test) was introduced recently along with the traditional culture-based techniques. This method allows identifying all participants of complex microbial communities, including non-culturable microorganisms. Given the limited number of valid comparative studies, RT PCR could not be widely recommended instead of culture-based techniques.

This study aimed to compare semen microbiota composition analyzed by means of culture-based technique and the RT PCR (Androflor test).

## METHODS

From January to May 2018, 86 semen samples were obtained from men who attended "Garmonia" Medical Center (Yekaterinburg) for resolving their reproduction problems. The patients were aged 18 to 57 years; mean age —  $34 \pm 6.7$  years. The inclusion criteria were: 3–5 days of sexual abstinence before performing the test in order to prevent semen contamination with female transient microflora (*Lactobacillus spp.*). The exclusion criteria were: detection of obligate pathogens (*Chlamydia trachomatis*, *Neisseria gonorrhoeae*, *Mycoplasma genitalium*, *Trichomonas vaginalis*). Prior to semen collection the patients urinated, completely emptying their bladders. The semen was collected into a 60 ml sterile container through masturbation; the patients were instructed not to touch the container's walls and lid with their hands. The samples were brought to the laboratory in a thermal container within 4 hours from collection. The semen culture and RT PCR were performed simultaneously from a given sample.

Semen cultures were performed at the Microbiological laboratory "Quality Med" (Yekaterinburg). One ml of semen was diluted with sterile saline (1 : 1) and centrifuged at 1500 rpm for 15 minutes. After removal of the supernatant, 10  $\mu$ l of the sediment were plated on 5 nutrient media (Bio-Rad; France): 5% blood agar with whey and yeast extract; chocolate agar based on blood agar; UriSelect4 chromogenic agar; Saburo agar; Mannitol salt agar. The samples were incubated at 37 °C for 24–48 h in aerobic conditions and in the 5% CO<sub>2</sub> atmosphere. The resulting colonies were identified with the matrix-assisted

laser desorption/ionization time-of-flight mass spectrometry (MALDI-TOF MS) in a Vitek MS analyzer (BioMerieux; France).

PCR tests were performed at the laboratory of the "Garmonia" Medical Center (Yekaterinburg). One ml of semen was put into an Eppendorf tube with 1 ml of transport medium with mucolytic (InterLabService; Russia), which was then shaken in the Fugue/Vortex Micro-Spin FV-2400 centrifuge (BioSan; Latvia) until the substances mixed completely. The tube was centrifuged at 13,000 rpm for 10 minutes. After removing the supernatant, 50  $\mu$ l of the precipitate was used for extraction of the DNA, using the PROBA-GS reagent kit (DNA-Technology; Russia) following the manufacturer's instructions. RT PCR was performed using the Androflor kit (DNA-Technology; Russia) and the DT-96 detection amplifier following the manufacturer's instructions (DNA-Technology; Russia) [9]. Once the amplification reaction was over, the special software (DNA-Technology; Russia) was used to automatically calculate the total bacterial load (TBL) and the proportion of particular species and groups of bacteria in relation to the TBL in the given sample. The quantity of identified microorganisms was expressed in genome equivalents per 1 ml (GE/ml). The kit allows identifying the following groups of OM: Gram-positive facultative anaerobes (*Streptococcus spp.*, *Staphylococcus spp.*, *Corynebacterium spp.*); Gram-negative facultative anaerobes (*Haemophilus spp.*, *Pseudomonas aeruginosa* / *Ralstonia spp.* / *Burkholderia spp.*); *Enterobacteriaceae* / *Enterococcus spp.* group; obligate anaerobes (*Gardnerella vaginalis*, *Eubacterium spp.*, *Sneathia spp.* / *Leptotrichia spp.* / *Fusobacterium spp.*, *Megasphaera spp.* / *Veillonella spp.* / *Dialister spp.*, *Bacteroides spp.* / *Porphyromonas spp.* / *Prevotella spp.*, *Anaerococcus spp.*, *Peptostreptococcus spp.*, *Atopobium cluster*), mycoplasmas (*Mycoplasma hominis*, *Ureaplasma urealyticum*, *Ureaplasma parvum*), transient microbiota (*Lactobacillus spp.*), yeast-like fungi (*Candida spp.*).

Microsoft Excel 2016 (Microsoft; USA) and WinPepi statistical software were used to process the data obtained. Differences in prevalence of microbiota types detected by culture technique and RT PCR were evaluated using Fisher's test; the statistical significance was set at  $p < 0.05$  for correction of multiple comparisons.

## RESULTS

### Semen culture results

Semen cultures were positive in 72 (83.7%) cases and 28 bacterial species were identified. Fourteen (16.3%) samples were culture negative.

The growth of a single bacterial culture was established in 33 (38.4%) samples. 10 bacterial species, mostly commensals, were identified. 21 (63.6%) of the 33 samples contained one of the Gram-positive facultative anaerobes: *Staphylococcus spp.* (*S. epidermidis*, *S. haemolyticus*, *S. hominis*); *Streptococcus spp.* (*S. anginosus*), *Corynebacterium coyleae*, *Dermabacter hominis*. In 8 (24.2%) cases *Enterococcus faecalis* was found, in 4 (12.2%) samples out of 33 — Gram-negative facultative anaerobes *Klebsiella oxytoca*, *E. coli*, *Moraxella osloensis* were detected.

The majority of the samples (28 out of 33, or 84.8%) have the colony count of less than  $10^2$ – $10^3$  CFU/ml, which is considered clinically insignificant. 6 (18.2%) samples have the colony count of  $10^4$  CFU/ml, and only in one sample the colony count was  $10^6$  CFU/ml.

Two bacterial cultures were detected in 27 (31.4%) out of 86 samples, 20 bacterial species were identified. Gram-positive facultative anaerobes were identified in 16 (59.3%) samples out

of 27. The most typical combinations were *S. mitis* / *S. oralis* (8 cases); *C. glucuronolyticum* / *S. epidermidis* and *E. faecalis* / *S. epidermidis* (2 cases each); *E. faecalis* / *S. haemolyticus*, *S. capitis* / *S. haemolyticus*, *S. epidermidis* / *S. agalactiae*, *C. glucuronolyticum* / *E. faecalis* (1 case each). Gram-negative facultative anaerobes (*Enterobacter hormaechei* / *Pseudomonas aeruginosa*) were established in one sample only. The combination of Gram-negative and Gram-positive facultative anaerobes was established in 5 (18.5%) samples. The most typical combinations were: *E. faecalis* / *E. coli* (2 cases); *Klebsiella pneumoniae* / *S. haemolyticus* (2 cases) and *E. Faecalis* / *K. oxytoca* (1 case). *G. vaginalis* was identified in 2 samples (7.4%), accompanied by *Actinomyces neuii* in one specimen and *S. epidermidis* in the other. Another 2 (7.4%) samples contained *Lactobacillus spp* in combination with Gram-positive cocci: *L. iners* / *S. gallolyticus*, *L. crispatis* / *S. warneri*.

The majority of samples (17 of 27 them, 62.9%) have the colony count of less than  $10^2$ – $10^3$  CFU/ml, which is considered clinically insignificant [10]. The colony count of  $10^4$  CFU/ml of at least one bacterial species (*E. faecalis*, *K. oxytoca*, *G. vaginalis*, *S. agalactiae*) was established in 9 (33.3%) specimens. The colony count of both isolated species (*K. pneumoniae* / *S. haemolyticus*) reached  $10^6$  CFU/ml just in one specimen.

Three bacterial cultures were detected in 9 samples (10.5%), 12 species were identified in various combinations. The mixed microbiota with Gram-positive facultative anaerobes was established in 4 (44.4%) out of 9 specimens: *C. glucuronolyticum*, *S. mitis* / *S. oralis*, *S. hominis*. Combinations of *C. glucuronolyticum* / *G. vaginalis* / *S. anginosus* were detected in 2 (22.2%) samples. The combinations of Gram-positive and Gram-negative facultative anaerobes were established in 3 cases: *S. agalactiae* / *E. coli* / *C. glucuronolyticum*; *Corynebacterium amycolatum* / *E. hormaechei* / *E. Faecalis* and *E. faecalis* / *E. coli* / *S. anginosus*.

The colony count was clinically insignificant (less than  $10^3$  CFU/ml) in 3 out of 9 samples. In 6 other specimens the colony count of at least one species was  $10^4$  CFU/ml or more with the prevalence of *C. glucuronolyticum*, *E. hormaechei*, *E. faecalis*, *S. anginosus*, *G. vaginalis* or *S. agalactiae*.

Four and more bacterial cultures were detected in just 3 samples. The combination of *C. gluconormum* / *E. faecalis* / *S. mitis* / *S. oralis* / *E. coli*, with *E. faecalis*  $10^4$  CFU/ml, was determined in one specimen. In two other cases the combinations of commensal Gram-positive bacteria with colony count less than  $10^3$  CFU/ml suggested potential contamination with skin microflora during semen collection.

### Semen RT PCR results

RT PCR identified microflora in all 86 semen specimens: from 8 to 15 groups of bacteria were detected in each, the amounts ranging from  $10^2$  to  $10^6$  GE/ml. A mathematical algorithm was applied to calculate the proportion of each group of microorganisms in the TBL; the predominant group of bacteria (the proportion of which in the TML exceeds that of other bacteria detected) was determined in the most samples.

Gram-positive facultative anaerobes — the UGT microbiota's *Streptococcus spp.*, *Staphylococcus spp.*, and *Corynebacterium spp.* — were abundant in 15 (17.4%) samples. Obligate anaerobes prevailed in 27 (31.4%) samples, Gram-negative facultative anaerobes (*P. aeruginosa* / *Ralstonia spp.* / *Burkholderia spp.* and *Haemophilus spp.*) — in 4 (4.7%) samples. *Enterobacteriaceae* / *Enterococcus spp.* group was abundant in 23 (26.7%) samples; transient microbiota (*Lactobacillus spp.*) — in 7 (8.1%) samples. Polymicrobial communities without a predominant group were identified in 10 (11.6%) samples. The latter demonstrates that RT PCR detected heterogeneous semen microbiota, culture technique failed to find.

When analysing the semen microbiota RT PCR results, we considered the fact that the microorganisms detected in semen could not be regarded as a microbial community or a microbiocenosis because they come from different parts of the man's UGT. Therefore, we suggest classifying the semen microbiota according to the predominant group of microorganisms. This criterion allowed discriminating 6 types of the semen microbiota; their detection rate was analyzed taking into account the TBL (Table 1).

**Table 1.** Semen microbiota variants, RT PCR data ( $n = 86$ )

Semen microbiota type	Predominant group of microorganisms in the semen microflora	TBM < $10^3$ GE/ml $n$ (%)	TBM $10^3$ < $10^4$ GE/ml $n$ (%)	TBM > $10^4$ GE/ml $n$ (%)	Significance of differences <sup>3</sup>
		1	2	3	
Microbiota type I	Gram-positive facultative anaerobes	4 (14.8)	9 (19.6)	2 (15.4)	$p_{1-2} > 0.05$ $p_{1-3} > 0.05$ $p_{2-3} > 0.05$
Microbiota type II	Gram-negative facultative anaerobes	2 (7.4)	2 (4.4)	0	$p_{1-2} > 0.05$ $p_{1-3} > 0.05$ $p_{2-3} > 0.05$
Microbiota type III	<i>Enterobacteriaceae spp.</i> / <i>Enterococcus spp.</i> group <sup>1</sup>	12 (44.4)	8 (17.4)	3 (23.1)	$p_{1-2} < 0.05$ $p_{1-3} < 0.05$ $p_{2-3} > 0.05$
Microbiota type IV	Obligate anaerobes	2 (7.4)	19 (41.3)	6 (46.2)	$p_{1-2} < 0.01$ $p_{1-3} < 0.01$ $p_{2-3} > 0.05$
Microbiota type V	Transient microflora ( <i>Lactobacillus spp.</i> )	1 (3.7%)	4 (8.7)	2 (15.4)	$p_{1-2} > 0.05$ $p_{1-3} > 0.05$ $p_{2-3} > 0.05$
Microbiota type VI	No predominant group (polymicrobial community) <sup>2</sup>	6 (22.2%)	4 (8.7)	0	$p_{1-2} > 0.05$ $p_{1-3} > 0.05$ $p_{2-3} > 0.05$
	Total group	27	46	13	

**Note:** <sup>1</sup> — this microbiota type was suggested due to the specifics of the Androflor test (*Enterobacteriaceae spp.* / *Enterococcus spp.* are detected in a tube separately from other Gram-positive and Gram-negative facultative anaerobes without species identification); <sup>2</sup> — this variant was applied when a proportion of several detected groups of microorganisms slightly differed from each other; <sup>3</sup> — Fisher's test enabled calculation of significance of the differences.

Several patterns were revealed while analysing the data. The higher semen TBL corresponded with the increased proportion of microbiota type IV (with predominance of obligate anaerobes) and lower detection rate of microbiota type III (with predominance of *Enterobacteriaceae spp./ Enterococcus spp.* group). We have also noted the increased detection rate of microbiota type V (with predominance of transient microbiota, *Lactobacillus spp.*); this can be the result of the patients not abstaining from intercourse for 3–5 days before the semen collection. Low TBL in semen samples often corresponded with microbiota type III and VI (mixed microbial community, no dominating group). As the TBL increased the microbiota composition changed.

Microbiota type I (with predominance of Gram-positive facultative anaerobes) was detected by RT PCR in 17.4% of samples only, while semen culture determined this variant in 50% cases.

### Comparison of the RT PCR and culture-based technique results

RT PCR in 100% of cases confirmed culture findings. However, in all culture-positive semen samples additional microorganisms were identified by molecular technique, mostly of the non-culturable or difficult to culture species. It should be noted specifically that RT PCR revealed obligate anaerobes, which cannot grow *in vitro*, in all samples.

According to the RT PCR results, microorganisms were found in all culture-negative samples. Microbiota type III (with predominance of *Enterobacteriaceae spp. / Enterococcus spp.* group) was determined in 5 (35.7%) samples out of 14; microbiota type I (with predominance of Gram-positive facultative anaerobes) — in 4 (28.5%) samples out of 14; microbiota type IV (with predominance of obligate anaerobes) — in 2 (14.3%) samples; microbiota type II, V and VI — in 1 sample each (7.2%). In all these samples the TBL was less than  $10^4$  GE/ml, which may partly explain why the cultures were negative.

Next, we analyzed the concordance of the determined predominant group of bacteria by culture method and by RT PCR (Table 2).

The culture results matched those of RT PCR in 21 (24.4%) of 86 cases. In these samples, the only isolated species or the quantitatively predominant species detected by culture method belonged to the same predominant group as detected by the RT PCR. In other cases, either culture was negative (14 (16.8%)) or RT PCR determined other groups of bacteria as predominant.

The TBL detected by RT PCR corresponded to colony count in culture technique in 41 (47.7%) of 86 samples; in 38 (44%) cases, there were 10 to 1000-fold difference. In 7 (8.3%) samples, the number of microorganisms identified by RT PCR was less than colony count by the culture technique. The discordant result occurred when the following species were cultured: *S. agalactiae* (2 samples), *S. anginosus* (2 samples), *S. mitis / S. oralis*, *S. hominis*, *L. crispatus* (1 sample each). The *in vitro* growth properties of bacteria can vary significantly, and some species could not stand even short-term transportation.

### DISCUSSION

Using culture technique, the clinically insignificant amounts of normal microbiota microorganisms, mainly Gram-positive facultative anaerobes, were detected in most semen samples. Their colony count was less than  $10^4$  CFU/ml in 43% of samples [10]. A number of commensal species cultured in the sample may indicate specimen contamination.

RT PCR in 100% of cases confirmed the results of semen cultures. The growth of a pure culture of a given microorganism corresponded to the positive signal in the relevant Androflor group, including all the 14 culture-negative samples. The lack of *in vitro* growth of most microorganism groups detected by RT PCR is quite understandable: most of them are either difficult to culture or non-culturable [11].

RT PCR and culture results mainly differed in determination of the predominant microbial group. The two methods gave identical results in 24.4% of cases. There are two possible reasons behind discordant results. Firstly, the bacteria have different *in vitro* growth properties, and secondly, some species may have not survived transportation. In addition, obligate anaerobic microorganisms cannot be detected using culture

**Table 2.** Comparison of the predominant groups of microorganisms according to culture-based technique and RT PCR results ( $n = 86$ )

Predominant group of bacteria according to RT PCR	Predominant group of bacteria according to culture-based technique						
	Gram-positive facultative anaerobes ( $n = 15$ )	Gram-negative facultative anaerobes ( $n = 4$ )	<i>Enterobacteriaceae spp./ Enterococcus spp.</i> group ( $n = 23$ )	Obligate anaerobes ( $n = 27$ )	Transient microflora ( $n = 7$ )	Mixed microflora ( $n = 10$ )	No microflora
Gram-positive facultative anaerobes ( $n = 15$ )	8	0	2	0	0	1	4
Gram-negative facultative anaerobes ( $n = 4$ )	0	0	0	0	0	1	2
<i>Enterobacteriaceae spp./ Enterococcus spp.</i> group ( $n = 23$ )	9	0	8	0	0	3	3
Obligate anaerobes ( $n = 27$ )	11	1	4	4	1	4	2
Transient microflora ( $n = 7$ )	5	0	0	0	1	0	1
Mixed microflora ( $n = 10$ )	7	0	2	0	0	0	1
No microflora	0	0	0	0	0	0	0

technique, which distorts the view of the semen microbiota's composition in general.

Culture technique and RT PCR determined the TBL per 1 ml differently in 52.3% of cases. In 44% of samples, the TBL determined using RT PCR exceeded that identified by the culture technique 10 to 1000-fold. In 7 (8.3%) cases, the situation was quite the opposite: culture technique identified higher total bacterial load than RT PCR. It should be noted here that we understand the flaws of direct comparison of microorganism amounts detected by RT PCR and culture technique. Semen's viscosity and uniformity are heterogeneous, thus, bacterial cells can be distributed unevenly throughout the examined sample. Moreover, prior to subjecting a sample to RT PCR testing, we treated it with a mucolytic medium, which reduced its viscosity and, probably, made the distribution of microorganisms in the sample more even.

The data obtained as a result of this research allow recommending RT PCR (Androflor test) as an alternative to the culture technique in the comprehensive examination of the semen microbiota.

## CONCLUSIONS

The advantages of RT PCR (Androflor test) for semen microbiota assessment were evaluated compared to culture method. Culture technique failed to reveal the majority of microorganisms in the samples; moreover, every sixth sample was considered culture negative. Using RT PCR, 8–15 bacterial groups in the amounts of  $10^2$ – $10^6$  GE/ml were identified in all samples. RT PCR established the predominant group of bacteria in most samples. Additional species other than those detected by the culture technique were registered in all 86 samples. As for the predominant bacterial groups, the culture results corresponded those of RT PCR in only 24.4% of cases; the discrepancies were mainly associated with the culture technique's inability to detect difficult to culture or non-culturable bacteria, whereas Androflor allows detecting such. The etiological significance of identifying certain predominant groups of microorganisms and their amounts requires further research that take into account the clinical data and the patient's diagnosis.

## References

1. Cornelia Gottschick, Zhi-Luo Deng, Marius Vital et al. The urinary microbiota of men and women and its changes in women during bacterial vaginosis and antibiotic treatment. *Microbiome*. 2017; 5 (99): 1–15.
2. Hou D, Zhou X, Zhong X, et al. Microbiota of the seminal fluid from healthy and infertile men. *FertilSteril*. 2013 Nov; 100(5): 1261–9.
3. Nelson DE, Dong Q, Van der Pol B, et al. Bacterial communities of the coronal sulcus and distal urethra of adolescent males. *PLoS One*. 2012; 7 (5): e36298.
4. Weng SL, Chiu CM, Lin FM, et al. Bacterial communities in semen from men of infertile couples: metagenomic sequencing reveals relationships of seminal microbiota to semen quality. *PLoS One*. 2014 Oct 23; 9 (10): e110152.
5. Domes T, Lo KC, Grober ED, et al. The incidence and effect of bacteriospermia and elevated seminal leukocytes on semen parameters. *Fertil Steril*. 2012 May; 97 (5): 1050–5.
6. Mändar R, Punab M, Korrovits P, et al. Seminal microbiome in men with and without prostatitis. *Int J Urol*. 2017 Mar; 24 (3): 211–6.
7. Schuppe H-C, Pilatz A, Hossain H, et al. Urogenital Infection as a Risk Factor for Male Infertility. *Deutsches Aerzteblatt Online*. 2017. DOI: 10.3238/arztebl.2017.0339.
8. Bozhedomov V. A. Hronicheskiy prostatit: novaja paradigma lechenija. *Urologija*. 2016; (36): 78–90. Russian.
9. Instrukcija po primeneniju nabora reagentov dlja issledovanija mikroflory urogenital'nogo trakta muzhchin metodom PCR v rezhime real'nogo vremeni Androflor® Skrin (ООО НПО «ДНК-Технология»). Dostupno po ssylke: <http://www.dna-technology.ru/information/aboutamethod/>. Russian.
10. Jungwirth A, Diemer T, Kopa Z, et al. EAU Guidelines on Male Infertility. 2017. Available from: [https://www.researchgate.net/publication/318239925\\_EAU\\_Guidelines\\_on\\_Male\\_Infertility\\_2017](https://www.researchgate.net/publication/318239925_EAU_Guidelines_on_Male_Infertility_2017).
11. Aragón IM, Herrera-Imbroda B, Queipo-Ortuño MI, et al. The Urinary Tract Microbiome in Health and Disease. *Eur Urol Focus*. 2018 Jan; 4 (1): 128–38.

## Литература

1. Cornelia Gottschick, Zhi-Luo Deng, Marius Vital et al. The urinary microbiota of men and women and its changes in women during bacterial vaginosis and antibiotic treatment. *Microbiome*. 2017; 5 (99): 1–15.
2. Hou D, Zhou X, Zhong X, et al. Microbiota of the seminal fluid from healthy and infertile men. *FertilSteril*. 2013 Nov; 100(5): 1261–9.
3. Nelson DE, Dong Q, Van der Pol B, et al. Bacterial communities of the coronal sulcus and distal urethra of adolescent males. *PLoS One*. 2012; 7 (5): e36298.
4. Weng SL, Chiu CM, Lin FM, et al. Bacterial communities in semen from men of infertile couples: metagenomic sequencing reveals relationships of seminal microbiota to semen quality. *PLoS One*. 2014 Oct 23; 9 (10): e110152.
5. Domes T, Lo KC, Grober ED, et al. The incidence and effect of bacteriospermia and elevated seminal leukocytes on semen parameters. *Fertil Steril*. 2012 May; 97 (5): 1050–5.
6. Mändar R, Punab M, Korrovits P, et al. Seminal microbiome in men with and without prostatitis. *Int J Urol*. 2017 Mar; 24 (3): 211–6.
7. Schuppe H-C, Pilatz A, Hossain H, et al. Urogenital Infection as a Risk Factor for Male Infertility. *Deutsches Aerzteblatt Online*. 2017. DOI: 10.3238/arztebl.2017.0339.
8. Божедомов В. А. Хронический простатит: новая парадигма лечения. *Урология*. 2016; (36): 78–90.
9. Инструкция по применению набора реагентов для исследования микрофлоры уrogenитального тракта мужчин методом ПЦР в режиме реального времени Андрофлор® Скрин (ООО НПО «ДНК-Технология»). Доступно по ссылке: <http://www.dna-technology.ru/information/aboutamethod/>.
10. Jungwirth A, Diemer T, Kopa Z, et al. EAU Guidelines on Male Infertility. 2017. Available from: [https://www.researchgate.net/publication/318239925\\_EAU\\_Guidelines\\_on\\_Male\\_Infertility\\_2017](https://www.researchgate.net/publication/318239925_EAU_Guidelines_on_Male_Infertility_2017).
11. Aragón IM, Herrera-Imbroda B, Queipo-Ortuño MI, et al. The Urinary Tract Microbiome in Health and Disease. *Eur Urol Focus*. 2018 Jan; 4 (1): 128–38.



According to the World Health Organization (WHO), stroke is the second leading cause of death worldwide. Each year more than 15 million people worldwide suffer stroke. Of these, 6 million die and another 5 million are permanently disabled [1]. The ischemic stroke is caused by angiostenosis or an abrupt blockage of cerebral arteries with resulting reduction in cerebral perfusion and rapid damage of brain tissues [2].

Recent studies show biochemical changes occurring in brain cells during ischemia. In particular, hypoxia increases extracellular concentration of glutamate, an important neurotransmitter, and its binding to glutamate receptors [3] leading to a sharp increase of intracellular calcium level. Uncontrolled  $\text{Ca}^{2+}$  regulation results in activation of  $\text{Ca}^{2+}$ -dependent proteins and upsetting the regulation of cellular cascades [4]. Biochemical changes result in reductions in cell pH and ATP production as well as changes in intracellular ionic ratios [5, 6]. At later stages of pathogenesis, DNA, proteins and lipids are damaged [7]. The pathologic events culminate in mitochondrial dysfunction and extensive cell death [8].

Lipids constitute about half of brain tissue dry weight and have important structural and metabolic functions. Glycerophospholipids and sphingolipids are major components of cellular membranes; cholesterol is a key component of lipid rafts, dynamic assemblies in the cell membrane, regulating membrane motility and signal transduction. Since lipids cannot pass through a blood-brain barrier (BBB), de novo synthesis of lipids occurs in nervous cells. NADPH plays the essential role in the lipid biosynthesis acting as a reducing equivalent in anabolic reactions.

Ischemia-reperfusion induces overproduction of reactive oxygen species (ROS) [9] leading to lipid peroxidation. Consequently, there are increased levels of lipid peroxidation products such as malondialdehyde and 4-hydroxynonenal [10] that can be used as markers of cellular oxidative stress.

In response to intracellular ROS increase, antioxidative defense mechanisms are activated in cells. Glutathione (GSH) plays a key role in thiol-disulfide exchange reactions [11, 12] while maintaining the redox state of the glutathione pool is mediated by NADPH-dependent systems [12]. Thus, both parameters are important in the regulation of protection processes against cell damage caused by oxidative stress during ischemia [13].

In our study, we estimated levels of the most important biochemical compounds related to lipid metabolism in rat brain tissues during ischemic damage. Measurements of metabolite concentrations were performed using commercially available kits and standard protocols (MDA, NADP(H)) [14, 15].

## METHODS

The study was carried out on male Wistar rats (weight ranging from 280 g to 330 g) obtained from Pushchino breeding facility (Moscow region; Russia). Animals were housed under standard vivarium conditions in plastic cages, three per cage. The animals had free access to food and water. The experimental work (surgeries and biochemical tests) was carried out within a month (June, 2018).

A middle cerebral artery occlusion (MCAO) was performed as described in [16]. Inhalation anesthesia with a mixture of isoflurane with air was used (Aerrane by Baxter; USA): 5% concentration for induction and 1.5% concentration for maintenance of general anesthesia.

The animals were analgesized with 5 mg/kg ketoprofen (Ketonal by Sandoz; Switzerland) administered subcutaneously; local analgesia was induced by administering 2% Novocaine.

0.185 mm MCAO (middle cerebral artery occlusion) sutures were used (403756PK10Re, Doccol; USA).

## Tissue sample preparation

The animals were randomized into five groups, four individuals each. The control group included intact animals. In the other four groups, the animals were subjected to permanent right middle cerebral artery occlusion (MCAO). Biochemical analysis was carried out at 5 time points: 1 hour (Group 2), 3 hours (Group 3), 6 hours (Group 4), and 24 hours (Group 5) post-ischemia.

Following 1 to 24 hours of occlusion, the animals were sacrificed and the brains were removed. Brain tissue without cerebellum and olfactory bulbs was frozen immediately in liquid nitrogen and then homogenized thoroughly. The received material was weighed and stored at  $-70\text{ }^{\circ}\text{C}$  until further processing.

## Measurement of FFA level

The quantification of free fatty acids in brain samples was performed with a Free Fatty Acid Quantification Assay Kit (Abcam; Cambridge, UK). At first, the free fatty acids are being converted to acyl-CoA under acyl-CoA synthetase action. Then specific enzyme oxidizes the obtained monoesters that is followed by reduction of colourless dye with formation of fluorescent compound (Ex. 535 nanometers; Em. 587 nanometers).

Tissue samples were thawed on ice and then homogenized in 200  $\mu\text{L}$  1% Triton X-100 in pure chloroform using a manual Potter homogenizer. The obtained homogenate was incubated on ice for 30 minutes to increase the efficiency of extraction. The extracts were centrifuged for 10 minutes at maximum speed, and after that, the organic phase was collected. To remove chloroform, the samples were air dried at  $50\text{ }^{\circ}\text{C}$  in a fume hood for an hour and then placed in vacuum dryer for the same time. The obtained lipid fraction was dissolved in 200  $\mu\text{L}$  Fatty Acid Assay Buffer by extensive vortexing.

Aliquots with volumes from 10 to 40  $\mu\text{L}$  were used for the assay. Sample volumes were adjusted to 50  $\mu\text{L}$  with Fatty Acid Assay Buffer solution. Also, a set of palmitic acid standards was prepared for standard curve plotting. 2  $\mu\text{L}$  ACS Reagent (the one with acyl-CoA synthetase activity) was added to each standard and sample well with subsequent incubation at  $37\text{ }^{\circ}\text{C}$  for 30 minutes. After that, 50  $\mu\text{L}$  of Reaction mix (45.6  $\mu\text{L}$  Assay Buffer; 0.4  $\mu\text{L}$  Fatty Acid Probe; 2  $\mu\text{L}$  Enzyme Mix; 2  $\mu\text{L}$  Enhancer) were added to each well, with following incubation at  $37\text{ }^{\circ}\text{C}$  for 30 minutes.

Fluorescence was measured using Tecan Infinite 200 Pro plate reader (Tecan; Switzerland) at Ex/Em = 535/587 nm. Based on standard readings, the dependence of fluorescence intensity on FFA content in the samples was determined. Based on that, concentrations of FFA in the test samples were calculated. The obtained values were normalized to corresponding tissue weight.

## Measurement of cholesterol level

Total cholesterol level (both free cholesterol and cholesteryl esters) in brain samples was quantified using commercially available Cholesterol/Cholesteryl Ester Detection Kit (Abcam; UK) according to the related protocol. In the assay, free cholesterol is oxidized by cholesterol dehydrogenase to generate NADH which reacts with a sensitive probe resulting in strong absorbance at 450 nm.

Tissue samples were thawed on ice and then homogenized in 200  $\mu\text{L}$   $\text{CHCl}_3$  : IPA : 10% NP-40 (7 : 11 : 0.1) using a manual Potter homogenizer. Each sample was centrifuged for 10 minutes at maximum speed, and after that, the organic phase was collected. To remove chloroform, the samples were air dried at 50  $^\circ\text{C}$  in a fume hood for an hour and then placed in vacuum dryer for the same time. The received lipid fraction was dissolved in 200  $\mu\text{L}$  Cholesterol Assay Buffer by extensive vortexing.

Aliquots with volumes from 10 to 40  $\mu\text{L}$  were used for the assay. Sample volumes were adjusted to 50  $\mu\text{L}$  with Cholesterol Assay Buffer. A set of cholesterol standards was prepared for standard curve plotting. 2  $\mu\text{L}$  Esterase (enzyme that hydrolyzes cholesterol esters to cholesterol) was added to each standard and sample well with following incubation at 37  $^\circ\text{C}$  for 30 minutes. After that, 48  $\mu\text{L}$  of Reaction mix (44  $\mu\text{L}$  Cholesterol Assay Buffer, 2  $\mu\text{L}$  Substrate Mix, 2  $\mu\text{L}$  Cholesterol Enzyme Mix) was added to each well, with subsequent incubation at 37  $^\circ\text{C}$  for 30 minutes.

The absorbance was measured using Tecan Infinite 200 Pro (Tecan; Switzerland) at 450 nm. Based on standard readings, the dependence of fluorescence intensity on cholesterol content in the samples was determined. After that the concentrations of total cholesterol in the test samples were calculated. The obtained values were normalized to corresponding tissue weight.

#### Measurement of NADP(H) level

NADP(H) content in brain samples was determined using nitro blue tetrazolium (NBT) and phenazine methosulfate (PMS). Acting as a donor of electrons, NADPH reduces NBT in the presence of PMS converting it into formazan that absorbs at 620 nm. To visualize presence of NADP<sup>+</sup>, an enzymatic reaction was used where glucose-6-phosphate dehydrogenase (G6PDHs) oxidized glucose-6-phosphate with reduction of cofactor.

About 300 mg of brain tissue were thawed on ice and homogenized using a manual Potter homogenizer in the presence of 1.5 ml of previously cooled carbonate buffer (100 mM  $\text{Na}_2\text{CO}_3$ , 20 mM  $\text{NaHCO}_3$ , 20 mM nicotinamide). The samples were centrifuged at 4  $^\circ\text{C}$  for 5 min at maximum speed. 10  $\mu\text{L}$  were taken out from the supernatant to determine the protein concentration in the solution while the remaining volume was further refined using Amicon® Ultra 0,5 mL 10 K columns (Merck Millipore; Germany) in accordance with the producer's protocol.

For analysis, the samples were placed to a 96-well plate in an amount of 10  $\mu\text{L}$ /well. A standard series of solutions with known NADP(H) content was prepared. Samples were brought up to 100  $\mu\text{L}$  with a reaction mixture of the following composition (per 10 reactions): 540  $\mu\text{L}$  MQ, 100  $\mu\text{L}$  1M TRIS-HCl buffer (pH 8.0), 50  $\mu\text{L}$  of 10 mM NBT, 150  $\mu\text{L}$  of 10 mM PMS, 50  $\mu\text{L}$  of a 100 mM EDTA solution, 10  $\mu\text{L}$  of 100 mM glucose-6-phosphate. Samples were incubated at +37  $^\circ\text{C}$  for 5 min, following which the reaction was initiated by adding 1  $\mu\text{L}$  of 250 U/ml glucose-6-phosphate dehydrogenase.

Absorbance at 620 nm was measured for each sample using Tecan Infinite 200 Pro plate reader (Tecan; Switzerland) in 10 min sessions. Each probe analysis was repeated without enzyme for the determination of background formazan formation under the action of cell lysate components. The dependence of the reaction rate on the content of NADP(H) in a sample was determined. The resulting calibration graph was used to determine the concentration of total NADP(H) in the experimental probes. The values obtained were normalized to the protein concentration.

#### Measurement of malondialdehyde level

To determine the intensity of lipid peroxidation in the samples, a modified TBARS assay was used. Malondialdehyde, which is one of the key products of lipid peroxidation, reacts with two 2-thiobarbituric acid (TBA) molecules to form a colored compound that intensively absorbs at 532 nm.

Approximately 100 mg of tissue were thawed on ice and homogenized in 750  $\mu\text{L}$  of previously cooled MQ-grade pure water using a manual Potter homogenizer. 5  $\mu\text{L}$  of butylated hydroxytoluene dissolved in methanol at a 10% concentration (w/v) were added to water to prevent *ex vivo* oxidation. The samples were centrifuged at 3000  $\times$  g for 15 min at 4  $^\circ\text{C}$  to obtain a soluble fraction containing cell membranes. At this stage, 10  $\mu\text{L}$  were removed from supernatant for further assessing protein concentration. 250  $\mu\text{L}$  of 40% trichloroacetic acid (TCA) were added to 350  $\mu\text{L}$  of samples for precipitation of proteins and stirred vigorously. The samples were again centrifuged at 3000  $\times$  g for 15 min at 4  $^\circ\text{C}$ .

For analysis, 500  $\mu\text{L}$  supernatant volume was mixed with 500  $\mu\text{L}$  of 0.67% TBA in 0.05 N NaOH. To prepare a standard solution series, 0.5 mM 1,1,3,3,-tetramethoxypropane (TMP) dissolved successively in 1 ml of 96% ethanol and 49 ml of MQ-grade water was used. Standard solutions were mixed with 500  $\mu\text{L}$  of 0.67% TBA in 0.05 N NaOH, after which all samples were incubated at +100  $^\circ\text{C}$  for 15 minutes. After the incubation, aliquots of 200  $\mu\text{L}$  were placed in a 96-well plate, and absorbance at 532 nm was measured using Tecan Infinite 200 Pro (Tecan; Switzerland). A calibration graph was created in accordance with the standard series samples, and MDA content was determined accordingly. The values obtained were normalized to the protein concentration.

#### Measurement of reduced glutathione (GSH) level

GSH in brain samples was quantified using commercially GSH/GSSG Ratio Detection Assay Kit, (Fluorometric-Green Abcam; UK). In the assay, non-fluorescent Thiol Green dye becomes strongly fluorescent upon reacting with GSH (Ex. 490, Em. 520).

Tissue material was thawed on ice and homogenized in 400  $\mu\text{L}$  of phosphate-saline buffer (pH 7.4) containing 0.5% NP-40 using a manual Potter homogenizer. The homogenates were centrifuged at maximum speed for 15 min at +4  $^\circ\text{C}$ . At the next stage, the samples were deproteinized by adding 1/5 volume of 100% (w/v) trichloroacetic acid (TCA). After intensive mixing and incubation on ice for 10 min, the samples were again centrifuged at 12,000  $\times$  g for 5 min at +4  $^\circ\text{C}$ . The TCA was neutralized by adding a  $\text{NaHCO}_3$  solution to the samples. Finally, the last centrifugation was carried out at 13,000  $\times$  g and +4  $^\circ\text{C}$  for 15 minutes.

For analysis, the supernatants were diluted by 10 times with Assay Buffer solution, and aliquots of 50  $\mu\text{L}$  of each sample were placed in a 96-well plate. A set of standards with known concentrations of GSH was also prepared. 50  $\mu\text{L}$  of Thiol Green solution were diluted by 100 times with Assay Buffer and then added to samples. The samples were incubated in the dark for one hour.

Fluorescence was measured using Tecan Infinite® 200 PRO (Tecan; Switzerland). Based on standard curve data, dependence of fluorescence intensity on the amount of glutathione in the sample was determined. The calibration graph was used to determine GSH content in each sample. The values obtained were normalized to starting tissue weight.

### Measurement of protein concentration

To determine concentration of proteins, a commercially available Bicinchoninic Acid Protein Assay Kit (Sigma-Aldrich; Germany) was used. In each series of experiment, a set of standards with known concentration of bovine serum albumin (BSA) protein was prepared. A mixture containing 1 part of 4% (w/v) copper (II) sulfate pentahydrate and 50 parts of the bicinchoninic acid solution was added to each sample. The samples were incubated at +37 °C for half an hour.

Absorbance at 562 nm was measured using Tecan Infinite 200 Pro (Tecan; Switzerland). Using standard curve, protein concentrations were estimated for each sample.

### RESULTS

A significant change in NADP(H) pool level was observed in 6 hours after MCAO. For control group, it was  $10.64 \pm 0.57$   $\mu\text{mol/mg}$  of protein while for damaged brain area, it was  $4.45 \pm 0.79$   $\mu\text{mol/mg}$  of protein. In 24 hours after MCAO, NADP(H) level was  $1.57 \pm 0.46$   $\mu\text{mol/mg}$  of protein that is about 7 times lower as compared to control group (Fig. 1A).

Since NADP(H) is involved in many biosynthetic processes including the lipid metabolism, we expected to observe a significant decrease in cholesterol and fatty acids levels in brain tissues. In our experiment, the level of total cholesterol (both

free cholesterol and cholesteryl esters) began to decrease in 6 h after MCAO:  $6.85 \pm 0.1$   $\mu\text{g/mg}$  of tissue while control value was  $7.29 \pm 0.20$   $\mu\text{g/mg}$  of tissue accordingly. In 24 hours after MCAO, the total cholesterol level in damaged tissues continued to decrease to value of  $5.95 \pm 0.4$   $\mu\text{g/mg}$  of tissue (Fig. 1B). For Group 3 (3 hours after MCAO), no difference in cholesterol level was observed as compared to control group. However, since a significant variation of values was observed for animals in Group 3, it is likely that 3 hours after MCAO, the cholesterol level started to decrease in damaged tissues.

The level of the free fatty acids (FFA) in damaged brain tissues differed from related control level in Group 5 (24 hours from MCAO) only:  $0.25 \pm 0.003$   $\text{nmol/mg}$  vs  $0.31 \pm 0.01$   $\text{nmol/mg}$  (Fig. 1C).

Malondialdehyde (MDA) is one of the lipid peroxidation markers. The tissue injury causes a slowdown in cell biosynthetic processes resulting in accumulation of biodegradation products accordingly. In control group, the MDA level was  $846.23 \pm 63.41$   $\text{pmol/mg}$  protein showing a normal functional level of cell biodegradation processes. A pathology occurs when cells fail to withstand the damage and maintain proper biosynthesis levels. In 24 hours after MCAO, MDA level in damaged brain tissues increased to  $1272.61 \pm 124.47$   $\text{pmol/mg}$  protein (Fig. 1D) in ischemic tissue. At this time an extensive cell death occurred that can be visualized by staining of brain slices using specific dye such as 2,3,5-triphenyltetrazolium chloride (TTC).

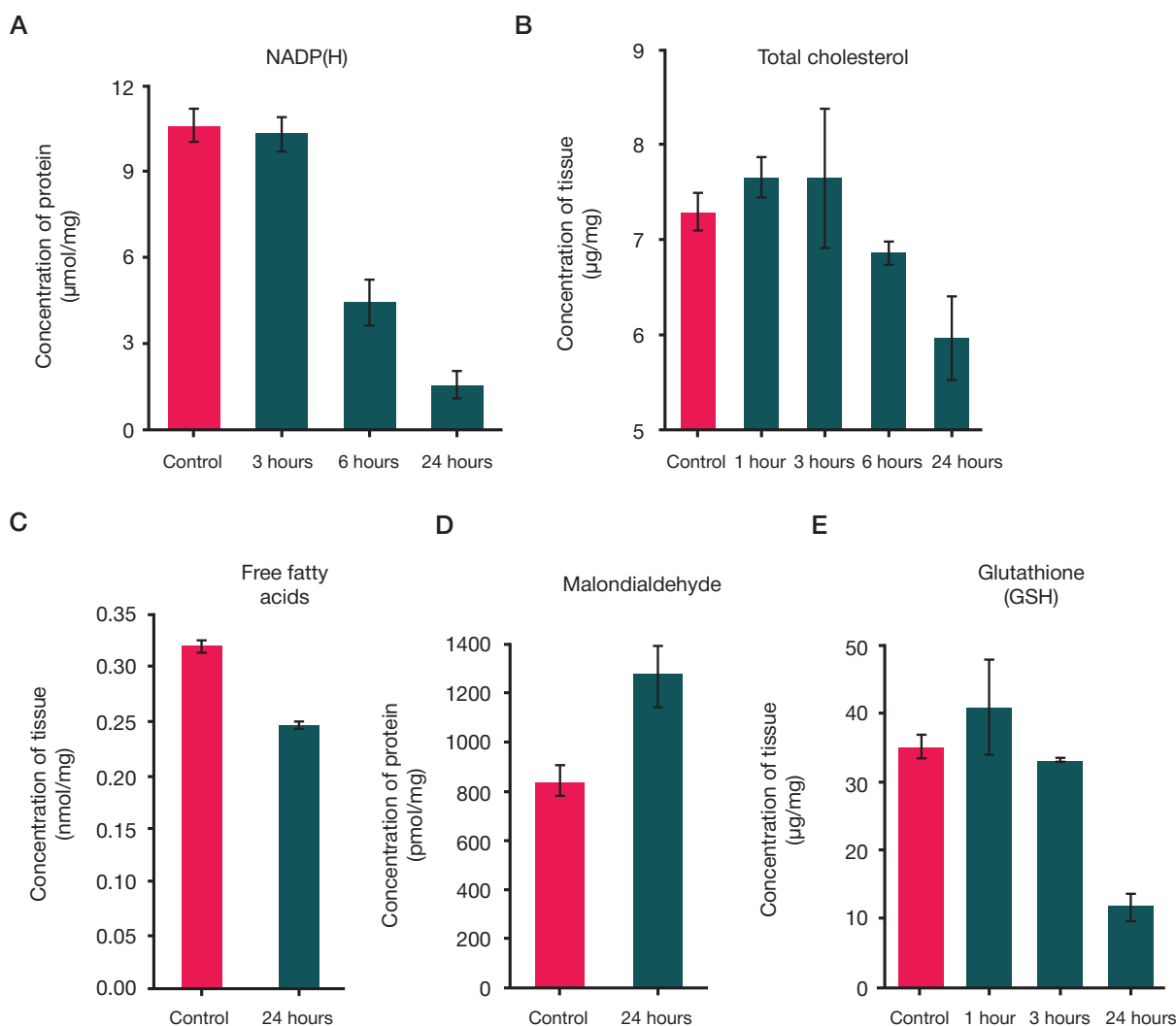


**Fig. 1.** Changes of biochemical parameters of brain tissues during permanent ischemia in rats. (A) NADP(H), (B) Total cholesterol, (C) Free fatty acids (FFA), (D) Malondialdehyde (MDA), (E) Glutathione (GSH)

The glutathione pool is an important redox component in cells. In particular, GSH is used by antioxidant enzymes such as glutathione peroxidase to neutralize ROS. Maintaining optimum GSH/GSSG ratio is essential to cell viability. NADPH is required for the regeneration of the reduced form of glutathione (GSH). In our study, no change was observed in the GSH levels for Groups 2–4 (within 6 hours from MCAO). In 24 hours after MCAO, GSH level in damaged brain tissues decreased to 11.8 µg/mg compared to 35.1 µg/mg in the control group (Fig. 1E).

Thus, levels of FFA, total cholesterol, GSH and MDA changed significantly in 24 hours after MCAO while the level of NADP(H) was found to decrease in 6 hours after MCAO. X-axis: Time, hours (after MCAO). Error levels correspond to a standard error of an average. 4 animals per group.

## DISCUSSION

Cerebral ischemic injury is a stress accompanied by structural damage at molecular or cellular level. Protection of tissues from the effects of ischemic damage occurs in different ways at many levels — through prevention of damage, repair and replacement of damaged structures.

Ischemic stroke is known to be accompanied by excessive and unregulated production of ROS [9] that are highly reactive compounds interacting with various cell compounds. One key target of ROS is lipids — both free and located within cell membranes. Lipid peroxidation is one of the common ways for the interaction of lipids and ROS. The process is a radical chain reaction, the end products of which are covalent aggregates of lipids as well as lipid hydroperoxides and lipid endoperoxides formed in the presence of oxygen [10]. The latter join intramolecular rearrangements with subsequent fragmentation of hydrocarbon tails. It is therefore feasible that an oxidative stress, while in the lipid phase, leads to an increase in the concentration of low molecular weight carbonyl compounds such as malondialdehyde (MDA). Most of the methods aimed at identifying oxidative stress are at least in some way based on registration of compounds of the above mentioned class [17, 18].

Interaction of lipids with reactive oxygen species may lead to a release of free fatty acids. Cell death in the foci of ischemia can also be followed by lipid hydrolysis [19]. It is known that free fatty acids can undergo auto-oxidation. Moreover, the cyclooxygenase pathway in the metabolism of arachidonic acid involves lipid hydroperoxides leading directly to the formation of oxygen radicals [10, 20]. Summing up the above, each and all of the mentioned factors will lead to an even greater contribution to peroxidation.

In practice, in many studies involving patients or laboratory animals, detection of MDA level in blood is performed. It was shown that MDA level increased significantly during the first 24 hours of ischemia, and it remained elevated for up to one week. A correlation of MDA level with a mortality rate has been shown for stroke patients [21]. Assessment of the concentration of MDA in ischemic brain can provide valuable information on the extent of tissue damage [22].

In our study, a model of permanent occlusion of the middle cerebral artery in rats was used. Under given conditions it was possible to register a noticeable increase in the concentration of MDA in 24 hours after MCAO. To better investigate the process, further studies are required involving ischemia/reperfusion model. Reperfusion is believed to be the key source of ROS generation. Cell death during permanent ischemia may be supposed to take place due to reasons other than lipid peroxidation; presence of dead tissue becomes visible

within a few hours after MCAO. In fact, the approach based on TBARS analysis may be subject to artifacts likely involved at the sample preparation stage. Addition of antioxidants like butylated hydroxytoluene reduces the formation of MDA in the presence of atmospheric oxygen, still does not completely eliminates it. Thus, detecting minor shifts of MDA concentration with reference to control probes may be very difficult.

The concentration of reduced glutathione (GSH) was used as one of the markers of the cell redox state. Similar to MDA, we did not detect any changes in GSH level during the active phase of ischemic damage. However, its concentration decreased significantly in 24 hours after MCAO. Since GSH is involved in thiol-disulfide exchange reactions, an increase in ROS level results in an increase of glutathione oxidized form due to activation of antioxidant enzymes. This suggests that a noticeable increase in occurrence of oxidized lipids with subsequent cell death may lead to a significant decrease of GSH level. Still, to confirm this, further investigations are necessary — specifically, using the ischemia/reperfusion model. On the one hand, prolonged peroxidation may lead to a depletion of the GSH pool; on the other hand, the shortage of GSH can drive the system to a state in which peroxidation (which until then could have been restrained) starts causing a damaging effect. Finally, decrease of GSH level may be not due to the functioning of antioxidant systems in membranes. For instance, tissue necrotization is characterized by inability to maintain the GSH pool due to poor functioning of related enzyme systems and the lack of reducing equivalents.

In our study, concentration of NADP(H) decreased by 2 times in the first 6 hours after MCAO and by almost 7 times in 24 hours after MCAO. The NADP(H) decrease is believed to have an adverse impact on the antioxidant systems performance as well as on the anabolic processes. As mentioned earlier, this factor is likely to contribute to the decrease of GSH pool as well as the increase of lipid peroxidation level.

Not all the lipids damaged during peroxidation can be repaired. We believe that during ischemic cerebral damage, anabolic pathways involved in lipid biosynthesis should be activated in order to replace damaged components. The NADP(H) abundance is known to be connected with an efficiency of the biosynthesis of fatty acids and cholesterol as these metabolic pathways require reducing equivalents. As it was mentioned, NADP(H) level changed during the experiment.

In a large number of lab and clinical studies, FFA level in blood plasma was detected as this index can be considered a potential biomarker for detection of early stages of ischemic stroke. Hydrolysis of brain phospholipids with release of FFA into blood stream occurs during a stroke that may be a reason of observing increased FFA level in blood in the first few hours [23]. Based on other research data available, there is a correlation between FFA occurrence and the severity of disorder: the higher the level of FFA, the higher severity level observed [24, 25]. Though changes in FFA profile are of substantial metabolic importance, there is still a lack of data related to brain tissues.

In this work, we detected FFA levels in brain samples at different time points. A significant decrease in FFA level was observed in 24 hours after MCAO; during the acute phase of stroke there was no difference between FFA levels in test groups and the control group. Thus, in our experiment no evidence was received in support of activation of the synthesis of fatty acids for replacement of damaged membrane components. A decrease in FFA level after 24 hours from MCAO is most likely due to cell death leading to depletion of NADP(H) content, disruption of the enzyme system and perhaps some other

factors. For the studied model of permanent ischemia in rats, it is likely that no accumulation of lipids hydrolyzed after cell death occurs in brain tissues.

Similar data were obtained with regard to cholesterol concentration however, in case of cholesterol the decrease was observed earlier — in 6 hours after MCAO. In comparison to the original level of metabolites, concentration of cholesterol and FFA decreased similarly in a time lapse of 24 hours after the occlusion (1.24 times for FFA and 1.27 times for cholesterol).

## References

- World Health Organization. Top ten causes of death. Available from: <http://www.who.int/mediacentre/factsheets/fs310/en/index.html> (accessed August 19, 2012).
- Hinkle JL, Guanci MM. Acute Ischemic Stroke Review. *Journal of Neuroscience Nursing*. 2007; 39 (5): 285–93. PubMed PMID: 17966295.
- Krzyżanowska W, Pomierny B, Filip M, Pera J. Glutamate transporters in brain ischemia: to modulate or not? *Acta Pharmacologica Sinica*. 2014; 35 (4): 444–62. PubMed PMID: 24681894.
- Berliocchi L, Bano D, Nicotera P. Ca<sup>2+</sup> signals and death programmes in neurons. *Philos Trans R Soc Lond B Biol Sci*. 2005; 360 (1464): 2255–8. PubMed PMID: 16321795.
- Klogeris T, Baines CP, Krenz M, Korthuis RJ. Ischemia/Reperfusion. *Compr Physiol*. 2016; (7): 113–70 PubMed PMID: 28135002.
- Kalogeris T, Baines CP, Krenz M, Korthuis RJ. Cell biology of ischemia/reperfusion injury. *Int Rev Cell Mol Biol*. 2012; (298): 229–317. PubMed PMID: 22878108.
- Allen CL, Bayraktutan U. Oxidative Stress and Its Role in the Pathogenesis of Ischaemic Stroke. *International Journal of Stroke*. 2009; 4 (6): 461–70. PubMed PMID: 19930058.
- Lesnefsky EJ, Chen Q, Tandler B, Hoppel CL. Mitochondrial dysfunction and myocardial ischemia-reperfusion: implications for novel therapies. *Annual review of pharmacology and toxicology*. 2017; (57): 535–65. PubMed PMID: 27860548.
- Vanden Hoek TL, Li C, Shao Z, Schumacker PT, Becker LB. Significant levels of oxidants are generated by isolated cardiomyocytes during ischemia prior to reperfusion. *J Mol Cell Cardiol*. 1997; (29): 2571–83. PubMed PMID: 9299379.
- Gaschler MM, Stockwell BR. Lipid peroxidation in cell death. *Biochem Biophys Res Commun*. 2017; 482 (3): 419–25. PubMed PMID: 28212725.
- Gaucher C, Boudier A, Bonetti J, Clarot I, Leroy P, Parent M. Glutathione: Antioxidant Properties Dedicated to Nanotechnologies. *Antioxidants (Basel)*. 2018; 7 (5): 62. PubMed PMID: 29702624.
- Bilan DS, Shohina AG, Lukjanov SA, Belousov VV. Osnovnye redoks-pary kletki. *Bioorganicheskaya himija*. 2015; (41): 385–402. Russian.
- Dringen R, Pawlowski PG, Hirrlinger J. Peroxide detoxification by brain cells. *Journal of Neuroscience Research*. 2004; 79 (1–2): 157–165. PubMed PMID: 15573410.
- Garcia YJ, Rodriguez-Malaver AJ, Penñaloza N. Lipid peroxidation measurement by thiobarbituric acid assay in rat cerebellar slices. *Journal of Neuroscience Methods*. 2005; (144): 127–35. PubMed PMID: 15848246.
- Charis WT, Scott MD. Single Extraction Method for the Spectrophotometric Quantification of Oxidized and Reduced Pyridine Nucleotides in Erythrocytes. *Analytical Biochemistry*. 1994; (222): 417–26. PubMed PMID: 7864367.
- Uluc K, Miranpuri A, Kujoth GC, Akture E, Baskaya MK. Focal cerebral ischemia model by endovascular suture occlusion of the middle cerebral artery in the rat. *J Vis Exp*. 2011 Feb 5; (48). PubMed PMID: 21339721.
- Gutteridge JMC, Halliwell B. The measurement and mechanism of lipid peroxidation in biological systems. *Trends in Biochemical Sciences*. 1990; 15 (4): 129–35. PubMed PMID: 2187293.
- Ceconi C, Cargnoni A, Pasini E, Condorelli E, Curello S, Ferrari R. Evaluation of phospholipid peroxidation as malondialdehyde during myocardial ischemia and reperfusion injury. *Am J Physiol*. 1991; 260 (4 Pt 2): H1057–61. PubMed PMID: 2012211.
- Bazan NG. Effects of ischemia and electroconvulsive shock on free fatty acid pool in the brain. *Biochimica et Biophysica Acta (BBA) — Lipids and Lipid Metabolism*. 1970; 218 (1): 1–10. PubMed PMID: 5473492.
- Braugher JM, Hall ED. Central nervous system trauma and stroke. I. Biochemical considerations for oxygen radical formation and lipid peroxidation. *Free Radic Biol Med*. 1989; (6): 289–301. PubMed PMID: 266366.
- Cojocar IM, Cojocar M, Sapira V, Ionescu A. Evaluation of oxidative stress in patients with acute ischemic stroke. *Rom J Intern Med*. 2013 Apr-Jun; 51 (2): 97–106. PubMed PMID: 24294813.
- Lorente L, Martin MM, Perez-Cejas A, Abreu-Gonzalez P, Ramos L, Argueso M et al. Association between total antioxidant capacity and mortality in ischemic stroke patients. *Ann Intensive Care*. 2016; 6 (1): 39. PubMed PMID: 27107565.
- Golovko SA, Golovko MI. Plasma Unesterified Fatty-Acid Profile Is Dramatically and Acutely Changed under Ischemic Stroke in the Mouse Model. *Lipids*. 2018; 52 (6): 641–645. PubMed PMID: 30206953.
- Niu Z, Hu H, Tang F. High Free Fatty Acid Levels Are Associated with Stroke Recurrence and Poor Functional Outcome in Chinese Patients with Ischemic Stroke. *J Nutr Health Aging*. 2017; 21 (10): 1102–1106. PubMed PMID: 29188867.
- Wang X, Feng A, Zhu C. Cerebrospinal fluid levels of free fatty acid associated with ischemic stroke recurrence and functional outcome. *Neurol Sci*. 2016; 37 (9): 1525–9. PubMed PMID: 27245354.

## CONCLUSIONS

In the permanent cerebral ischemia experiment, the levels of total cholesterol, FFA, MDA, GSH, and NADP(H) in brain tissues of rats have been measured. It was shown that in 24 hours from the onset of ischemia, there was a significant decrease in levels of FFA, total cholesterol and GSH, and an increase in the level of MDA, a marker of lipid peroxidation. NADP(H) level decreased twice in 6 hours from MCAO.

## Литература

- World Health Organization. Top ten causes of death. Available from: <http://www.who.int/mediacentre/factsheets/fs310/en/index.html> (accessed August 19, 2012).
- Hinkle JL, Guanci MM. Acute Ischemic Stroke Review. *Journal of Neuroscience Nursing*. 2007; 39 (5): 285–93. PubMed PMID: 17966295.
- Krzyżanowska W, Pomierny B, Filip M, Pera J. Glutamate transporters in brain ischemia: to modulate or not? *Acta*

- Pharmacologica Sinica. 2014; 35 (4): 444–62. PubMed PMID: 24681894.
4. Berliocchi L, Bano D, Nicotera P.  $Ca^{2+}$  signals and death programmes in neurons. *Philos Trans R Soc Lond B Biol Sci*. 2005; 360 (1464): 2255–8. PubMed PMID: 16321795.
  5. Klogeris T, Baines CP, Krenz M, Korthuis RJ. Ischemia/Reperfusion. *Compr Physiol*. 2016; (7): 113–70 PubMed PMID: 28135002.
  6. Klogeris T, Baines CP, Krenz M, Korthuis RJ. Cell biology of ischemia/reperfusion injury. *Int Rev Cell Mol Biol*. 2012; (298): 229–317. PubMed PMID: 22878108.
  7. Allen CL, Bayraktutan U. Oxidative Stress and Its Role in the Pathogenesis of Ischaemic Stroke. *International Journal of Stroke*. 2009; 4 (6): 461–70. PubMed PMID: 19930058.
  8. Lesnefsky EJ, Chen Q, Tandler B, Hoppel CL. Mitochondrial dysfunction and myocardial ischemia-reperfusion: implications for novel therapies. *Annual review of pharmacology and toxicology*. 2017; (57): 535–65. PubMed PMID: 27860548.
  9. Vanden Hoek TL, Li C, Shao Z, Schumacker PT, Becker LB. Significant levels of oxidants are generated by isolated cardiomyocytes during ischemia prior to reperfusion. *J Mol Cell Cardiol*. 1997; (29): 2571–83. PubMed PMID: 9299379.
  10. Gaschler MM, Stockwell BR. Lipid peroxidation in cell death. *Biochem Biophys Res Commun*. 2017; 482 (3): 419–25. PubMed PMID: 28212725.
  11. Gaucher C, Boudier A, Bonetti J, Clarot I, Leroy P, Parent M. Glutathione: Antioxidant Properties Dedicated to Nanotechnologies. *Antioxidants (Basel)*. 2018; 7 (5): 62. PubMed PMID: 29702624.
  12. Билан Д. С., Шохина А. Г., Лукьянов С. А., Белоусов В. В. Основные редокс-пары клетки. *Биоорганическая химия*. 2015; (41): 385–402.
  13. Dringen R, Pawlowski PG, Hirrlinger J. Peroxide detoxification by brain cells. *Journal of Neuroscience Research*. 2004; 79 (1–2): 157–165. PubMed PMID: 15573410.
  14. Garcia YJ, Rodriguez-Malaver AJ, Penãloza N. Lipid peroxidation measurement by thiobarbituric acid assay in rat cerebellar slices. *Journal of Neuroscience Methods*. 2005; (144): 127–35. PubMed PMID: 15848246.
  15. Charis WT, Scott MD. Single Extraction Method for the Spectrophotometric Quantification of Oxidized and Reduced Pyridine Nucleotides in Erythrocytes. *Analytical Biochemistry*. 1994; (222): 417–26. PubMed PMID: 7864367.
  16. Uluc K, Miranpuri A, Kujoth GC, Akture E, Baskaya MK. Focal cerebral ischemia model by endovascular suture occlusion of the middle cerebral artery in the rat. *J Vis Exp*. 2011 Feb 5; (48). PubMed PMID: 21339721.
  17. Gutteridge JMC, Halliwell B. The measurement and mechanism of lipid peroxidation in biological systems. *Trends in Biochemical Sciences*. 1990; 15 (4): 129–35. PubMed PMID: 2187293.
  18. Ceconi C, Cargnoni A, Pasini E, Condorelli E, Curello S, Ferrari R. Evaluation of phospholipid peroxidation as malondialdehyde during myocardial ischemia and reperfusion injury. *Am J Physiol*. 1991; 260 (4 Pt 2): H1057–61. PubMed PMID: 2012211.
  19. Bazan NG. Effects of ischemia and electroconvulsive shock on free fatty acid pool in the brain. *Biochimica et Biophysica Acta (BBA) — Lipids and Lipid Metabolism*. 1970; 218 (1): 1–10. PubMed PMID: 5473492.
  20. Braughler JM, Hall ED. Central nervous system trauma and stroke. I. Biochemical considerations for oxygen radical formation and lipid peroxidation. *Free Radic Biol Med*. 1989; (6): 289–301. PubMed PMID: 266366.
  21. Cojocaru IM, Cojocaru M, Sapira V, Ionescu A. Evaluation of oxidative stress in patients with acute ischemic stroke. *Rom J Intern Med*. 2013 Apr-Jun; 51 (2): 97–106. PubMed PMID: 24294813.
  22. Lorente L, Martin MM, Perez-Cejas A, Abreu-Gonzalez P, Ramos L, Argueso M et al. Association between total antioxidant capacity and mortality in ischemic stroke patients. *Ann Intensive Care*. 2016; 6 (1): 39. PubMed PMID: 27107565.
  23. Golovko SA, Golovko MI. Plasma Unesterified Fatty-Acid Profile Is Dramatically and Acutely Changed under Ischemic Stroke in the Mouse Model. *Lipids*. 2018; 52 (6): 641–645. PubMed PMID: 30206953.
  24. Niu Z, Hu H, Tang F. High Free Fatty Acid Levels Are Associated with Stroke Recurrence and Poor Functional Outcome in Chinese Patients with Ischemic Stroke. *J Nutr Health Aging*. 2017; 21 (10): 1102–1106. PubMed PMID: 29188867.
  25. Wang X, Feng A, Zhu C. Cerebrospinal fluid levels of free fatty acid associated with ischemic stroke recurrence and functional outcome. *Neurol Sci*. 2016; 37 (9): 1525–9. PubMed PMID: 27245354.

## HEART INJURIES: MAIN CLINICAL SYMPTOMS

Maslyakov VV <sup>✉</sup>, Krjukov EV, Barsukov VG, Kurkin KG, Dorzhiev PA, Gorbelyk VR

Reaviz Medical University, Saratov, Russia

Injuries to the heart are uncommon in peacetime, yet they result in life-threatening conditions, which makes timely diagnostics a crucial factor in saving patients' lives. In this connection, it is important to define the main signs of heart injuries. This study aimed to analyze the basic clinical symptoms associated with various wounds to the heart. We have retrospectively analyzed such symptoms registered in 86 patients with varying chest injuries that affect the heart. All patients were treated in the emergency surgery unit of the Engels Town Hospital from 1991 to 2017. 41 (47.6%) patient had stab wounds, and there were 45 (52.3%) cases of gunshot wounds. 23 (26.7%) patients had chest injuries affecting heart exclusively, while for 63 (73.2%) the consequences were wounds to other organs. We found that the clinical picture depends on the kind of injury to the heart: stab and slash wounds translate into more pronounced symptoms, while gunshot wounds do not produce such an effect. Accepting patients, practitioners should take this fact into account. The misdiagnosis rate for stab and slash heart wounds is 9.7%, that for gunshot wounds — 17.7%, the latter being the result of vagueness of the clinical picture. The clinical signs are most pronounced in the cases of stab and slash wounds to the heart.

**Keywords:** heart wounds, diagnostics, diagnostic mistakes

**Author contribution:** Barsukov VG — study design and general concept development; Gorbelyk VR — data collection, analysis and interpretation; Kurkin KG, Dorzhiev PA — manuscript writing; Maslyakov VV — drafting the manuscript, compilation of its first version and critical evaluation of the content; Maslyakov VV, Krjukov EV — final decision on the manuscript's readiness for publication.

**Compliance with ethical standards:** the study was approved by Reaviz Medical University local ethics committee (minutes #12 of December 21, 2018). All patients signed the informed voluntary consent form.

✉ **Correspondence should be addressed:** Vladimir V. Maslyakov  
Verkhny Rynok 10, Saratov, 410012; e-mail: maslyakov@inbox.ru

**Received:** 03.07.2018 **Accepted:** 17.07.2018 **Published online:** 27.02.2019

**DOI:** 10.24075/brsmu.2019.003

## ОСНОВНЫЕ КЛИНИЧЕСКИЕ СИМПТОМЫ ПРИ РАНЕНИЯХ СЕРДЦА

В. В. Масляков <sup>✉</sup>, Е. В. Крюков, В. Г. Барсуков, К. Г. Куркин, П. А. Доржиев, В. Р. Горбелик

Саратовский медицинский университет «Реавиз», Саратов, Россия

Ранения сердца в мирное время нельзя отнести к самым распространенным, однако повреждение этого органа угрожает жизни, и своевременная диагностика влияет на спасение жизни. В связи с этим актуальным является выявление основных признаков повреждения сердца. Целью исследования было провести анализ основных клинических симптомов, возникающих при различных ранениях сердца. Был проведен ретроспективный анализ основных симптомов, возникающих при различных ранениях груди с повреждением сердца у 86 пациентов, находившихся на лечении в экстренном хирургическом отделении городской больницы города Энгельса в период с 1991 по 2017 г. Из общего количества пациентов колото-резаные ранения были зарегистрированы в 41 (47,6%), огнестрельные — в 45 (52,3%) случаях. При ранении груди только ранение сердца наблюдалось в 23 (26,7%) случаях, в остальных 63 (73,2%) случаях зарегистрированы повреждения других органов. Установлено, что различные ранения сердца имеют неодинаковую клиническую картину: она более выражена при колото-резаных и менее выражена при огнестрельных ранениях, что необходимо учитывать при поступлении таких пациентов. Диагностические ошибки при колото-резаных ранениях сердца встречаются в 9,7% случаев, при огнестрельных ранениях — в 17,7% случаев. Наиболее выражены клинические симптомы при колото-резаных ранениях сердца.

**Ключевые слова:** ранения сердца, диагностика, диагностические ошибки

**Информация о вкладе авторов:** В. Г. Барсуков — разработка общей концепции и дизайна исследования; В. Р. Горбелик — сбор, анализ и интерпретация данных; К. Г. Куркин, П. А. Доржиев — написание рукописи; В. В. Масляков — составление проекта и первичного варианта рукописи, критическая оценка интеллектуального содержания рукописи; В. В. Масляков, Е. В. Крюков — принятие окончательного решения о готовности рукописи к публикации.

**Соблюдение этических стандартов:** исследование было одобрено местным этическим комитетом Саратовского медицинского университета «Реавиз» (протокол № 12 от 21 декабря 2018 г.). Все пациенты дали письменное информированное добровольное согласие.

✉ **Для корреспонденции:** Владимир Владимирович Масляков  
ул. Верхний рынок, корпус 10, г. Саратов, 410012; e-mail: maslyakov@inbox.ru

**Статья получена:** 03.07.2018 **Статья принята к печати:** 17.07.2018 **Опубликована онлайн:** 27.02.2019

**DOI:** 10.24075/vrgmu.2019.003

According to the literature, 10 to 19.5% of penetrating chest wounds result in injuries to the heart [1, 2, 3, 4, 5]. The associated mortality rate is up to 50% [6–8], with the main reasons thereof being massive blood loss, acute cardiac tamponade, extensive damage to intracardiac structures [3–7]. The common complications registered in patients with heart injuries shortly after surgery are pericarditis, post-traumatic pulpitis, pleurisy [9–11], as well as myocardial ischemia, surgical wound suppuration [12–15]. Diagnosing an injury to the heart, practitioners examine wound in its projection and signs of damage the organ may have received. In most cases, such examination is only visual, thus, the key task before the

surgeon is to correctly diagnose the heart wound within a very short period of time and operate on it as soon as possible.

This study aimed to analyze the basic clinical symptoms associated with various wounds to the heart.

## PATIENTS AND METHODS

To achieve the goal set, we have retrospectively analyzed the basic clinical symptoms registered in 86 patients with varying chest injuries that affect the heart. All patients were treated in the emergency surgery unit of the Engels Town Hospital from 1991 to 2017.

Inclusion criteria: a gunshot or a stab wound to the chest resulting in a heart injury; age from 18 to 50. Exclusion criteria: age under 18; agonal state at the time of admission; concomitant head, neck, limb injuries.

41 (47.6%) patient had stab wounds, and there were 45 (52.3%) cases of gunshot wounds. 23 (26.7%) patients had chest injuries affecting heart exclusively, for 63 (73.2%) the consequences were wounds to other organs and in 4 (4.6%) cases the patients had concomitant wounds to the abdomen. The other organs damaged in connection with the chest wounds were lungs (52 cases, 85.7%), ribs (4 cases, 6.3%), thoracic esophagus (3 cases, 4.7%), inferior vena cava (2 cases 3.1%), diaphragm and liver (1 case, 1.5%). None of the patients had the pericardial injury greater than 3 cm. The volume of blood found in pericardial cavities of the patients ranged from 300 to 700 ml. In most cases, clots plugged the injuries to the heart. 46 (53.4%) patients had non-penetrating wounds, while those in 40 (46.5%) patients were penetrating. 38 (44.1%) slash/stab victims exhibited penetrating wounds to their hearts, 3 (4.5%) — non-penetrating wounds; gunshots resulted mainly in non-penetrating wounds, which were diagnosed in 43 (50%) patients, while only 2 (2.3%) had gun-related penetrating wounds. All penetrating wounds were pinpoint.

In addition to hemopericardium, 75 (87.2%) patients had hemothorax; in 58 (77.3%) of them the volume of blood accumulated in the pleural cavity was 500 ml, 14 (18.6%) had about 1 l of blood there and 3 (4%) suffered from a total hemothorax. All patients were male, their mean age was  $31 \pm 2$  years.

With heart wounds, time is one of the crucial factors shaping the prognosis. Having analyzed the available data, we learned that chest slash/stab victims were brought to the hospital within  $26.7 \pm 5$  minutes from wound infliction, gunshot victims — within  $21.3 \pm 6$  minutes. 37 (43%) slash/stab victims were brought to the hospital by an ambulance, only 4 (4.7%) arrived in a private vehicle. As for the patients with gunshot wounds, all of them were delivered to the hospital by an ambulance. Thus, the majority of the wounded people considered in this study arrived to the hospital in a specialized vehicle, where the ambulance crews gave them infusions (79 patients (91.8%), in most cases — 100–1000 ml of polyglucin solution intravenously at the rate of 60–80 drops/minute), non-narcotic analgesics (56 patients (65.1%)), dressed the wound (83 patients (96.5%), including 74 (86%) occlusive dressings). Undoubtedly, these measures had their effects on the outcomes.

At admission, 67 (77.9%) patients were experiencing shock of varying degree; they were 27 (31.3%) slash/stab victims and 40 (46.5%) men with gunshot wounds. The data show that patients with gunshot wounds are more prone to shock than those slashed or stabbed, the difference between the two groups being statistically significant ( $p < 0.05$ ). As for the degrees of shock registered, 34 patients (39.5%) had the first-degree shock, 26 (30.2%) had the second-degree shock, 7 (8.1%) experienced the third degree. Thus, at the time of admission most patients experienced first- and second-degree shock.

The condition of the patients at admission was assessed with the help of the AIS scale, where code 1 means minor severity; code 2 — moderate; 3 — serious, but not life-threatening; 4 — severe, life-threatening; 5 — critical, survival doubtful; 6 — maximum, fatal damage. Applied to the slash/stab victims considered, AIS assessment yielded the following results: 21 (24.4%) patients — code 2; 12 (13.9%) patients — code 3; 8 (9.3%) patients — code 4. As for the patients with

gunshot wounds, 18 (20.9%) of them were put into the code 2 group, the condition of 7 (8.1%) was classified as code 3, code 4 was assigned to 11 (12.7%) patients and code 5 to 9 (10.4%). Thus, gunshot victims were registered with the most severe conditions.

Assessing localization of the wounds, we delimited the "heart zone" with second rib on top, subcostal line at the bottom, midclavicular line from the right and anterior axillary line from the left. Out of the 86 patients studied, 50 (58.1%) had injuries in this zone, 38 (92.6%) of them slash/stab wounds, 12 (26.6%) — gunshot wounds.

84 patients underwent anterior-lateral thoracotomy, one patient had a sternotomy, and another had a laparotomy. In 96.7% of the patients the heart wound was sutured with interrupted stitches, 3.3% received U-shaped stitches. Separate apposition stitches were used to suture pericardial sacs in all the patients; pleural cavity drainage was placed in the II and VII intercostal spaces.

It should be noted specifically that the emergency hospital that received the patients is a level II trauma center; in such centers, ultrasound examinations are typically done around the clock. However, the patients considered in this study were not subjected to this type of examination, which, without a doubt, affected the outcomes, since sonography facilitates diagnosing and could have reduced the number of diagnostic mistakes.

We used Excel 2007, part of the Microsoft Office 2007 package, to process the data. The difference between the compared values was considered statistically significant at  $p < 0.05$ .

## RESULTS

The symptoms of penetrating wounds to the heart include signs of rapidly increasing internal bleeding, cardiac tamponade and shock. The table below contains the main symptoms registered in the patients with heart injuries.

Patients with slash/stab wounds to the heart have exhibited more clinical symptoms. The most frequent of them were localization of the wound in the heart zone (38 (92.6%) cases) and tachycardia (over 90 beats per minute, 38 (92.6%) cases), as well as expansion of the cardiac dullness percussion boundaries (31 (75.6 %) cases). Tachycardia can be explained by the body's compensatory response to acute blood loss. Symptoms observed less frequently: precordialgia (28 (68.2%) cases), venous hypertension (27 (65.8%) cases), arterial hypotension due to hemorrhagic shock (25 (60.9%) cases), dyspnea (23 (24.3%) cases), no pulse in the peripheral arteries (23 (56%) cases).

The least frequent symptoms were feeling short of breath (16 (39%) cases), neck vein swelling (10 (11.6%) cases), blue face and neck (9 (21.9%) cases). Thus, slash/stab wounds to the heart produce a fairly pronounced clinical picture, with the signs of hemorrhagic shock and cardiac tamponade at the forefront. Only 6 (14.6%) cases did not offer a clear clinical picture, the state of the patients in questions being satisfactory upon admission, without any signs of shock and cardiac tamponade. The aforementioned factors allowed diagnosing the heart injury promptly, and most of the patients were brought straight to the operating room for immediate surgery. In this group, only 10 (24.3%) patients received primary surgical treatment, while the remaining 13 (31.7%) underwent thoracotomy. 17 (41.4%) patients were subjected to additional examinations; in most cases, it was AP view chest X-ray imaging and ECG, which were mostly performed in the operating room. The well-pronounced clinical picture associated with slash/

**Table.** Frequency of occurrence of the main symptoms associated with wounds to the heart ( $M \pm m$ )

Symptoms	Frequency of symptoms by group	
	Slash/stab wounds ( $n = 41$ )	Gunshot wounds ( $n = 45$ )
Precordialgia	$28 \pm 2^*$	$10 \pm 1$
Feeling short of breath	$16 \pm 2^*$	$6 \pm 1$
Wound localization in the heart zone	$38 \pm 2^*$	$12 \pm 1$
Blue face and neck	$9 \pm 1$	$9 \pm 2$
Neck vein swelling	$10 \pm 1$	$10 \pm 1$
Dyspnea (over 25–30 per min)	$23 \pm 2^*$	$11 \pm 1$
Expansion of the cardiac dullness percussion boundaries	$31 \pm 5^*$	$7 \pm 2$
Tachycardia (over 90 beats per min)	$38 \pm 4^*$	$8 \pm 1$
No pulse in the peripheral arteries	$23 \pm 4^*$	$3 \pm 2$
Arterial hypotension (SBP less than 100 mm Hg)	$25 \pm 2^*$	$5 \pm 0,3$
Venous hypertension (CVP more than 140 mm water column)	$27 \pm 4^*$	$7 \pm 1$

Note: \* — ( $p < 0.05$ ).

stab wounds to the heart minimized the number of diagnostic mistakes made: only 4 (9.7%) patients went into surgery with a delay. In those cases, the picture was unclear, and diagnostic examinations (chest X-ray, ECG) revealed no signs of heart injury and cardiac tamponade. All these patients received primary surgical treatment. Thoracotomy was performed 3-4 hours after admission following the appearance of signs of hemorrhagic shock.

Gunshot wounds to the chest resulting in heart injuries produced a different clinical picture. Only 12 (26.6%) patients had the wound in the heart zone, while the remaining 33 (73.3%) gunshot victims had it out of this zone, which complicated diagnosing. The clinical symptoms most commonly registered in this group of patients were: dyspnea (10 (24.4%) cases), precordialgia (10 (22.2%) cases), neck vein swelling (10 (24.4%) cases), blue face and neck (9 (20%) cases), tachycardia (8 (17.7%) cases). 7 (15.5%) patients exhibited signs of expansion of the cardiac dullness percussion boundaries; 6 (13.3%) gunshot victims felt short of breath. Compared to the slash/stab wound group, patients with gunshot wounds showed signs of hemorrhagic shock less frequently; the signs were arterial hypotension (5 (11.1%) cases) and no pulse in the peripheral arteries (3 (6.6%) cases). It is safe to say that the lack of pronounced signs of heart injuries and manifestations of hemorrhagic shock made diagnosing the cases a more complicated process. At admission, with just the objective wound data available, only 12 (26.6%) patients were diagnosed with heart injuries and allowed straight into the operating room. The remaining 33 (73.3%) patients were subjected to diagnostic examinations in the reception ward, which delayed surgery. 38 (84.4%) patients underwent chest X-ray examination; in 30 cases, the results thereof allowed suspecting a wound to the heart. 29 (64.4%) patients underwent ECG, and 18 (40%) were subjected to pleural puncture. 40 patients received primary surgical treatment in the operating room. In 8 (17.7%) cases belonging to this group, the delay to surgery was from 2 to 3 hours, all of which are attributed to the unclear clinical picture. The patients went into surgery when their condition deteriorated and the signs of hemorrhagic shock became more vivid.

Having analyzed the data covering the immediate post-surgery period, we learned that in the slash/stab wound group 21 (24.4%) patients developed complications, and 12 (13.9%) cases ended in a fatality. In the gunshot wound group,

complications were registered in 34 (39.5%) cases, fatality — in 23 (26.7%) cases.

## DISCUSSION

This study shows that the clinical picture depends on the kind of injury to the heart: stab and slash wounds translate into more pronounced symptoms, while gunshot wounds do not produce such an effect; this fact should be taken into account when admitting such patients into the hospital. The main reason behind the unclear clinical picture in gunshot wound cases is the severity of the patients' condition, which results from the shock: it was registered in 46.5% gunshot victims compared to 31.3% patients with slash/stab wounds. The nature of the wound is another important factor influencing the clinical picture: for example, most of the slash/stab wounds were penetrating, which made the clinical signs more pronounced. The data we obtained are in line with the relevant research results published [16]. It should be noted that the treatment results in the gunshot wound group were worse than in the slash/stab wound group: the former group registered complications in 39.5% of cases (immediate post-surgery period) and fatalities in 26.7% of cases, whereas in the latter group the figures were 24.4% and 13.9%, respectively. The reasons behind the greater share of developed complications and fatalities associated with gunshot wounds to the heart should be researched separately and were not a subject of this study. At that, the relevant reports published indicate that the number of fatalities and complications developed following gunshot wounds can be a consequence of heart bruising resulting from the projectile's hydrodynamic impact, which influences the post-surgery recovery process significantly [17].

## CONCLUSIONS

The misdiagnosis rate for stab and slash heart wounds is 9.7%, that for gunshot wounds — 17.7%, the latter being the result of vagueness of the clinical picture. The clinical signs are most pronounced in the cases of stab and slash wounds to the heart. In order to reduce the number of diagnostic mistakes, it is necessary to apply the notion of "heart zone" when diagnosing chest injuries, subject patients to US examinations of the heart, pleural cavities, etc.

## References

1. Vinokurov MM, Gogolev NM. Ranenie serdca i perikarda. Acta Biomedica Scientifica. 2005; (3): 160. Russian.
2. Volkov VE, Vanyukov VP, Volkov SV, Zhamkov DG. Neposredstvennye rezul'taty hirurgicheskogo lechenija ranenij serdca. Zdravoohranenie Chuvashii. 2017; 3 (52): 32–4. Russian.
3. Volkov VE, Volkov SV. Ranenija serdca: sostojanie problemy i perspektivy. Acta Medica Eurasica. 2017; (1): 17–21. Russian.
4. Ivchenko DR, Koltovich AP. Faktory tanatogeneza pri ognestrel'nyh ranenijah grudi. Medicinskij vestnik MVD. 2013; 2 (63): 31–5. Russian.
5. Kovalchuk VI. Otkrytye ranenija serdca u detej. Zdravoohranenie (Minsk). 2015; (4): 62–5. Russian.
6. Novoselov VP, Savchenko SV, Gricinger VA. Ocenka reaktivnyh izmenenij miokarda pri pronikajushhix koloto-rezanyh ranenijah grudi s povrezhdeniem serdca. Medicinskaja jekspertiza i pravo. 2013; (2): 8–10. Russian.
7. Tarasenko VS, Arkushenko VA, Mhoyan SA. Hirurgicheskaja taktika pri ranenijah grudi. Medicinskij vestnik Bashkortostana. 2014; (3): 40–3. Russian.
8. Topolnickij EB, Sivolap MP. Analiz povrezhdenij i letal'nosti u postradavshih s ranenijami serdca v mirnoe vremja. Acta Biomedica Scientifica. 2007; (1): 199–200. Russian.
9. Maslyakov VV, Barsukov VG, Kurkin KG. Neposredstvennye rezul'taty lechenija ognestrel'nyh ranenij grudi grazhdanskogo naselenija v uslovijah lokal'nyh voennyh konfliktov. Novosti hirurgii. 2016; (4): 379–84. Russian.
10. Maslyakov VV, Dorzhiev PS. Neposredstvennye i otdalennye rezul'taty lechenija otkrytyh travm serdca. Hirurg. 2013; (5): 42–7. Russian.
11. Novoselov VP, Savchenko SV, Fedorov SA, Kiryanova KS. Morfologija povrezhdenij serdca pri pronikajushhix koloto-rezanyh ranenijah grudi. Sibirskij medicinskij zhurnal (Tomsk). 2009; 24 (4–2): 49–51. Russian.
12. Selezov EA, Zhigo PT, Beloborodov AA, Polikarpov LS. Diagnostika i lechenie ranenij serdca i perikarda. Sibirskoe medicinskoe obozrenie. 2005; 4 (37): 41–2. Russian.
13. Topolnickij EB. Rezul'taty i osnovnye principy hirurgicheskogo lechenija ranenij serdca. Vestnik hirurgii im. I. I. Grekova. 2010; 2 (169): 85–9. Russian.
14. Fomin VN, Fomina RV. Uspeshnoe lechenie ranenija serdca v uslovijah central'noj rajonnoj bol'nicy. Vestnik hirurgii im. I. I. Grekova. 2015; 6 (174): 89–90. Russian.
15. Shajmardanov RSh, Gubaev RF, Korobkov VN, Filippov VA. Diagnostika i hirurgicheskaja taktika pri ranenijah serdca. Vestnik sovremennoj klinicheskoj mediciny. 2014; (7): 205–8. Russian.
16. Rozanov VE, Bolotnikov AI, Lebedev VN, Bondarenko AV, Kil'djashov AV. Osobennosti diagnostiki i lechenija sochetannyh ranenij serdca. Medicina jekstremal'nyh situacij. 2012; (3): 15–30. Russian.
17. Samohvalov IM, Gavrilov SV, Kuzmin AM, Meshakov DP, Nedomolkin SV, Denisov VA, Suprun TV, Zhirnova NA. Ushib serdca pri ognestrel'nyh ranenijah. Voenno-medicinskij zhurnal. 2018; (9): 21–8. Russian.

## Литература

1. Винокуров М. М., Гоголев Н. М. Ранение сердца и перикарда. Acta Biomedica Scientifica. 2005; (3): 160.
2. Волков В. Е., Ванюков В. П., Волков С. В., Жамков Д. Г. Непосредственные результаты хирургического лечения ранений сердца. Здравоохранение Чувашии. 2017; 3 (52): 32–4.
3. Волков В. Е., Волков С. В. Ранения сердца: состояние проблемы и перспективы. Acta Medica Eurasica. 2017; (1): 17–21.
4. Ивченко Д. Р., Колтович А. П. Факторы танатогенеза при огнестрельных ранениях груди. Медицинский вестник МВД. 2013; 2 (63): 31–5.
5. Ковальчук В. И. Открытые ранения сердца у детей. Здравоохранение (Минск). 2015; (4): 62–5.
6. Новоселов В. П., Савченко С. В., Грицингер В. А. Оценка реактивных изменений миокарда при проникающих колото-резаных ранениях груди с повреждением сердца. Медицинская экспертиза и право. 2013; (2): 8–10.
7. Тарасенко В. С., Аркушенко В. А., Мхоян С. А. Хирургическая тактика при ранениях груди. Медицинский вестник Башкортостана. 2014; (3): 40–3.
8. Топольницкий Е. Б., Сиволап М. П. Анализ повреждений и летальности у пострадавших с ранениями сердца в мирное время. Acta Biomedica Scientifica. 2007; (1): 199–200.
9. Масляков В. В., Барсуков В. Г., Куркин К. Г. Непосредственные результаты лечения огнестрельных ранений груди гражданского населения в условиях локальных военных конфликтов. Новости хирургии. 2016; (4): 379–84.
10. Масляков В. В., Доржиев П. С. Непосредственные и отдаленные результаты лечения открытых травм сердца. Хирург. 2013; (5): 42–7.
11. Новоселов В. П., Савченко С. В., Федоров С. А., Кирьянова К. С. Морфология повреждений сердца при проникающих колото-резаных ранениях груди. Сибирский медицинский журнал (Томск). 2009; 24 (4–2): 49–51.
12. Селезов Е. А., Жиго П. Т., Белобородов А. А., Поликарпов Л. С. Диагностика и лечение ранений сердца и перикарда. Сибирское медицинское обозрение. 2005; 4 (37): 41–2.
13. Топольницкий Е. Б. Результаты и основные принципы хирургического лечения ранений сердца. Vestnik hirurgii im. I. I. Grekova. 2010; 2 (169): 85–9.
14. Фомин В. Н., Фомина Р. В. Успешное лечение ранения сердца в условиях центральной районной больницы. Vestnik hirurgii im. I. I. Grekova. 2015; 6 (174): 89–90.
15. Шаймарданов Р. Ш., Губаев Р. Ф., Коробков В. Н., Филиппов В. А. Диагностика и хирургическая тактика при ранениях сердца. Vestnik sovremennoj klinicheskoj mediciny. 2014; (7): 205–8.
16. Розанов В. Е., Болотников А. И., Лебедев В. Н., Бондаренко А. В., Кильдяшов А. В. Особенности диагностики и лечения сочетанных ранений сердца. Медицина экстремальных ситуаций. 2012; (3): 15–30.
17. Самохвалов И. М., Гаврилов С. В., Кузьмин А. М., Мешаков Д. П., Недомолкин С. В., Денисов В. А., Супрун Т. В., Жирнова Н. А. Ушиб сердца при огнестрельных ранениях. Военно-медицинский журнал. 2018; (9): 21–8.

## HUMORAL RESPONSE TO EPSTEIN-BARR VIRAL INFECTION IN PATIENTS WITH ALLERGIES

Svirshchetskaya EV<sup>1</sup> ✉, Simonova MA<sup>1</sup>, Matushevskaya EV<sup>2</sup>, Fattakhova GV<sup>1</sup>, Khlgatian SV<sup>3</sup>, Ryazantsev DY<sup>1</sup>, Chudakov DB<sup>1</sup>, Zavriev SK<sup>1</sup><sup>1</sup> Shemyakin-Ovchinnikov Institute of Bioorganic Chemistry, Moscow, Russia<sup>2</sup> Institute of Continuing Vocational Education, Federal Medical Biological Agency, Moscow, Russia<sup>3</sup> Mechnikov Research Institute of Vaccines and Sera, Moscow, Russia

Type I hypersensitivity is mediated by the production of IgE antibodies in response to normally harmless substances. Debate still continues about the mechanisms underlying allergic reactions. Reduced barrier tissue function can be one of the risk factors for allergies. The aim of the present work was to compare the humoral immune response to Epstein-Barr virus in patients allergic to the *A. alternata* fungus or *D. farinae* house dust mites and healthy donors. It is known that up to 90% of the world population are infected with EBV. This infection occurs at early age when a child develops allergy. The antibodies were analyzed using immuno-PCR and the recombinant EBV protein rEBNA. We were able to demonstrate that infection occurs at early age in both allergic patients and healthy donors. The proportion of EBP-seropositive individuals was comparable between the groups (75 and 74%). The proportion of patients with high IgG<sub>1</sub> titers among patients with allergies was lower (7%) than in healthy donors (18%), suggesting a lower viral load. In patients with allergies (but not in healthy donors) IgG<sub>1</sub> titers declined as children grew older ( $p = 0.037$ ). Besides, IgA<sub>1</sub> titers were increased in patients with allergies in comparison with healthy donors, but differed between patients allergic to *A. alternata* and house dust mites. In allergic individuals, production of IgM against EBV was triggered earlier than in healthy donors. We conclude that IgM production and the IgA<sub>1</sub>-mediated humoral response occur earlier in patients with allergies, causing a decline in IgG<sub>1</sub> titers over time.

**Keywords:** allergy, house dust mites, *A. alternata*, recombinant allergens, Epstein-Barr virus, immuno-PCR

**Author contribution:** Svirshchetskaya EV measured IgE titers against allergens in the sera of allergic individuals and healthy donors, processed the obtained data and participated in the writing of this article; Khlgatian SV selected sera samples for the study and conducted RIDA assays; Fattakhova GV and Chudakov DB measured IgE titers against allergens in the sera of patients with allergies and healthy donors; Matushevskaya EV collected sera samples from patients with allergies, participated in the discussion of the study results and in the writing of this article; Simonova MA and Ryazantsev DY performed iPCR; Ryazantsev DY expressed recombinant proteins of EBV, *A. alternata* and *D. farinae*; Chudakov DB synthesized, purified and characterized the sufficient amount of recombinant proteins for the study; Zavriev SK optimized PCR and participated in the discussion of the study results.

**Compliance with ethical standards:** the study was approved by the Ethics Committee of Mechnikov Research Institute of Vaccines and Sera (Protocol 35 dated September 12, 2018).

✉ **Correspondence should be addressed:** Elena V. Svirshchetskaya  
Miklouho-Maclay 16/10, Moscow, 117997; esvir@mail.ibch.ru

**Received:** 12.09.2018 **Accepted:** 15.02.2019 **Published online:** 01.03.2019

**DOI:** 10.24075/brsmu.2019.004

## ГУМОРАЛЬНЫЙ ОТВЕТ НА ВИРУС ЭПШТЕЙНА-БАРР ПРИ АЛЛЕРГИИ

Е. В. Свирищевская<sup>1</sup> ✉, М. А. Симонова<sup>1</sup>, Е. В. Матушевская<sup>2</sup>, Г. В. Фаттахова<sup>1</sup>, С. В. Хлгатян<sup>3</sup>, Д. Ю. Рязанцев<sup>1</sup>, Д. Б. Чудаков<sup>1</sup>, С. К. Завриев<sup>1</sup><sup>1</sup> Институт биоорганической химии имени М. М. Шемякина и Ю. А. Овчинникова, Москва, Россия<sup>2</sup> Институт повышения квалификации Федерального медико-биологического агентства, Москва, Россия<sup>3</sup> Научно-исследовательский институт вакцин и сывороток имени И. И. Мечникова, Москва, Россия

Аллергия I типа опосредована формированием IgE-антител к безвредным веществам. Механизмы возникновения аллергии остаются дискуссионными. Одним из факторов риска может быть снижение защитных функций барьерных тканей. Целью работы было проанализировать гуморальный иммунный ответ на вирус Эпштейна-Барр (ВЭБ) у больных с аллергией на гриб *A. alternata* и клещей домашней пыли *D. farinae* (КДП) и у здоровых людей. Известно, что до 90% населения инфицированы ВЭБ. Инфицирование происходит в раннем возрасте параллельно с формированием аллергических реакций. Анализ антител проводили методом иммуно-ПЦР с использованием рекомбинантного белка ВЭБ rEBNA1. Показали, что инфицирование как у больных, так и у доноров происходит в детстве; доля сероположительных по ВЭБ индивидов была сравнимой в группах (75 и 74%). Доля пациентов с высокими титрами IgG<sub>1</sub> среди больных с аллергией была ниже (7%) по сравнению с донорами (18%), что соответствует меньшей вирусной нагрузке. У больных с аллергией, но не у здоровых людей, наблюдали снижение титров IgG<sub>1</sub> с возрастом ( $p = 0,037$ ). Кроме того, при аллергии повышены титры IgA<sub>1</sub> по сравнению с донорами, однако IgA<sub>1</sub>-ответы при аллергии на гриб *A. alternata* и на КДП различались. При аллергии также раньше формировались IgM к ВЭБ. Таким образом, при аллергии быстрее формируется IgM и IgA<sub>1</sub> гуморальный ответ, что приводит к снижению с возрастом IgG<sub>1</sub>-титров.

**Ключевые слова:** аллергия, клещи домашней пыли, грибы *A. alternata*, рекомбинантные аллергены, вирус Эпштейна-Барр, иммуно-ПЦР

**Информация о вкладе авторов:** Е. В. Свирищевская — определение IgE титров на аллергены в сыворотках больных с аллергией и доноров, обработка данных, написание статьи; С. В. Хлгатян — подбор сывороток больных с аллергией и доноров различного возраста, типирование методом RIDA; Г. В. Фаттахова, Д. Б. Чудаков — определение IgE титров на аллергены в сыворотках больных с аллергией и доноров; Е. В. Матушевская — сбор сывороток больных с аллергией, обсуждение результатов и написание статьи; М. А. Симонова, Д. Ю. Рязанцев — постановка ПЦР; Д. Ю. Рязанцев — экспрессия в *E. coli* рекомбинантных белков ВЭБ, *A. alternata* и *D. Farinae*; Д. Ю. Чудаков — наработка, очистка и характеристика рекомбинантных белков; С. К. Завриев — оптимизация ПЦР, участие в обсуждении результатов.

**Соблюдение этических стандартов:** исследование одобрено этическим комитетом Института вакцин и сывороток им. И. И. Мечникова (протокол № 35 от 12 сентября 2018 г.).

✉ **Для корреспонденции:** Елена Викторовна Свирищевская  
ул. Миклухо-Маклая, 16/10, г. Москва, 117997; esvir@mail.ibch.ru

**Статья получена:** 12.09.2018 **Статья принята к печати:** 15.02.2019 **Опубликована онлайн:** 01.03.2019

**DOI:** 10.24075/vrgmu.2019.004

The Epstein–Barr virus (EBV) is a DNA virus that belongs to the *Herpesviridae* family and causes a broad range of pathologies in humans, from respiratory diseases to cancer. So far, 8 herpesvirus types are known that infect humans. Among them, herpes simplex virus (types 1 and 2), varicella zoster (type 3), EBV (type 4), and cytomegalovirus (type 5) are widely spread in the human population. In contrast, infections caused by types 6 and 7 herpesviruses and Kaposi sarcoma-associated herpesvirus are much rarer. Almost every adult is infected with at least one type of herpesvirus. The diagnosis is established based on the presence of specific antibodies in the blood serum. About 80 to 95% of the world population are latently infected with EBV or cytomegalovirus [1]. Latent EBV infection is associated with some cancers [1–3], multiple sclerosis [4–5], and systemic lupus erythematosus [6]; it also aggravates the course of HIV infection [7] and triggers production of autoantibodies against human DNA and proteins [8–9]. The main EBV antigens are the viral capsid antigen, the early antigen and the nuclear antigen 1 (EBNA1) [10–11]. EBNA1 ensures persistence of the virus in its latent state. Type G antibodies (IgG) against EBNA1 are produced by the organism every time the virus reactivates and reflect the total body viral load.

EBV is spread through bodily contacts, such as kissing, sharing personal hygiene items, eating utensils or the like. Airborne transmission is quite rare though possible. Mother-to-child transmission occurs during pregnancy, childbirth or breastfeeding. According to some researchers, antibodies against EBV are detected in 50% of children under 3 years of age [12–13]. In such cases, the virus is likely to be spread through sharing eating utensils and kissing.

Type I hypersensitivity is characterized by a IgE-mediated humoral response to the proteins contained in small, normally harmless particles, such as pollen, house dust mites (HDM), animal dander, etc. [14–15]. The skin and bronchial epithelium of patients with allergies differ considerably from barrier tissues of healthy individuals [16–17]. The aim of the present study was to measure a humoral response to EBV in patients allergic to *A. alternata* and *D. farinæ*.

Previously, we proposed a method for measuring IgG<sub>1</sub> titers against EBV and other allergens based on the quantitative polymerase chain reaction (PCR) [18–19]. Immuno-PCR (iPCR) is a sensitive technique that can detect antibodies in biological fluids [20–21]. Its advantage is the linearity of titration curves in a wide range of concentrations, which enables detection of specific antibodies using a smaller number of dilutions [18–19].

## METHODS

### Sera

Serum samples used in the present study were collected from children and adults with hypersensitivity to HDM and the *Alternaria alternata* fungus at Mechnikov Research Institute of Vaccines and Sera (Moscow, Russia) between 2009 and 2017. Informed consent was obtained from all donors or their representatives. Allergy tests were performed using commercial RIDA panels (Germany). The samples collected from patients with allergies were included in the study if IgE titers against *A. alternata* or *D. farina* measured by RIDA were interpreted as classes 3 through 6. Patients who had previously undergone allergen-specific immunotherapy or had cross-sensitivity to *A. alternata* or *D. farinæ* were excluded from the study. Individuals of different ages who had no IgE against pollen, fungi or domestic allergens included in the RIDA panel were considered healthy donors.

### Materials

The following reagents and equipment were used in the study: high protein-binding capacity well-plates (Costar; USA), Nunc TopYield strips for qPCR (ThermoFisher Scientific; USA), Tween-20, a ready-for-use 3,3',5,5'-tetramethylbenzidine solution (Sigma; USA), goat serum (Bovogen Biologicals; Australia), biotinylated monoclonal anti-human IgG<sub>1</sub>–IgG<sub>4</sub> and anti-IgE antibodies (Southern Biotech; USA), mouse anti-human IgA<sub>1</sub> and IgA<sub>2</sub> antibodies, a conjugate of goat anti-mouse IgG and biotin and a conjugate of streptavidin and horseradish peroxidase (BD Pharmigen; USA), biotinylated oligodeoxyribonucleotide (ODN) (Lumiprobe; Moscow), streptavidin (Sigma; USA) and recombinant proteins rEBNA1, Der f 2 and Alt a 1 synthesized in our laboratory [18, 22–23]. Other reagents were purchased from Fluka (Switzerland).

### Immuno-PCR

The 10 µg/ml solution of the recombinant rEBNA1 antigen in carbonate-bicarbonate buffer (0.05 M, pH 9.6) was pipetted into the TopYield wells (50 µl per well) and incubated overnight at 4 °C. In the morning the wells were washed with TETBS (20 mM Tris-HCl, 150 mM NaCl, 0.1 mM EDTA, 0.1% Tween-20, pH 7.5) three times. Serum samples were diluted tenfold with TETBS containing 20% goat serum, and a series of 1 : 5 dilutions was prepared for each sample. Each diluted sample was pipetted into the well-plates (25 µl per well) in three replicates. Six replicates of fetal bovine serum (FBS) were used as a negative control. The plate with the samples was incubated on the shaker at room temperature for 30 min. Then, the plate was washed with TETBS three times. Solutions of biotinylated anti-human IgG<sub>1</sub>, IgG<sub>2</sub>, IgG<sub>3</sub>, and IgG<sub>4</sub> antibodies or mouse anti-human IgA<sub>1</sub>, IgA<sub>2</sub> and IgM antibodies in TETBS containing 20%-goat serum (1 : 1,000) were introduced into the wells (50 µl per well). The plates were incubated on the shaker at room temperature for 30 min and then washed three times with TETBS. To measure IgA<sub>1</sub>, IgA<sub>2</sub> and IgM concentrations, the samples were further incubated with goat anti-mouse IgG antibodies conjugated to biotin. After washing, 50 µl of 1 µg/ml streptavidin were introduced into the wells, incubated for 10 min, and washed. Then, 50 µl of 5 pM ODN solution in TETBS containing 20% goat serum were added into each well and incubated on the shaker at room temperature for 10 min. After incubation, the wells were washed 3 times with TBS (20 mM Tris-HCl, 150 mM NaCl, pH 7.5). Thirty-five µl of the PCR mix were added in the wells and overlaid with 30 µl of mineral oil per well. Real-time PCR was performed in the DTprime thermocycler (DNA-Technology; Russia). Briefly, the protocol included initial 5-min denaturation at 94 °C followed by 40 cycles of annealing and extension at 60 °C for 15 s and denaturation at 94 °C for 5 s. For each cycle, fluorescence from the probe was recorded at 520 nm wavelength. PCR results were analyzed using the thermocycler software provided by the vendor. For each sample, a mean threshold cycle value (C<sub>q</sub>) and a standard deviation were computed. The detection threshold was calculated as 3 standard deviations for (C<sub>q</sub>-), where (C<sub>q</sub>-) is a threshold cycle value in negative samples. The titers were determined as a maximal dilution of a serum sample at which the sample was positive for a measured analyte.

### Statistical analysis

Mean and standard deviations were computed in Excel (Microsoft Office, 2003). The correlation between IgG1-antibody titers

and the groups of patients was evaluated using the parametric Pearson's  $\chi^2$ -test and Student's *t*-test. The differences were considered significant at  $p < 0.05$  yielded by the two-tailed analysis.

## RESULTS

### Specifics of iPCR

The iPCR-based method used in this study is described in the Table. On the whole, steps 0-3 of iPCR are similar to those of ELISA: the antigen is applied onto a plate (step 0); incubated with a blood serum sample (step 1); then with biotinylated anti-human IgG1 antibodies (step 2); streptavidin-ODN (PCR) or a streptavidin-horseradish peroxidase conjugate (ELISA, step 3). Step 3 in iPCR is divided into two substeps and includes incubation with streptavidin followed by incubation with biotin-ODN, which enhances iPCR sensitivity. Step 4 is purely PCR or the addition of a substrate for horseradish peroxidase (ELISA).

In ELISA, the substrate-based detection step remains unstandardized and depends on the day of experiment and the time of reaction termination. Using iPCR, one can reduce the time required for the reaction by as much as 1 hour. The iPCR makes the analysis more standardized and therefore less dependent on the operator. It also increases the sensitivity of the analysis due to a stronger linearity of the obtained data [18–19].

### IgE-mediated response to allergens

Serum samples collected from allergic individuals were assayed using commercial RIDA panels. Those containing IgE antibodies against *Dermatophagoides farinae* and *Alternaria alternata* were included in the initial phase of the study. Specifically, we selected the samples interpreted as class 3 and above, according to RIDA scores. Fig. 1 shows distribution of the allergic patients into groups based on RIDA classes. In

some samples, no IgE antibodies were detected against any of 15 allergens present in the panel (pollens, fungi and domestic allergens). Such sera were used as healthy donor samples. Ultimately, a total of 30 samples were selected representing patients with allergies and healthy donors aged 0 to 15 years.

### Total humoral response to EBV

A pool of 10 RIDA class 5 and 6 serum samples was used to profile the repertoire of anti-EBV antibodies in patients aged 3–15 years with respiratory allergies to HDM and *A. alternata*. A pool of samples collected from 10 healthy donors of the same age was used as a control. The titers of rEBNA1-recognizing immunoglobulins were as follows: IgM > IgG<sub>1</sub> > IgA<sub>1</sub> > IgA<sub>2</sub> > IgG<sub>2</sub> (Fig. 2) in donors and IgM > IgA<sub>1</sub> > IgG<sub>1</sub> > IgA<sub>2</sub> > IgG<sub>2</sub> in patients with allergies. The titers of IgG<sub>3</sub> and IgG<sub>4</sub> were low in both groups. Significant differences between allergic patients and healthy donors were observed only for IgG<sub>1</sub> and IgA<sub>1</sub>. The IgG<sub>1</sub> to IgA<sub>1</sub> ratio was 9 and 0.4 for healthy donors and allergic patients, respectively, suggesting that the IgA-mediated response prevailed in the studied cohort of patients whereas the IgG<sub>1</sub>-mediated response prevailed in healthy donors.

### Analysis of IgG<sub>1</sub>-mediated response to EBV

Viral infections normally trigger production of class IgG<sub>1</sub> antibodies. Fig. 3A shows age-based distribution of IgG<sub>1</sub> titers against EBV in the sera of patients allergic to HDM and/or *A. alternata* and healthy donors. The analysis revealed that infection had been acquired at early age in both groups. A few 4–6-year-old children in both groups had IgG<sub>1</sub> levels above 1,000. Mean IgG<sub>1</sub> titers were 330 and 1,500 in the group of patients aged 3 to 10 years and healthy donors, respectively. In patients aged 11–20 years and healthy donors of the same age, the titers were 720 and 490, respectively, indicating a tendency to early infection or early immune response. Because of the considerable variability in the data, no significant differences

**Table.** Comparison of iPCR and ELISA steps

Steps	0	1	2	3	4	
PCR	Antigen	Serum	algG1-bio*	Streptavidin/ODN	PCR	Time
	Overnight	30 min	30 min	10/10 min	1 h	3–4 h
ELISA	Antigen	Serum	algG1-bio	Streptavidin-HP**	Substrate	
	Overnight	1 h	1 h	1 h	20 min	4–5 h

**Note:** \*algG1-bio represents any biotinylated antibody to any class or subclass of antibodies (G, A, E); \*\*HP is horseradish peroxidase.

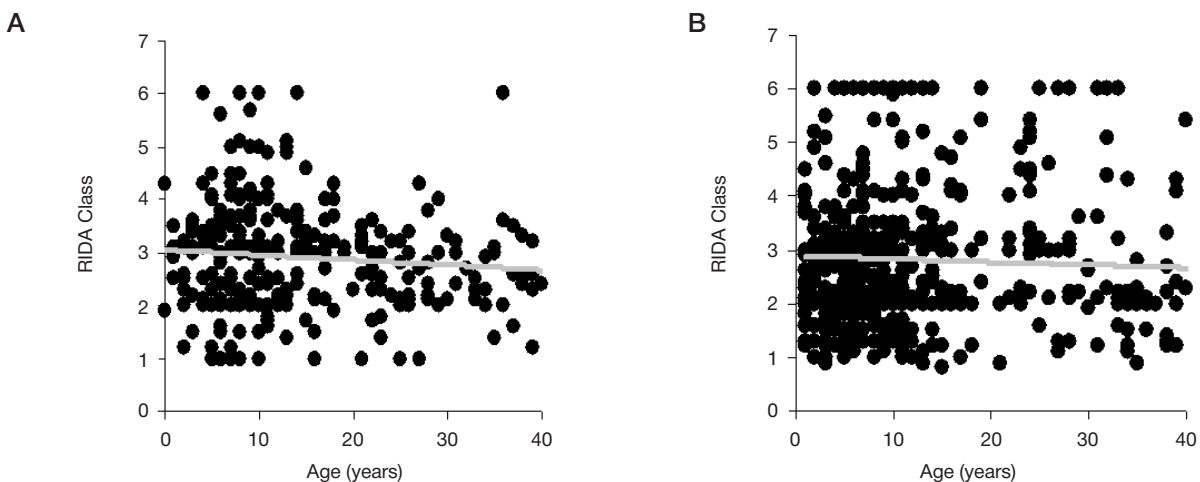


**Fig. 1.** IgE-mediated response in patients with allergies measured by RIDA. IgE levels in the serum samples of patients allergic to house dust mites (A) and *A. alternata* (B) were interpreted as classes 0–6 proportional to IgE titers

were observed between the groups. No differences were found in the level of antibodies against EBV between patients allergic to HDM or *A. alternata* and healthy donors (Fig. 3B).

While determining the proportions of individuals who did not have antibodies against EBV and those who had low (< 100), moderate (100–1,000) or high (>1,000) IgG<sub>1</sub> titers, we established that 75% of children in both groups aged 3–15 years had a latent EBV infection (Fig. 4A) and 45% of individuals in both groups had low titers of antibodies. The groups differed in terms of high IgG<sub>1</sub> titers: the titers over 1,000 (2,000–8,000) were observed in 20% of healthy donors and only 7% of allergic children (Fig. 4A). This suggests a better resistance to the viral infection in allergic patients. Anti-EBV antibody levels were comparable in both groups (Fig. 4B).

### Analysis of IgA<sub>1</sub> and IgM-mediated responses to EBV

As shown above, IgA<sub>1</sub> antibodies were slightly though reliably increased in patients with allergies ( $p = 0.03$ ). A more detailed analysis revealed that the most pronounced difference could

be observed at early stages of the viral infection (Fig. 5A). Moderate anti-EBV IgA<sub>1</sub> titers in patients with allergies and healthy donors aged 3 to 10 years reached 425 and 265, respectively; in patients aged 11–30 years, they were 690 and 370, respectively. Besides, IgA<sub>1</sub> titers tended to increase with age in both groups (Fig. 5A). Interestingly, IgA<sub>1</sub> titers against EBV were indicative of the difference in response to the viral infection between patients with different allergies. The levels of IgA<sub>1</sub> against EBV were significantly higher in patients with allergies to HDM (Fig. 5B) than in patients with IgE against *A. alternata* and in healthy donors.

In both healthy donors and patients with allergies, moderate IgM titers against EBV were higher than class G and A immunoglobulin titers by one order of magnitude. The obtained data were split into two groups: low titers (< 5,000) and high titers (> 15,000) (Fig. 5C, D). The proportion of individuals with high IgM titers in both groups was  $\approx 60\%$ . No differences in IgM levels depending on the age and mean titer were observed in the high IgM subgroup (Fig. 5C). In the low IgM subgroup, patients with allergies produced anti-EBV antibodies earlier

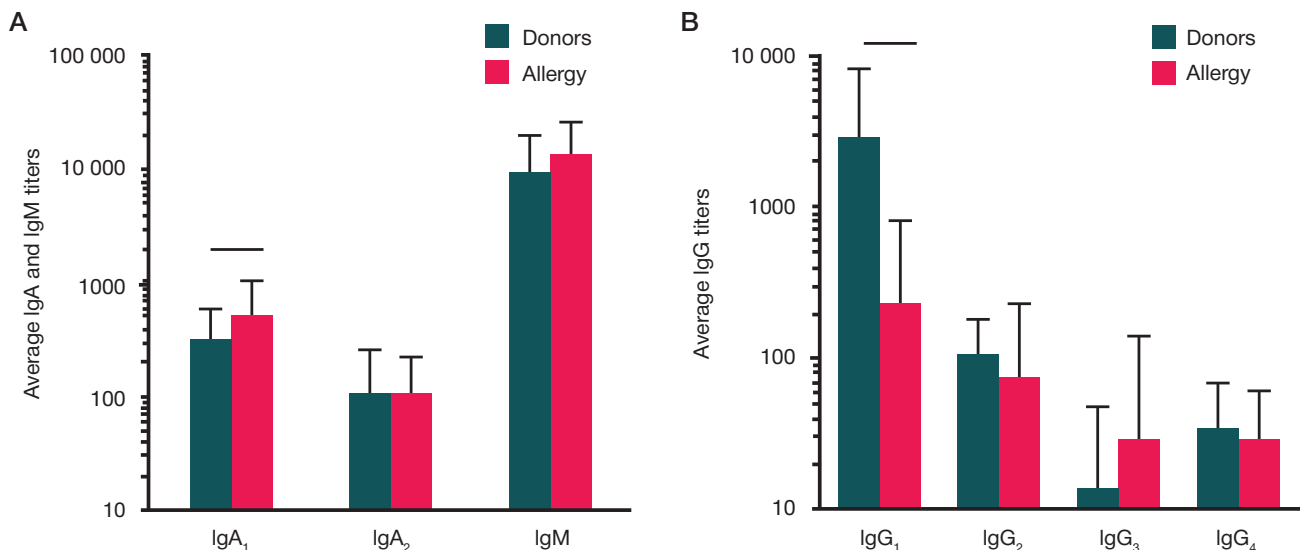


**Fig. 2.** Analysis of rEBNA1-recognizing immunoglobulins present in the sera of healthy donors and patients with allergies. Analysis of IgA<sub>1</sub>, IgA<sub>2</sub>, IgM (A), IgG<sub>1</sub>, IgG<sub>2</sub>, IgG<sub>3</sub>, and IgG<sub>4</sub> (B) in the pooled sera of 10 donors and 10 allergic patients. The figures are presented as mean values  $\pm$  a standard deviation. Statistically significant differences ( $p < 0.05$ ) are marked with a vertical line with a cross-bar

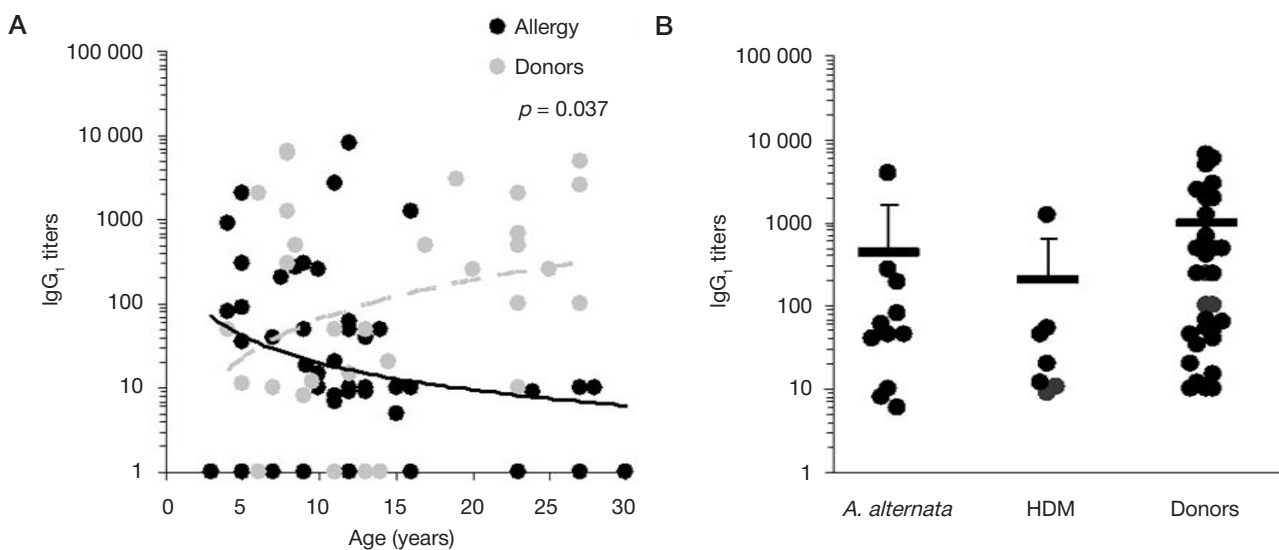


**Fig. 3.** Analysis of rEBNA1-specific IgG<sub>1</sub> in the sera of healthy donors and patients with allergies. **A.** Analysis of IgG<sub>1</sub> titers in individual sera of patients allergic to *A. alternata* ( $n = 15$ ), house dust mites ( $n = 9$ ) and healthy donors ( $n = 38$ ). Vertical lines with cross-bars indicate mean values  $\pm$  a standard deviation. **B.** Relationship between rEBNA1-specific IgG<sub>1</sub> titers and age in the individual samples of sera collected from allergic patients ( $n = 53$ ) and healthy donors ( $n = 34$ ). Power approximation is marked with lines and t-test probability is also shown

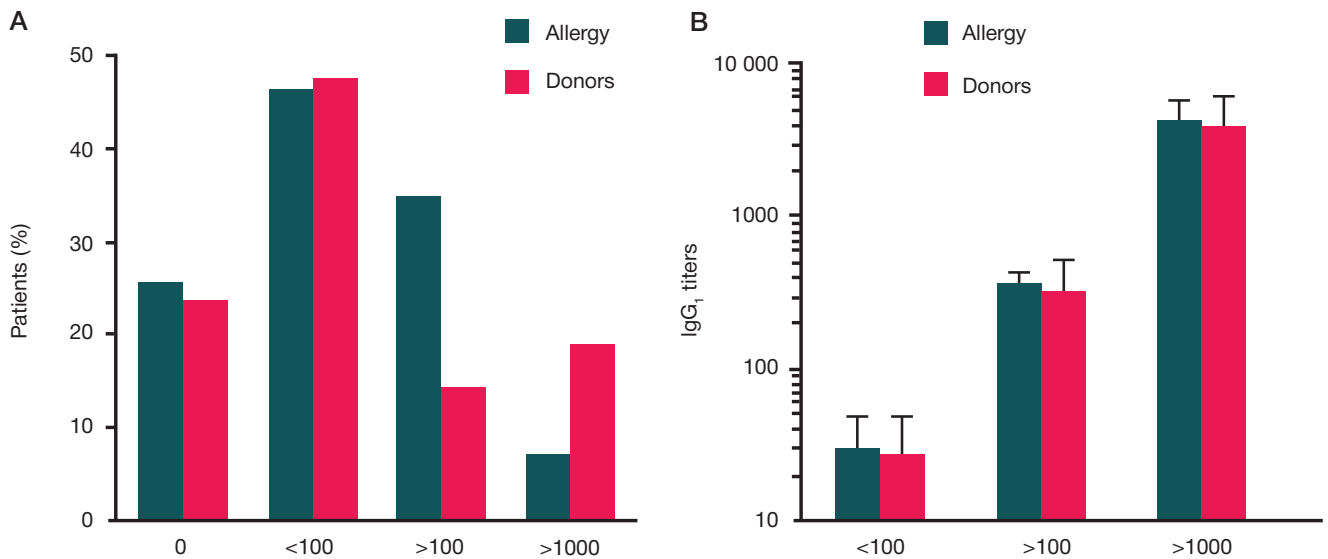


**Fig. 4.** Analysis of rEBNA1-specific IgG<sub>1</sub> present in the sera of healthy donors and patients with allergies. The proportion (%) of patients and healthy donors with different IgG<sub>1</sub> titers (A) and the mean titers in these groups (B)

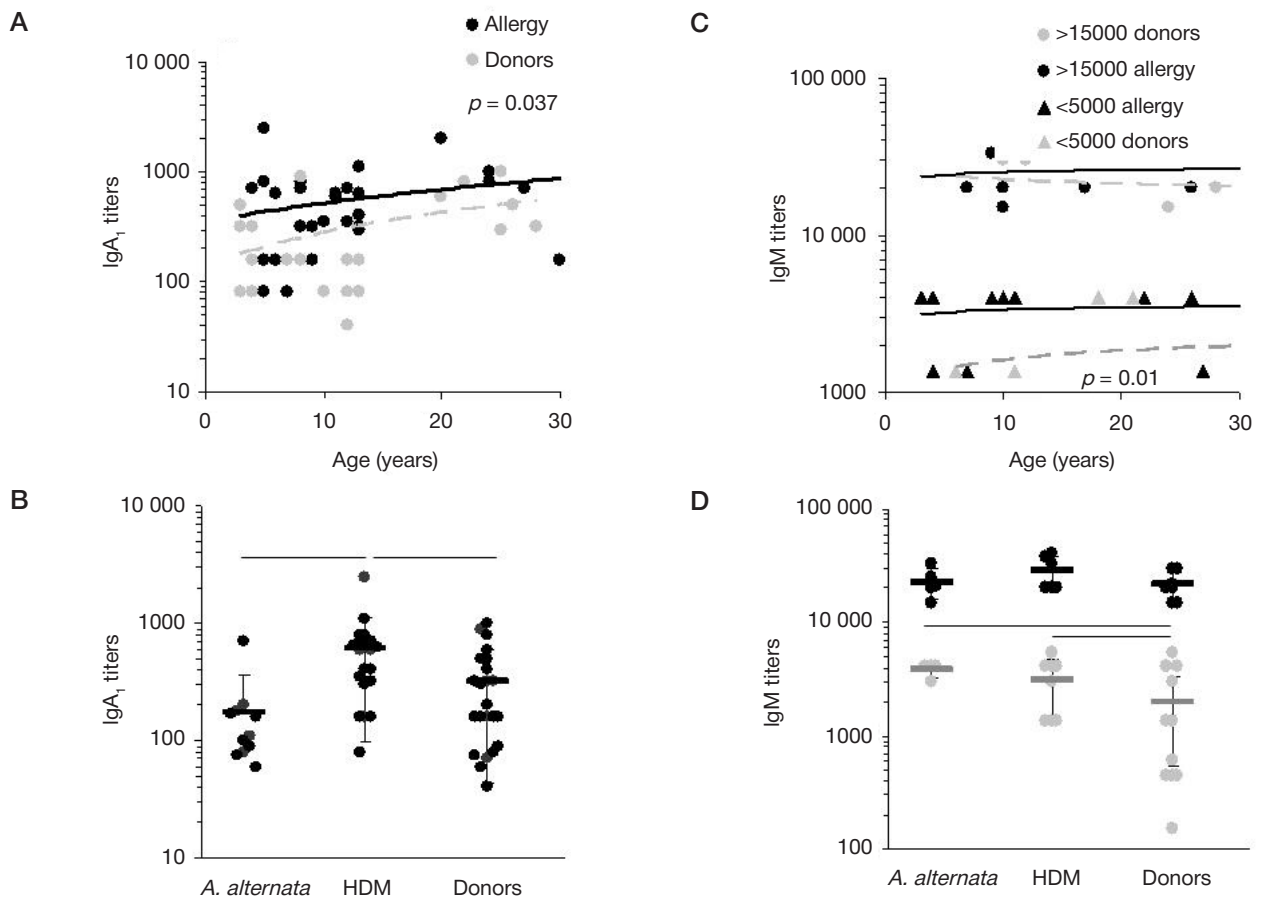


**Fig. 5.** Analysis of rEBNA1-specific IgA<sub>1</sub> and IgM in the sera of healthy donors and patients with allergies. Distribution of IgA<sub>1</sub> (A) and (B) titers in the individual serum samples of patients allergic to *A. alternata* ( $n = 11$ ), house dust mites ( $n = 21$ ) and healthy donors ( $n = 23$ ) depending on donors' age. Distribution of rEBNA1-specific IgA<sub>1</sub> (C) and IgM (D) in the sera of healthy donors and patients with allergies. IgM data are given for the sera with low (grey circles) and high (black circles) IgM titers. Vertical lines with cross-bars show mean values  $\pm$  a standard deviation. Significant differences ( $p < 0.05$ ) are marked with horizontal bars

than healthy donors (Fig. 5D). A rise in IgM titers in the low IgM subgroup was detected in patients allergic to both HDM and *A. alternata* (Fig. 5D).

DISCUSSION

After primary infection with EBV, the organism starts to produce different (sub)classes of antibodies. A human body is capable

of producing isotypes M, A, G and E that also include the IgG<sub>1</sub>-IgG<sub>4</sub> and IgA<sub>1</sub>-IgA<sub>2</sub> subtypes. The main pool of class M antibodies represents innate immunity; IgM titers increase during primary infection. IgA is involved in mucosal defense. IgE rises in response to parasitic infections and allergens. At present, it is believed that IgA and IgE are adaptive immunity components because their production requires B-cells to "switch" from secreting IgM to other immunoglobulins. However,

recently there has been a lot of debate about the possibility of such “switch” occurring without participation of T cells [23, 24], which is how innate immunity functions. Class A antibodies are produced in response to exposure to early antigens, such as VCA and EA [25]. IgA and IgM antibodies to early antigens are markers of viral reactivation or secondary infection. IgA titers against the late EBNA1 antigen are also significantly increased in patients with nasopharyngeal cancer [26].

The data yielded by our experiment demonstrate that patients with allergies responded to EBV infection by an early and significant increase in IgA<sub>1</sub> and IgM titers. Their IgA<sub>2</sub> titers were lower than IgA<sub>1</sub> and did not differ significantly between the groups (these data are not provided in the present article). Allergies are accompanied by mucosal inflammation and increased production of cytokines and chemokines [17, 24], leading to the activation of B cells. IgM production was comparable between healthy donors and allergic patients (both with a strong serological response) indicating an equally strong immune response to the reactivation of IgM-secreting B cells by the virus.

IgG proteins are the main protective component of the adaptive humoral response. The “switch” of B cells to IgG production occurs only in parallel with the antigen-specific T-dependent response to EBV. It is known that IgG1 secretion dominates antiviral response [27–28]. According to the literature,

antibody titers produced in response to hepatitis B infection are as follows: IgG<sub>1</sub> > IgG<sub>4</sub> > IgG<sub>3</sub> > IgG<sub>2</sub> [27]; the pattern changes in the case of EBV: IgG<sub>1</sub> >> IgG<sub>2</sub>, IgG<sub>3</sub>, IgG<sub>4</sub> [28]. The data obtained for healthy donors are consistent with the EBV response pattern dominated by IgG<sub>1</sub> production. For patients with allergies, mean IgG<sub>1</sub> concentrations were lower than in healthy donors and comparable with IgG<sub>2</sub> concentrations ( $p = 0.14$ ). Statistical analysis revealed that significant differences in IgG<sub>1</sub> titers between allergic patients and healthy donors increase with age. So far, the antiviral response in patients with allergies has not been studied. On the whole, the data yielded by our experiment suggest that respiratory allergy is accompanied by an increase in IgA<sub>1</sub>- and IgM-antibodies against EBV, which prevents the virus from penetrating the epithelial barrier and reduces the total body viral load.

## CONCLUSIONS

Allergy is characterized by hypersensitivity of epithelial barriers caused by an interaction between IgE and allergens. Hyperreactivity of the innate immune system seems to enhance the antiviral response to the Epstein-Barr virus, causes a rise in IgA<sub>1</sub> and IgM titers and a reduction in IgG<sub>1</sub> titers correlating to the latent viral load.

## References

- Kayamba V, Monze M, Asombang AW, Zyambo K, Kelly P. Serological response to Epstein-Barr virus early antigen is associated with gastric cancer and human immunodeficiency virus infection in Zambian adults: a case-control study. *Pan Afr Med J*. 2016; (23): 45. DOI: 10.11604/pamj.2016.23.45.8503.
- Banko AV, Lazarevic IB, Folic MM, Djukic VB, Cirkovic AM, Karalic DZ, Cupic MD, Jovanovic TP. Characterization of the Variability of Epstein-Barr Virus Genes in Nasopharyngeal Biopsies: Potential Predictors for Carcinoma Progression. *PLoS One*. 2016; 11 (4): e0153498. DOI: 10.1371/journal.pone.0153498.
- Frappier L. EBNA1. *Curr Top Microbiol Immunol*. 2015; (391): 3–34. DOI: 10.1007/978-3-319-22834-1\_1.
- Myhr KM, Riise T, Barrett-Connor E, Myrmet H, Vedeler C, Grønning M, Kalvenes MB, Nyland H. Altered antibody pattern to Epstein-Barr virus but not to other herpesviruses in multiple sclerosis: a population based case-control study from western Norway. *J Neurol Neurosurg Psychiatry*. 1998; 64 (4): 539–42.
- Lomakin Y, Arapidi GP, Chernov A, Ziganshin R, Tcyganov E, Lyadova I, Butenko IO, Osetrova M, Ponomarenko N, Telegin G, Govorun VM, Gabibov A, Belogurov A Jr. Exposure to the Epstein-Barr Viral Antigen Latent Membrane Protein 1 Induces Myelin-Reactive Antibodies In Vivo. *Front Immunol*. 2017; (8): 777. DOI: 10.3389/fimmu.2017.00777.
- Piroozmand A, Haddad Kashani H, Zamani B. Correlation between Epstein-Barr Virus Infection and Disease Activity of Systemic Lupus Erythematosus: a Cross-Sectional Study. *Asian Pac J Cancer Prev*. 2017; (18): 523–7.
- Pan R, Liu X, Zhou S, Ning Z, Zheng H, Gao M, Ding Y, Yao W, Liao X, He N. Differential prevalence and correlates of whole blood Epstein-Barr virus DNA between HIV-positive and HIV-negative men who have sex with men in Shanghai, China. *Epidemiol Infect*. 2017; 145 (11): 2330–40. DOI: 10.1017/S0950268817001054.
- Lindsey JW, deGannes SL, Pate KA, Zhao X. Antibodies specific for Epstein-Barr virus nuclear antigen-1 cross-react with human heterogeneous nuclear ribonucleoprotein L. *Mol Immunol*. 2016 Jan; (69): 7–12. DOI: 10.1016/j.molimm.2015.11.007.
- Lindsey JW. Antibodies to the Epstein-Barr virus proteins BFRF3 and BRRF2 cross-react with human proteins. *Neuroimmunol*. 2017; (310): 131–4.
- Al Sidairi H, Binkhamis K, Jackson C, Roberts C, Heinsteinst C, MacDonald J, Needle R, Hatchette TF, LeBlanc JJ. Comparison of two automated instruments for Epstein-Barr virus serology in a large adult hospital and implementation of an Epstein-Barr virus nuclear antigen-based testing algorithm. *J Med Microbiol*. 2017; 66 (11): 1628–34. DOI: 10.1099/jmm.0.000616.
- Maylin S, Feghouli L, Salmona M, Herda A, Mercier-Delarie S, Simon F, Legoff J. Evaluation the Architect EBV VCA IgM, VCA IgG, and EBNA-1 IgG chemiluminescent immunoassays to assess EBV serostatus prior transplantation. *J Med Virol*. 2017; 89 (11): 2003–10. DOI: 10.1002/jmv.24889.
- Simon KC, Saghafiyan-Hedengren S, Sverremark-Ekström E, Nilsson C, Ascherio A. Age at Epstein-Barr virus infection and Epstein-Barr virus nuclear antigen-1 antibodies in Swedish children. *Mult Scler Relat Disord*. 2012; 1 (3): 136–8. DOI: 10.1016/j.msard.2012.03.002.
- Xiong G, Zhang B, Huang MY, Zhou H, Chen LZ, Feng QS, Luo X, Lin HJ, Zeng YX. Epstein-Barr virus (EBV) infection in Chinese children: a retrospective study of age-specific prevalence. *PLoS One*. 2014; 9 (6): e99857. DOI: 10.1371/journal.pone.0099857.
- Feng C, Kim JH. Beyond Avoidance: the Psychosocial Impact of Food Allergies. *Clin Rev Allergy Immunol*. 2018. DOI: 10.1007/s12016-018-8708-x.
- Licari A, Castagnoli R, Brambilla I, Marseglia A, Tosca MA, Marseglia GL, Ciprandi G. Asthma Endotyping and Biomarkers in Childhood Asthma. *Pediatr Allergy Immunol Pulmonol*. 2018; 31 (2): 44–55. DOI: 10.1089/ped.2018.0886.
- Tsakok T, Woolf R, Smith CH, Weidinger S, Flohr C. Atopic dermatitis: the skin barrier and beyond. *Br J Dermatol*. 2018. DOI: 10.1111/bjd.16934.
- Carsin A, Mazenq J, Ilstad A, Dubus JC, Chanez P, Gras D. Bronchial epithelium in children: a key player in asthma. *Eur Respir Rev*. 2016; 25 (140): 158–69. DOI: 10.1183/16000617.0101-2015.
- Pivovarov VD, Ryazantsev DY, Simonova MA, Dimitrieva TV, Khlgatian SV, Zavriev SK, Svirshchetskaya EV. Razrabotka test-sistemy dlja analiza antitel k virusu Jepshtejna-Barr metodom immuno-PCR. *Molekuljarnaja biologija*. 2018; 52 (4): 727–34.
- Simonova MA, Pivovarov VD, Ryazantsev DY, Dolgova AS,

- Berzhets VM, Zavriev SK, Svirshchevskaya EV. Comparative diagnostics of allergy using quantitative immuno-PCR and ELISA. *Bioanalysis*. 2018. DOI: 10.4155/bio-2017-0194.
20. Chang L, Li J, Wang L. Immuno-PCR: An ultrasensitive immunoassay for biomolecular detection. *Anal Chim Acta*. 2016; (910): 12–24. DOI:10.1016/j.aca.2015.12.039.
  21. Jani D, Savino E, Goyal J. Feasibility of immuno-PCR technology platforms as an ultrasensitive tool for the detection of anti-drug antibodies. *Bioanalysis*. 2015; (7): 285–94.
  22. Ryazantsev DYu, Drobyazina PE, Khlgatian SV, Zavriev SK, Svirshchevskaya EV. Jekspressija allergenov kleshhej domashnej pyli Der f 1 i Der f 2 v list'jah Nicotiana benthamiana. *Bioorganicheskaja himija*. 2014; 40 (4): 468–78.
  23. Svirshchevskaya E, Fattakhova G, Khlgatian S, Chudakov D, Kashirina E, Ryazantsev D, Kotsareva O, Zavriev S. Direct versus sequential immunoglobulin switch in allergy and antiviral responses. *Clin Immunol*. 2016; (170): 31–8. DOI: 10.1016/j.clim.2016.07.022.
  24. Takaki H, Ichimiya S, Matsumoto M, Seya T. Mucosal Immune Response in Nasal-Associated Lymphoid Tissue upon Intranasal Administration by Adjuvants. *J Innate Immun*. 2018; (10): 515–21. DOI: 10.1159/000489405.
  25. Bhaduri-McIntosh S, Landry ML, Nikiforow S, Rotenberg M, El-Guindy A, Miller G. Serum IgA antibodies to Epstein-Barr virus (EBV) early lytic antigens are present in primary EBV infection. *J Infect Dis*. 2007; 195 (4): 483–92.
  26. Cai YL, Li J, Lu AY, Zheng YM, Zhong WM, Wang W, Gao JQ, Zeng H, Cheng JR, Tang MZ. Diagnostic significance of combined detection of Epstein-Barr virus antibodies, VCA/IgA, EA/IgA, Rta/IgG and EBNA1/IgA for nasopharyngeal carcinoma. *Asian Pac J Cancer Prev*. 2014; 15 (5): 2001–6.
  27. Wang L, Tsai TH, Huang CF, Ho MS, Lin DB, Ho YC, Lin SS, Wei JC, Chou MC, Yang CC. Utilizing self-prepared ELISA plates for a cross-population study of different anti-HBe IgG subclass profiles. *J Med Virol*. 2007; 79 (5): 495–2.
  28. Wakiguchi H, Hisakawa H, Hosokawa T, Kubota H, Kurashige T. Analysis of IgG subclasses in chronic active Epstein-Barr virus infection. *Pediatr Int*. 2000; 42 (1): 21–5.

## Литература

1. Kayamba V, Monze M, Asombang AW, Zyambo K, Kelly P. Serological response to Epstein-Barr virus early antigen is associated with gastric cancer and human immunodeficiency virus infection in Zambian adults: a case-control study. *Pan Afr Med J*. 2016; (23): 45. DOI: 10.11604/pamj.2016.23.45.8503.
2. Banko AV, Lazarevic IB, Folic MM, Djukic VB, Cirkovic AM, Karalic DZ, Cupic MD, Jovanovic TP. Characterization of the Variability of Epstein-Barr Virus Genes in Nasopharyngeal Biopsies: Potential Predictors for Carcinoma Progression. *PLoS One*. 2016; 11 (4): e0153498. DOI: 10.1371/journal.pone.0153498.
3. Frappier L. EBNA1. *Curr Top Microbiol Immunol*. 2015; (391): 3–34. DOI: 10.1007/978-3-319-22834-1\_1.
4. Myhr KM, Riise T, Barrett-Connor E, Myrnes H, Vedeler C, Grønning M, Kalvenes MB, Nyland H. Altered antibody pattern to Epstein-Barr virus but not to other herpesviruses in multiple sclerosis: a population based case-control study from western Norway. *J Neurol Neurosurg Psychiatry*. 1998; 64 (4): 539–42.
5. Lomakin Y, Arapidi GP, Chernov A, Ziganshin R, Tcyganov E, Lyadova I, Butenko IO, Osetrova M, Ponomarenko N, Telegin G, Govorun VM, Gabibov A, Belogurov A Jr. Exposure to the Epstein-Barr Viral Antigen Latent Membrane Protein 1 Induces Myelin-Reactive Antibodies In Vivo. *Front Immunol*. 2017; (8): 777. DOI: 10.3389/fimmu.2017.00777.
6. Piroozmand A, Haddad Kashani H, Zamani B. Correlation between Epstein-Barr Virus Infection and Disease Activity of Systemic Lupus Erythematosus: a Cross-Sectional Study. *Asian Pac J Cancer Prev*. 2017; (18): 523–7.
7. Pan R, Liu X, Zhou S, Ning Z, Zheng H, Gao M, Ding Y, Yao W, Liao X, He N. Differential prevalence and correlates of whole blood Epstein-Barr virus DNA between HIV-positive and HIV-negative men who have sex with men in Shanghai, China. *Epidemiol Infect*. 2017; 145 (11): 2330–40. DOI: 10.1017/S0950268817001054.
8. Lindsey JW, deGannes SL, Pate KA, Zhao X. Antibodies specific for Epstein-Barr virus nuclear antigen-1 cross-react with human heterogeneous nuclear ribonucleoprotein L. *Mol Immunol*. 2016 Jan; (69): 7–12. DOI: 10.1016/j.molimm.2015.11.007.
9. Lindsey JW. Antibodies to the Epstein-Barr virus proteins BFRF3 and BRRF2 cross-react with human proteins. *Neuroimmunol*. 2017; (310): 131–4.
10. Al Sidairi H, Binkhamis K, Jackson C, Roberts C, Heinstejn C, MacDonald J, Needle R, Hatchette TF, LeBlanc JJ. Comparison of two automated instruments for Epstein-Barr virus serology in a large adult hospital and implementation of an Epstein-Barr virus nuclear antigen-based testing algorithm. *J Med Microbiol*. 2017; 66 (11): 1628–34. DOI: 10.1099/jmm.0.000616.
11. Maylin S, Feghoul L, Salmona M, Herda A, Mercier-Delarue S, Simon F, Legoff J. Evaluation the Architect EBV VCA IgM, VCA IgG, and EBNA-1 IgG chemiluminescent immunoassays to assess EBV serostatus prior transplantation. *J Med Virol*. 2017; 89 (11): 2003–10. DOI: 10.1002/jmv.24889.
12. Simon KC, Sagharian-Hedengren S, Sverremark-Ekström E, Nilsson C, Ascherio A. Age at Epstein-Barr virus infection and Epstein-Barr virus nuclear antigen-1 antibodies in Swedish children. *Mult Scler Relat Disord*. 2012; 1 (3): 136–8. DOI: 10.1016/j.msard.2012.03.002.
13. Xiong G, Zhang B, Huang MY, Zhou H, Chen LZ, Feng QS, Luo X, Lin HJ, Zeng YX. Epstein-Barr virus (EBV) infection in Chinese children: a retrospective study of age-specific prevalence. *PLoS One*. 2014; 9 (6): e99857. DOI: 10.1371/journal.pone.0099857.
14. Feng C, Kim JH. Beyond Avoidance: the Psychosocial Impact of Food Allergies. *Clin Rev Allergy Immunol*. 2018. DOI: 10.1007/s12016-018-8708-x.
15. Licari A, Castagnoli R, Brambilla I, Marseglia A, Tosca MA, Marseglia GL, Ciprandi G. Asthma Endotyping and Biomarkers in Childhood Asthma. *Pediatr Allergy Immunol Pulmonol*. 2018; 31 (2): 44–55. DOI: 10.1089/ped.2018.0886.
16. Tsakok T, Woolf R, Smith CH, Weidinger S, Flohr C. Atopic dermatitis: the skin barrier and beyond. *Br J Dermatol*. 2018. DOI: 10.1111/bjd.16934.
17. Carsin A, Mazonq J, Iltstad A, Dubus JC, Chanez P, Gras D. Bronchial epithelium in children: a key player in asthma. *Eur Respir Rev*. 2016; 25 (140): 158–69. DOI: 10.1183/16000617.0101-2015.
18. Пивоваров В. Д., Рязанцев Д. Ю., Симонова М. А., Димитриева Т. В., Хлгатын С. В., Завриев С. К., Свирщевская Е. В. Разработка тест-системы для анализа антител к вирусу Эпштейна-Барр методом иммуно-ПЦР. Молекулярная биология. 2018; 52 (4): 727–34.
19. Simonova MA, Pivovarov VD, Ryazantsev DY, Dolgova AS, Berzhets VM, Zavriev SK, Svirshchevskaya EV. Comparative diagnostics of allergy using quantitative immuno-PCR and ELISA. *Bioanalysis*. 2018. DOI: 10.4155/bio-2017-0194.
20. Chang L, Li J, Wang L. Immuno-PCR: An ultrasensitive immunoassay for biomolecular detection. *Anal Chim Acta*. 2016; (910): 12–24. DOI:10.1016/j.aca.2015.12.039.
21. Jani D, Savino E, Goyal J. Feasibility of immuno-PCR technology platforms as an ultrasensitive tool for the detection of anti-drug antibodies. *Bioanalysis*. 2015; (7): 285–94.
22. Рязанцев Д. Ю., Дробязина П. Е., Хлгатын С. В., Завриев С. К., Свирщевская Е. В. Экспрессия аллергенов клещей домашней пыли Der f 1 и Der f 2 в листьях Nicotiana benthamiana. Биоорганическая химия. 2014; 40 (4): 468–78.
23. Svirshchevskaya E, Fattakhova G, Khlgatian S, Chudakov D, Kashirina E, Ryazantsev D, Kotsareva O, Zavriev S. Direct versus sequential immunoglobulin switch in allergy and antiviral responses. *Clin Immunol*. 2016; (170): 31–8. DOI: 10.1016/j.clim.2016.07.022.

- clim.2016.07.022.
24. Takaki H, Ichimiya S, Matsumoto M, Seya T. Mucosal Immune Response in Nasal-Associated Lymphoid Tissue upon Intranasal Administration by Adjuvants. *J Innate Immun.* 2018; (10): 515–21. DOI: 10.1159/000489405.
  25. Bhaduri-McIntosh S, Landry ML, Nikiforow S, Rotenberg M, El-Guindy A, Miller G. Serum IgA antibodies to Epstein–Barr virus (EBV) early lytic antigens are present in primary EBV infection. *J Infect Dis.* 2007; 195 (4): 483–92.
  26. Cai YL, Li J, Lu AY, Zheng YM, Zhong WM, Wang W, Gao JQ, Zeng H, Cheng JR, Tang MZ. Diagnostic significance of combined detection of Epstein–Barr virus antibodies, VCA/IgA, EA/IgA, Rta/IgG and EBNA1/IgA for nasopharyngeal carcinoma. *Asian Pac J Cancer Prev.* 2014; 15 (5): 2001–6.
  27. Wang L, Tsai TH, Huang CF, Ho MS, Lin DB, Ho YC, Lin SS, Wei JC, Chou MC, Yang CC. Utilizing self-prepared ELISA plates for a cross-population study of different anti-HBe IgG subclass profiles. *J Med Virol.* 2007; 79 (5): 495–2.
  28. Wakiguchi H, Hisakawa H, Hosokawa T, Kubota H, Kurashige T. Analysis of IgG subclasses in chronic active Epstein–Barr virus infection. *Pediatr Int.* 2000; 42 (1): 21–5.

## A CORRELATION BETWEEN THE FLUCTUATIONS OF CYTOKINE CONCENTRATIONS MEASURED IN THE MORNING AND EVENING AND THE CIRCADIAN BLOOD PRESSURE RHYTHM IN PATIENTS WITH STAGE II ESSENTIAL HYPERTENSION

Radaeva OA<sup>1</sup>, Simbirtsev AS<sup>2</sup>, Khovryakov AV<sup>3</sup>

<sup>1</sup> National Research Mordovia State University, Saransk, Russia

<sup>2</sup> State Research Institute of Highly Pure Biopreparations, FMBA, St. Petersburg, Russia

<sup>3</sup> Mordovian Republican Clinical Hospital No.4, Saransk, Russia

Today, increasing attention is being paid to the role of circadian rhythms in pathology. There are time-of-day-dependent immune markers that provide valuable information about disease progression. The aim of this study was to measure evening and morning concentrations of a few cytokines (interleukins, adhesion molecules, tumor necrosis/growth factors, etc.) in the peripheral blood of patients with stage II essential hypertension and to investigate how they correlate with a nocturnal blood pressure decline. Blood samples were collected from 90 patients with stage II EH at 7:00 a.m. and 8:00 p.m. Cytokine concentrations were measured using immunoassays. Based on 24-h blood pressure monitoring, the patients were distributed into 3 groups: dippers, non-dippers and night-peakers. The morning to evening ratios of cytokine concentrations in patients with EH differed from those in healthy controls due to an increase in the evening concentrations of somnogenic cytokines (IL1 $\beta$ , IL1 $\alpha$ ) and LIF, sLIFr, and M-CSF whose daily fluctuations patterns remain understudied. On the whole, the fluctuation patterns of the measured cytokines in patients with stage II EH who had had the condition for 10 to 14 years and were receiving no antihypertensive treatment at the time of our study differed from those displayed by healthy controls. A twenty percent rise in the evening concentrations of IL1 $\alpha$ , LIF, sLIFr, M-CSF, and erythropoietin contributes significantly to pathological blood pressure rhythms (as demonstrated by the groups of non-dippers and night-peakers) in patients with stage II EH receiving no antihypertensive therapy. Understanding the pathophysiological role of cytokine levels and their fluctuations over a 24-h cycle could inspire new methods for EH prevention and reduce end-organ damage.

**Keywords:** cytokines, essential hypertension, Dipper, Non-dipper, Night-peaker

**Author contribution:** Radaeva OA recruited the study participants, collected blood samples, interpreted the results, analyzed the literature, and helped to write a draft of the manuscript. Simbirtsev AS supervised the research group, identified the aims and objectives of the study, proposed a methodology, and provided critical feedback. Khovryakov AV recruited the study participants, collected blood samples and wrote the manuscript.

**Compliance with ethical standards:** the study was approved by the Ethics Committee of Ogariov Mordovian State University (Protocol 12 dated December 14, 2008). All patients gave their informed consent to participate. Blood samples were collected in full compliance with the Declaration of Helsinki (2000) and the Protocol of the Convention on Human Rights and Biomedicine of the Council of Europe (1999).

✉ **Correspondence should be addressed:** Olga A. Radaeva  
Ulianova 26/a, Saransk, 430030; vtlbwbyf\_79@mail.ru

**Received:** 16.07.2018 **Accepted:** 01.03.2019 **Published online:** 12.03.2019

**DOI:** 10.24075/brsmu.2019.011

## СВЯЗЬ СУТОЧНЫХ КОЛЕБАНИЙ СОДЕРЖАНИЯ ЦИТОКИНОВ С ИЗМЕНЕНИЕМ РИТМОВ АРТЕРИАЛЬНОГО ДАВЛЕНИЯ ПРИ ЭССЕНЦИАЛЬНОЙ АРТЕРИАЛЬНОЙ ГИПЕРТЕНЗИИ ВТОРОЙ СТАДИИ

О. А. Радаева<sup>1</sup>, А. С. Симбирцев<sup>2</sup>, А. В. Ховряков<sup>3</sup>

<sup>1</sup> Мордовский государственный университет имени Н. П. Огарева, Саранск, Россия

<sup>2</sup> Государственный научно-исследовательский институт особо чистых биопрепаратов Федерального медико-биологического агентства, Санкт-Петербург, Россия

<sup>3</sup> ГБУЗ РМ «Республиканская клиническая больница № 4», Саранск, Россия

Все больше внимания уделяется исследованию роли суточных ритмов в патологических процессах в организме. Безусловно, существуют суточные иммунные маркеры, позволяющие судить о прогрессировании ряда заболеваний. Целью исследования было изучить содержание цитокинов (интерлейкинов, молекул адгезии, факторов некроза опухоли, роста и др.) в сыворотке периферической крови больных эссенциальной артериальной гипертензией (ЭАГ) II стадии в утреннее/вечернее время и его корреляцию со степенью снижения артериального давления (АД) в ночное время. У 90 пациентов с ЭАГ II стадии проводили забор крови в 7.00 и 20.00 ч, определяли иммуноферментным методом в сыворотке периферической крови цитокины и проводили анализ данных суточного мониторинга АД с выделением групп: «Dipper», «Non-dipper», «Night-peaker». Обнаружено изменение отношения утренних и вечерних концентраций при сравнении со здоровыми, за счет повышения степени роста в вечернее время как цитокинов из группы «somnogenic» (IL1 $\beta$ , IL1 $\alpha$ ), так и мало изученных в аспекте суточных закономерностей LIF, sLIFr, M-CSF. Динамика и уровни исследуемых показателей у пациентов с ЭАГ II стадией и анамнезом заболевания 10–14 лет без гипотензивной терапии отличались от таковых в группе здоровых добровольцев (контроля). Повышение концентраций IL1 $\alpha$ , LIF, sLIFr, M-CSF, эритропоэтина в 20.00 ч на 20% и более является значимым компонентом формирования патологических околосуточных ритмов АД («Non-dipper» и «Night-peaker») у больных ЭАГ II стадии при длительности заболевания 10–14 лет (без приема гипотензивных препаратов). Понимание патофизиологической роли изменения не только количественных характеристик цитокинов сыворотки периферической крови у больных ЭАГ II стадии, но и особенностей их суточной динамики может стать основой создания новых систем профилактики прогрессирования ЭАГ и снизить частоту повреждения органов-мишеней.

**Ключевые слова:** цитокины, эссенциальная артериальная гипертензия, «Dipper», «Non-dipper», «Night-peaker»

**Информация о вкладе авторов:** О. А. Радаева: набор группы пациентов, забор материала для исследования, интерпретация результатов исследования и литературных данных, подготовка первоначального варианта текста статьи, компьютерная работа с текстом; А. С. Симбирцев: научное руководство, определение цели и задач, методологии исследования, критический анализ полученных результатов и доработка текста; А. В. Ховряков: набор группы пациентов, забор материала для исследования, компьютерная работа с текстом.

**Соблюдение этических стандартов:** исследование одобрено этическим комитетом ФГБОУ «МГУ им. Н. П. Огарева» (протоколы № 12 от 14 декабря 2008 г.); отбор биологического материала для исследования (кровь) произвели с учетом положений Хельсинской Декларации ВМА (2000) и протокола Конвенции Совета Европы о правах человека и биомедицине (1999); все участники исследования подписали добровольное информированное согласие на участие в эксперименте.

✉ **Для корреспонденции:** Ольга Александровна Радаева  
ул. Ульянова, д. 26а, г. Саранск, 430030; vtlbwbyf\_79@mail.ru

**Статья получена:** 16.07.2018 **Статья принята к печати:** 01.03.2019 **Опубликована онлайн:** 12.03.2019

**DOI:** 10.24075/vrgmu.2019.011

Circadian rhythms are adaptive oscillations in behavior and physiology that follow a roughly 24-h cycle and prepare an organism for the environmental effects of the Earth's rotation [1]. The circadian clock originated in cyanobacteria and is found in all multicellular organisms and mammals in particular. In 2017, the Nobel prize in physiology or medicine was awarded to Jeffrey C. Hall, Michael Rosbash and Michael W. Young "for their discoveries of molecular mechanisms controlling the circadian rhythm". This award has emphasized the importance of research into the role of daily cycles in health and pathology. In 1960 Halberg et al. articulated the basic principles of circadian rhythm research in immunology after discovering a circadian pattern of sensitivity to an endotoxin administered to mice at different times of day. The sleep/wake cycle is one of the most well-studied manifestations of the circadian rhythm, correlating with the immune response and blood pressure (BP) dynamics [2]. It is currently assumed that proinflammatory cytokines are somnogenic, i.e. increasingly synthesized during the resting phase, whereas anti-inflammatory cytokines, such as IL10, are activated upon awakening and inhibit sleep. In this respect, IL1 $\beta$ , TNF $\alpha$ , IFN $\gamma$ , IL6, IL4, and IL10 are currently the best studied [1, 3, 4, 5]. Blood pressure control is exerted by the following neuroendocrine mechanisms: the monoaminergic systems that regulate the physiological activity of the autonomous nervous system and the secretion of biogenic amines; the hypothalamic-pituitary-adrenal and hypothalamic-pituitary-thyroid axes; the opioid, renin-angiotensin-aldosterone and endothelial systems, and vasoactive peptides [6, 7]. Recently, there has been growing interest in circadian rhythms and their effect on the immune system, but in spite of significant advances in the understanding of their mechanisms, many circadian phenotypes are yet to be explained. A number of experimental studies have suggested an association between the fluctuations of cytokine levels at different times of day and end-organ damage [8] and also a nocturnal decline in BP [9]. Progredient essential hypertension (EH) accompanied by stably high BP with very slight fluctuations in the evening correlates with the levels of certain cytokines. This suggests the existence of time-of-day-dependent immune markers that promote cardiovascular diseases and provides rationale for our study. This work aims to investigate the association between the morning/evening levels of certain cytokines (interleukins, adhesion molecules, tumor necrosis/growth factors, etc.), as well as erythropoietin, in the peripheral blood of patients with stage II EH and the nocturnal BP decline registered in such patients.

## METHODS

The study was carried out at the facilities of the Regional Vascular Center of Mordovian Republican Clinical Hospital No.4, Mordovian Republican Clinical Hospital No.3 and the Department of Immunology, Microbiology, and Virology of Ogariov Mordovian State University. The study recruited 90 patients (40 men and 50 women). Fifty healthy volunteers with no signs of EH constituted the control group. The groups were comparable in terms of age and sex. The following inclusion criteria were applied: age of  $57.5 \pm 1.17$  years; stage II EH (duration of 10 to 14 years); no antihypertensive treatment received. Exclusion criteria included comorbidities; types I and II diabetes mellitus; metabolic syndrome; autoimmune disorders; allergies; symptomatic therapy aimed to normalize blood pressure; infections 1 month before the study; alcoholism or drug addiction; refusal to participate in the study. Peripheral blood samples were collected from the patients and healthy

controls at 7:00 a.m. and 20:00 p.m. The interval between blood collection and meals was at least 6 h. The following cytokines were assayed: IL1 $\beta$ , IL1 $\alpha$ , IL1ra, IL18, IL18BP, IL37, IL6, sIL6r, LIF, sLIFr, TNF $\alpha$ , sTNF-RI, IL2, IL10, TGF- $\beta$ 1, IL8, CX3CL1, CXCL10, INF $\gamma$ , M-CSF, erythropoietin, and a few vasoactive peptides, including NO, iNOS, eNOS, ADMA, SDMA, Nt-proCNP, and Nt-proBNP. In 20% of patients, blood sampling was repeated a month later to test the reproducibility of the results. The variance was 3 to 6%. Time for blood collection was chosen based on the literature [1, 8, 10] and our own pilot study which we had conducted in 5 healthy individuals and 24 patients with stage II EH with different circadian BP rhythms. In that study, we had analyzed the levels of 6 cytokines, including IL1 $\alpha$ , LIF, sLIFr, M-CSF, and erythropoietin, measured at 6:00 a.m., 8:00 a.m., 12:00 a.m., 4:00 p.m., 8:00, and midnight.

Peripheral blood concentrations of the studied cytokines and vasoactive peptides were determined with ELISA using the Personal Lab TM analyzer (Adaltis; Italy) at the laboratory of the Department of Immunology (Ogariov Mordovian State University; laboratory license 13.01.04. 0001.L.000005.06.11 issued 23.06.2011).

All study participants had their blood pressure monitored at the Regional Vascular Center of the Mordovian Republican Clinical Hospital 4 and Mordovian Republican Clinical Hospital 3 using Space Labs Medical 90702 (Spacelabs Medical, Inc.; USA) according to the recommendations of the Fourth International Consensus Conference on Ambulatory Blood Pressure Monitoring (Belgium, 1994); the obtained blood pressure values were added to the patients' medical histories. The patients were divided into 3 groups depending on the degree of BP fluctuations at night: dippers (10–20% decline), non-dippers (< 10% decline); night-peakers (elevated BP).

The data were processed in Statistica ver. 8.0. (StatSoft Inc.; USA). Normality of data distribution was tested using the one-sample Kolmogorov-Smirnoff test. If the distribution was normal, the data were presented as an arithmetic mean (M) and a standard deviation (SD); if the distribution deviated from the norm, the data were presented as a median (Me) and the interquartile range (C25–C75). Depending on the normality of data distribution and the sample size, the two-sample t-test and the Mann-Whitney U-test were used to compare unrelated samples; related samples were analyzed using the paired t-test and Wilcoxon signed rank test.

## RESULTS

The patients with stage II EH who had been suffering from this condition for 10 to 14 years and were not receiving antihypertensive therapy around the time of the study, had higher morning concentrations of IL1 $\beta$ , IL1 $\alpha$ , IL18, IL18BP, IL6, sIL6r, LIF, TNF $\alpha$ , sTNF-RI, IL10, TGF- $\beta$ 1, IL8, CX3CL1, CXCL10, INF $\gamma$ , M-CSF, and erythropoietin ( $p < 0.001$ ) and lower morning concentrations of IL1ra ( $p < 0.001$ ) than the healthy controls (Table 1). The following dynamics were observed in the control group in the evening: IL1 $\beta$  levels rose by 14.1% (0.37),  $p < 0.05$ ; IL1 $\alpha$ , by 14.8% (0.33),  $p < 0.05$ ; IL6, by 29.2% (0.98),  $p < 0.001$ ; TNF $\alpha$ , by 12.3% (0.78),  $p < 0.01$ ; sTNF-RI, by 12.6% (0.65),  $p < 0.05$ ; IL1ra dropped by 14.6% (0.32),  $p < 0.01$ ; IL10, by 23% (0.58),  $p < 0.01$ , and sIL6r, by 30.4% (1.54),  $p < 0.001$ . In the patients with stage II EH the pattern was the same as in the controls, but the changes were more pronounced: IL1 $\beta$  concentrations rose by 21.3% (0.92),  $p < 0.001$  and IL1 $\alpha$ , by 31.2% (1.12),  $p < 0.001$ . The most significant, clinically relevant differences registered in the group of patients with EH were observed for LIF concentrations that increased by 16% (0.43),

$p < 0.01$ , and for sLIFr that demonstrated a 22% rise (0.63),  $p < 0.001$ . In our hypertensive patients, M-CSF levels increased by 20.2% (0.42),  $p < 0.001$ , and erythropoietin, by 36.5% (1.22),  $p < 0.001$ , whereas IL18BP concentrations declined by 11% (0.27),  $p < 0.05$  and IL37, by 21.7% (0.86),  $p < 0.001$ , in contrast to the control group. The evening rise in the IL6 and TNF $\alpha$  concentrations was comparable between the two groups: IL6 levels surged by 31% (1.02) and 29.2% (0.98),  $p < 0.001$ , respectively, while TNF $\alpha$  levels rose by 12.3% (0.78) and 12.2% (0.66),  $p < 0.01$ , respectively. In the healthy volunteers, sIL6r levels decreased in the evening ( $p < 0.001$ ), attenuating IL6 activity after 8 p.m. In contrast, the patients with elevated blood pressure did not have this protective sIL6r decline. The analysis of evening IL10 concentrations revealed a comparable decline ( $p < 0.01$ ) in the levels of this proinflammatory cytokine between the groups, which reached 17% (0.58) and 15% (0.63) in the healthy individuals and patients with EH, respectively.

The analysis of concentrations of cytokines and vasoactive peptides measured at different times of day yielded strong direct correlations between the evening concentrations of IL1 $\alpha$  and ADMA,  $r = 0.76$ ,  $p < 0.01$  (for their diurnal levels  $r = 0.58$ ,  $p < 0.05$ ); sLIFr and SDMA,  $r = 0.85$ ,  $p < 0.001$  (for their diurnal levels  $r = 0.69$ ,  $p < 0.05$ ); beM-CSF and SDMA,  $r = 0.81$ ,  $p < 0.01$  (for their diurnal levels  $r = 0.51$ ,  $p < 0.05$ ). The strength and the direction of correlations between the levels of IL1 $\beta$ , IL1ra, IL18, IL18BP, IL37, IL6, sIL6r, LIF, TNF $\alpha$ , sTNF-RI, IL2, IL10, TGF- $\beta$ 1, IL8, CX3CL1, CXCL10, INF $\gamma$ , and the concentrations of vasoactive peptides in the blood serum measured in the

evening did not differ from the results obtained for the samples that were collected at 7:00 a.m.

A pronounced increase in the concentrations of the cytokines that correlated with vasopressor factors in patients with stage II EH suggests that there might be a correlation between the morning/evening levels of these cytokines and the BP phenotypes (dipper, non-dipper and night-peaker).

The dippers, whose BP dropped by normal 10–20% at nighttime, as well as other patients with stage II EH, had higher concentrations of proinflammatory cytokines. In this subgroup, the dynamics observed for IL1 $\beta$ , IL18, IL18BP, IL37, LIF, sLIFr, TNF $\alpha$ , sTNF-RI, IL2, IL8, IL10, INF $\gamma$ , CX3CL1, CXCL10, TGF $\beta$ 1, and M-CSF were the same as in the healthy individuals (Table 2). Only 6 cytokines demonstrated a different behavior: IL6 and sIL6r (a less pronounced rise in IL6 in the evening accompanied by high and stable sIL6r concentrations); protective IL1ra and erythropoietin that did not decline as in the healthy volunteers; elevated evening IL1 $\alpha$  that demonstrated a more than 20% rise in comparison with its morning concentrations. The analysis of the cyclic dynamics demonstrated by 21 studied cytokines established that evening deviations from morning concentrations by more than 20% were the most pathogenic in terms of their contribution to the progression of hypertension. In the dipper group, such deviations were observed only for IL1 $\alpha$  associated with increased ADMA in patients with stage II EH.

The non-dippers, whose BP dropped by only 10% at the most, demonstrated a more pronounced change in cytokine concentrations in the evening than the healthy controls and the dippers (Table 2). Only 9 cytokines followed a similar pattern

**Table 1.** Morning and evening concentrations of cytokines (pg/ml) in the serum samples of patients with stage II EH (duration of 10 to 14 years, no antihypertensive treatment applied)

Cytokines	Healthy controls (n = 50)		Patients with stage II EH (n = 90)	
	7.00 a.m.	8:00 p.m.	7.00 a.m.	8:00 p.m.
	1	2	3	4
IL1 $\beta$	5.2 (1.87)	5.95 (1.37) <sup>11</sup>	18.7 (5.8) <sup>*1</sup>	22.8 (6.12) <sup>*2,3</sup>
IL1 $\alpha$	3.83 (1.17)	4.37 (0.98) <sup>11</sup>	13.2 (3) <sup>*1</sup>	17.2 (2.93) <sup>*2,3</sup>
IL1ra	691 (99)	598 (96) <sup>^1</sup>	575 (108) <sup>*1</sup>	582 (96.2)
IL18	197 (59)	201 (48)	371 (84) <sup>*1</sup>	382 (83) <sup>*2</sup>
IL18BP	4934 (1173)	4903 (1122)	6710(1980) <sup>*1</sup>	5970 (1783) <sup>^2,3</sup>
IL37	90 (25.6)	88 (17.3)	92 (24.5)	71.6 (18.2) <sup>11</sup>
IL6	3.12 (0.63)	4.03 (0.69) <sup>*11</sup>	23.7 (4.2) <sup>*1</sup>	27.2 (3.92) <sup>*2,3</sup>
sIL6r	681 (52)	478 (50) <sup>*1</sup>	1826 (263) <sup>*1</sup>	1902 (255) <sup>*2</sup>
LIF	1.41 (0.61)	1.47 (0.54)	7.54 (2.4) <sup>*1</sup>	9.08 (2.24) <sup>*2,3</sup>
sLIFr	3920 (1123)	4003 (1223)	4100 (1200)	5100 (1420) <sup>*2,3</sup>
TNF- $\alpha$	7.56 (1.83)	8.49 (1.64) <sup>^1</sup>	21.4 (4) <sup>*1</sup>	23.2 (3.84) <sup>*2 ^3</sup>
sTNF-RI	1620 (367)	1817 (367) <sup>11</sup>	2770 (670) <sup>*1</sup>	2810 (627) <sup>*2</sup>
IL2	10.1 (2.12)	10.7 (1.97)	10.8 (3.11)	10.4 (2.82)
IL8	8.75 (1.82)	9.21 (2.03)	29 (7.83) <sup>*1</sup>	31.2 (6.61) <sup>*2</sup>
IL10	18.2 (5.7)	15.9 (4.83) <sup>^1</sup>	26.2 (7.9) <sup>*1</sup>	22.3 (6.87) <sup>*2,3</sup>
INF $\gamma$	8.97 (2.23)	8.84 (2.14)	18.4 (4.3) <sup>*1</sup>	18.7 (3.96) <sup>*2</sup>
M-CSF	202 (51)	197 (47)	389 (92) <sup>*1</sup>	463 (87) <sup>*2,3</sup>
CX3CL1	422 (61.3)	436 (58.1)	520 (120) <sup>*1</sup>	503 (112) <sup>^2</sup>
CXCL10	8.83 (1.73)	8.97 (1.24)	18.2 (4.5) <sup>*1</sup>	17.9 (3.84) <sup>*2</sup>
TGF $\beta$ 1	11.5 (3.23)	10.2 (2.84)	21.4 (4.64) <sup>*1</sup>	20.2 (4.24) <sup>*2</sup>
Erythropoietin	3.93 (1.31)	4.27 (1.01)	12.6 (3.8) <sup>*1</sup>	17.2 (3.43) <sup>*2,3</sup>

**Note:** significance of differences: <sup>1</sup> —  $p < 0.05$ , <sup>^</sup> —  $p < 0.01$ , <sup>\*</sup> —  $p < 0.001$  (comparison with the specified group). The data are presented as an arithmetic mean (M) and a standard deviation (SD).

of morning-to-evening changes as in the healthy controls, including IL18, TNF $\alpha$ , sTNF-RI, IL2, IL8, IFN $\gamma$ , TGF $\beta$ 1, CX3CL1, and CXCL10. Evening deviations from morning concentrations reaching over 20% were observed for IL1 $\beta$ , IL1 $\alpha$ , IL37, LIF, sLIFr, IL10, M-CSF, and erythropoietin and were statistically significant between the non-dippers and the healthy controls. IL37 and IL10, which might be protective against the progression of EH, as suggested by the study results, demonstrated a more pronounced evening drop in the patients with insufficiently low nocturnal BP than in the healthy individuals. In contrast, IL1 $\beta$ , IL1 $\alpha$ , LIF, sLIFr, M-CSF, and erythropoietin concentrations tended to grow in the evening in such patients. It should be noted that evening and morning levels of IL1ra in the non-dippers did not differ, whereas a significant IL1ra decline was observed in the controls, suggesting protection against rising IL1 $\beta$  and IL1 $\alpha$ , just like in the dippers.

In the night-peakers with elevated nocturnal BP, the daily dynamics of IL1ra, IL18, TNF $\alpha$ , sTNF-RI, IL2, IL8, CX3CL1, CXCL10, and TGF $\beta$ 1 were similar to those observed in the controls (Table 2). Evening deviations from morning concentrations reaching over 20% were noticed for IL1 $\beta$ , IL1 $\alpha$ , IL37, LIF, sLIFr, M-CSF, neopterin, and erythropoietin and were statistically significant between the night-peakers and the healthy controls. IL37, which could be relatively protective against the progression of hypertension in patients with elevated BP, exhibited a more pronounced evening decline as compared to the controls, whereas for IL1 $\beta$ , IL1 $\alpha$ , LIF, sLIFr, M-CSF, neopterin and erythropoietin, a more pronounced rise

was observed. It should be noted that in the night-peakers, IL10 concentrations did not differ between morning and evening, although they did go down in the healthy controls; this tendency might be protective against the rising levels of proinflammatory cytokines. In our study, the cytokine synthesis pattern was similar in the night-peakers and the non-dippers, differing only in the behavior of IL1ra. The evening concentrations of this cytokine dropped significantly in the night-peakers; however, proinflammatory IL10 did not drop at all, which was not the case with the non-dippers. This makes the night-peaker and non-dipper groups somewhat equivalent in terms of protection against EH progression. In the night-peakers, the evening levels of IL1 $\alpha$ , M-CSF and erythropoietin increased more than in the non-dippers (> 35% at 8:00 p.m.), but the overall pattern of their dynamics was the same.

## DISCUSSION

Cytokines, including IL1 $\beta$ , TNF $\alpha$ , IFN $\gamma$ , IL6, IL4, and IL10, affect the biological activity of neurotransmitters/neuromodulators and exert a direct effect on neurons in some areas of the brain, regulating the sleep cycle, which remains the most well-studied circadian rhythm [2]. This means that these cytokines are involved in the processes indirectly related to the sleep/wake cycle, including blood pressure fluctuations. We have found that the daily dynamics of cytokine concentrations is abnormal in patients with stage II EH (duration of 10 to 14 years) in comparison with healthy controls: concentrations of somnogenic

**Table 2.** The relationships between morning and evening concentrations of cytokines (pg/ml) in the serum samples of patients with stage II EH (duration of 10 to 14 years, no antihypertensive treatment applied) AND the blood pressure phenotype

Cytokines	«Dipper» (n = 36)		«Non-dipper» (n = 30)		«Night-peaker» (n = 24)	
	7.00 a.m.	8:00 p.m.	7.00 a.m.	8:00 p.m.	7.00 a.m.	8:00 p.m.
	1	2	3	4	5	6
IL1 $\beta$	16.3 [3.24–25.1]	18.7 [10.3–29.4] <sup>^1</sup>	16.8 [3.32–26.4]	22.3 [15.6–32.8] <sup>^2*3</sup>	22.4 [10.4–32.2] <sup>^1,3</sup>	29.4 [18.9–36.3] <sup>^2,5^4</sup>
IL1 $\alpha$	12.5 [5.72–17.3]	15.2 [10.4–21.3] <sup>^*1</sup>	12.8 [5.23–17.9]	17.3 [13.8–23.1] <sup>^2*3</sup>	16.2 [10.1–20.2] <sup>^*1,3</sup>	23.7 [17.2–24.8] <sup>^2,5,4</sup>
IL1ra	570 [493–670]	591 [517–691]	567 [488–691]	586 [504–652]	589 [468–702]	514 [387–601] <sup>^2,4,5</sup>
IL18	370 [311–432]	400 [322–465]	362 [291–421]	407 [319–467]	389 [298–444]	397 [263–450]
IL18BP	6740 [5370–8457]	5990 [4700–7100] <sup>^1</sup>	6940 [5128–8620]	6103 [4620–7130] <sup>^3</sup>	6630 [4970–8520]	5930 [4550–7310] <sup>^5</sup>
IL37	87.5 [70.2–110]	82.3 [59.3–109]	90.1 [67.5–106]	60.4 [32.2–83.3] <sup>^2,3</sup>	85.4 [68.7–114]	62.5 [33.4–80.9] <sup>^2,5</sup>
IL6	23.9 [20.8–26.7]	27.2 [24.5–29.9] <sup>^1</sup>	24.3 [20–26.9]	27.7 [24–29.3] <sup>^3</sup>	23.7 [21.2–26.5]	26.8 [24.8–30] <sup>^5</sup>
sIL6r	1826 [1648–2003]	1902 [1730–2073]	1793 [1615–2121]	1837 [1710–2113]	1804 [1583–2107]	1924 [1698–2107]
LIF	8.07 [4.68–10.3]	8.56 [6.86–9.93]	7.09 [4.92–9.12]	10.8 [9.92–12.1] <sup>^2*3</sup>	8.32 [5.13–9.3]	11.3 [8.43–12.9] <sup>^2,5</sup>
sLIFr	4140 [3120–4820]	4320 [3270–5240]	4060 [3230–4770]	5930 [4600–7720] <sup>^2,3</sup>	3980 [3040–4910]	6030 [4580–7810] <sup>^2,5</sup>
TNF- $\alpha$	21.2 [18.3–24]	23.6 [20.9–26.1] <sup>^1</sup>	20.7 [18.9–23.5]	23.1 [20.2–25.7] <sup>^3</sup>	20.9 [17.9–24.3]	23.9 [21.6–26.7] <sup>^5</sup>
sTNF-RI	2790 [2320–3220]	3030 [2607–3450] <sup>^1</sup>	2810 [2280–3110]	3110 [2406–3640] <sup>^3</sup>	2720 [2120–3310]	3090 [2540–3620] <sup>^5</sup>
IL2	10.6 [8.92–12.9]	10.4 [8.5–12.2]	10.9 [8.83–12.4]	11.1 [8.69–12.5]	10 [8.63–11.7]	10.4 [8.57–12.1]
IL8	29.1 [23.7–34.3]	31.2 [26.8–35.6]	30.4 [23.9–34.8]	32.4 [27.7–36.2]	29.8 [22.9–33.8]	30.9 [25.9–35.3]
IL10	26.2 [20.9–31.5]	22.3 [17.7–27] <sup>^1</sup>	27.8 [19.7–32.6]	21.6 [16.9–26.3] <sup>^3</sup>	25.7 [19.1–30.3]	23.5 [18.5–28.1]
IFN $\gamma$	18.4 [15.5–21.3]	19.3 [16–21.8]	18.9 [16.7–22.3]	20.2 [17.3–22.4]	17.9 [14.7–21.8]	21.1 [17.4–24.3] <sup>^2,5</sup>
M-CSF	371 [320–448]	402 [345–484] <sup>^1</sup>	378 [314–452]	451 [391–540] <sup>^2*3</sup>	394 [322–440]	517 [410–614] <sup>^2,4,5</sup>
CX3CL1	520 [439–607]	503 [427–579]	553 [455–647]	544 [409–597]	546 [461–639]	519 [447–602]
CXCL10	18.6 [15.2–21.3]	17.7 [15.1–20.5]	19.5 [16.3–22.1]	18.2 [15.8–21.3]	17.9 [14.7–21.9]	18.9 [15.4–21.3]
TGF $\beta$ 1	21.4 [18.3–24.9]	20.3 [17.2–23.1]	22.1 [18.1–24.3]	19.7 [16.8–22.9]	20.9 [17.9–24.5]	20.6 [17.7–23.3]
Erythropoietin	15.5 [10.2–20.3]	15.7 [9.62–19.9]	12.5 [9.12–15.6] <sup>^1</sup>	17.2 [12.9–22.3] <sup>^2*3</sup>	12.7 [7.8–16.9] <sup>^1</sup>	20.3 [16.2–24.7] <sup>^2,5,4</sup>

**Note:** significance of differences: <sup>^1</sup> — < 0.05, <sup>^2</sup> — < 0.01, <sup>^3</sup> — < 0.001 (comparison with the specified group); 1 — 7:00 a.m., dippers, 2 — 8:00 p.m., dippers, 3 — 7:00 a.m., non-dippers, 4 — 8:00 p.m., non-dippers, 5 — 7:00 a.m., night-peakers, 6 — 8:00 p.m., night-peakers. The data are presented as a median (Me) and an interquartile range [C25-C75].

IL1 $\beta$  and IL1 $\alpha$  and a few other cytokines whose circadian dynamics remain understudied (LIF, sLIFr and M-CSF) significantly increase in the evening in hypertensive patients. In healthy individuals, evening concentrations of LIF, sLIFr, and M-CSF undergo a less pronounced rise (<10%), whereas IL1 $\alpha$  and erythropoietin increase by 10–15%. Importantly, patients with stage II EH (duration of 10–14 years, no antihypertensive therapy) demonstrate a more than 20% increase in the evening levels of IL1 $\alpha$ , LIF, sLIFr, M-CSF, and erythropoietin. Such high values correlate with a rise in the concentrations of vasopressor peptides, in particular with ADMA and SDMA. ADMA competes with L-arginine for binding to eNOS [11]. SDMA is a structural ADMA isomer that has a role in arginine binding to a transmembrane transporter by limiting its availability to eNOS and curbing the subsequent synthesis of NO [12]. A substantial increase in the evening levels of the mentioned cytokines contributes to EH progression, which has been confirmed in a number of recent experimental studies. IL1 $\alpha$  has a direct stimulating effect on the proliferation of vascular smooth muscle cells, activates fibrosis and enhances the expression of angiotensin II and endothelin I receptor mRNA on the surface of the smooth muscle cells of the vascular wall [13]. Previously, we reported that IL1 $\alpha$  caused a secondary increase in LIF levels in the blood of patients with EH [14], which can stimulate the LIF-mediated influx of Ca<sup>2+</sup> and ER $\beta$ -dependent activation of MAPK [15]. Growing concentrations of M-CSF inhibit eNOS activity [16] and suppress the mRNA expression of its own receptor IL34 (PTP- $\zeta$ ) [17]. These findings are consistent with our experimental data. A decline in IL34 concentrations occurring in the background of rising M-CSF [18] inhibits its protective effect on the brain. Together, these processes can cause vasodilation and increase the sensitivity of blood vessels to vasopressors. They unfold in the background of declining IL37 concentrations (the cytokine has a protective effect in patients with EH) and stable IL10 levels and are more pronounced in individuals with a pathological daily BP cycle (non-dippers and night-peakers).

In the dippers whose BP dropped at nighttime by over 10%, the studied cytokines, including IL1 $\beta$ , IL18, IL18BP, IL37, LIF, sLIFr, TNF $\alpha$ , sTNF-R1, IL2, IL8, IL10, IFN $\gamma$ , CX3CL1, CXCL10, TGF $\beta$ 1, and M-CSF, followed the same pattern as in healthy individuals: except for IL6/sIL6r and erythropoietin, all these cytokines underwent a less than 15% drop in the

evening. A more than 20% increase in IL1 $\beta$ , IL1 $\alpha$ , LIF, sLIFr, M-CSF and erythropoietin concentrations registered in the evening is a potential isofactor that changes the tone of blood vessels and interferes with blood pressure regulation by the central nervous system. Under these circumstances, blood pressure does not decline sufficiently at night, and evening concentration of the mentioned cytokines rise by 35%, which is associated with elevated nocturnal BP. These changes can be explained by the established correlations with vasopressor factors and are consistent with the experimental data provided above. Changes in the protective cytokine mechanisms that distinguish healthy individuals from patients with EH illustrate resistance to the effect of proinflammatory cytokines. In dippers, as well as in healthy volunteers, IL10 concentrations decline in the evening, but IL1ra does not go down, which is a compensatory antagonistic effect against growing IL1 $\beta$  and IL1 $\alpha$  (sIL6r does not decline in antihypertensive patients but does decrease in healthy individuals), which adds to the activity of IL6. In non-dippers, evening concentrations of IL37 display a negative dynamic. In night-peakers, IL10 does not decline in the evening, suggesting a compensatory effect against the rising proinflammatory cytokines; however, IL1ra levels do drop in this group of patients.

## CONCLUSIONS

We have identified a number of changes in the daily dynamics of peripheral blood cytokine concentrations in patients with stage II EH that are associated with abnormal daily BP cycles (non-dippers and night-peakers). Here, the major contribution is done by a more than 20% rise in LIF, sLIFr, M-CSF, IL1 $\alpha$ , and erythropoietin. In the night-peaker group, the rise is over 35%. Patients with a sufficient drop in BP at night (dippers) have higher concentrations of proinflammatory cytokines than healthy controls but the overall daily dynamics are the same in these two groups.

Understanding the pathophysiological role of cytokine levels and their fluctuations over a 24-h cycle in patients with stage II EH could inspire new methods for EH prevention, reducing end-organ damage and tailoring treatment strategies to an individual patient. This proves the importance of research into the dynamics of physiological parameters with respect to circadian rhythms.

## References

- Geiger SS, Fagundes CT, Siegel RM. Chrono-immunology: progress and challenges in understanding links between the circadian and immune systems. *Immunology*. 2015; 146 (3): 349–58.
- Rico-Rosillo MG, Vega-Robledo GB. Sleep and immune system. *Rev Alerg Mex*. 2018; 65 (2): 160–70.
- Labrecque N, Cermakian N. Circadian Clocks in the Immune System. *J Biol Rhythms*. 2015; 30 (4): 277–90.
- Bennardo M, Alibhai F, Tsimakouridze E, et al. Day-night dependence of gene expression and inflammatory responses in the remodeling murine heart post-myocardial. *Am J Physiol Regul Integr Comp Physiol*. 2016; 311 (6): 1243–54.
- Paganelli R, Petrarca C, Gioacchino M. Biological clocks: their relevance to immune-allergic diseases. *Clin Mol Allerg*. 2018; 16 (1). PMID: 29344005. DOI: 10.1186/s12948-018-0080-0.
- Portaluppi F. The circadian organization of the cardiovascular system in health and disease. *Indian J Exp Biol*. 2014; 52 (5): 395–8.
- Xing CY, Tarumi T, Meijers RL, et al. Arterial Pressure, Heart Rate, and Cerebral Hemodynamics Across the Adult Life Span. *Hypertension*. 2017; 69 (4): 712–20.
- Cuesta M, Boudreau P, Dubeau-Laramee G, et al. Simulated Night Shift Disrupts Circadian Rhythms of Immune Functions in Humans. *J Immunol*. 2016; 196 (6): 2466–75.
- Su D, Song A, Yan B, et al. Circadian Blood Pressure Variations in Postmenopausal Females with Hypertension. *Int Heart J*. 2018; 59 (2): 361–6.
- Sartini C, Whincup PH, Wannamethee SG, et al. Associations of time of day with cardiovascular disease risk factors measured in older men: results from the British Regional Heart Study. *BMJ Open*. 2017; 7 (11): e018264. DOI: 10.1136/bmjopen-2017-018264.
- Shin S, Thapa SK, Fung H-L. Cellular interactions between L-arginine and asymmetric dimethylarginine: Transport and metabolism. *PLoS ONE*. 2017; 12 (5): e0178710. DOI:10.1371/journal.pone.0178710.
- Dahlem DP, Neiger R, Schweighauser A. Plasma Symmetric Dimethylarginine Concentration in Dogs with Acute Kidney Injury and Chronic Kidney Disease. *J Veterin Int Med*. 2017; 31 (3): 899–04.
- Ahnstedt H, Stenman E, Cao L, et al. Cytokines and growth factors modify the upregulation of contractile endothelin ET(A) and ET(B) receptors in rat cerebral arteries after organ culture. *Acta Physiol*. 2012; 205 (2): 266–78.

14. Radaeva OA, Simbircev AS. Gendernye osobennosti sistemy interlejkina-1 u zhenshchin s ehssencial'noj arterial'noj gipertenziej. *Citokiny i vospalenie*. 2014; 3 (13): 31–8. Russian.
15. Dey D, Shepherd A, Pachuau J, Martin M. Leukemia inhibitory factor regulates trafficking of T-type Ca<sup>2+</sup> channels. *Am J Physiol Cell Physiol*. 2011; 300 (3): 576–87.
16. Hsu CP, Zhao JF, Lin SJ, et al. Asymmetric Dimethylarginine Limits the Efficacy of Simvastatin Activating Endothelial Nitric Oxide Synthase. *J Am Heart Assoc*. 2016; 5 (4): e003327. DOI: 10.1161/JAHA.116.003327.
17. Hawley CA, Rojo R, Raper A. Csf1r-mApple Transgene Expression and Ligand Binding In Vivo Reveal Dynamics of CSF1R Expression within the Mononuclear Phagocyte System. *J Immunol*. 2018 Mar 15; 200 (6): 2209–23. DOI: 10.4049/jimmunol.1701488.
18. Radaeva OA, Simbircev AS. M-CSF, IL-34, VEGF-A kak faktory riska razvitiya infarkta miokarda, ostrogo narusheniya mozgovogo krovoobrashcheniya u bol'nyh ehssencial'noj arterial'noj gipertenziej. *Rossijskij immunologicheskij zhurnal*. 2015; 9 (1): 93–101. Russian.

## Литература

1. Geiger SS, Fagundes CT, Siegel RM. Chrono-immunology: progress and challenges in understanding links between the circadian and immune systems. *Immunology*. 2015; 146 (3): 349–58.
2. Rico-Rosillo MG, Vega-Robledo GB. Sleep and immune system. *Rev Alerg Mex*. 2018; 65 (2): 160–70.
3. Labrecque N, Cermakian N. Circadian Clocks in the Immune System. *J Biol Rhythms*. 2015; 30 (4): 277–90.
4. Bennardo M, Alibhai F, Tsimakouridze E, et al. Day-night dependence of gene expression and inflammatory responses in the remodeling murine heart post-myocardial. *Am J Physiol Regul Integr Comp Physiol*. 2016; 311 (6): 1243–54.
5. Paganelli R, Petrarca C, Gioacchino M. Biological clocks: their relevance to immune-allergic diseases. *Clin Mol Allerg*. 2018; 16 (1). PMID: 29344005. DOI: 10.1186/s12948-018-0080-0.
6. Portaluppi F. The circadian organization of the cardiovascular system in health and disease. *Indian J Exp Biol*. 2014; 52 (5): 395–8.
7. Xing CY, Tarumi T, Meijers RL, et al. Arterial Pressure, Heart Rate, and Cerebral Hemodynamics Across the Adult Life Span. *Hypertension*. 2017; 69 (4): 712–20.
8. Cuesta M, Boudreau P, Dubeau-Laramée G, et al. Simulated Night Shift Disrupts Circadian Rhythms of Immune Functions in Humans. *J Immunol*. 2016; 196 (6): 2466–75.
9. Su D, Song A, Yan B, et al. Circadian Blood Pressure Variations in Postmenopausal Females with Hypertension. *Int Heart J*. 2018; 59 (2): 361–6.
10. Sartini C, Whincup PH, Wannamethee SG, et al. Associations of time of day with cardiovascular disease risk factors measured in older men: results from the British Regional Heart Study. *BMJ Open*. 2017; 7 (11): e018264. DOI: 10.1136/bmjopen-2017-018264.
11. Shin S, Thapa SK, Fung H-L. Cellular interactions between L-arginine and asymmetric dimethylarginine: Transport and metabolism. *PLoS ONE*. 2017; 12 (5): e0178710. DOI:10.1371/journal.pone.0178710.
12. Dahlem DP, Neiger R, Schweighauser A. Plasma Symmetric Dimethylarginine Concentration in Dogs with Acute Kidney Injury and Chronic Kidney Disease. *J Veterin Int Med*. 2017; 31 (3): 899–04.
13. Ahnstedt H, Stenman E, Cao L, et al. Cytokines and growth factors modify the upregulation of contractile endothelin ET(A) and ET(B) receptors in rat cerebral arteries after organ culture. *Acta Physiol*. 2012; 205 (2): 266–78.
14. Радаева О. А., Симбирцев А. С. Гендерные особенности системы интерлейкина-1 у женщин с эссенциальной артериальной гипертензией. *Цитокины и воспаление*. 2014; 3 (13): 31–8.
15. Dey D, Shepherd A, Pachuau J, Martin M. Leukemia inhibitory factor regulates trafficking of T-type Ca<sup>2+</sup> channels. *Am J Physiol Cell Physiol*. 2011; 300 (3): 576–87.
16. Hsu CP, Zhao JF, Lin SJ, et al. Asymmetric Dimethylarginine Limits the Efficacy of Simvastatin Activating Endothelial Nitric Oxide Synthase. *J Am Heart Assoc*. 2016; 5 (4): e003327. DOI: 10.1161/JAHA.116.003327.
17. Hawley CA, Rojo R, Raper A. Csf1r-mApple Transgene Expression and Ligand Binding In Vivo Reveal Dynamics of CSF1R Expression within the Mononuclear Phagocyte System. *J Immunol*. 2018 Mar 15; 200 (6): 2209–23. DOI: 10.4049/jimmunol.1701488.
18. Радаева О. А., Симбирцев А. С. M-CSF, IL-34, VEGF-A как факторы риска развития инфаркта миокарда, острого нарушения мозгового кровообращения у больных эссенциальной артериальной гипертензией. *Российский иммунологический журнал*. 2015; 9 (1): 93–101.

## INJECTABLE COLLAGEN IN CORRECTION OF AGE-RELATED SKIN CHANGES: EXPERIMENTAL AND CLINICAL PARALLELS

Manturova NE<sup>1</sup>, Stenko AG<sup>2</sup>, Petinati YaA<sup>3</sup>, Chaikovskaya EA<sup>2</sup> ✉, Bolgarina AA<sup>4</sup>

<sup>1</sup> Pirogov Russian National Research Medical University, Moscow, Russia

<sup>2</sup> Institute of plastic surgery and cosmetology, Moscow, Russia

<sup>3</sup> Izmerov Research Institute of Occupational Health, Moscow, Russia

<sup>4</sup> LLC Nearmedic PLUS, Moscow, Russia

To a large extent, age-related facial skin changes, wrinkles and flabbiness, are attributed to the structural alterations in dermis, including of collagen fibers fragmentation and disorganization. There are various cosmetological correction methods that aim to activate neocollagenesis and dermal remodeling. From this perspective, intradermal injections of exogenous collagen preparations seem logical. This study aimed to investigate the efficacy and safety of Collost 7% collagen complex applied to correct the age-related facial skin changes, as well as clarify the possible mechanisms of skin rejuvenation resulting from a course of intradermal injections. 35 participants entered the study, 30 of them finished it. A set of indicators describing age-related skin changes was assessed with the help of clinical scales; the assessment revealed a pronounced improvement in the quality of the patients' skin, including smoothed relief in the area of localization of fine wrinkles. The therapy resulted in a statistically significant improvement of the skin's elasticity, which, combined with the changes discovered through US scanning (greater dermis thickness and echodensity), is an indirect indication of skin restructuring associated with accumulation of fibrous protein structures. These results allow parallels with the experimental data that shows activation of neocollagenesis in the skin of laboratory animals after a course of Collost 7% gel. The research revealed no serious adverse events. A course of collagen administered intradermally can be recommended as an aesthetic correction procedure, as well as means of prevention of atrophy that has a significant effect on skin's appearance and health status.

**Keywords:** skin ageing, skin rejuvenation, collagen injection

**Acknowledgements:** the authors would like to thank "Nearmedic Plus" (Moscow) for the support of the clinical observational study, as well as Natalya Indilova, Galina Sofinskaya, Evgenia Ikonnikova, medical researchers of the Institute of Plastic Surgery and Cosmetology, and Olga Bondareva and Olesya Sidorova, doctors with Cosmoprodtest SPC, for the assistance they provided in the context of this study.

**Author contribution:** Manturova NE — research planning and data interpretation; Stenko AG, Petinati YaA — selection of participants, conducting research, data interpretation; Chaikovskaya EA — research planning, data collection and interpretation, manuscript preparation; Bolgarina AA — literature analysis, research planning.

**Compliance with ethical standards:** the study was approved by the Society of Aesthetic Medicine ethical committee (Protocol №2 of September 07, 2017). Registration number at [www.ClinicalTrials.gov](http://www.ClinicalTrials.gov): NCT03677258.

✉ **Correspondence should be addressed:** Ekaterina A. Chaikovskaya  
Olkhovskaya, 27, Moscow, 105066; [ktchaikovskaya@yandex.ru](mailto:ktchaikovskaya@yandex.ru)

**Received:** 27.09.2018 **Accepted:** 25.02.2019 **Published online:** 09.03.2019

**DOI:** 10.24075/brsmu.2019.010

## ИНЪЕКЦИОННЫЙ КОЛЛАГЕН В КОРРЕКЦИИ ВОЗРАСТНЫХ ИЗМЕНЕНИЙ КОЖИ: ЭКСПЕРИМЕНТАЛЬНО-КЛИНИЧЕСКИЕ ПАРАЛЛЕЛИ

Н. Е. Мантурова<sup>1</sup>, А. Г. Стенько<sup>2</sup>, Я. А. Петинати<sup>3</sup>, Е. А. Чайковская<sup>2</sup> ✉, А. А. Болгарина<sup>4</sup>

<sup>1</sup> Российский национальный исследовательский медицинский университет имени Н. И. Пирогова, Москва, Россия

<sup>2</sup> АО «Институт пластической хирургии и косметологии», Москва, Россия

<sup>3</sup> Научно-исследовательский институт медицины труда имени академика Н. Ф. Измерова, Москва, Россия

<sup>4</sup> ООО «Ниармедик Плюс», Москва, Россия

Возрастные изменения лица в виде морщин, дряблости кожи во многом связаны со структурными изменениями дермы, в том числе с фрагментацией и дезорганизацией коллагеновых волокон. Различные методы косметологической коррекции направлены на активизацию неоколлагенеза и ремоделирование дермы. С этой точки зрения логичным видится проведение внутрикожных инъекций препаратов экзогенного коллагена. Целью исследования было изучить эффективность и безопасность применения коллагенового комплекса Коллост 7% в коррекции возрастных изменений кожи лица, а также уточнить возможные механизмы развития эффекта омоложения кожи после курса внутрикожных инъекций. В исследование были включены 34 участницы, завершили его 30 участниц. Оценка комплекса показателей возрастных изменений кожи с помощью клинических шкал продемонстрировала выраженное улучшение качества кожи и разглаживание ее рельефа, особенно в области локализации тонких морщин. После завершения курса лечения достоверно повысилась эластичность кожи лица, что вкупе с изменениями, выявленными при УЗ-сканировании (повышение толщины дермы и ее акустической плотности), косвенно свидетельствует о структурной перестройке кожи с накоплением белковых волокнистых структур. Полученные результаты позволяют проводить параллели с данными экспериментальных исследований, показывающими активизацию неоколлагенеза в коже лабораторных животных после курсового введения геля Коллост 7%. Серьезных нежелательных явлений при проведении исследования не выявлено. Курсовое внутрикожное введение коллагена можно рекомендовать как процедуру эстетической коррекции, а также в качестве профилактики развития атрофических процессов, которые существенно сказываются на внешнем виде и здоровье кожи.

**Ключевые слова:** старение кожи, омоложение кожи, инъекции коллагена

**Благодарности:** авторы благодарят компанию ООО «Ниармедик Плюс» (Москва) за поддержку клинического наблюдательного исследования, а также благодарят Наталью Индилову, Галину Софинскую, Евгению Иконникову — врачей-исследователей АО «Институт пластической хирургии и косметологии»; Ольгу Бондареву, Олесю Сидорову — врачей НПЦ «Космопротест» за помощь в проведении исследования.

**Информация о вкладе авторов:** Н. Е. Мантурова — планирование исследования и интерпретация данных; А. Г. Стенько, Я. А. Петинати — подбор участников, проведение исследования, интерпретация данных; Е. А. Чайковская — планирование исследования, сбор и интерпретация данных, подготовка рукописи; А. А. Болгарина — анализ литературы, планирование исследования.

**Соблюдение этических стандартов:** исследование одобрено этическим комитетом Общества эстетической медицины (протокол № 2 от 7 сентября 2017 г.). Регистрационный номер на портале [www.ClinicalTrials.gov](http://www.ClinicalTrials.gov) — NCT03677258.

✉ **Для корреспонденции:** Екатерина Александровна Чайковская  
ул. Ольховская, д. 27, г. Москва, 105066; [ktchaikovskaya@yandex.ru](mailto:ktchaikovskaya@yandex.ru)

**Статья получена:** 27.09.2018 **Статья принята к печати:** 25.02.2019 **Опубликована онлайн:** 09.03.2019

**DOI:** 10.24075/vrgmu.2019.010

In the body, skin is multifunctional: it is a barrier and thermal regulator, immune defense forefront and producer of a wide range of hormones. Lately, its social function has been drawing much attention, since appearance of the face, its aesthetic qualities and signs of diseases thereon, largely define the person's "external" age. Youthfulness and attractiveness of the face help people communicate, socialize and maintain the desired level of social life, which, one way or another, affects their quality of life and determines personal and professional success [1]. Therefore, medical researchers continue to study all the aspects of correction of age-related facial skin changes, with a certain number of such efforts addressing the topics of efficacy and safety of the products and methods developed.

Assessing external age, people primarily focus on how noticeable facial wrinkles and skin folds are [2, 3]. The wrinkles and folds depend on biomechanical properties of skin [4, 5], which, in turn, are a reflection of the state of dermis' extracellular matrix, or connective tissue layer.

Collagen is the basic protein of any connective tissue, and half of its total amount resides in surface tissues, making up about 70% of the skin proteins [6]. The main structural components of the dermis are fiber-forming collagens of types I and III. Their complex architectonics define skin's sturdiness, elasticity, ability to repair [1, 5, 7, 8]. With age, collagen matrix changes significantly. In part, the change is the results of the predetermined normal ageing processes, but there are other factors that speed up these processes, including diseases, endocrine profile alterations, smoking, unhealthy nutritional habits, UV radiation, pollutants found in the environment [1, 9–12]. The studies conducted to date show that the content of collagen in dermis decreases progressively as people age. After 40, a woman loses approximately 20% of her skin's collagen every 10 years [7]. Different research contain different specific data [13–16], but the trend is the same: as people age, proliferative and synthesizing functions of fibroblasts fade, their pool diminishes, cells convert to an inactive "collapsed" phenotype [17]. The quality of collagen fibers changes together with the quantity: they become compacted due to the development of additional covalent cross-links of polypeptide chains. Such structures are more resistant to the action of matrix metalloproteinases, which catabolize proteins and thus incite their renewal. Randomly positioned fragmented collagen fibers that lose focal contacts with fibroblasts accumulate in extracellular matrix. Cells lose structural and functional contact with the matrix and convert to an inactive phenotype [9, 12, 17–19]. Thus forms the vicious circle: the changes of the skin's structure that draw the clinical picture of an "aged face" consolidate. This thesis is confirmed by the fact that in systemic scleroderma patients, whose skin is thicker and contains a greater amount of collagen, age-related facial changes — wrinkles, folds and enlarged pores — manifest themselves much later [20].

The above justifies the need for further examination of various cosmetic methods to restore the collagen framework of dermis. Along with the aesthetic aspect, it is very important to work on restoring the skin's reparative resource: as an organized fiber network, collagen participates in regulation of migration, proliferation, differentiation of cells and their interaction [8, 21].

Topical retinoid preparations, laser irradiation and intradermal injection of fillers (gels of stabilized hyaluronic acid, polylactic acid, calcium hydroxyapatite particles) were proven to reliably induce neocollagenesis [22–26]. The action mechanisms of these means differ, but the result of their application is the same: affected skin develops a dense fibrous collagen

network. The same purpose drives research of such methods as intracutaneous injection of active peptides, microgranules of polycaprolactone, implantation of polycaprolactone threads, exposure to radio frequencies and microfocused ultrasound, mechanical microperforation of skin, etc. Injecting the dermis proper with collagen appears etiologically sound. Aesthetic collagen therapy has been officially recognized about 40 years ago: in 1981, FDA (Food and Drug Administration) registered the first injection material based on this substance. Medical products developed around cow skin collagen are safe and show good biocompatibility [27]. The assumed pattern of action of collagen materials administered intradermally includes temporary hydration of dermis, optimization of the extracellular matrix properties, and stimulating effect of short peptides (matricins), a product of biodegradation of exogenous collagen [8, 28, 29]. Via the biological feedback mechanism, protein fragments accumulation per se stimulates synthesis of protein de novo [30].

Collost 7% and Collost 15% collagen material in the form of sterile gel products were developed and are produced in Russia by BioPHARMAHOLDING; the gels find use in various situations related to medical treatment, including cosmetological procedures. The collagen for Collost is derived from cattle hides; it is purified to remove the impurities without breaking the native fibrous structure and corrupting properties of the protein. The material is registered as an injectable medical product (FSR 2008/02112 of February 26, 2016). In cosmetology, Collost gels are prescribed to counter skin ageing and atrophy. Intradermal injections of the material instantly eliminate the soft tissue volume deficiency; administered as a course, it guarantees lasting results [31, 32]. A test for hypersensitivity to animal collagen is a mandatory measure before any procedures involving Collost gels.

Metabolism and biochemical effects of a Collost 7% gel implanted into the skin were detailed in the context of recent experimental studies [21]. Laboratory animals (rats) were injected with the material intradermally twice. Throughout the entire observation period, which lasted 37 weeks, the researchers noted constant growth of the levels of total collagen and its soluble fraction. According to the researchers, within the several few days after the injection (2<sup>nd</sup> and 7<sup>th</sup> days) collagen level grows due to the presence of exogenous protein, whereas after a considerable period of time (21<sup>st</sup> and 37<sup>th</sup> days) the same trend signals of activation of neocollagenesis in the skin. This hypothesis is also confirmed by the fact that within the same timespans there was registered a significant intensification of incorporation of radiomarked C14 amino acids into the skin protein. Through the seven days of observation, collagenolytic tissue activity was accelerating, which may be the result of the foreign protein biodegradation. The discovered processes suggest that exogenous collagen that has its native structure preserved stimulates synthesis of the skin's native protein while biodegrading.

One of the objectives of the prospective observational study "Investigation of efficacy and safety of Collost 7% collagen recovery complex applied to correct age-related skin changes" was to clarify, applying non-invasive diagnostic methods, the possible mechanisms of skin rejuvenation during and after a course of intradermal injections.

## PATIENTS AND METHODS

The study lasted from October 2017 to June 2018; it was conducted at the Institute of Plastic Surgery and Cosmetology and Izmerov Research Institute of Occupational Health. Thirty-

four participants were screened for fitness to accept a course of Collost injections, 30 were found fit.

Inclusion criteria: female; age 35–65 years; skin phototypes I–III; signs of facial skin age-related changes; no chronic diseases at the stage of decompensation; abstention from any cosmetic procedures during the study. Exclusion criteria: pregnancy; lactation; infection; dermatosis; malignant skin neoplasms in the supposed correction zone; systemic connective tissue diseases that damage skin and subcutaneous tissue (systemic lupus erythematosus, ring granuloma, discoid lupus erythematosus, scleroderma, dermatomyositis, etc.); exacerbation or decompensation of chronic somatic diseases; infectious, oncological diseases; coagulation disorders, including iatrogenic caused by drugs taken; use of isotretinoin within the previous 6 months; propensity hypertrophic and keloid scars; use of antihistamines, glucocorticoids, NSAIDs, immunosuppressants and other drugs that affect skin reactivity; hypersensitivity to the components of the studied medical product.

The participants were 36 to 64 years old, (average age — 48.50; 25<sup>th</sup> and 75<sup>th</sup> percentiles — 43.00 and 57.00 years), Caucasian, with a body weight of 52–80 kg and body mass index less than 30. To avoid skewing the clinical picture of facial skin ageing, the participants maintained a stable body weight (fluctuations of 2 kg max.) through the entire observation period. No allergies were found in the histories of 93.33% of participants; all of them had no allergic reaction to local anesthetics. The majority of patients (24 people, 80.00%) were non-smoking, all adhered to a mixed diet. The skin of 16.67% of them was highly sensitive; the thickness and sensitivity of skin of other participants was normal. The "average" participant of this study could be described as follows: a woman about 50 years old with fair skin, photoaging picture fitting her age, with signs of age-related deformational changes on her face that are largely the result of progressing flabbiness, i. e., changes in the skin's biomechanical properties.

Following a detailed examination, the research program included a description of the overall condition of facial skin using 8 indicators (scored against the 5-point Gejnic, Alexiades-Armenakas scale [33, 34]) calculated into an integral skin condition indicator, as well as assessment of wrinkles in 7 zones applying the 5-point MAS (Merz Aesthetic Scale) validated grading scale [35].

The equipment-aided tests were:

- skin elasticity test (cutometry) on forehead, paraorbital zone, cheek, the devices enabling the test were Multi Skin Test Center MC-900 and Cutometer Dual MPA-580 (Courage + Khazaka electronic GmbH; Germany);
- epidermis and dermis thickness test, dermis acoustic density test, implying ultrasound scanning of the equivalent collateral patches of skin using DUB SkinScanner (Taberna pro medicum; Germany) and DermaScan C-System (Cortex Technology; Denmark) featuring 20–22 MHz sensors.

Both medical researchers and participants of the study assessed the efficacy of cosmetological correction course. The latter applied the universal Global Aesthetic Improvement Scale (GAIS) [35].

The results were documented using the LifeViz system (QuantifiCare; France) that makes and enables analysis of 3D images of the face.

To assess the safety of Collost intradermal injections, each procedure was followed by registration of adverse events, immediate and delayed, that could be connected to the individual response to collagen material and/or injection itself.

The study design implied five visits, screening based on inclusion and exclusion criteria, allergy testing as prescribed by the Collost gel material leaflet. Allergy history of the participants and the result of their allergy tests were scrutinized by an immunologist.

The participants received intradermal injections of Collost 7% three times with an interval of 3 weeks between each. To make the procedures comfortable, they had Acriol Pro anesthetic cream applied to their skin 1 hour prior to injection. The injected amount was 2 ml stored in prefilled syringes that were preheated in a thermostat at 40 °C. The skin was cleaned and disinfected with the help of 0.05% chlorhexidine digluconate solution; Traumeel gel was applied to the patients' facial skin at the end of each procedure. The participants underwent full examination before the course, prior to each procedure (evaluating the results of the previous ones) and 3 weeks after the course was over.

Statistica 6.0 (Statsoft; Russia) software was used to perform statistical analysis; we used nonparametric methods. The data are presented as medians (Me), 25<sup>th</sup> and 75<sup>th</sup> percentiles. The two groups of dependent markers were compared through the Wilcoxon test; the differences were considered statistically significant at  $p < 0.05$ .

## RESULTS

### Safety profile analysis

During the study, all participants exhibited the expected local reactions in the form of skin reddening, slight edemas, palpable pimples at the injection sites. The reactions occurred after the procedures and lasted several hours to several days. In spite of the injection being considerably traumatic, in most cases bleeding took form of petechiae (point hemorrhages), which may be explained by the hemostatic properties of collagen.

### Efficacy analysis

Statistical analysis showed a significant improvement of the clinical and aesthetic properties of facial skin and face on the whole. The integral indicator used to assess the changes decreased significantly ( $p < 0.05$ ; screening data compared to data collected after the third procedure) (Table 1): the reduction median was 24.26%. It should be explained here that the integral indicator grows together with the level of contribution of specific markers (wrinkles, folds, rough skin pattern, telangiectasia, etc.) to the "aged face" picture. Thus, when this indicator goes down, the face rejuvenates.

We have registered significant positive trend in the wrinkle depth change ( $p < 0.05$ ; screening data compared to data

**Table 1.** Skin quality indicators, screening and post-course ( $p < 0.05$ )

Indicator	Screening	Post-course
Integral skin condition indicator, points	14 (10; 17)*	11.5 (8; 13)
Wrinkle visibility (consolidated indicator, 7 zones), points	12 (11; 16)	8 (7; 11)

**Note:** \* — this Table and Table 2 provide median values, brackets contain values of 25<sup>th</sup> and 75<sup>th</sup> percentiles.

collected after the third procedure) (Table 1); the reduction median reflecting the overall visibility of wrinkles on the MAS scale was 28.57%. The detailed analysis of wrinkles in certain zones showed that the most visible changes (skin relief smoothing) occurred on the forehead, paraorbital areas ("crow's feet" wrinkles), lower eyelid and upper lip (Fig. 1).

Skin elasticity in 77% of participants has improved significantly (Table 2): the indicator growth median was 30.90% for forehead, 19.10% for paraorbital area and 15.75% for cheeks. All changes are significant ( $p < 0.05$ ; screening data compared to data collected after the third procedure).

According to the results of the sonography, the following indicators have improved significantly in all participants post-course: there was an increase in epidermis thickness (by 30.7–39.3%), dermis thickness (by 18.7–22.3%), dermis acoustic density (by 28.7–44.5%, all or some zones of the face) (Table 2, Fig. 2 and 3) ( $p < 0.05$ ; screening data compared to data collected after the third procedure).

All (100%) participants considered the Collost 7% gel injection course to be effective. Applying the GAIS scale, half of them called the result satisfactory and expressed a wish to have it improved, while another half was fully satisfied with the result (Fig. 4). From a medical doctor's point of view, a third of participants had the result at the optimal level for them, whereas the majority did not enjoy a full correction but only a considerable improvement. In 2 participants, the improvement was insignificant, an opinion shared by the participants themselves and the medical researcher.

DISCUSSION

This clinical study confirmed the efficacy of Collost 7% as a correction product for involutional skin changes. The study

employed non-invasive diagnostic methods exclusively, which enabled thorough examination of all participants.

The criteria suggested by Gejnic et al, Alexiades-Armenakas [33, 34] were used to assess the overall condition of skin, including photodamage / photoaging symptoms (modified assessment pattern). The integrated indicator combined scores reflecting the state of micro- and macro-relief of the skin, its color, texture, pigmentation, vascular pattern, elastosis and keratosis. Post-course, the indicator has decreased significantly; detailing the results, the visible changes at the skin relief and color levels (wrinkle and folds reduction) should be noted. Two patients with thin skin around eyelids saw the blues spots under their eyes disappear, which was perceived extremely positively by the patients themselves and their close ones. Overall, the skin of most participants, acquired a pink hue and a healthier look.

In the forehead, paraorbital and upper lip zones wrinkles smoothed out the best. These zones have superficial wrinkles associated with the dermal skin layer atrophy/alterations [36]. Restoration of the collagen framework of dermis enables effective correction of skin relief in these areas. However, correcting deep folds (e. g., nasolabial furrows) requires intervention at the level of subcutaneous fat.

Most researchers see a connection between biomechanical properties of the skin and quality of the dermis' fibrous collagen framework. It is logical to assume that the significant skin elasticity improvement registered in the participants may be the result of neocollagenesis, generation of mature fibers with intact structure and sufficient hydrophilicity. The other indirect confirmations of the skin's restructuring are the increased thickness of dermis and growth of its acoustic density, which were detected by ultrasound scanning. According to the earlier research [37, 38], reduction of dermis thickness and acoustic

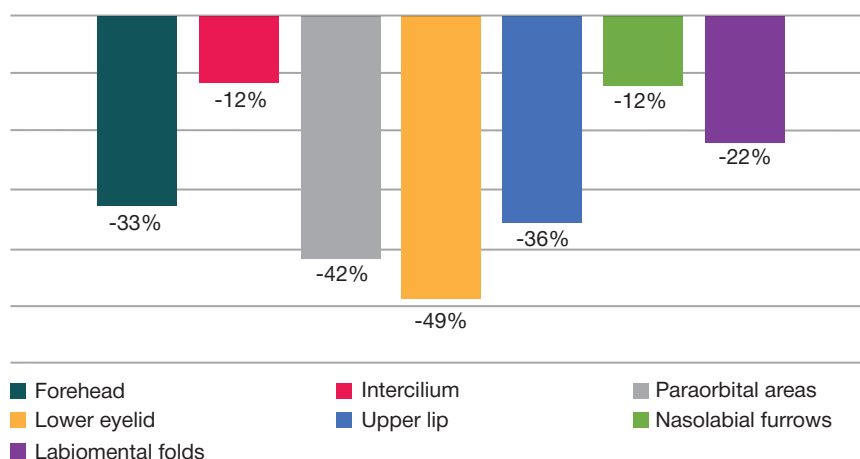


Fig. 1. Wrinkle visibility change dynamics by face zones (screening data compared to post-course data)

Table 2. Structural and functional skin indicators, screening and post-course ( $p < 0.05$ )

Indicators	Screening			Post-course		
	Zones			Zones		
	Forehead	Paraorbital area	Cheek	Forehead	Paraorbital area	Cheek
Epidermis thickness (US scan), mm	0.128 (0.105; 0.158)	0.110 (0.105; 0.133)	0.132 (0.108; 0.158)	0.177 (0.151; 0.192)	0.163 (0.150; 0.184)	0.186 (0.162; 0.199)
Dermis thickness (US scan), mm	1.330 (1.195; 1.531)	1.206 (1.086; 1.376)	1.592 (1.256; 1.869)	1.628 (1.411; 1.790)	1.496 (1.344; 1.672)	1.855 (1.685; 2.094)
Dermis acoustic density (US scan), c. u.	5.102 (3.741; 13.190)	5.738 (3.778; 13.470)	5.794 (2.877; 11.906)	7.236 (5.672; 13.540)	9.071 (6.026; 17.010)	6.611 (4.739; 13.230)
Skin elasticity (cutometry), c. u.	52.63 (46.00; 61.45)	55.08 (49.85; 62.65)	55.06 (49.30; 62.00)	66.75 (56.03; 93.39)	65.65 (58.00; 74.16)	63.25 (55.50; 61.50)

density is an age-related phenomenon, associated with diseases or steroid-induced atrophy that can be caused by the decreasing content of structural fibrillar proteins. Thus, the growing thickness and acoustic density reflect accumulation of fibrous structures, restructuring of the skin [39, 40]. According to our research, the manifestation of these changes was most evident 3 weeks post-course, which allows a parallel with the afore-mentioned experimental studies that registered the peak of collagen content in the laboratory animals' skin 2–4 weeks after the final Collost 7% injection.

It should be noted that improvement of the skin's biomechanical properties, the structural changes observed after a course Collost 7% injections do not only enhance the appearance but help to prevent the age-related changes associated with atrophy and contribute to healing of the skin.

CONCLUSIONS

According to our study, the course of intradermal injections of Collost 7% improves the aesthetic appearance of facial skin, reliably normalizes its color, reduces visibility of wrinkles. Moreover, the positive clinical dynamics occur against the background of improving biomechanical properties of the skin (better elasticity) and structural changes identified by US scanning, which indirectly signal of the dermis

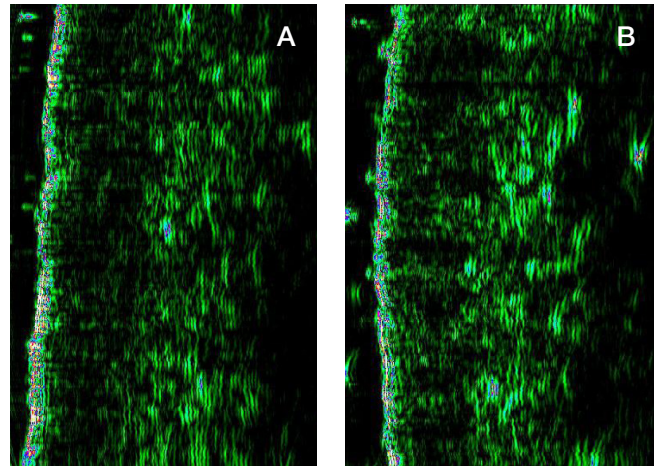


Fig. 3. US scans of forehead skin: screening (A), post-course (B)

collagen framework remodeling process. Thus, Collost 7% intradermal injections can be considered an effective and safe method of aesthetic correction. Perhaps, the results of this study will contribute to the development of etiologically and pathogenetically substantiated protocols of combined correction of age-related skin changes that would include administration of HA, polylactic acids and high-energy methods.

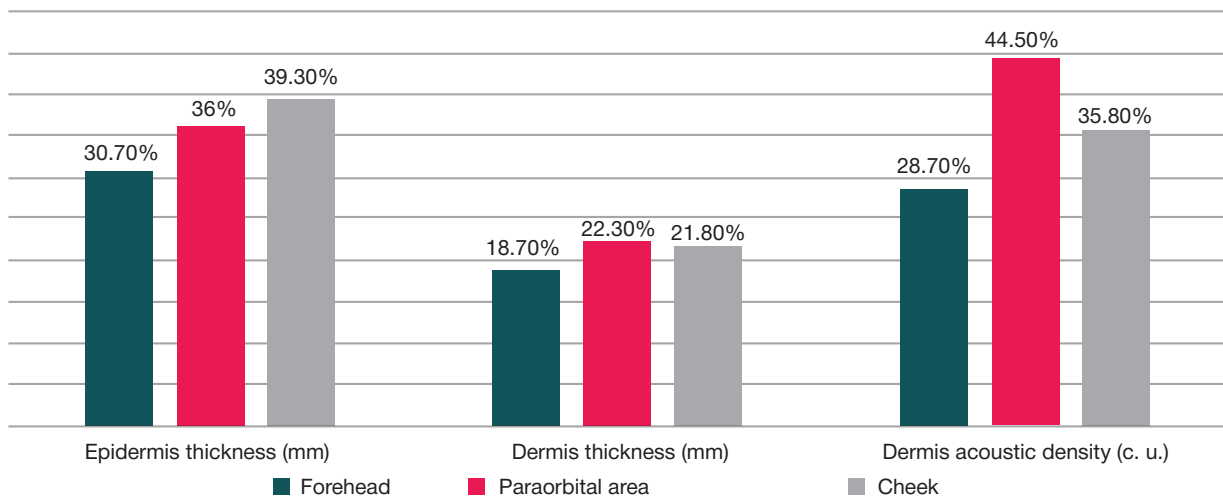


Fig. 2. Dynamics of alteration of skin structure indicators, US scans (post-course median against screening data)

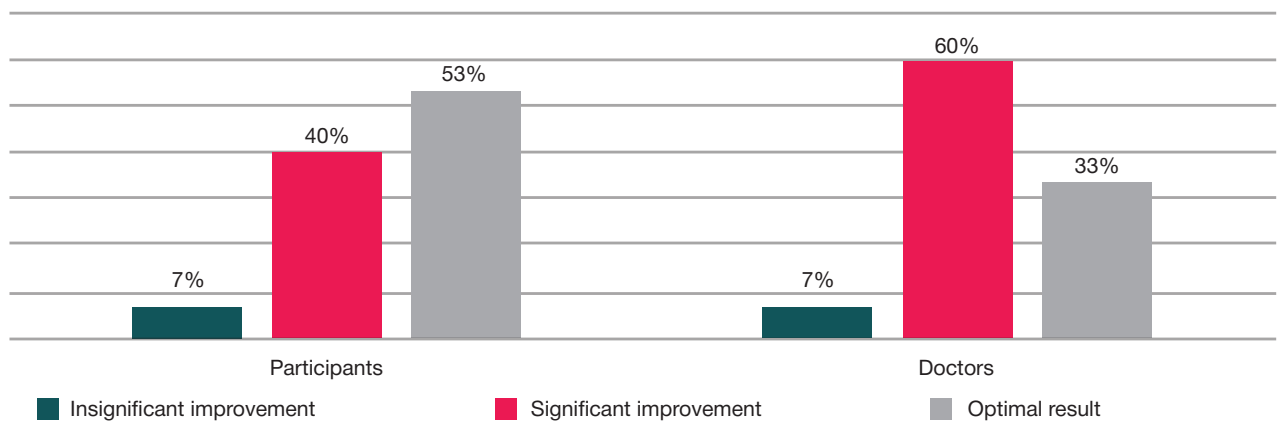


Fig. 4. Injection course efficacy assessment, GAIS, applied by participants and medical researchers

## References

- Rittié L, Fisher GJ. Natural and sun-induced aging of human skin. *Cold Spring Harb Perspect Med*. 2015; 5 (1): a015370.
- Gunn DA, Rexbye H, Griffiths CE, Murray PG, Fereday A, Catt SD, et al. Why Some Women Look Young for Their Age. *Tregenza T*, ed. *PLoS ONE*. 2009; 4 (12): e8021.
- Nkengne A, Bertin C, Stamatas GN, Giron A, Rossi A, Issachar N, et al. Influence of facial skin attributes on the perceived age of Caucasian women. *J Eur Acad Dermatol Venereol*. 2008; 22 (8): 982–91.
- Hussain SH, Limthongkul B, Humphreys TR. The biomechanical properties of the skin. *Dermatol Surg*. 2013; 39 (2): 193–203.
- Aziz J, Shezali H, Radzi Z, Yahya NA, Abu Kassim NH, Czernuszka J, et al. Molecular Mechanisms of Stress-Responsive Changes in Collagen and Elastin Networks in Skin. *Skin Pharmacol Physiol*. 2016; 29 (4): 190–203.
- Czekalla C, Schönborn KH, Döge N, Jung S, Darvin ME, Lademann J, et al. Impact of Body Site, Age, and Gender on the Collagen/Elastin Index by Noninvasive in vivo Vertical Two-Photon Microscopy. *Skin Pharmacol Physiol*. 2017; 30 (5): 260–7.
- Baroni Edo R, Biondo-Simões Mde L, Auersvald A, Auersvald LA, Montemor Netto MR, Ortolan MC, et al. Influence of aging on the quality of the skin of white women: the role of collagen. *Acta Cir Bras*. 2012; 27 (10): 736–40.
- Kapuler O, Selskaja B, Galeeva A, Kamilov F. Metabolizm kollagenovih volokon na fone vozrastnyh izmenenij. *Vrach*. 2015; (8): 64–9.
- Quan T, Fisher GJ. Role of Age-Associated Alterations of the Dermal Extracellular Matrix Microenvironment in Human Skin Aging: A Mini-Review. *Gerontology*. 2015; 61 (5): 427–34.
- Calleja-Agius J, Brincat M, Borg M. Skin connective tissue and ageing. *Best Pract Res Clin Obstet Gynaecol*. 2013; 27 (5): 727–40.
- Danby FW. Nutrition and aging skin: sugar and glycation. *Clin Dermatol*. 2010; 28 (4): 409–11.
- Ahmed T, Nash A, Clark KE, Ghibaudo M, de Leeuw NH, Potter A, et al. Combining nano-physical and computational investigations to understand the nature of "aging" in dermal collagen. *Int J Nanomedicine*. 2017; (12): 3303–14.
- Moragas A, Garcia-Bonafé M, Sans M, Torán N, Huguet P, Martin-Plata C. Image analysis of dermal collagen changes during skin aging. *Analyt Quant Cytol Histol*. 1998; (20): 493–9.
- El-Domyati M, Attia S, Saleh F, Brown D, Birk DE, Gasparro F, et al. Intrinsic aging VS photoaging: a comparative histopathological, immunohistochemical and ultrastructural study of skin. *Exp Dermatol*. 2002; (11): 398–405.
- Yaar M, Eller MS, Gilchrist BA. Fifty years of skin aging. *J Invest Dermatol*. 2002; (7): 51–8.
- Cheng W, Yan-hua R, Fang-gang N, Guo-an Z. The content and ratio of type I and III collagen in skin differ with age and injury. *African J Biotechnol*. 2011; 10 (13): 2524–9.
- Fisher GJ, Varani J, Voorhees JJ. Looking older: fibroblast collapse and therapeutic implications. *Arch Dermatol*. 2008; 144 (5): 666–72.
- Cole MA, Quan T, Voorhees JJ, Fisher GJ. Extracellular matrix regulation of fibroblast function: redefining our perspective on skin aging. *J Cell Commun Signal*. 2018; 12 (1): 35–43.
- Varani J, Spearman D, Perone P, Fligel SE, Datta SC, Wang ZQ, et al. Inhibition of type I procollagen synthesis by damaged collagen in photoaged skin and by collagenase-degraded collagen in vitro. *Am J Pathol*. 2001; 158 (3): 931–42.
- Sawamura S, Jinnin M, Kajihara I, Makino K, Aoi J, Ichihara A, et al. Do scleroderma patients look young? Evaluation by using facial imaging system. *Drug Discov Ther*. 2017; 11 (6): 342–5.
- Kamilov FH, Selskaja BN, Danilova OV, Kapuler OM. Metabolizm kollagena v kozhe jeksperimental'nyh zhivotnyh pri intradermal'noj in'ekcii nemozificirovannogo bych'ego kollagena tipa I. *Vestnik Udmurtskogo universiteta*. 2017; 27 (3): 356–61.
- Kruglikov I. Neocollagenesis in Non-Invasive Aesthetic Treatments. *J Cosmet Dermatol Sci Appl*. 2013; 3 (1A): 1–5.
- Shao Y, He T, Fisher GJ, Voorhees JJ, Quan T. Molecular basis of retinol anti-ageing properties in naturally aged human skin in vivo. *Int J Cosmet Sci*. 2017; 39 (1): 56–65.
- Wang F, Garza LA, Kang S, Varani J, Orringer JS, Fisher GJ, et al. In vivo stimulation of de novo collagen production caused by cross-linked hyaluronic acid dermal filler injections in photodamaged human skin. *Arch Dermatol*. 2007; 143 (2): 155–63.
- Yutskovskaya Y, Kogan E, Leshunov E. A randomized, split-face, histomorphologic study comparing a volumetric calcium hydroxylapatite and a hyaluronic acid-based dermal filler. *J Drugs Dermatol*. 2014; 13 (9): 1047–52.
- Stein P, Vitavska O, Kind P, Hoppe W, Wiczorek H, Schürer NY. The biological basis for poly-L-lactic acid-induced augmentation. *J Dermatol Sci*. 2015; 78 (1): 26–33.
- Rao KP. Recent developments of collagen-based materials for medical applications and drug delivery systems. *J Biomater Sci Polymer Ed*. 1995; 7 (7): 623–45.
- Katayama K, Armendariz-Borunda J, Raghov R, Kang AH, Seyer JM. A pentapeptide from type I procollagen promotes extracellular matrix production. *J Biol Chem*. 1993; 268 (14): 9941–4.
- Maquart FX, Pasco S, Ramont L, Hornebeck W, Monboisse JC. An introduction to matrikines: extracellular matrix-derived peptides which regulate cell activity. Implication in tumor invasion. *Crit Rev Oncol Hematol*. 2004; 49 (3): 199–202.
- Abojanc RK, Istranov LP, Istranova EV, Rudenko TG. Plasticheskie materialy napravlennoho dejstvija na osnove kollagena. *Jelektronnyj sbornik nauchnyh trudov "Zdorov'e i obrazovanie v XXI veke"*. 2011; (4): 184.
- Kubanova AA, Smoljannikova VA, Sluzhaeva NG. Starenie kozhi i vozmozhnosti korrrekcii preparatom kollagena. *Vestnik dermatologii i venerologii*. 2007; (5): 70–3.
- Kapuler OM, Kuramshina ER. Prikladnye aspekty kollagenoterapii v jesteticheskoj medicine. *Jeksperimental'naja i klinicheskaja dermatokosmetologija*. 2013; (5): 40–3.
- Gejnic AV, Kiani A, Okushko SS. Novye vozmozhnosti primenenija glubokoj i poverhnostnoj frakcionnoj ablacii v anti-age terapii. *Plasticheskaja hirurgija i kosmetologija*. 2013; (4): 625–32.
- Alexiades-Armenakas M, Newman J, Willey A, Kilmer S, Goldberg D, Garden J, et al. Prospective multicenter clinical trial of a minimally invasive temperature-controlled bipolar fractional radiofrequency system for rhytid and laxity treatment. *Dermatol Surg*. 2013; 39 (2): 263–73.
- Carruthers A, Carruthers J. A validated facial grading scale: the future of facial ageing measurement tools? *J Cosmet Laser Ther*. 2010; 12 (5): 235–41.
- Tsukahara K, Tamatsu Y, Sugawara Y, Shimada K. The relationship between wrinkle depth and dermal thickness in the forehead and lateral canthal region. *Arch Dermatol*. 2011; 147 (7): 822–8.
- Waller JM, Maibach HI. Age and skin structure and function, a quantitative approach (I): blood flow, pH, thickness, and ultrasound echogenicity. *Skin Res Technol*. 2005; (11): 221–35.
- Jasaitiene D, Valiukeviciene S, Linkeviciute G, et al. Principles of high-frequency ultrasonography for investigation of skin pathology. *J Eur Acad Dermatol Venereol*. 2011; (25): 375–82.
- Kozarova A, Kozar M, Minarikova E, Pappova T. Identification of the age related skin changes using high-frequency ultrasound. *Acta Medica Martiniana*. 2017; 17 (1): 15–20.
- Lacarrubba F, Tedeschi A, Nardone B, Micali G. Mesotherapy for skin rejuvenation: assessment of the subepidermal low-echogenic band by ultrasound evaluation with cross-sectional B-mode scanning. *Dermatol Ther*. 2008; 21 (Suppl 3): 1–5.

## Литература

- Rittié L, Fisher GJ. Natural and sun-induced aging of human skin. *Cold Spring Harb Perspect Med*. 2015; 5 (1): a015370.
- Gunn DA, Rexbye H, Griffiths CE, Murray PG, Fereday A, Catt SD, et al. Why Some Women Look Young for Their Age. *Tregenza T*, ed. *PLoS ONE*. 2009; 4 (12): e8021.

- ed. PLoS ONE. 2009; 4 (12): e8021.
3. Nkengne A, Bertin C, Stamatas GN, Giron A, Rossi A, Issachar N, et al. Influence of facial skin attributes on the perceived age of Caucasian women. *J Eur Acad Dermatol Venereol*. 2008; 22 (8): 982–91.
  4. Hussain SH, Limthongkul B, Humphreys TR. The biomechanical properties of the skin. *Dermatol Surg*. 2013; 39 (2): 193–203.
  5. Aziz J, Shezali H, Radzi Z, Yahya NA, Abu Kassim NH, Czernuszka J, et al. Molecular Mechanisms of Stress Responsive Changes in Collagen and Elastin Networks in Skin. *Skin Pharmacol Physiol*. 2016; 29 (4): 190–203.
  6. Czekalla C, Schönborn KH, Döge N, Jung S, Darvin ME, Lademann J, et al. Impact of Body Site, Age, and Gender on the Collagen/Elastin Index by Noninvasive in vivo Vertical Two-Photon Microscopy. *Skin Pharmacol Physiol*. 2017; 30 (5): 260–7.
  7. Baroni Edo R, Biondo-Simões Mde L, Auersvald A, Auersvald LA, Montemor Netto MR, Ortolan MC, et al. Influence of aging on the quality of the skin of white women: the role of collagen. *Acta Cir Bras*. 2012; 27 (10): 736–40.
  8. Капулер О., Сельская Б., Галеева А., Камилов Ф. Метаболизм коллагеновых волокон на фоне возрастных изменений. *Врач*. 2015; (8): 64–9.
  9. Quan T, Fisher GJ. Role of Age-Associated Alterations of the Dermal Extracellular Matrix Microenvironment in Human Skin Aging: A Mini-Review. *Gerontology*. 2015; 61 (5): 427–34.
  10. Calleja-Agius J, Brincat M, Borg M. Skin connective tissue and ageing. *Best Pract Res Clin Obstet Gynaecol*. 2013; 27 (5): 727–40.
  11. Danby FW. Nutrition and aging skin: sugar and glycation. *Clin Dermatol*. 2010; 28 (4): 409–11.
  12. Ahmed T, Nash A, Clark KE, Ghibaud M, de Leeuw NH, Potter A, et al. Combining nano-physical and computational investigations to understand the nature of "aging" in dermal collagen. *Int J Nanomedicine*. 2017; (12): 3303–14.
  13. Moragas A, Garcia-Bonafé M, Sans M, Torán N, Huguet P, Martin-Plata C. Image analysis of dermal collagen changes during skin aging. *Analyt Quant Cytol Histol*. 1998; (20): 493–9.
  14. El-Domyati M, Attia S, Saleh F, Brown D, Birk DE, Gasparro F, et al. Intrinsic aging VS photoaging: a comparative histopathological, immunohistochemical and ultrastructural study of skin. *Exp Dermatol*. 2002; (11): 398–405.
  15. Yaar M, Eller MS, Gilchrist BA. Fifty years of skin aging. *J Invest Dermatol*. 2002; (7): 51–8.
  16. Cheng W, Yan-hua R, Fang-gang N, Guo-an Z. The content and ratio of type I and III collagen in skin differ with age and injury. *African J Biotechnol*. 2011; 10 (13): 2524–9.
  17. Fisher GJ, Varani J, Voorhees JJ. Looking older: fibroblast collapse and therapeutic implications. *Arch Dermatol*. 2008; 144 (5): 666–72.
  18. Cole MA, Quan T, Voorhees JJ, Fisher GJ. Extracellular matrix regulation of fibroblast function: redefining our perspective on skin aging. *J Cell Commun Signal*. 2018; 12 (1): 35–43.
  19. Varani J, Spearman D, Perone P, Fligel SE, Datta SC, Wang ZQ, et al. Inhibition of type I procollagen synthesis by damaged collagen in photoaged skin and by collagenase-degraded collagen in vitro. *Am J Pathol*. 2001; 158 (3): 931–42.
  20. Sawamura S, Jinnin M, Kajihara I, Makino K, Aoi J, Ichihara A, et al. Do scleroderma patients look young? Evaluation by using facial imaging system. *Drug Discov Ther*. 2017; 11 (6): 342–5.
  21. Камилов Ф. Х., Сельская Б. Н., Данилова О. В., Капулер О. М. Метаболизм коллагена в коже экспериментальных животных при интрадермальной инъекции немодифицированного бычьего коллагена типа I. *Вестник Удмуртского университета*. 2017; 27 (3): 356–61.
  22. Kruglikov I. Neocollagenesis in Non-Invasive Aesthetic Treatments. *J Cosmet Dermatol Sci Appl*. 2013; 3 (1A): 1–5.
  23. Shao Y, He T, Fisher GJ, Voorhees JJ, Quan T. Molecular basis of retinol anti-ageing properties in naturally aged human skin in vivo. *Int J Cosmet Sci*. 2017; 39 (1): 56–65.
  24. Wang F, Garza LA, Kang S, Varani J, Orringer JS, Fisher GJ, et al. In vivo stimulation of de novo collagen production caused by cross-linked hyaluronic acid dermal filler injections in photodamaged human skin. *Arch Dermatol*. 2007; 143 (2): 155–63.
  25. Yutskovskaya Y, Kogan E, Leshunov E. A randomized, split-face, histomorphologic study comparing a volumetric calcium hydroxylapatite and a hyaluronic acid-based dermal filler. *J Drugs Dermatol*. 2014; 13 (9): 1047–52.
  26. Stein P, Vitavska O, Kind P, Hoppe W, Wieczorek H, Schürer NY. The biological basis for poly-L-lactic acid-induced augmentation. *J Dermatol Sci*. 2015; 78 (1): 26–33.
  27. Rao KP. Recent developments of collagen-based materials for medical applications and drug delivery systems. *J Biomater Sci Polymer Ed*. 1995; 7 (7): 623–45.
  28. Katayama K, Armendariz-Borunda J, Raghow R, Kang AH, Seyer JM. A pentapeptide from type I procollagen promotes extracellular matrix production. *J Biol Chem*. 1993; 268 (14): 9941–4.
  29. Maquart FX, Pasco S, Ramont L, Hornebeck W, Monboisse JC. An introduction to matrikines: extracellular matrix-derived peptides which regulate cell activity. Implication in tumor invasion. *Crit Rev Oncol Hematol*. 2004; 49 (3): 199–202.
  30. Абоянц Р. К., Истранов Л. П., Истранова Е. В., Руденко Т. Г. Пластические материалы направленного действия на основе коллагена. Электронный сборник научных трудов «Здоровье и образование в XXI веке». 2011; (4): 184.
  31. Кубанова А. А., Смольяникова В. А., Служаева Н. Г. Старение кожи и возможности коррекции препаратом коллагена. *Вестник дерматологии и венерологии*. 2007; (5): 70–3.
  32. Капулер О. М., Курамшина Е. Р. Прикладные аспекты коллагенотерапии в эстетической медицине. *Экспериментальная и клиническая дерматокосметология*. 2013; (5): 40–3.
  33. Гейниц А. В., Киани А., Окушко С. С. Новые возможности применения глубокой и поверхностной фракционной абляции в anti-age терапии. *Пластическая хирургия и косметология*. 2013; (4): 625–32.
  34. Alexiades-Armenakas M, Newman J, Willey A, Kilmer S, Goldberg D, Garden J, et al. Prospective multicenter clinical trial of a minimally invasive temperature-controlled bipolar fractional radiofrequency system for rhytid and laxity treatment. *Dermatol Surg*. 2013; 39 (2): 263–73.
  35. Carruthers A, Carruthers J. A validated facial grading scale: the future of facial ageing measurement tools? *J Cosmet Laser Ther*. 2010; 12 (5): 235–41.
  36. Tsukahara K, Tamatsu Y, Sugawara Y, Shimada K. The relationship between wrinkle depth and dermal thickness in the forehead and lateral canthal region. *Arch Dermatol*. 2011; 147 (7): 822–8.
  37. Waller JM, Maibach HI. Age and skin structure and function, a quantitative approach (I): blood flow, pH, thickness, and ultrasound echogenicity. *Skin Res Technol*. 2005; (11): 221–35.
  38. Jasaitiene D, Valiukeviciene S, Linkeviciute G, et al. Principles of high-frequency ultrasonography for investigation of skin pathology. *J Eur Acad Dermatol Venereol*. 2011; (25): 375–82.
  39. Kozarova A, Kozar M, Minarikova E, Pappova T. Identification of the age related skin changes using high-frequency ultrasound. *Acta Medica Martiniana*. 2017; 17 (1): 15–20.
  40. Lacarubba F, Tedeschi A, Nardone B, Micali G. Mesotherapy for skin rejuvenation: assessment of the subepidermal low-echogenic band by ultrasound evaluation with cross-sectional B-mode scanning. *Dermatol Ther*. 2008; 21 (Suppl 3): 1–5.

## GLYCOPROTEIN GP AS A BASIS FOR THE UNIVERSAL VACCINE AGAINST EBOLA VIRUS DISEASE

Dolzhikova IV <sup>✉</sup>, Tukhvatulin AI, Gromova AS, Grousova DM, Tukhvatulina NM, Tokarskaya EA, Logunov DY, Naroditskiy BS, Gintsburg AL

N.F. Gamaleya Research Institute of Epidemiology and Microbiology, Moscow, Russia

Ebola virus disease (EVD) is one of the deadliest viral infections affecting humans and nonhuman primates. Of 6 known representatives of the *Ebolavirus* genus responsible for the disease, 3 can infect humans, causing acute highly contagious fever characterized by up to 90% fatality. These include Bundibugyo ebolavirus (BDBV), Zaire ebolavirus (ZEBOV) and Sudan ebolavirus (SUDV). The majority of the reported EVD cases are caused by ZEBOV. Vaccine development against the virus started in 1976, immediately after the causative agent of the infection was identified. So far, 4 vaccines have been approved. All of them are based on the protective epitope of the ZEBOV glycoprotein GP. Because SUDV and BDBV can also cause outbreaks and epidemics, it is vital to design a vaccine capable of conferring protection against all known ebolaviruses posing a threat to the human population. This article presents systematized data on the structure, immunogenicity and protective properties of ebolavirus glycoprotein GP, looks closely at the immunodominant epitopes of ZEBOV, SUDV and BDBV glycoprotein GP required to elicit a protective immune response, and offers a rational perspective on the development of a universal vaccine against EVD that relies on the use of vectors expressing two variants of GP represented by ZEBOV and SUDV.

**Keywords:** Ebola virus disease, EVD, vaccines, cross-reactive immunity, cross-protective immunity

**Author contribution:** Dolzhikova IV, Tukhvatulin AI and Logunov DY conceived and planned the study, analyzed the literature, collected, analyzed and interpreted the data; Gromova AS, Grousova DM, Tukhvatulina NM, and Tokarskaya EA helped to collect and analyze the data; Naroditskiy BS and Gintsburg AL contributed to data interpretation; Dolzhikova IV wrote this manuscript.

✉ **Correspondence should be addressed:** Inna V. Dolzhikova  
Gamalei 18, Moscow, 123098; i.dolzhikova@gmail.com

**Received:** 06.12.2018 **Accepted:** 20.02.2019 **Published online:** 03.03.2019

**DOI:** 10.24075/brsmu.2019.005

## ИСПОЛЬЗОВАНИЕ ГЛИКОПРОТЕИНА GP ДЛЯ СОЗДАНИЯ УНИВЕРСАЛЬНОЙ ВАКЦИНЫ ПРОТИВ ЛИХОРАДКИ ЭБОЛА

И. В. Должикова <sup>✉</sup>, А. И. Тухватулин, А. С. Громова, Д. М. Гроусова, Н. М. Тухватулина, Е. А. Токарская, Д. Ю. Логунов, Б. С. Народицкий, А. Л. Гинцбург

Национальный исследовательский центр эпидемиологии и микробиологии имени Н. Ф. Гамалеи, Москва, Россия

Болезнь, вызванная вирусом Эбола (БВБЭ) — одно из самых высоклетальных вирусных заболеваний, поражающих человека и приматов. Возбудителем БВБЭ является вирус Эбола. В настоящее время известно шесть видов этого вируса, три из них патогенны для человека — это виды Заир (ZEBOV), Судан (SUDV) и Бундибугио (BDBV), вызывающие острые вирусные высококонтагиозные лихорадки у людей и приматов с летальностью до 90%. В большинстве случаев БВБЭ вызвана видом ZEBOV. Разработка вакцин против БВБЭ началась сразу после идентификации возбудителя в 1976 г. На сегодняшний день в мире зарегистрировано четыре вакцинных препарата для профилактики БВБЭ. Все они основаны на протективном антигене — гликопротеине (GP) вируса Эбола вида ZEBOV. В силу того что виды SUDV и BDBV также могут быть причиной вспышек и эпидемий БВБЭ, очевидна необходимость разработки вакцин, способных обеспечить защиту от всех известных патогенных для человека видов вируса Эбола. В статье систематизированы данные относительно структуры, иммуногенных и протективных свойств GP вируса Эбола, проведен анализ иммунодоминантных эпитопов гликопротеина вирусов ZEBOV, SUDV и BDBV, необходимых для формирования протективного иммунитета, а также предложен рациональный, на наш взгляд, подход создания возможных вариантов вакцин против БВБЭ, вызванной разными видами вируса Эбола, состоящий в использовании векторных конструкций, экспрессирующих как минимум два варианта гликопротеина — GP вируса Эбола вида ZEBOV и вида SUDV.

**Ключевые слова:** болезнь, вызванная вирусом Эбола; БВБЭ; вакцины; кросс-реактивный иммунитет; кросс-протективный иммунитет

**Информация о вкладе авторов:** И. В. Должикова — анализ литературы, планирование исследования, сбор, анализ и интерпретация данных, подготовка рукописи; А. И. Тухватулин — анализ литературы, планирование исследования, сбор, анализ, интерпретация данных; А. С. Громова, Д. М. Гроусова, Н. М. Тухватулина, Е. А. Токарская — сбор и анализ данных; Д. Ю. Логунов — анализ литературы, планирование исследования, анализ и интерпретация данных; Б. С. Народицкий — интерпретация данных; А. Л. Гинцбург — интерпретация данных.

✉ **Для корреспонденции:** Инна Вадимовна Должикова  
ул. Гамалеи, д. 18, г. Москва, 123098; i.dolzhikova@gmail.com

**Статья получена:** 06.12.2018 **Статья принята к печати:** 20.02.2019 **Опубликована онлайн:** 03.03.2019

**DOI:** 10.24075/vrgmu.2019.005

Ebola virus disease (EVD) is one of the most dangerous viral infections afflicting humans and nonhuman primates. Its first reported outbreak occurred in 1976 in Yambuku, a village in the Democratic Republic of the Congo (former Zaire), and Nzara, a town in South Sudan. That same year, the causative agent of the disease — *Ebolavirus*, a member of the *Filoviridae* family — was first isolated from an infected individual who lived in the Ebola river valley that gave its name to the virus [1]. So far, 6 ebolaviruses are known including *Bundibugyo ebolavirus* (BDBV), *Zaire ebolavirus* (ZEBOV), *Reston ebolavirus* (RESTV), *Sudan ebolavirus* (SUDV), *Tai forest ebolavirus* (TAFV), and *Bombali ebolavirus* (BOMV). ZEBOV, SUDV and BDBV are capable of infecting humans and therefore pose a serious threat [2–3]. Since 1976, the world has seen more than 20 outbreaks

of EVD caused by ZEBOV, SUDV and BDBV. The largest outbreak that occurred in 2014–2016 in West Africa grew into an epidemic and killed over 12,000 people. The majority of all reported EVD cases have been attributed to ZEBOV (Table 1) [4].

ZEBOV, SUDV and BDBV cause acute, highly contagious fever in humans and nonhuman primates. RESTV is not known to cause EVD in humans; however, antibodies against this species are detected in the blood serum of individuals who work with monkeys and apes infected with RESTV [4]. The reasons behind such different pathogenicity of RESTV and other pathogenic types of Ebola virus are still unknown.

The epidemic of 2014–2016 urged the researchers all around the globe to put increasing effort into developing a vaccine against EVD. To date, over 10 vaccines have been developed,

of which 4 have already been approved for clinical use [5]. Both candidate and approved vaccines confer 100% protection against ZEBOV-associated EBV in nonhuman primates. Their efficacy against other ebolaviruses varies. Because SUDV and BDBV can also cause outbreaks and epidemics and because new ZEBOV strains are emerging, the world is faced with a pressing need for vaccine capable of protecting the human population against all known pathogenic ebolaviruses.

### The structure of the virus

Ebolaviruses have a filamentous structure that comes in different shapes and length. The virions consist of an envelope, a nucleocapsid, a polymerase complex and a matrix [6] (Fig. 1). The nucleocapsid core of the virion contains a replication complex composed of a single-stranded RNA genome and a few proteins, including NP, VP35, VP30, and polymerase L. The virus has an outer lipid membrane with glycoprotein (GP) spikes on its surface. The protein matrix formed by proteins VP40 and VP24 lies immediately beneath the outer membrane [6].

The viral genome is represented by negative single-stranded RNA (Fig. 2) [6] carrying 7 genes that code for a total of 9 proteins: the nucleoprotein (NP), the viral polymerase cofactor VP35, the major matrix protein VP40, 3 glycoproteins (the secreted sGP, the full-length GP and the small secreted ssGP), the minor nucleoprotein VP30, the membrane-associated protein VP24, and the viral polymerase L [6–7].

The GP glycoprotein of the *Ebolavirus* is the only protein located on the surface of the virion. It plays a key role in the early stages of infection helping the virion to attach to and enter the cell [7].

### Synthesis and proteolytic processing of GP

The ebolavirus glycoprotein gene codes for 3 proteins: pre-sGP, pre-ssGP (they both are precursors of secreted nonstructural glycoproteins) and pre-GP (a precursor of the structural transmembrane glycoprotein). The nucleotide sequence of the glycoprotein gene contains 7 consecutive uracils at positions 880–886, where a hairpin loop is formed. It is difficult for the viral L polymerase to read through the hairpin [7–8]; therefore, this RNA region undergoes editing. As a result, 3 transcripts are produced:

- a transcript containing 7 uracils (~71%), coding for sGP (364 aa);
- a transcript containing 8 uracils (~25%), coding for GP (676 aa);
- a transcript containing 9 uracils (~4%), coding for ssGP (298 aa).

The first 295 amino acids bases in GP, sGP and ssGP are identical; however, the proteins differ in their C-terminus, which naturally affects their function. A newly synthesized pre-sGP is processed by cell proteases, leading to the formation of secreted sGP, that reduces the efficacy of humoral response

by misdirecting antibodies and  $\Delta$ -peptide responsible for pore formation in the cell membrane (Fig. 2) [8–9].

Pre-GP is also cleaved by cell proteases into two subunits: GP1 and GP2. The subunits form heterodimers that are trimerized and constitute spikes on the surface of the viral particle. GP1 contains a receptor-binding domain, a glycan cap and a mucin-like domain required for the interaction with cell surface receptors. GP2 is a transmembrane domain, anchoring the complex in the membrane (Fig. 2). GP2 has a binding site for the TACE protease; in proteolytic cleavage, the glycoprotein is cut off from the membrane and another type of GP is formed: the shed GP [8].

Mature surface GP exerts one of the most crucial functions in the lifecycle of the virus: it interacts with cell receptors, promoting fusion of the virion with the membrane. The virus is taken up into the endocytic/macropinocytic pathway; then, the mucin-like domain and the glycan cap of the glycoprotein are cut off by furin and cathepsins in the cell endosome. The truncated GP binds to Niemann-Pick C1 (NCP1) cholesterol transporter, initiating fusion of the endosomal and viral membranes and allowing the nucleocapsid to enter the cytoplasm [10–11].

### Structural and immunogenic features of different GP forms

All secretory forms of GP (sGP, ssGP and shed GP) serve to protect the virus from being neutralized by the host's natural defenses. Cells infected with *Ebolavirus* secrete these proteins thereby guiding the humoral response against the limited number of epitopes [12–13]. Produced in abundance, sGP, ssGP and shed GP misdirect the majority of IgG, reducing the efficacy of the host's humoral response [14]. These glycoproteins (especially sGP and ssGP) trigger production of antibodies that have zero or weak virus-neutralizing potential, causing the phenomenon of antibody-dependent enhancement of the infection: the antibodies recognize the virus and interact with Fc-receptors of phagocytes, "ordering" the latter to take up the virus-antibody complexes via Fc $\gamma$ R-mediated phagocytosis [15]. Importantly, although secreted forms of GP have binding sites for the protective antibodies, not all animals vaccinated with truncated forms of proteins develop protective immunity against the virus. A strong immune response against EVD can be achieved in all vaccinated animals only when a full-length GP is used [16–18]. This is probably due to the presence of additional neutralization sites and T-cell epitopes in the structure of the full-length protein. This hypothesis is supported by a few observations. Firstly, there are reports that apart from GP1 (glycan cap)-recognizing antibodies isolated from convalescent patients, those that specifically bind to the submembrane domain of GP2 also have protective potential [18–21]. Secondly, a study of CD8<sup>+</sup>-memory cells in convalescent patients has identified glycoprotein epitopes crucial for provoking a protective T-cell response, among which are regions of the receptor-binding domain and the glycan cap of GP [22].

**Table 1.** EVD case fatality in patients infected with different ebolaviruses. The table shows summarized data on the total number individuals with EVD in all reported outbreaks [4]

Species	Number of infected individuals	Number of deaths	Fatality rate, %
ZEBOV	30154	12503	40–90
SUDV	792	426	36–65
BDBV	206	66	25–51
RESTV	0/13*	0	0
TAFV	1	0	0
BOMV	0	0	0

**Note:** \* — clinical symptoms not observed; antibodies against RESTV detected in the blood serum.

Because a full-fledged protective immune response can be induced by using a full-length glycoprotein or structures expressing the *gp* gene, the majority of candidate and approved vaccines against ebolaviruses are based on the GP glycoprotein [23–24].

**Analysis of cross-reactive immunity in vaccinated individuals and patients recovered from EVD**

An ideal EVD vaccine must ensure protection against all variants of *Ebolavirus* that infect humans. Therefore, it is important to understand whether immune response can be induced against both homologous and phylogenetically distant species. The vaccine based on the recombinant vesicular stomatitis virus (rVSV-ZEBOV) that expresses glycoprotein GP of the ebolavirus isolated in 1995 has been reported to protect non-human primates against infection with any of known ZEBOV strains (isolated in 1976, 1995 and 2014) [25]. Studies of sera samples obtained from patients recovering from ZEBOV confirm those findings: IgG antibodies detected in the sera of the patients were capable of cross-reacting with glycoproteins of heterologous species SUDV and BDBV [26–27]. The studies of cross-

protective immunity in non-human primates demonstrate that the use of ZEBOV glycoprotein (as a component of the rVSV vaccine) confers protection against the lethal BDBV infection in 100% of animals; in contrast, the rVSV-SUDV vaccine does not protect all animals against ZEBOV and BDBV [28–30].

Research into cross-protective immunity against EVD in animals has revealed that postvaccination immunity is cross-protective against ZEBOV and BDBV but not against these species and SUDV.

In search of explanation for this phenomenon, we compared the structure of GP in different species of the ebolavirus. We aligned amino acid sequences of ZEBOV, SUDV and BDBV and mapped immunodominant GP epitopes (i. e., those with the highest immunogenicity; IE) in 1,548 Ebola virus isolates; 10 BDBV, 23 SUDV and 1,515 ZEBOV sequences were taken from a public database [31].

The detailed analysis of immunodominant regions carried out in T Cell Epitope Prediction Tools in the deimmunization mode [32] allowed us to identify 22 IE (Table 2 and 3). The vastest diversity was observed for the mucin domain of GP1; the lowest, for GP2. Paired comparison of IE revealed that homology between ZEBOV and BDBV immunodominant

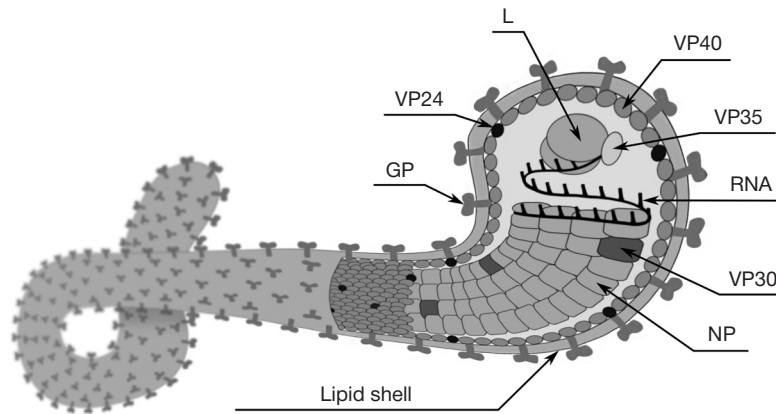


**Fig. 1.** The structure of Ebolavirus. GP — glycoprotein; L — catalytic subunit of the viral RNA-dependent RNA polymerase; NP — nucleoprotein; VP24 — minor matrix protein; VP30 — minor nucleoprotein; VP35 — nucleocapsid protein; VP40 — matrix protein

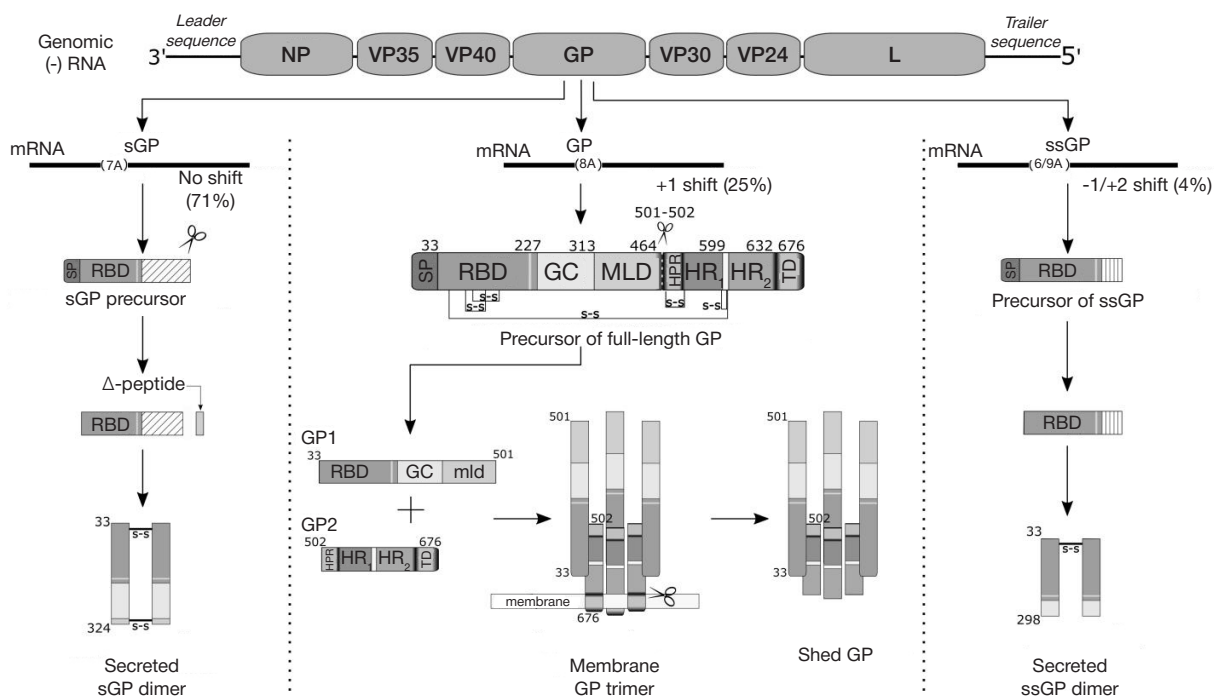


**Fig. 2.** Forms of *Ebolavirus* glycoprotein in eukaryotic cells. GC — glycan cap (glycan cap); HR — heptad repeat; HPR — hydrophobic region; MLD — mucin-like domain (mucin domain); RBD — receptor-binding domain; SP — signal peptide; TD — transmembrane domain

glycoprotein epitopes was 75.8%; between ZEBOV and SUDV, 63.2%; and between SUDV and BDBV, 61.5% (Table 2). It should be noted that glycoproteins representing different of ZEBOV isolates dating back to 1976, 1995, 2014 and 2018 are almost identical and only have minor differences in the region of the glycan cap and the mucin domain (Table 3). On average, IE homology was 98.7–100%.

The obtained data suggest closer phylogenetic relationship between ZEBOV and BDBV, in comparison with SUDV, but do not explain the difference in their ability to induce immune response in animals immunized with the corresponding variants of GP. So, we decided to analyze the sites that bind antibodies conferring cross-protective immunity against the lethal infection caused by various ebolavirus species. Such antibodies are specific to both GP1 and the regions adjacent to the transmembrane domain of GP2 [19–21, 33]. A few recent works point to the fact that protective antibodies bind to the conformational epitopes of GP and not to the linear ones [34–36]. Our analysis of GP sequences has revealed that positions of key amino acids essential for antibody binding are quite conserved. The analysis of sites for binding antibodies with protective potential shows that the positions of key amino acids (i.e., those whose substitution fully blocks the ability of the antibodies to bind to GP) in ZEBOV epitopes are absolutely identical to the positions of amino acids BDBV GP epitopes. Homology between these

amino acids and those found in SUDV glycoprotein varies from 30 to 60% (Fig. 3). In our opinion, mutations at such amino acid positions inhibit the protective potential of the antibodies. It seems that homology of the sites that bind the protective antibodies to the glycoproteins representing different *Ebolavirus* species is the factor that ensures cross-protective immunity against ZEBOV and BDBV and the lack of cross-protective immune response against these two species and SUDV.

The discovery of universal antibodies capable of protecting humans against pathogenic ebolaviruses [19–21, 33–34, 36] will boost the development of effective EBD therapies and inspire new approaches to the design vaccines against this virus. Studies of cross-protective immunity and antibodies isolated from convalescent patients with EVD give us hope that a ZEBOV GP-based vaccine inducing immunity against both ZEBOV и BDBV is not just wishful thinking. Adding SUDV glycoprotein to the vaccine would make it effective against SUDV species, as well.

CONCLUSIONS

The comparative analysis of GP in 1,548 ZEBOV, SUDV and BDBV isolates has demonstrated a high variability of amino acid sequences in the glycoproteins representing different ebolaviruses (~60–65% homology). Further analysis of epitope

**Table 2.** Homology of amino acid sequences of glycoprotein IE in ZEBOV, SUDV and BDBV viruses. The search for IE was conducted in T Cell Epitope Prediction Tools [32]; amino acid sequences were compared in Geneious® 10.2.3 (Biomatters; Auckland, New Zealand). The heat map shows homology is expressed as %: dark gray stands for 100%, white represents 0%

		Amino acid positions	Homology of amino acid sequences of GP in ZEBOV, SUDV and BDBV, %			
			ZEBOV vs SUDV vs BDBV	ZEBOV vs SUDV	ZEBOV vs BDBV	SUDV vs BDBV
GP1	RBD	93–127*	82.9	91.4	88.6	82.9
		151–165	86.7	93.3	93.3	93.3
		156–170	86.7	93.3	93.3	86.7
		161–175	73.3	86.7	86.7	73.3
		171–185	66.7	80.0	86.7	66.7
		190–204**	40.0	53.3	73.3	53.3
	Glycan cap	211–225	26.7	26.7	40.0	53.3
		214–247*	26.5	29.4	58.8	35.3
		231–245	40.0	46.7	73.3	40.0
		236–250	40.0	46.7	86.7	40.0
		241–255	53.3	53.3	86.7	53.3
		246–260	66.7	66.7	80.0	66.7
		251–265	53.3	53.3	73.3	53.3
	Mucin	271–285**	26.7	40.0	66.7	26.7
		389–405**	0.0	17.6	5.9	11.8
401–417**		5.9	5.9	17.6	17.6	
GP2	476–490**	33.3	53.3	53.3	40.0	
	505–519**	66.7	73.3	73.3	66.7	
	566–580	100	100	100	100	
	571–585	86.7	86.7	100	86.7	
	576–590	86.7	86.7	100	86.7	
	581–595	80.0	80.0	100	80.0	
	599–631**	90.9	90.9	97.0	93.9	
632–651**	70.0	70.0	90.0	75.0		
Average homology (%)			58.0	63.2	75.8	61.5

**Note:** \* — IE essential for inducing protective T-cell-mediated immune response [22]; \*\* — IE essential for inducing protective B-cell-mediated immune response [20, 34–38].

**Table 3.** Homology of amino acid sequences of ZEBOV glycoprotein IE (isolates from 1976, 1995, 2014 and 2018). The search for IE was conducted in T Cell Epitope Prediction Tools [32]; amino acid sequences were compared in Geneious® 10.2.3 (Biomatters; Auckland, New Zealand). The heat map shows homology is expressed as %: dark gray stands for 100%, white represents 0%

		Amino acid positions	Homology of amino acid sequences of ZEBOV glycoprotein in the isolates from 1976, 1995, 2014 and 2018, %						
			1976–1995–2014–2018	1976–1995	1976–2014	1976–2018	1995–2014	1995–2018	2014–2018
GP1	RBD	93–127*	100	100	100	100	100	100	100
		151–165	100	100	100	100	100	100	100
		156–170	100	100	100	100	100	100	100
	Glycan cap	161–175	100	100	100	100	100	100	100
		171–185	100	100	100	100	100	100	100
		190–204**	100	100	100	100	100	100	100
		211–225	100	100	100	100	100	100	100
		214–247*	100	100	100	100	100	100	100
		231–245	100	100	100	100	100	100	100
	Mucin	236–250	100	100	100	100	100	100	100
		241–255	100	100	100	100	100	100	100
		246–260	100	100	100	100	100	100	100
		251–265	93.3	100	93.3	100	93.3	100	93.3
		271–285**	100	100	100	100	100	100	100
		389–405**	94.1	100	94.1	100	94.1	100	94.1
	GP2	401–417**	88.2	100	88.2	100	88.2	100	88.2
		476–490**	93.3	100	100	93.3	100	93.3	93.3
		505–519**	100	100	100	100	100	100	100
GP2	566–580	100	100	100	100	100	100	100	
	571–585	100	100	100	100	100	100	100	
	576–590	100	100	100	100	100	100	100	
	581–595	100	100	100	100	100	100	100	
	599–631**	100	100	100	100	100	100	100	
	632–651**	100	100	100	100	100	100	100	
	Average homology (%)		98.7	100	99.0	99.7	99.0	99.7	98.7

**Note:** \* — IE essential for inducing protective T-cell-mediated immune response [22]; \*\* — IE essential for inducing protective B-cell-mediated immune response [20, 34–38].

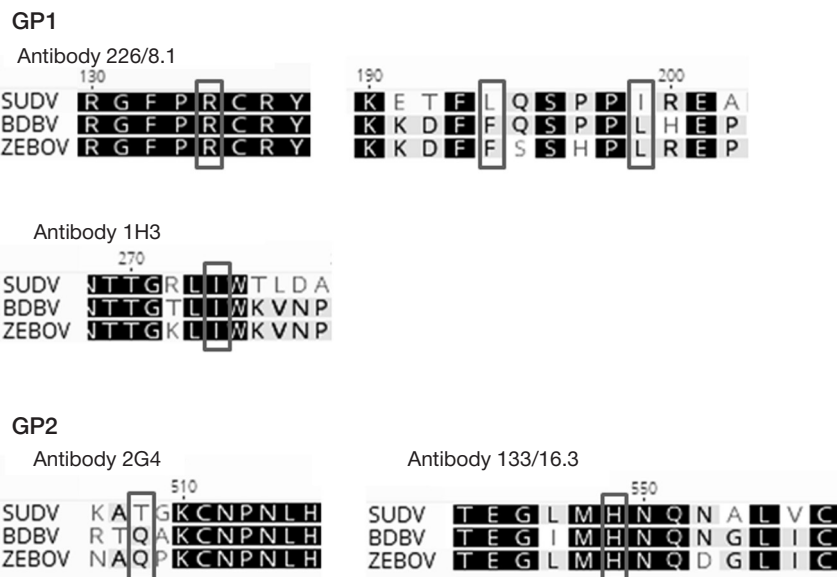


**Fig. 3.** The aligned consensus amino acid sequences of glycoprotein of ZEBOV, SUDV and BDBV species. Key amino acid positions essential for antibody binding are marked by a rectangle [34, 36]

homology in the glycoproteins of ZEBOV, SUDV and BDBV, accounting for the tertiary protein structure, has established that ZEBOV and BDBV glycoproteins have identical amino acids capable of binding to the protective antibodies and thus neutralizing these viral species characterized by low homology of linear amino acid sequences. These findings are fully consistent with the reports of the ability of candidate and approved vaccines against *Ebolavirus* to induce cross-immunity

against ZEBOV and BDBV. Protection against the lethal infection caused by SUDV can be ensured only by vaccines based on SUDV GP.

We believe that the facts listed above clearly establish that development of effective vaccine protecting humans against pathogenic *Ebolavirus* species should focus on vectors expressing at least two glycoprotein types: of ZEBOV and SUDV.

## References

- Beer B, Kurth R, Bukreyev A. Characteristics of Filoviridae: Marburg and Ebola viruses. *Naturwissenschaften*. 1999; 86 (1): 8–17.
- Kuhn JH, Becker S, Ebihara H, Geisbert TW, Johnson KM, Kawaoka Y, et al. Proposal for a revised taxonomy of the family Filoviridae: Classification, names of taxa and viruses, and virus abbreviations. *Archives of Virology*. 2010; 155 (12): 2083–103.
- Goldstein T, Anthony SJ, Gbakima A, Bird BH, Bangura J, Tremeau-Bravard A, et al. The discovery of Bombali virus adds further support for bats as hosts of ebolaviruses. *Nature Microbiology*. 2018; 3 (10): 1084–89.
- CDC. Cases and Outbreaks of EVD by Year [updated 2018 Nov 9; cited 2018 Nov 12]. Available from: <https://www.cdc.gov/vhf/ebola/history/chronology.html>.
- Lévy Y, Lane C, Piot P, Beavogui AH, Kieh M, Leigh B, et al. Prevention of Ebola virus disease through vaccination: where we are in 2018. *Lancet*. 2018; 392 (10149): 787–90.
- Bharat TA, Noda T, Riches JD, Kraehling V, Kolesnikova L, Becker S, et al. Structural dissection of Ebola virus and its assembly determinants using cryo-electron tomography. *Proc Natl Acad Sci USA*. 2012; 109 (11): 4275–80.
- Volchkov VE, Becker S, Volchkova VA, Ternovoj VA, Kotov AN, Netesov SV, et al. GP mRNA of Ebola virus is edited by the Ebola virus polymerase and by T7 and vaccinia virus polymerases. *Virology*. 1995; 214 (2): 421–30.
- Cook JD, Lee JE. The Secret Life of Viral Entry Glycoproteins: Moonlighting in Immune Evasion. *PLoS Pathog*. 2013; 9 (5): e1003258.
- He J, Melnik LI, Komin A, Wiedman G, Fuselier T, Morris CF, et al. Ebola Virus Delta Peptide is a Viroporin. *J Virol*. 2017; 91 (16): e00438–17.
- Lee JE, Saphire EO. Ebolavirus glycoprotein structure and mechanism of entry. *Future virology*. 2009; 4 (6): 621–35.
- Wang H, Shi Y, Song J, Qi J, Lu G, Yan J, et al. Ebola Viral Glycoprotein Bound to Its Endosomal Receptor Niemann-Pick C1. *Cell*. 2016; 164 (1–2): 258–68.
- Sanchez A, Yang ZY, Xu L, Nabel GJ, Crews T, Peters CJ. Biochemical Analysis of the Secreted and Virion Glycoproteins of Ebola Virus. *J Virol*. 1998; 72 (8): 6442–47.
- Dolinik O, Volchkova V, Garten W, Carbonnelle C, Becker S, Kahnt J, et al. Ectodomain shedding of the glycoprotein GP of Ebola virus. *EMBO J*. 2004; 23 (10): 2175–84.
- Ito H, Watanabe S, Takada A, Kawaoka Y. Ebola Virus Glycoprotein: Proteolytic Processing, Acylation, Cell Tropism, and Detection of Neutralizing Antibodies. *J Virol*. 2001; 75 (3): 1576–80.
- Kuzmina NA, Younan P, Gilchuk P, Santos RI, Flyak AI, Ilinykh PA, et al. Antibody-Dependent Enhancement of Ebola Virus Infection by Human Antibodies Isolated from Survivors. *Cell Rep*. 2018; 24 (7): 1802–15.
- Sullivan NJ, Geisbert TW, Geisbert JB, Shedlock DJ, Xu L, Lamoreaux L, et al. Immune protection of nonhuman primates against Ebola virus with single low-dose adenovirus vectors encoding modified GPs. *PLoS Med*. 2006; 3 (6): e177.
- Li W, Ye L, Carrion R, Nunneley J, Staples H, Ticer A, et al. Characterization of Immune Responses Induced by Ebola Virus Glycoprotein (GP) and Truncated GP Isoform DNA Vaccines and Protection Against Lethal Ebola Virus Challenge in Mice. *J Infect Dis*. 2015; 212 (Suppl 2): S398–403.
- Saphire EO, Schendel SL, Fusco ML, Gangavarapu K, Gunn BM, Wec AZ, et al. Systematic Analysis of Monoclonal Antibodies against Ebola Virus GP Defines Features that Contribute to Protection. *Cell*. 2018; 174 (4): 938–52.
- Wec AZ, Herbert AS, Murin CD, Nyakatura EK, Abelson DM, Fels JM, et al. Antibodies from a Human Survivor Define Sites of Vulnerability for Broad Protection against Ebolaviruses. *Cell*. 2017; 169 (5): 878–90.
- Gilchuk P, Kuzmina N, Ilinykh PA, Huang K, Gunn BM, Bryan A, et al. Multifunctional Pan-ebolavirus Antibody Recognizes a Site of Broad Vulnerability on the Ebolavirus Glycoprotein. *Immunity*. 2018; 49 (2): 363–74.
- Flyak AI, Kuzmina N, Murin CD, Bryan C, Davidson E, Gilchuk P, et al. Broadly neutralizing antibodies from human survivors target a conserved site in the Ebola virus glycoprotein HR2-MPER region. *Nat Microbiol*. 2018; 3 (6): 670–77.
- Sakabe S, Sullivan BM, Hartnett JN, Robles-Sikisaka R, Gangavarapu K, Cubitt B, et al. Analysis of CD8+ T cell response during the 2013–2016 Ebola epidemic in West Africa. *Proc Natl Acad Sci USA*. 2018; 115 (32): E7578–E7586.
- Lévy Y, Lane C, Piot P, Beavogui AH, Kieh M, Leigh B, et al. Prevention of Ebola virus disease through vaccination: where we are in 2018. *Lancet*. 2018; 392 (10149): 787–90.
- Dolzhikova IV, Tokarskaya EA, Dzharullaeva AS, Tukhvatulin AI, Shcheblyakov DV, Voronina OL, et al. Virus-Vectored Ebola Vaccines. *Acta Naturae*. 2017; 9 (3): 4–11.
- Marzi A, Robertson SJ, Haddock E, Feldmann F, Hanley PW, Scott DP, et al. EBOLA VACCINE. VSV-EBOV rapidly protects macaques against infection with the 2014/15 Ebola virus outbreak strain. *Science*. 2015; 349 (6249): 739–42.
- Macneil A, Reed Z, Rollin PE. Serologic cross-reactivity of human IgM and IgG antibodies to five species of Ebola virus. *PLoS Negl Trop Dis*. 2011; 5 (6): 1175.
- Natesan M, Jensen SM, Keasey SL, Kamata T, Kuehne AI, Stonier SW, et al. Human Survivors of Disease Outbreaks Caused by Ebola or Marburg Virus Exhibit Cross-Reactive and Long-Lived Antibody Responses. *Clin Vaccine Immunol*. 2016; (23): 717–24.
- Hensley LE, Mulangu S, Asiedu C, Johnson J, Honko AN, Stanley D, et al. Demonstration of cross-protective vaccine immunity against an emerging pathogenic Ebolavirus Species. *PLoS Pathog*. 2010; 6 (5): e1000904.
- Mire CE, Geisbert JB, Marzi A, Agans KN, Feldmann H, Geisbert TW. Vesicular stomatitis virus-based vaccines protect nonhuman primates against Bundibugyo ebolavirus. *PLoS Negl Trop Dis*. 2013; (7): e2600.
- Marzi A, Ebihara H, Callison J, Groseth A, Williams KJ, Geisbert TW, et al. Vesicular stomatitis virus-based Ebola vaccines with improved cross-protective efficacy. *J Infect Dis*. 2011; 204 (Suppl 3): S1066–74.
- Hatcher EL, Zhdanov SA, Bao Y, Blinkova O, Nawrocki EP, Ostapchuck Y, et al. Virus Variation Resource — improved response to emergent viral outbreaks. *Nucleic Acids Res*. 2016; 45 (D1): 482–90.
- T Cell Epitope Prediction Tools [cited 2018 Nov 12]. Available from: <http://tools.iedb.org/main/tcell/>.
- Ilinykh PA, Santos RI, Gunn BM, Kuzmina NA, Shen X, Huang K, et al. Asymmetric antiviral effects of ebolavirus antibodies targeting glycoprotein stem and glycan cap. *PLoS Pathog*. 2018; 14 (8): e1007204.
- Audet J, Wong G, Wang H, Lu G, Gao GF, Kobinger G,

- et al. Molecular characterization of the monoclonal antibodies composing ZMAb: a protective cocktail against Ebola virus. *Sci Rep.* 2014; (4): 6881.
35. Murin CD, Fusco ML, Bornholdt ZA, Qiu X, Olinger GG, Zeitlin L, et al. Structures of protective antibodies reveal sites of vulnerability on Ebola virus. *Proc Natl Acad Sci USA.* 2014; 111 (48): 17182–7.
36. Ponomarenko J, Vaughan K, Sette A, Maurer-Stroh S. Conservancy of mAb Epitopes in Ebolavirus Glycoproteins of Previous and 2014 Outbreaks. *PLoS Curr.* 2014; (6).
37. Zhao X, Howell KA, He S, Brannan JM, Wec AZ, Davidson E, et al. Immunization-Elicited Broadly Protective Antibody Reveals Ebolavirus Fusion Loop as a Site of Vulnerability. *Cell.* 2017; 169 (5): 891–904.
38. Misasi J, Gilman MS, Kanekiyo M, Gui M, Cagigi A, Mulangu S, et al. Structural and molecular basis for Ebola virus neutralization by protective human antibodies. *Science.* 2016; 351 (6279): 1343–6.

Литература

1. Beer B, Kurth R, Bukreyev A. Characteristics of Filoviridae: Marburg and Ebola viruses. *Naturwissenschaften.* 1999; 86 (1): 8–17.
2. Kuhn JH, Becker S, Ebihara H, Geisbert TW, Johnson KM, Kawaoka Y, et al. Proposal for a revised taxonomy of the family Filoviridae: Classification, names of taxa and viruses, and virus abbreviations. *Archives of Virology.* 2010; 155 (12): 2083–103.
3. Goldstein T, Anthony SJ, Gbakima A, Bird BH, Bangura J, Tremeau-Bravard A, et al. The discovery of Bombali virus adds further support for bats as hosts of ebolaviruses. *Nature Microbiology.* 2018; 3 (10): 1084–89.
4. CDC. Cases and Outbreaks of EVD by Year [updated 2018 Nov 9; cited 2018 Nov 12]. Available from: <https://www.cdc.gov/vhf/ebola/history/chronology.html>.
5. Lévy Y, Lane C, Piot P, Beavogui AH, Kieh M, Leigh B, et al. Prevention of Ebola virus disease through vaccination: where we are in 2018. *Lancet.* 2018; 392 (10149): 787–90.
6. Bharat TA, Noda T, Riches JD, Kraehling V, Kolesnikova L, Becker S, et al. Structural dissection of Ebola virus and its assembly determinants using cryo-electron tomography. *Proc Natl Acad Sci USA.* 2012; 109 (11): 4275–80.
7. Volchkov VE, Becker S, Volchkova VA, Ternovoj VA, Kotov AN, Netesov SV, et al. GP mRNA of Ebola virus is edited by the Ebola virus polymerase and by T7 and vaccinia virus polymerases. *Virology.* 1995; 214 (2): 421–30.
8. Cook JD, Lee JE. The Secret Life of Viral Entry Glycoproteins: Moonlighting in Immune Evasion. *PLoS Pathog.* 2013; 9 (5): e1003258.
9. He J, Melnik LI, Komin A, Wiedman G, Fuselier T, Morris CF, et al. Ebola Virus Delta Peptide is a Viroporin. *J Virol.* 2017; 91 (16): e00438–17.
10. Lee JE, Saphire EO. Ebolavirus glycoprotein structure and mechanism of entry. *Future virology.* 2009; 4 (6): 621–35.
11. Wang H, Shi Y, Song J, Qi J, Lu G, Yan J, et al. Ebola Viral Glycoprotein Bound to Its Endosomal Receptor Niemann-Pick C1. *Cell.* 2016; 164 (1–2): 258–68.
12. Sanchez A, Yang ZY, Xu L, Nabel GJ, Crews T, Peters CJ. Biochemical Analysis of the Secreted and Virion Glycoproteins of Ebola Virus. *J Virol.* 1998; 72 (8): 6442–47.
13. Dolnik O, Volchkova V, Garten W, Carbonnelle C, Becker S, Kahnt J, et al. Ectodomain shedding of the glycoprotein GP of Ebola virus. *EMBO J.* 2004; 23 (10): 2175–84.
14. Ito H, Watanabe S, Takada A, Kawaoka Y. Ebola Virus Glycoprotein: Proteolytic Processing, Acylation, Cell Tropism, and Detection of Neutralizing Antibodies. *J Virol.* 2001; 75 (3): 1576–80.
15. Kuzmina NA, Younan P, Gilchuk P, Santos RI, Flyak AI, Ilinykh PA, et al. Antibody-Dependent Enhancement of Ebola Virus Infection by Human Antibodies Isolated from Survivors. *Cell Rep.* 2018; 24 (7): 1802–15.
16. Sullivan NJ, Geisbert TW, Geisbert JB, Shedlock DJ, Xu L, Lamoreaux L, et al. Immune protection of nonhuman primates against Ebola virus with single low-dose adenovirus vectors encoding modified GPs. *PLoS Med.* 2006; 3 (6): e177.
17. Li W, Ye L, Carrion R, Nunneley J, Staples H, Ticer A, et al. Characterization of Immune Responses Induced by Ebola Virus Glycoprotein (GP) and Truncated GP Isoform DNA Vaccines and Protection Against Lethal Ebola Virus Challenge in Mice. *J Infect Dis.* 2015; 212 (Suppl 2): S398–403.
18. Saphire EO, Schendel SL, Fusco ML, Gangavarapu K, Gunn BM, Wec AZ, et al. Systematic Analysis of Monoclonal Antibodies against Ebola Virus GP Defines Features that Contribute to Protection. *Cell.* 2018; 174 (4): 938–52.
19. Wec AZ, Herbert AS, Murin CD, Nyakatura EK, Abelson DM, Fels JM, et al. Antibodies from a Human Survivor Define Sites of Vulnerability for Broad Protection against Ebolaviruses. *Cell.* 2017; 169 (5): 878–90.
20. Gilchuk P, Kuzmina N, Ilinykh PA, Huang K, Gunn BM, Bryan A, et al. Multifunctional Pan-ebolavirus Antibody Recognizes a Site of Broad Vulnerability on the Ebolavirus Glycoprotein. *Immunity.* 2018; 49 (2): 363–74.
21. Flyak AI, Kuzmina N, Murin CD, Bryan C, Davidson E, Gilchuk P, et al. Broadly neutralizing antibodies from human survivors target a conserved site in the Ebola virus glycoprotein HR2-MPER region. *Nat Microbiol.* 2018; 3 (6): 670–77.
22. Sakabe S, Sullivan BM, Hartnett JN, Robles-Sikisaka R, Gangavarapu K, Cubitt B, et al. Analysis of CD8+ T cell response during the 2013–2016 Ebola epidemic in West Africa. *Proc Natl Acad Sci USA.* 2018; 115 (32): E7578–E7586.
23. Lévy Y, Lane C, Piot P, Beavogui AH, Kieh M, Leigh B, et al. Prevention of Ebola virus disease through vaccination: where we are in 2018. *Lancet.* 2018; 392 (10149): 787–90.
24. Dolzhikova IV, Tokarskaya EA, Dzharullaeva AS, Tukhvatulin AI, Shcheblyakov DV, Voronina OL, et al. Virus-Vectored Ebola Vaccines. *Acta Naturae.* 2017; 9 (3): 4–11.
25. Marzi A, Robertson SJ, Haddock E, Feldmann F, Hanley PW, Scott DP, et al. EBOLA VACCINE. VSV-EBOV rapidly protects macaques against infection with the 2014/15 Ebola virus outbreak strain. *Science.* 2015; 349 (6249): 739–42.
26. Macneil A, Reed Z, Rollin PE. Serologic cross-reactivity of human IgM and IgG antibodies to five species of Ebola virus. *PLoS Negl Trop Dis.* 2011; 5 (6): 1175.
27. Natesan M, Jensen SM, Keasey SL, Kamata T, Kuehne AI, Stonier SW, et al. Human Survivors of Disease Outbreaks Caused by Ebola or Marburg Virus Exhibit Cross-Reactive and Long-Lived Antibody Responses. *Clin Vaccine Immunol.* 2016; (23): 717–24.
28. Hensley LE, Mulangu S, Asiedu C, Johnson J, Honko AN, Stanley D, et al. Demonstration of cross-protective vaccine immunity against an emerging pathogenic Ebolavirus Species. *PLoS Pathog.* 2010; 6 (5): e1000904.
29. Mire CE, Geisbert JB, Marzi A, Agans KN, Feldmann H, Geisbert TW. Vesicular stomatitis virus-based vaccines protect nonhuman primates against Bundibugyo ebolavirus. *PLoS Negl Trop Dis.* 2013; (7): e2600.
30. Marzi A, Ebihara H, Callison J, Groseth A, Williams KJ, Geisbert TW, et al. Vesicular stomatitis virus-based Ebola vaccines with improved cross-protective efficacy. *J Infect Dis.* 2011; 204 (Suppl 3): S1066–74.
31. Hatcher EL, Zhdanov SA, Bao Y, Blinkova O, Nawrocki EP, Ostapchuk Y, et al. Virus Variation Resource — improved response to emergent viral outbreaks. *Nucleic Acids Res.* 2016; 45 (D1): 482–90.
32. T Cell Epitope Prediction Tools [cited 2018 Nov 12]. Available from: <http://tools.iedb.org/main/tcell/>.
33. Ilinykh PA, Santos RI, Gunn BM, Kuzmina NA, Shen X, Huang K, et al. Asymmetric antiviral effects of ebolavirus antibodies targeting glycoprotein stem and glycan cap. *PLoS Pathog.* 2018; 14 (8): e1007204.
34. Audet J, Wong G, Wang H, Lu G, Gao GF, Kobinger G, et al. Molecular characterization of the monoclonal antibodies composing ZMAb: a protective cocktail against Ebola virus. *Sci*

- Rep. 2014; (4): 6881.
35. Murin CD, Fusco ML, Bornholdt ZA, Qiu X, Olinger GG, Zeitlin L, et al. Structures of protective antibodies reveal sites of vulnerability on Ebola virus. *Proc Natl Acad Sci USA*. 2014; 111 (48): 17182–7.
  36. Ponomarenko J, Vaughan K, Sette A, Maurer-Stroh S. Conservancy of mAb Epitopes in Ebolavirus Glycoproteins of Previous and 2014 Outbreaks. *PLoS Curr*. 2014; (6).
  37. Zhao X, Howell KA, He S, Brannan JM, Wec AZ, Davidson E, et al. Immunization-Elicited Broadly Protective Antibody Reveals Ebolavirus Fusion Loop as a Site of Vulnerability. *Cell*. 2017; 169 (5): 891–904.
  38. Misasi J, Gilman MS, Kanekiyo M, Gui M, Cagigi A, Mulangu S, et al. Structural and molecular basis for Ebola virus neutralization by protective human antibodies. *Science*. 2016; 351 (6279): 1343–6.

## A GENETICALLY ENCODED BIOSENSOR ROKATE FOR MONITORING THE REDOX STATE OF THE GLUTATHIONE POOL

Shokhina AG<sup>1</sup>, Belousov VV<sup>1,2</sup>, Bilan DS<sup>1</sup> ✉

<sup>1</sup> Shemyakin-Ovchinnikov Institute of Bioorganic Chemistry, Moscow, Russia

<sup>2</sup> Institute of Translational Medicine, Pirogov Russian National Research Medical University, Moscow, Russia

Genetically encoded fluorescent sensors are exploited to study a variety of biological processes in living organisms in real time. In recent years, a whole family of biosensors has been developed, serving to visualize changes in the glutathione redox state. The aim of our experiment was to design a biosensor based on the red fluorescent protein mKate2 for measuring the 2GSH/GSSG ratio. A pair of cysteine amino acid residues were introduced into the structure of the fluorescent protein using site-directed mutagenesis. These residues form a disulfide bridge when the surrounding glutathione pool is oxidized, affecting the spectral characteristics of the protein. Our biosensor, which we called roKate, was tested *in vitro* on an isolated protein. Specifically, we examined the spectral characteristics, pH and the redox potential of the sensor. Additionally, the performance of roKate was evaluated using the culture of living mammalian cells. The fluorescent signal emitted by the sensor was very bright and remarkably stable under pH conditions varying in the physiological range. Irreversibly oxidized in mammalian cells, roKate stands out from other members of this biosensor family. This biosensor should be preferred in the experiments when the time between the manipulations with the biological object and the subsequent analysis of the induced effect is substantial, as is the case with long sample preparation.

**Keywords:** genetically encoded fluorescent sensor, glutathione, 2GSH/GSSG ratio, roKate

**Funding:** this work was supported by the Russian Foundation for Basic Research (Project mol\_a\_dk No.16-34-60175).

**Author contribution:** Shokhina AG was responsible for the experimental part of the study. Belousov VV and Bilan DS supervised the study and prepared this manuscript.

✉ **Correspondence should be addressed:** Dmitry S. Bilan  
Miklouho-Maclay, 16/10, Moscow, 117997; d.s.bilan@gmail.com

**Received:** 26.12.2018 **Accepted:** 02.03.2019 **Published online:** 14.03.2019

**DOI:** 10.24075/brsmu.2019.013

## ГЕНЕТИЧЕСКИ КОДИРУЕМЫЙ БИОСЕНСОР РОКАТЕ ДЛЯ РЕГИСТРАЦИИ РЕДОКС-СОСТОЯНИЯ ПУЛА ГЛУТАТИОНА

А. Г. Шохина<sup>1</sup>, В. В. Белоусов<sup>1,2</sup>, Д. С. Билан<sup>1</sup> ✉

<sup>1</sup> Институт биоорганической химии имени М. М. Шемякина и Ю. А. Овчинникова РАН, Москва, Россия

<sup>2</sup> Научно-исследовательский институт трансляционной медицины, Российский национальный исследовательский медицинский университет имени Н. И. Пирогова, Москва, Россия

Генетически кодируемые биосенсоры на основе флуоресцентных белков представляют собой инструмент исследования ряда биологических процессов в живых системах в режиме реального времени. За последние годы было создано целое семейство биосенсоров, позволяющих визуализировать в живых клетках изменения редокс-состояния пула глутатиона. Целью настоящей работы была разработка нового биосенсора для регистрации соотношения 2GSH/GSSG на основе красного флуоресцентного белка mKate2. Для этого методом направленного мутагенеза в структуру флуоресцентного белка вносили пару аминокислотных остатков цистеина, которые при окислении окружающего пула глутатиона формируют дисульфидную связь, что приводит к изменению спектральных характеристик. Полученный биосенсор был протестирован *in vitro* на выделенном препарате белка, в частности, были исследованы спектральные характеристики, pH-чувствительность белка, окислительно-восстановительный потенциал. Кроме того, биосенсор, названный roKate, был протестирован в культуре живых клеток млекопитающих. Он отличается высокой яркостью и повышенной стабильностью сигнала при изменениях pH в физиологическом диапазоне. От других представителей данного семейства биосенсоров roKate отличается необратимым изменением сигнала при окислении в клетках млекопитающих. Применение данного сенсора предпочтительно в экспериментах с наличием длительного промежутка времени между воздействием на биологическую систему и последующим анализом вызванного эффекта, например в условиях длительной пробоподготовки.

**Ключевые слова:** генетически кодируемый флуоресцентный биосенсор, глутатион, соотношение 2GSH/GSSG, roKate

**Финансирование:** работа выполнена при поддержке гранта РФФИ мол\_a\_дк № 16-34-60175.

**Информация о вкладе авторов:** А. Г. Шохина проводила экспериментальную работу; В. В. Белоусов и Д. С. Билан руководили исследованиями, писали текст статьи.

✉ **Для корреспонденции:** Дмитрий Сергеевич Билан  
ул. Миклухо-Маклая, д. 16/10, г. Москва, 117997; d.s.bilan@gmail.com

**Статья получена:** 26.12.2018 **Статья принята к печати:** 02.03.2019 **Опубликована онлайн:** 14.03.2019

**DOI:** 10.24075/vrgmu.2019.013

Research into redox reactions is a burgeoning field of contemporary biomedicine. The ratio of reduced (GSH) to oxidized (GSSG) glutathione is an important characteristic of a cell's redox state. Essentially, glutathione is an abundant tripeptide ( $\gamma$ -L-glutamyl-L-cysteinyl-glycine), whose intracellular concentrations can be as high as 10 mM [1]. The biological function of glutathione relies on the ability of its two reduced molecules (2GSH) to pass on a pair of electrons to an acceptor molecule. During this process, glutathione is oxidized to a

disulfide form that can be further converted back to GSH by glutathione reductase (GR) [2]. GSH plays a key role in the reduction of oxidative stress products, including lipid and hydrogen peroxides. Glutathione reduces reversible disulfide bonds that largely determine the structure and function of many cellular proteins [3]. Summing up, firstly, glutathione is a critical component of the thiol-disulfide exchange and secondly, it is involved in protein glutathionylation, playing a crucial role in intracellular redox signaling and protein folding.

Defects in the regulatory systems controlling the intracellular levels of glutathione or its redox homeostasis (the 2GSH/GSSG ratio) can promote pathology. Impaired glutathione synthesis caused by mutations in the genes coding for the subunits of  $\gamma$ -glutamyl-cysteine-synthase is linked to diabetes mellitus [4], asthma [5], schizophrenia [6], and other diseases. Deficient activity of glutathione reductase that maintains the GSH pool is associated with systemic lupus erythematosus [7] and some forms of favism [8]. By contrast, in cancer cells this enzyme is often hyperactive, causing an increase in GSH concentrations and strengthening the antioxidant defense of malignant cells [9]. Changes in the 2GSH/GSSG ratio that characterizes the redox state of the intracellular environment can indicate both pathological and normal physiological processes, such as differentiation [10, 11], proliferation [12], or apoptosis [13]. However, if these changes are massive and uncontrolled, they can cause a wide range of disorders, including neurodegenerative, immune, cardiovascular, etc. [14]. Among other functions of glutathione in the living organism is participation in the metabolism of xenobiotics that includes conjugation to GSH in the reaction catalyzed by glutathione transferases [15].

In a biological sample, GSH and GSSG can be measured by high-performance liquid chromatography (HPLC). Another approach to investigating the redox state of the glutathione pool involves the use of chemical dyes. Prior to staining with the classic Ellman's reagent [16], cells need to be lysed or tissue homogenate needs to be prepared. By contrast, synthetic dyes like ThiolQuant Green [17] and RealThiol [18] can be used in intact cells; however, they provide information about GSH concentrations only. At present, genetically encoded sensors based on redox-sensitive fluorescent proteins (roFP) have become very popular as tools for monitoring the dynamics of the GSH redox ratio. Such sensors rely on the oxidation of two surface cysteine residues incorporated into the structure of a fluorescent protein by site-directed mutagenesis. The oxidation degree of the redox-sensitive cysteine residues is determined by the surrounding glutathione pool. Being in close proximity to each other, the cysteine residues form a disulfide bond when oxidized in response to change in the GSH redox ratio. This leads to conformational rearrangements affecting the spectral characteristics of the fluorescent protein. Depending on the 2GSH/GSSG value, roFP can be either in reduced or oxidized forms distinguished by their spectra. Because such biosensors are protein-based, they can be expressed in a wide range of biological system, from individual cell organelles to transgenic organism tissue. The history of this biosensor family started with a yellow fluorescent protein [19]; green protein sensors appeared shortly afterwards [20, 21]. Today, we have an arsenal of diverse redox-sensitive sensors at our disposal that can be employed to monitor the 2GSH/GSSG dynamics in living systems in real time. They vary in their spectral characteristics, redox potential, reaction rate, and specificity [22].

The most convenient fluorescent sensors for *in vivo* experiments are those emitting in the far-red spectrum [23]; over this wavelength range, light absorption by water, hemoglobin, melanin and other tissue compounds is minimal. Besides, the green light used to excite a chromophore of a red protein is less toxic for cells in comparison with blue and violet used to induce fluorescence of green biosensors. The aim of this study was to create a new version of a redox biosensor based on the mKate2 red fluorescent protein. The sensor that we called roKate exhibits increased pH stability and brightness. The distinctive feature of the roKate biosensor is its irreversible response in mammalian cells upon oxidation, which

allows researchers to use it as a sensor that has an "oxidation memory" of glutathione pool oxidation.

## METHODS

### Genetic constructs

Point mutations were introduced into the structure of the red fluorescent protein mKate2. The sample for DNA amplification contained thermally stable Tersus polymerase in a buffer (Evrogen; Russia) and an equimolar mixture of dNTP (200  $\mu$ M), primers (10  $\mu$ M) and a DNA template (100 ng). The PCR protocol included 22 cycles of denaturation (95  $^{\circ}$ C, 30 s), annealing (60  $^{\circ}$ C, 45 s) and elongation (72  $^{\circ}$ C, 90 s).

Random mutagenesis was performed to improve the properties of the genetic constructs. The reaction mix contained thermally stable Taq polymerase in a buffer (Evrogen; Russia), primers (10  $\mu$ M), dATP (200  $\mu$ M), dTTP (200  $\mu$ M), dCTP (200  $\mu$ M), dGTP (360  $\mu$ M), MnSO<sub>4</sub> (640  $\mu$ M), and a DNA template (20 pg). The PCR protocol included 27 cycles of denaturation (95  $^{\circ}$ C, 30 s), annealing (60  $^{\circ}$ C, 45 s) and elongation (72  $^{\circ}$ C, 105 s). The expected number of mutations was 4–5 per construct [24]. The obtained samples were cloned into plasmid vectors: pQe30 (to facilitate expression in bacterial cells) and pC1 (to facilitate expression in mammalian cells).

### Bacterial cells

We used strain XL1-Blue of *E. coli*. The cells were cultured in an LB broth or in a solid medium in Petri dishes (1.5% LB agar). The medium contained 100  $\mu$ kg/ml ampicillin (for pQe30) or 25  $\mu$ kg/ml kanamycin (for pC1).

The US SZX12 fluorescence microscope (Olympus; Japan) was used to select the brightest fluorescent colonies that were subsequently transferred onto the solid substrate. Further measurements were carried out using Varian Cary Eclipse fluorescence spectrophotometer (Agilent; USA). Briefly, the bacterial biomass was suspended in 1 ml of PBS and fluorescence emission and excitation spectra were recorded at  $\lambda_{ex}$  = 585 nm and  $\lambda_{em}$  = 624 nm, respectively. To change the redox state of the cells, H<sub>2</sub>O<sub>2</sub> was added to the suspension at the final concentrations of 100  $\mu$ M — 2 mM. The data were processed in OriginPro 9.0 (OriginLab; USA).

### The recombinant protein

XL1-Blue *E. coli* cells were transformed with the roKate pQe30 plasmid. The mKate2 protein expressed by the cells had a histidine tag (His-tag) at its C-terminus. The bacterial clones were cultured in LB broth containing 100  $\mu$ kg/ml ampicillin for 16 h at room temperature under continuous stirring at 200 rpm. The obtained bacterial suspension was pelleted by centrifugation for 15 min at 2,000 g and 4  $^{\circ}$ C. Cell lysis was aided by the commercial B-PER™ Bacterial Protein Extraction Reagent (ThermoFisher; USA). Then, the samples were again centrifuged for 20 min at 18,000 g and 4  $^{\circ}$ C. The supernatant was applied to the chromatography column containing TALON purification resin (Clontech; USA) capable of binding to the His-tag. The protein was eluted from the column using a PBS solution (pH 7.0) containing 250 mM imidazole. To separate imidazole from the recombinant protein, the latter was run through a gel filtration column packed with Sephadex G-50 (GE Healthcare Life Sciences; UK). The sample was incubated in a PBS solution containing 20 mM dithiothreitol for 30 min to reduce disulfide bonds.

### *In vitro* tests of the biosensor

An aliquot of the purified protein was added to 1 ml of PBS (pH 7.0) at a final concentration of 100 nM in a spectrophotometry cuvette. Fluorescence emission and excitation spectra were recorded by Varian Cary Eclipse (Agilent; USA) at  $\lambda_{ex} = 585$  nm and  $\lambda_{em} = 624$  nm. GSSG or GSH were added to the sample at concentrations ranging between 50  $\mu$ M and 2 mM; the spectra were recorded subsequently.

The purified protein was titrated with glutathione solutions with the GSH/GSSG ratio varying from 10 : 0 to 0 : 10. Then, the following approach was applied to measure the redox potential of the tested biosensor. First, Y was calculated by the formula:  $Y = (F_n - F_{min}) / (F_{max} - F_n)$ , where  $F_n$  is fluorescence intensity in the sample with a known GSH/GSSG value;  $F_{min}$  is fluorescence intensity in the sample containing 1 mM GSSG;  $F_{max}$  is fluorescence intensity in the sample containing 1 mM GSH. Then, logY was plotted against log([GSSG]/[GSH]). A GSSG/2GSH ratio was determined at which the signal intensity changed by 50%; the obtained value was designated as A. The equilibrium constant  $K_{eq}$  was calculated by the formula:  $\log K_{eq} = \log(F_{max}/F_{min}) - \log A$ . The redox potential (E) was calculated by the formula:  $E = E_0 - (RT/nF) \cdot \ln K_{eq}$ , where  $E_0$  is the redox potential of glutathione (-240 mV) at pH = 7.0; R is the gas constant (8.314 J/mol·K); T is temperature (K); n is the number of electrons participating in the exchange; F is the Faraday constant (96,490 J/mol·V).

For samples with a known GSH:GSSG ratio, the oxidation degrees (OxD) of the glutathione pool and roKate were calculated by the following formulas:

$$\begin{aligned} \text{OxD}_{\text{GSH}} &= 2[\text{GSH}] / (2[\text{GSSG}] + [\text{GSH}]), \\ \text{OxD}_{\text{roKate}} &= [\text{GSH}] / ([\text{GSSG}] (K_{eq} + [\text{GSH}] / [\text{GSSG}])). \end{aligned}$$

The quantum yield of the biosensor was calculated by the formula:  $QY = (Em_{\text{roKate}} \cdot Abs_{\text{mKate2}}) / (Em_{\text{mKate2}} \cdot Abs_{\text{roKate}}) \cdot QY_{\text{mKate2}}$ , where  $Em_{\text{roKate}}$  and  $Em_{\text{mKate2}}$  are intensities of the fluorescent signals emitted by roKate and the reference mKate2 protein with the emission peak at  $\lambda = 624$  nm;  $Abs_{\text{roKate}}$  and  $Abs_{\text{mKate2}}$  are absorbances of roKate and the reference mKate2 protein at  $\lambda = 590$  nm;  $QY_{\text{mKate2}}$  is the quantum yield of mKate2 (a precalculated value, 0.4).

To determine the extinction coefficient ( $\xi$ ), absorption spectra were recorded at  $\lambda = 590$  nm for native roKate and roKate denatured in 1 mM NaOH. Following the assumption that  $\xi$  of the denatured roKate chromophore equals  $\xi$  of mKate2 (62,500 M<sup>-1</sup> · cm<sup>-1</sup>), we calculated the extinction coefficient for the native protein by the formula:  $\xi_{\text{native}} = (Abs_{\text{native}} \cdot \xi_{\text{denat}}) / Abs_{\text{denat}}$ .

$pK_a$  of the biosensor was measured using a series of buffer solutions with a known pH ranging from 3.0 to 11.0 (at 0.5 increments). An aliquot of the protein was added to each of the solutions at a final concentration of 100 nM and the fluorescence excitation spectrum was recorded; then, the fluorescence intensity/pH curve was built.

### Mammalian cell culture

In our experiment, we used the HeLa Kyoto cell line cultured in DMEM supplemented with 10% FBS, 2 mM glutamine, 1% of penicillin and streptomycin. The cells were grown at 37 °C in a 5% CO<sub>2</sub> atmosphere.

Prior to transfection, the cells were plated and cultured in 35 mm glass-bottom microscopy dishes FluoroDishes (World Precision Instruments; USA). Plasmid DNA was mixed with the

FuGene HD transfection reagent (Promega; USA) following the manufacturer's protocol. After the transfection solution was added to the cell culture, the dishes were put in the incubator. Microscopy was performed on the following day.

### Fluorescent microscopy

Microscopy was performed using the DMI 6000 B microscope (Leica; Germany) equipped with a 120W HXP mercury lamp (Osram; Germany) and a CoolSNAP HQ CCD-camera (Photometrics; USA). The TX2 filter (Excitation: BP560/40; Emission: BP645/75) was used to record fluorescence in the far-red spectrum. Prior to microscopy, the DMEM medium was replaced with a Hanks' balanced salt solution containing 15 mM Hepes. Microscopy was performed in 1 ml of the medium at 37 °C. One hundred  $\mu$ L of hydrogen peroxide brought to a final concentration of 750  $\mu$ M was added to the cells in order to oxidize the intracellular glutathione pool. Dithiothreitol taken at a final concentration of 2 mM was used as a reductant. The images were analyzed in Leica Application Suite Advanced Fluorescence software (Leica; Germany). Final image processing was done in ImageJ (EMBL; Germany) and OriginPro 9.0 (OriginLab; USA).

## RESULTS

### Genetic constructs

The red fluorescent protein mKate2 is a monomer that produces very bright fluorescence and is stable under physiological pH conditions [23]. So, we selected this protein to design a redox biosensor capable of reporting shifts in the 2GSH/GSSG ratio. A pair of cysteine (Cys) residues was introduced into the protein structure by site-directed mutagenesis in such way that they could form a disulfide bond when oxidized. In total, 10 protein variants were obtained differing in the positions of Cys insertions: 142/198, 142/196, 141/161, 144/196, 141/198, 141/161, 141/196, 107/118, 140/214, and 200/214. It is known that it takes quite a time for the equilibrium between the redox-active cysteine residues of previously designed rYFP and roGFP biosensors and the glutathione pool to settle. However, if glutaredoxin (Grx) concentrations are increased in the vicinity of these proteins, the reaction accelerates. Therefore, rYFP and roGFP were fused to human Grx1 at the gene level via a polypeptide linker [25, 26] to speed up the reaction. All mKate2-based constructs contained human Grx1 attached by a linker (Gly-Gly-Ser-Gly-Gly)<sub>6</sub> to their N-terminus. Fig. 1A is a schematic representation of how the obtained biosensor is expected to function.

### roKate expression in bacterial cells

The obtained genetic constructs were expressed in XL1 Blue *E. coli* bacterial cells. Twenty-four hours later, fluorescence intensity was measured in the grown colonies. To assess the functional activity of each fluorescent biosensor variant, we recorded changes in the fluorescence excitation spectra before and after H<sub>2</sub>O<sub>2</sub> (the final concentration of 1 mM) was added to the bacterial suspension. H<sub>2</sub>O<sub>2</sub> is a powerful oxidant that significantly affects the redox state of the intracellular environment if taken in excess. It also leads to the increased production of GSSG. Grx1-mKate2 was used as a negative control. This protein does not contain redox-active Cys in the chromophore environment of the fluorescent protein and, therefore, does not respond to oxidation by changing

its spectral properties. After the measurements, two proteins with Cys at positions 141/198 and 141/196 were selected for further experiments. Other mutants either lacked fluorescent properties or were insensitive to oxidation.

Fluorescence intensity of the selected mutants declined by less than 10% in response to oxidation with  $\text{H}_2\text{O}_2$ . Random mutagenesis was performed to improve the properties of the proteins. This method produces a fixed number of random mutations in a targeted gene and can be used to obtain thousands of variants of the same protein that differ in only a few amino acid substitutions. Since even a single mutation can significantly affect the properties of a protein, further screening should be performed to identify the optimal mutants. After running a few cycles of random mutagenesis, we selected the brightest clones that were further tested under the conditions of oxidative stress. Finally, we opted for a mutant that contained redox-active Cys141 and Cys198 and additional mutations Lys12Glu and Asn21Asp in the structure of the fluorescent protein. This mutant protein was named roKate. It responded to oxidation by at least a 40% drop in fluorescence intensity.

### Measuring roKate characteristics *in vitro*

The roKate protein was purified for further in-depth analysis. This protein has one fluorescence excitation peak at 585 nm and one emission peak at 624 nm (Fig. 1B). Because during the initial screening  $\text{H}_2\text{O}_2$  concentrations were high, the first thing to test was whether  $\text{H}_2\text{O}_2$  could directly oxidize the redox-active Cys residues of the protein.  $\text{H}_2\text{O}_2$  at a final concentration of 1 mM was added to the protein sample (100 nM), causing no changes to the excitation spectra of the sample (Fig. 1C). However, fluorescence intensity dropped by 40% when 1 mM of GSH was added to the sample before 1 mM of  $\text{H}_2\text{O}_2$  was added, which can be explained by GSH oxidation (Fig. 1D). The same fluorescence pattern was observed when pre-oxidized GSSG (1 mM) was added to the protein sample (Fig. 1E). That reaction was reversible *in vitro*. If glutathione reductase (GR) and NADPH were introduced into the same sample, fluorescence intensity went back to its initial value (Fig. 1E). Thus, changes in the signal intensity were mediated by the changes in the glutathione redox state.

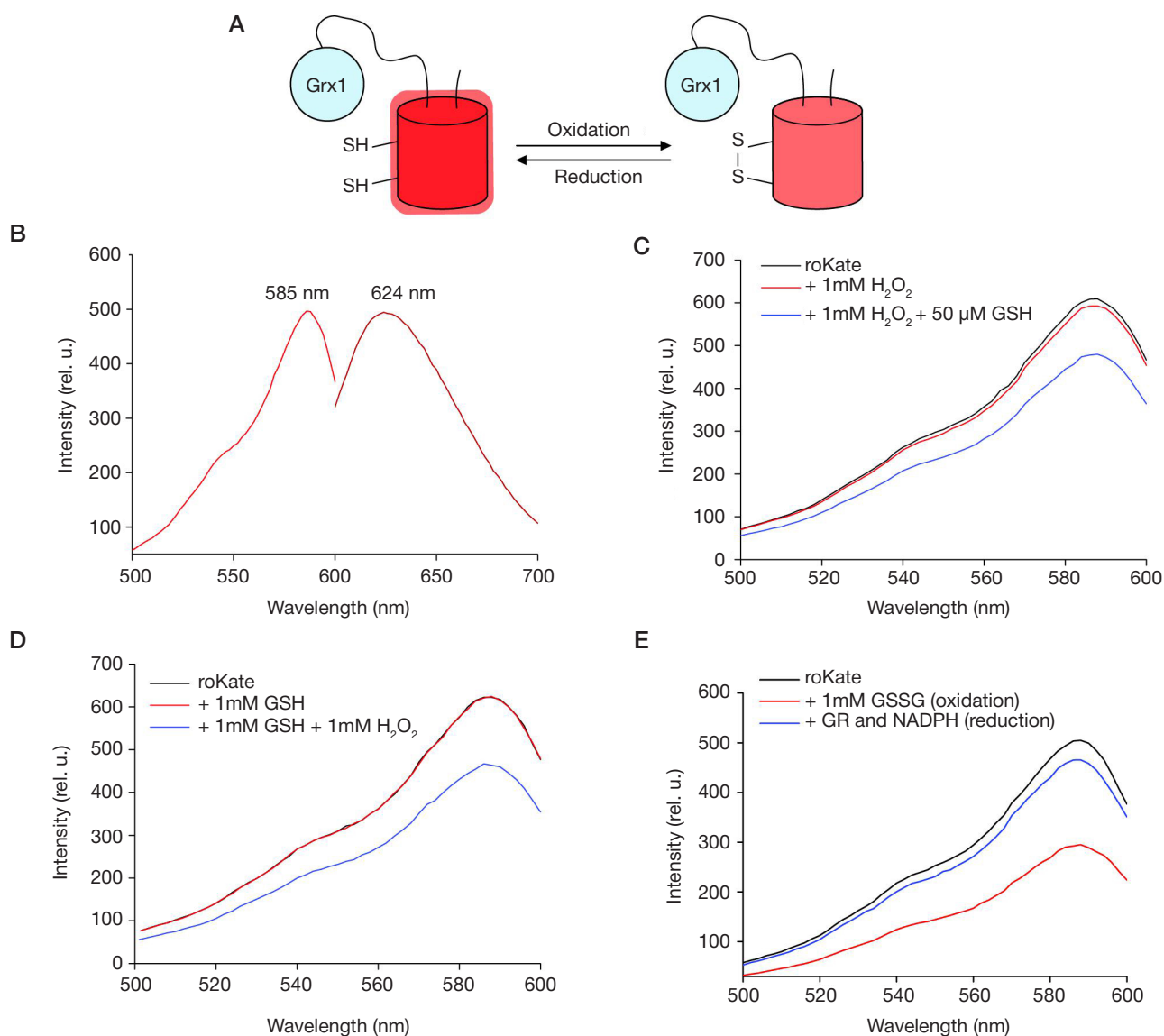


**Fig. 1.** **A.** A schematic representation of roKate's functioning. Two closely positioned cysteine amino acid residues were incorporated into the protein's structure. When oxidized, the residues form a disulfide bond in the presence of human glutaredoxin 1 (Grx1). Oxidation is accompanied by a drop in fluorescence intensity. **B.** The fluorescence emission and excitation spectra of the biosensor. **C.** Changes in the fluorescence excitation spectra in response to the presence of hydrogen peroxide and the subsequent addition of GSH. **D.** Changes in the fluorescence excitation spectra in response to the presence of GSH and the subsequent addition of hydrogen peroxide. **E.** Changes in the fluorescence excitation spectra in the isolated protein sample accompanying oxidation (the addition of GSSG) and subsequent reduction (enzymatic reaction of glutathione reduction in the presence of GR and NADPH)

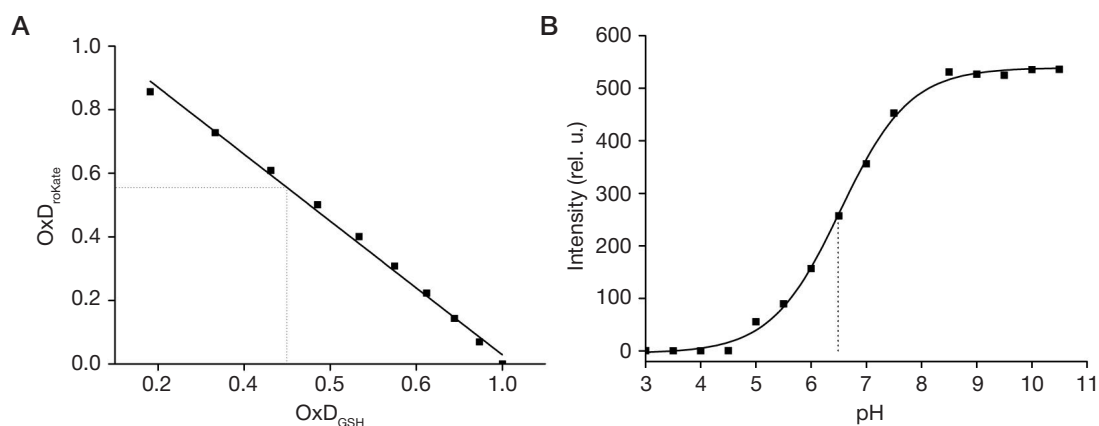


Fig. 2. **A.** Relationship between roKate and glutathione oxidation degrees. **B.** Relationship between roKate's fluorescence intensity and pH

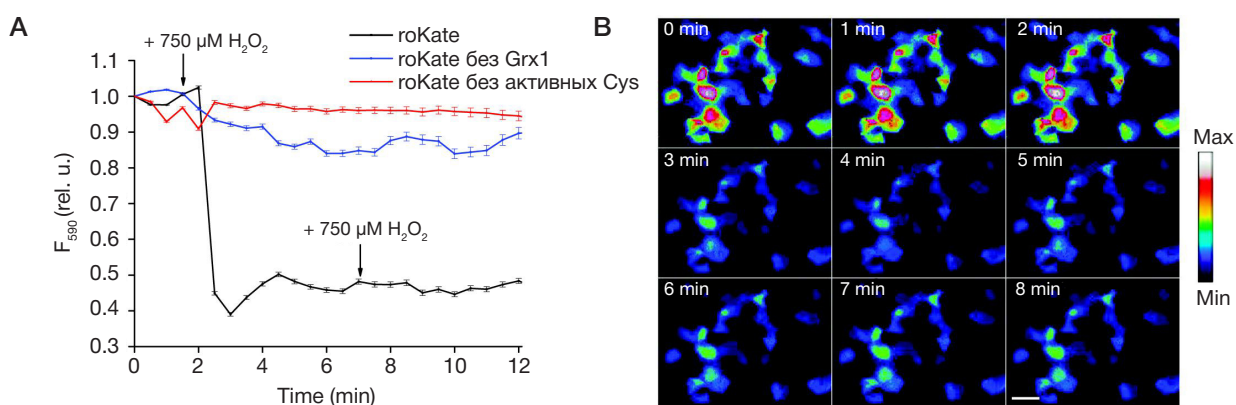


Fig. 3. **The roKate biosensor in HeLa Kyoto cells.** **A.** Fluorescence intensity dynamics of roKate (the black curve), its variant without Grx1 (the blue curve) and its variant without redox-active cysteine residues (the red curve) in the cytoplasm of living HeLa Kyoto cells in response to the addition of hydrogen peroxide to the medium (the moment hydrogen peroxide was added is marked by an arrow). Error bars show the standard deviation from the mean. **B.** Images of HeLa Kyoto cells expressing the roKate biosensor before and after the addition of hydrogen peroxide (the time on the images corresponds to that on the graph). The images are shown in pseudo colors corresponding to signal intensity. Scale: 40 μm

The purified roKate protein was titrated with solutions with different GSH /GSSG ratios ranging from 10 : 0 to 0 : 10. This was necessary to evaluate roKate's redox potential. Fig. 2A shows the relationship between roKate and glutathione oxidation degrees. The redox potential of the biosensor was  $-245$  mV.

The pH sensitivity of the protein was tested using a standard series of buffer solutions with a known pH. The chromophore of fluorescent proteins can exist in a protonated or deprotonated state due to the presence of an amino acid tyrosine residue in its structure. Therefore, the intensity of the fluorescent signal depends on pH. In an experimental system, it is important to keep in mind that the amplitude of changes that the fluorescent signal undergoes under different pH conditions varying in the physiological range (6.0–8.0). We found that  $pK_a$  of the roKate biosensor was 6.5. As pH went up from 6.0 to 8.0, fluorescence increased threefold (Fig. 2B).

We also calculated the extinction coefficient and the quantum yield of roKate. They were  $36,400 \text{ M}^{-1} \text{ cm}^{-1}$  and 0.3, respectively.

### roKate expression in eukaryotic cells

The roKate gene was cloned into the pC1 vector for further expression in mammalian cells. For the human HeLa Kyoto cell line, the maximum amplitude of the response was 55% under the conditions of oxidative stress caused by H<sub>2</sub>O<sub>2</sub> (the highest concentration was 750 μM) (Fig. 3A and B). H<sub>2</sub>O<sub>2</sub> was added to the cell culture repeatedly to identify the maximum change in the signal intensity during oxidation. Normally, the cells do not require any extra reductants to reduce biosensors similar

to roKate. However, roKate was not reduced in the cytoplasm of HeLa Kyoto cells even when the cells were incubated with different reductants, including dithiothreitol, β-mercaptoethanol, and tris(2-carboxyethyl) phosphine). The construct bearing no Grx1 at the N-terminus was inferior to the full-sized biosensor in terms of the reaction rate (Fig. 2A). This means that Grx1 has a key role in supporting the equilibrium between the intracellular glutathione pool and the redox-active cysteine residues of the sensor. The mutant without roKate2 cysteine residues did not change its fluorescence in the eukaryotic system.

In mammalian cells, roKate is oxidized irreversibly, meaning that the sensor can only report the oxidation dynamics of the glutathione pool and is unable to sense its reverse reduction.

### DISCUSSION

We have developed a genetically encoded biosensor based on the red fluorescent protein mKate2. The biosensor is capable of reporting the redox state of the glutathione pool. The properties and design of roKate differ from those of a previously proposed rxRFP sensor [27] that was based on a circularly permuted red fluorescent cpApple protein. Circularly permuted fluorescent proteins are obtained by connecting (at the gene level) the "native" N- and C-termini to each other by a polypeptide linker sequence; the new N- and C-termini are formed in close proximity to a chromophore. The structure of a circularly permuted protein is more conformationally flexible, affecting its spectral characteristics. In rxRFP, redox-active cysteine residues are located at the N- and C-termini of the circularly permuted protein, but the protein is not fused to Grx [27], i. e.

endogenous Grx is needed to support the equilibrium between the redox state of the surrounding glutathione pool and the protein. Besides, chromophores of circular permutants are more susceptible to the environment in comparison with native proteins. This explains why the rXRF biosensor is sensitive to physiological fluctuations of pH.

Another member of the red fluorescent protein-based biosensor family specialized in monitoring the 2GSH/GSSG ratio is called Grx1-roCherry. It has a classic structure composed of a mCherry protein containing a pair of redox-active cysteines and Grx1 fused to the protein by a polypeptide linker sequence. Its redox potential (–311 mV) is different from roKate's; it also differs from our biosensor in the ability to be reversibly reduced in mammalian cells [28].

Red fluorescent proteins are more convenient when it comes to *in vivo* experiments in living systems. They can be used in parallel with green sensors for multiparameter microscopy. This approach yields a wealth of valuable information since it allows researchers to monitor the behavior of several parameters within one biological system or one parameter in different cell compartments [29].

The reason why the oxidized roKate sensor does not get reduced in mammalian cells is unknown. But the protein

can be used as a “memory sensor” that reports the moment of oxidation in living cells or tissue. This could be convenient when the time between the manipulations with the biological object and fluorescence measurements is quite substantial, as is the case with long sample preparation. The time required for sample preparation can be sufficient for the cells to restore their glutathione pool, thereby skewing the results of the experiment. In mammalian cells, roKate gets irreversibly oxidized allowing us to detect glutathione oxidation. Besides, the biosensor can be used to monitor the oxidation dynamics of the intracellular glutathione pool in real time.

## CONCLUSIONS

We have designed a new genetically encoded red-protein based biosensor, which we called roKate, capable of reporting the redox state of the glutathione pool. The biosensor can be used to study redox reactions related to the fluctuations in the 2GSH/GSSG ratio in bacterial cells. In mammalian cells, roKate gets irreversibly oxidized and therefore can be employed as a “memory sensor” reporting the oxidation dynamics of the glutathione pool.

## References

- Lushchak VI. Glutathione homeostasis and functions: potential targets for medical interventions. *J Amino Acids*. 2012; 2012: 736837.
- Couto N, Wood J, Barber J. The role of glutathione reductase and related enzymes on cellular redox homeostasis network. *Free Radic Biol Med*. 2016; (95): 27–42.
- Nagy P. Kinetics and mechanisms of thiol-disulfide exchange covering direct substitution and thiol oxidation-mediated pathways. *Antioxid Redox Signal*. 2013; 18 (13): 1623–41.
- Bekris LM, Shephard C, Janer M, Graham J, McNeney B, Shin J, Zarghami M, Griffith W, Farin F, Kavanagh TJ, Lernmark A. Glutamate cysteine ligase catalytic subunit promoter polymorphisms and associations with type 1 diabetes age-at-onset and GAD65 autoantibody levels. *Exp Clin Endocrinol Diabetes*. 2007; 115 (4): 221–28.
- Polonikov AV, Ivanov VP, Solodilova MA, Khoroshaya IV, Kozhuhov MA, Panfilov VI. The relationship between polymorphisms in the glutamate cysteine ligase gene and asthma susceptibility. *Respir Med*. 2007; 101 (11): 2422–4.
- Tosic M, Ott J, Barral S, Bovet P, Deppen P, Gheorghita F, Matthey ML, Parnas J, Preisig M, Saraga M, Solida A, Timm S, Wang AG, Werge T, Cuenod M, Do KQ. Schizophrenia and oxidative stress: glutamate cysteine ligase modifier as a susceptibility gene. *Am J Hum Genet*. 2006; 79 (3): 586–92.
- Ramos PS, Oates JC, Kamen DL, Williams AH, Gaffney PM, Kelly JA, et al. Variable association of reactive intermediate genes with systemic lupus erythematosus in populations with different African ancestry. *J Rheumatol*. 2013; 40 (6): 842–9.
- Kamerbeek NM, van Zwielen R, de Boer M, Morren G, Vuil H, Bannink N, et al. Molecular basis of glutathione reductase deficiency in human blood cells. *Blood*. 2007; 109 (8): 3560–6.
- Backos DS, Franklin CC, Reigan P. The role of glutathione in brain tumor drug resistance. *Biochem Pharmacol*. 2012; 83 (8): 1005–12.
- Huh YJ, Kim JM, Kim H, Song H, So H, Lee SY, et al. Regulation of osteoclast differentiation by the redox-dependent modulation of nuclear import of transcription factors. *Cell Death Differ*. 2006; 13 (7): 1138–46.
- Kim JM, Kim H, Kwon SB, Lee SY, Chung SC, Jeong DW, et al. Intracellular glutathione status regulates mouse bone marrow monocyte-derived macrophage differentiation and phagocytic activity. *Biochem Biophys Res Commun*. 2004; 325 (1): 101–8.
- Suthanthiran M, Anderson ME, Sharma VK, Meister A. Glutathione regulates activation-dependent DNA synthesis in highly purified normal human T lymphocytes stimulated via the CD2 and CD3 antigens. *Proc Natl Acad Sci USA*. 1990; 87 (9): 3343–7.
- Garcia-Ruiz C, Fernandez-Checa JC. Redox regulation of hepatocyte apoptosis. *J Gastroenterol Hepatol*. 2007; (22 Suppl 1): 38–42.
- Ballatori N, Krance SM, Notenboom S, Shi S, Tieu K, Hammond CL. Glutathione dysregulation and the etiology and progression of human diseases. *Biol Chem*. 2009; 390 (3): 191–214.
- Armstrong RN. Glutathione S-transferases: reaction mechanism, structure, and function. *Chem Res Toxicol*. 1991; 4 (2): 131–40.
- Sedlak J, Lindsay RH. Estimation of total, protein-bound, and nonprotein sulfhydryl groups in tissue with Ellman's reagent. *Anal Biochem*. 1968; 25 (1): 192–205.
- Jiang X, Yu Y, Chen J, Zhao M, Chen H, Song X, et al. Quantitative imaging of glutathione in live cells using a reversible reaction-based ratiometric fluorescent probe. *ACS Chem Biol*. 2015; 10 (3): 864–74.
- Jiang X, Chen J, Bajic A, Zhang C, Song X, Carroll SL, et al. Quantitative real-time imaging of glutathione. *Nat Commun*. 2017; (8): 16087.
- Ostergaard H, Henriksen A, Hansen FG, Winther JR. Shedding light on disulfide bond formation: engineering a redox switch in green fluorescent protein. *EMBO J*. 2001; 20 (21): 5853–62.
- Hanson GT, Aggeler R, Oglesbee D, Cannon M, Capaldi RA, Tsien RY, et al. Investigating mitochondrial redox potential with redox-sensitive green fluorescent protein indicators. *J Biol Chem*. 2004; 279 (13): 13044–53.
- Dooley CT, Dore TM, Hanson GT, Jackson WC, Remington SJ, Tsien RY. Imaging dynamic redox changes in mammalian cells with green fluorescent protein indicators. *J Biol Chem*. 2004; 279 (21): 22284–93.
- Schwarzlander M, Dick TP, Meyer AJ, Morgan B. Dissecting Redox Biology Using Fluorescent Protein Sensors. *Antioxid Redox Signal*. 2016; 24 (13): 680–712.
- Shcherbo D, Murphy CS, Ermakova GV, Solovieva EA, Chepurnykh TV, Shcheglov AS, et al. Far-red fluorescent tags for protein imaging in living tissues. *Biochem J*. 2009; 418 (3): 567–74.
- Available from: [www.clontech.com](http://www.clontech.com), протокол № PT3393-1.
- Bjornberg O, Ostergaard H, Winther JR. Mechanistic insight provided by glutaredoxin within a fusion to redox-sensitive yellow

- fluorescent protein. *Biochemistry*. 2006; 45 (7): 2362–71.
26. Gutscher M, Pauleau AL, Marty L, Brach T, Wabnitz GH, Samstag Y, et al. Real-time imaging of the intracellular glutathione redox potential. *Nat Methods*. 2008; 5 (6): 553–9.
  27. Fan Y, Chen Z, Ai HW. Monitoring redox dynamics in living cells with a redox-sensitive red fluorescent protein. *Anal Chem*. 2015; 87 (5): 2802–10.
  28. Shokhina AG, Kostyuk AI, Ermakova YG, Panova AS, Staroverov DB, Egorov ES, et al. Red fluorescent redox-sensitive biosensor Grx1-roCherry. *Redox Biol*. 2019; (21): 101071.
  29. Kostyuk AI, Panova AS, Bilan DS, Belousov VV. Redox biosensors in a context of multiparameter imaging. *Free Radic Biol Med*. 2018; (128): 23–39.

## Литература

1. Lushchak VI. Glutathione homeostasis and functions: potential targets for medical interventions. *J Amino Acids*. 2012; 2012: 736837.
2. Couto N, Wood J, Barber J. The role of glutathione reductase and related enzymes on cellular redox homeostasis network. *Free Radic Biol Med*. 2016; (95): 27–42.
3. Nagy P. Kinetics and mechanisms of thiol-disulfide exchange covering direct substitution and thiol oxidation-mediated pathways. *Antioxid Redox Signal*. 2013; 18 (13): 1623–41.
4. Bekris LM, Shephard C, Janer M, Graham J, McNeney B, Shin J, Zarghami M, Griffith W, Farin F, Kavanagh TJ, Lernmark A. Glutamate cysteine ligase catalytic subunit promoter polymorphisms and associations with type 1 diabetes age-at-onset and GAD65 autoantibody levels. *Exp Clin Endocrinol Diabetes*. 2007; 115 (4): 221–28.
5. Polonikov AV, Ivanov VP, Solodilova MA, Khoroshaya IV, Kozhuhov MA, Panfilov VI. The relationship between polymorphisms in the glutamate cysteine ligase gene and asthma susceptibility. *Respir Med*. 2007; 101 (11): 2422–4.
6. Tosic M, Ott J, Barral S, Bovet P, Deppen P, Gheorghita F, Matthey ML, Parnas J, Preisig M, Saraga M, Solida A, Timm S, Wang AG, Werge T, Cuenod M, Do KQ. Schizophrenia and oxidative stress: glutamate cysteine ligase modifier as a susceptibility gene. *Am J Hum Genet*. 2006; 79 (3): 586–92.
7. Ramos PS, Oates JC, Kamen DL, Williams AH, Gaffney PM, Kelly JA, et al. Variable association of reactive intermediate genes with systemic lupus erythematosus in populations with different African ancestry. *J Rheumatol*. 2013; 40 (6): 842–9.
8. Kamerbeek NM, van Zwieten R, de Boer M, Morren G, Vuil H, Bannink N, et al. Molecular basis of glutathione reductase deficiency in human blood cells. *Blood*. 2007; 109 (8): 3560–6.
9. Backos DS, Franklin CC, Reigan P. The role of glutathione in brain tumor drug resistance. *Biochem Pharmacol*. 2012; 83 (8): 1005–12.
10. Huh YJ, Kim JM, Kim H, Song H, So H, Lee SY, et al. Regulation of osteoclast differentiation by the redox-dependent modulation of nuclear import of transcription factors. *Cell Death Differ*. 2006; 13 (7): 1138–46.
11. Kim JM, Kim H, Kwon SB, Lee SY, Chung SC, Jeong DW, et al. Intracellular glutathione status regulates mouse bone marrow monocyte-derived macrophage differentiation and phagocytic activity. *Biochem Biophys Res Commun*. 2004; 325 (1): 101–8.
12. Suthanthiran M, Anderson ME, Sharma VK, Meister A. Glutathione regulates activation-dependent DNA synthesis in highly purified normal human T lymphocytes stimulated via the CD2 and CD3 antigens. *Proc Natl Acad Sci USA*. 1990; 87 (9): 3343–7.
13. Garcia-Ruiz C, Fernandez-Checa JC. Redox regulation of hepatocyte apoptosis. *J Gastroenterol Hepatol*. 2007; (22 Suppl 1): 38–42.
14. Ballatori N, Krance SM, Notenboom S, Shi S, Tieu K, Hammond CL. Glutathione dysregulation and the etiology and progression of human diseases. *Biol Chem*. 2009; 390 (3): 191–214.
15. Armstrong RN. Glutathione S-transferases: reaction mechanism, structure, and function. *Chem Res Toxicol*. 1991; 4 (2): 131–40.
16. Sedlak J, Lindsay RH. Estimation of total, protein-bound, and nonprotein sulfhydryl groups in tissue with Ellman's reagent. *Anal Biochem*. 1968; 25 (1): 192–205.
17. Jiang X, Yu Y, Chen J, Zhao M, Chen H, Song X, et al. Quantitative imaging of glutathione in live cells using a reversible reaction-based ratiometric fluorescent probe. *ACS Chem Biol*. 2015; 10 (3): 864–74.
18. Jiang X, Chen J, Bajic A, Zhang C, Song X, Carroll SL, et al. Quantitative real-time imaging of glutathione. *Nat Commun*. 2017; (8): 16087.
19. Ostergaard H, Henriksen A, Hansen FG, Winther JR. Shedding light on disulfide bond formation: engineering a redox switch in green fluorescent protein. *EMBO J*. 2001; 20 (21): 5853–62.
20. Hanson GT, Aggeler R, Oglesbee D, Cannon M, Capaldi RA, Tsien RY, et al. Investigating mitochondrial redox potential with redox-sensitive green fluorescent protein indicators. *J Biol Chem*. 2004; 279 (13): 13044–53.
21. Dooley CT, Dore TM, Hanson GT, Jackson WC, Remington SJ, Tsien RY. Imaging dynamic redox changes in mammalian cells with green fluorescent protein indicators. *J Biol Chem*. 2004; 279 (21): 22284–93.
22. Schwarzlander M, Dick TP, Meyer AJ, Morgan B. Dissecting Redox Biology Using Fluorescent Protein Sensors. *Antioxid Redox Signal*. 2016; 24 (13): 680–712.
23. Shcherbo D, Murphy CS, Ermakova GV, Solovieva EA, Chepurnykh TV, Shcheglov AS, et al. Far-red fluorescent tags for protein imaging in living tissues. *Biochem J*. 2009; 418 (3): 567–74.
24. Доступно по ссылке: [www.clontech.com](http://www.clontech.com), протокол № PT3393-1.
25. Bjornberg O, Ostergaard H, Winther JR. Mechanistic insight provided by glutaredoxin within a fusion to redox-sensitive yellow fluorescent protein. *Biochemistry*. 2006; 45 (7): 2362–71.
26. Gutscher M, Pauleau AL, Marty L, Brach T, Wabnitz GH, Samstag Y, et al. Real-time imaging of the intracellular glutathione redox potential. *Nat Methods*. 2008; 5 (6): 553–9.
27. Fan Y, Chen Z, Ai HW. Monitoring redox dynamics in living cells with a redox-sensitive red fluorescent protein. *Anal Chem*. 2015; 87 (5): 2802–10.
28. Shokhina AG, Kostyuk AI, Ermakova YG, Panova AS, Staroverov DB, Egorov ES, et al. Red fluorescent redox-sensitive biosensor Grx1-roCherry. *Redox Biol*. 2019; (21): 101071.
29. Kostyuk AI, Panova AS, Bilan DS, Belousov VV. Redox biosensors in a context of multiparameter imaging. *Free Radic Biol Med*. 2018; (128): 23–39.

## TAKAYASU'S ARTERITIS: THE RETROSPECTIVE ANALYSIS OF PATIENTS FROM THE URAL POPULATION

Borodina IE<sup>1,2</sup>✉, Popov AA<sup>2</sup>, Salavatova GG<sup>1</sup>, Shardina LA<sup>2</sup><sup>1</sup> Sverdlovsk Regional Clinical Hospital No.1, Yekaterinburg, Russia<sup>2</sup> Ural State Medical University, Yekaterinburg, Russia

Takayasu's arteritis (TA) is a rare disease that can be overlooked during the first visit to a GP, rheumatologist, or any other medical specialist due to a variety of its symptoms. The aim of this study was to describe the clinical presentation and the course of patients with TA residing in the Middle Ural. A retrospective analysis was conducted using the medical records of 183 patients treated at the Sverdlovsk Regional Clinical Hospital 1 from 1979 through 2018. The male to female ratio was 1:3. The mean age was 33.5 years for women and 35.2 for men. The most frequently involved arteries were subclavian (101 cases; 55%), carotid (98 cases; 53%) and renal (77 cases; 42%). Type V was the most common angiographic type. Arterial stenosis was present in 94 (51%) patients. Sixty-six patients received surgical interventions. Of all patients included in the analysis, 31 died. The observed 5-year survival was 92%, 10-year survival, 90% and 15-year survival, 80%. Seventy-two patients (39%) developed major adverse cardiovascular events (MACE), including myocardial infarction, ischemic stroke, and thrombosis of large arteries/veins. The clinical presentation of TA may vary in different geographical regions.

**Keywords:** Takayasu's arteritis, clinical symptoms, renal artery

**Author contribution:** all authors participated in conceiving and planning the study, processing the data, discussing the results, and writing the manuscript. Borodina IE and Salavatova GG collected the medical records for the electronic database.

**Compliance with ethical standards:** the study was approved by the Ethics Committee of Ural State Medical University (Protocol No. 9 dated November 23, 2018).

✉ **Correspondence should be addressed:** Irina E. Borodina  
Repina 3, Yekaterinburg, Sverdlovsk region, 620014; borodysik@mail.ru

**Received:** 10.08.2018 **Accepted:** 02.03.2019 **Published online:** 14.03.2019

**DOI:** 10.24075/brsmu.2019.012

## АРТЕРИИТ ТАКАЯСУ: РЕЗУЛЬТАТЫ РЕТРОСПЕКТИВНОГО АНАЛИЗА ПАЦИЕНТОВ УРАЛЬСКОЙ ПОПУЛЯЦИИ

И. Э. Бородина<sup>1,2</sup>✉, А. А. Попов<sup>2</sup>, Г. Г. Салаватова<sup>1</sup>, Л. А. Шардина<sup>2</sup><sup>1</sup> Свердловская областная клиническая больница № 1, Екатеринбург, Россия<sup>2</sup> Уральский государственный медицинский университет, Екатеринбург, Россия

Артериит Такаясус (АТ) — редкое заболевание, которое ревматологи, врачи общей практики и другие специалисты могут не распознать при первичном посещении пациента из-за различных клинических проявлений. Целью исследования было оценить клиническую картину и течение АТ у 183 пациентов Среднего Урала. В ретроспективную часть исследования вошли 183 страдающих АТ пациентов, наблюдавшиеся в Свердловской областной клинической больнице № 1 в период с 1979 по 2018 г. Соотношение мужчин и женщин составляло 1 : 3. Средний возраст женщин — 33,5 года, мужчин — 35,2 лет. Наиболее часто были зарегистрированы поражения следующих артерий: подключичной — 101 (55%) случай, сонной — 98 (53%) случаев и почечных — 77 (42%) случаев. Наиболее часто встречался ангиографический тип V, а типичным ангиографическим признаком был артериальный стеноз — 94 (51%). Хирургические вмешательства выполнены 66 пациентам. За период исследования зарегистрирован 31 летальный исход, пятилетняя выживаемость составила 92%; 10-летняя — 90%, а 15-летняя — 80%. У 72 (39%) пациентов развились клинически значимые сердечно-сосудистые события: инфаркт миокарда, ишемический инсульт, тромбоз крупной артерии и венозный тромбоз. В разных географических зонах АТ может иметь широкий спектр клинических проявлений.

**Ключевые слова:** артериит Такаясус, клинические проявления, почечная артерия

**Информация о вкладе авторов:** все авторы принимали участие в планировании работы, статистической обработке, обсуждении результатов, написании и редактировании текста. И. Э. Бородина и Г. Г. Салаватова проводили сбор первичного материала и формирование электронной базы данных.

**Соблюдение этических стандартов:** исследование одобрено этическим комитетом ФБГОУ ВО УГМУ Министерства здравоохранения России, протокол № 9 от 23 ноября 2018 г.

✉ **Для корреспонденции:** Ирина Эдуардовна Бородина  
ул. Репина, д. 3, г. Екатеринбург, Свердловская обл., 620014; borodysik@mail.ru

**Статья получена:** 10.08.2018 **Статья принята к печати:** 02.03.2019 **Опубликована онлайн:** 14.03.2019

**DOI:** 10.24075/vrgmu.2019.012

Takayasu's arteritis (TA) is a granulomatous vasculitis of the aorta and its major branches. Although TA predominantly affects Asian and South American ethnic groups, rare cases of the disease are reported in other races, too [1]. TA incidence varies from 0.8 to 2.6 cases per 1, 000, 000 adult population depending on the geographical area of residence and ethnicity [2]. At present, no epidemiological data are available on the prevalence of this disease in the Russian Federation. Because of untimely diagnosis and delayed treatment, patients with TA can develop major adverse cardiovascular events (MACE) leading to premature yet preventable death.

At its onset, TA can mimic a wide range of conditions. Specific symptoms that may not be present in the early

stages include asymmetric pulse or blood pressure in the upper extremities accompanied by pronounced hypertension, impaired vision, and abdominal pain.

The aim of this retrospective study was to describe the clinical manifestations, laboratory and radiographic findings, the course and outcome of TA in 183 patients residing in the Middle Ural.

## METHODS

Our retrospective cohort study included 183 patients (139 females and 44 males) with verified TA who had received treatment at Sverdlovsk Clinical Hospital No. 1 between 1979

and 2018. The age at diagnosis was 9 to 62 years in females (mean: 33.5; median: 35; 25%–75% IQR: 24–43) and 12 to 59 years in male patients (mean: 35.18; median: 34; 25%–75% IQR: 26.5–42). The duration of the disease was 0.6 to 64 years in women (mean: 12.3 years; median: 10 years; 25%–75% IQR: 4–18) and 0.6 to 32 years in men (mean: 9 years; median: 7 years; 25%–75% IQR: 4–14.5). The time elapsed between the onset of the first clinical symptoms and the established diagnosis was 0.6–54 years in females (mean: 5.7 years; median: 3 years; 25%–75% IQR: 1–7) and 0.6–33 years in men (mean: 6 years; median: 4 years; 25%–75% IQR: 1.5–8) (Table 1).

The primary diagnosis of TA specified in the patients' medical records was verified according to the criteria proposed by the American College of Rheumatology in 1990 [3].

Following the unified protocol, we collected and analyzed demographic data, clinical, laboratory and angiography findings, and information about TA-related surgical interventions. Moriwaki's classification criteria were applied to

describe arterial damage [4]. Because our retrospective study covered a long time period that had seen an evolution in clinical practices and technologies, the imaging modalities used to identify arterial stenosis, occlusion, dilation, dissection, etc. were different and included conventional catheter angiography and/or CTA and/or MRA and/or ultrasonography. Importantly, for every patient, ultrasonography findings were confirmed by at least one contrast-enhanced imaging technique.

To obtain information about the clinical manifestations and angiographic demonstration of the disease in other ethnicities, we searched the PubMed database using *Takayasu's arteritis* as keywords. Similar to the present study, the inclusion criteria used in the PubMed articles were based on ACR 1990 [3]. Among them were: the presence of 3 or more TA symptoms (90% sensitivity, 97.8% specificity), including 40 years at onset, claudication (muscle weakness and pain in the extremities during movement), pulse deficit in one or both brachial arteries, blood pressure difference > 10 mmHg in the brachial arteries,

**Table 1.** Characteristics of the patients with Takayasu's arteritis included in the study

Characteristics	Patients		
	Females 139 (76%)	Males 44 (24%)	Total n = 183 (100%)
Age at diagnosis, years, Me [25%–75%]	35 [24–43]	34 [26.5–42]	35 [24–43]
Duration of the disease, years, Me [25%–75%]	10 [4–18]	7 [4–14.5]	13.5 [6–20]
Time between the onset of the first symptoms and diagnosis, Me [25%–75%]	3 [1–7]	4 [1.5–8]	3 [1–8]

**Table 2.** Clinical and laboratory findings

	Patients (n = 183)
Hypertension	98 (53%)
Pain, weakness, numbness, and asymmetric pulse in the upper extremities	89 (49%)
Malaise	87 (47.5%)
Headache	86 (47%)
Fever	65 (35.5%)
Weight loss	44 (24%)
Claudication	40 (22%)
Dizziness	40 (2%)
Blood pressure difference > 10 mmHg	37 (20%)
Chronic abdominal ischemia	36 (20%)
Chest pain	31 (17%)
Pain, weakness, numbness in the lower extremities	26 (14%)
Shortness of breath	16 (8%)
Arthralgias	13 (7%)
<b>Laboratory tests</b>	
ESR (mm/h), Me [25%–75%]	18 [6–28]
CRP (g/l), Me [25%–75%]	0.3 [0–6]
WBC (10 <sup>9</sup> /l), Me [25%–75%]	6.2 [4–8.7]
Hg (g/l), Me [25%–75%]	119 [97–128]
<b>TA type (Moriwaki's classification)</b>	
1	60 (33%)
2a	9 (5%)
2b	1 (0.5%)
3	3 (2%)
4	32 (17%)
5	78 (43%)

**Note:** Me — median; 25% — the lower quartile; 75% — the upper quartile.

bruits over the subclavian arteries or abdominal aorta, and a narrowed lumen or occlusion of the aorta or its major branches in the proximal upper and lower extremities not associated with atherosclerosis, fibromuscular dysplasia and spasm.

A reference dataset was compiled from Elibrary, a free Russian academic database of research works on biomedicine and natural sciences. We ran a search using *Takayasu's arteritis* and *TA* as keywords in order to obtain information about clinical and angiographic TA manifestations in Russian patients [1, 14, 19, 20].

### Statistical analysis

The data were processed in Statistica 7.0 (Statsoft inc; USA). Categorical variables were analyzed using a chi-square test. All statistical tests applied were two-tailed; differences were considered significant at  $p < 0.05$ . The Kaplan–Meier method was used to analyze the factors affecting patients' survival. Between the groups, survival distributions were compared using the log-rank test.

## RESULTS

### Demographic data and clinical manifestations of the disease

At the time of examination, the most common clinical symptoms were malaise (47.5%), elevated blood pressure (53%), pulse asymmetry in the upper extremities (49%), pain, weakness or numbness in the upper extremities (49%), and headache (47%) (Table 2).

Erythrocyte sedimentation rate (ESR), C-reactive protein (CRP) and high-sensitivity CRP were elevated (Table 2). The most common pattern of arterial involvement was Moriwaki's type V (the aortic arch, its major branches, the abdominal aorta and/or renal arteries).

Pathological lesions were typically found in the subclavian, carotid and renal arteries. Stenosis was the most common pathology (Table 3).

Surgical interventions were performed on 66 (36%) patients (23 men and 43 women). Among the indications for surgery were: hemodynamically significant stenosis, occlusion or thrombosis of the involved vessels; hypertension caused by renal artery or subtotal aortic stenosis; symptoms of end-stage upper/lower limb ischemia. The surgical interventions performed can be broken down into two groups: endovascular procedures (stenting, bypass grafting, angioplasty) and open reconstructive surgeries. Besides, one patient with aneurysm and thrombosis of renal arteries had to undergo nephrectomy and kidney autotransplantation (Table 4).

In the majority of cases, medication therapy included glucocorticoids (96 patients; 52%) and antiplatelet agents, such as aspirin and dipyridamole (116 patients; 63%) (Table 5).

Since 1979, 31 patients have died, including 18 men and 13 women. The mean age at death was 38 years in women (Me [25%–75%] — 36 [32–44]) and 49 years in men (Me [25%–75%] — 50 [40–57]). On average, the time elapsed from the established diagnosis to the moment of death was 9.25 years (6.5 [3–16]) in men and 9 years (5 [3–10]) in women. Information about the causes of death was obtained from autopsy protocols ( $n = 22$ ) and in conversations with the close relatives of the deceased ( $n = 9$ ) (Table 6).

Data on the patients' survival is shown in Fig. 1. The 5-year survival rate was 92%; 10-year survival, 90%; and 15-year survival, 80%. (median: 34 [20–41]).

A total of 72 patients (27 men and 45 women) developed cardiovascular complications. On average, age at TA onset was Me [25%–75%] — 33 [26–43]. TA duration before the onset of a cardiovascular event was Me [25%–75%] — 10 [5–20]. Age at the onset of cardiovascular complications was 38 [30–49.5] (Table 7).

## DISCUSSION

In spite of being considered a rare disease, Takayasu's arteritis is studied all over the world because it poses a significant social and economic burden: patients with TA develop serious cardiovascular complications causing disabilities and premature death in young people.

Although the arsenal of available diagnostic techniques is vast, the diagnosis of TA still remains a challenge due to the variability of its symptoms and the lack of knowledge of the disease demonstrated by public health practitioners. This leads to misdiagnosis during the initial examination or delays the correct diagnosis.

Our sample of the Ural residents was dominated by women: 139 (76%) of 183 participants were female. In other countries, the male to female ratio varies between 1 : 2.4 and 1 : 8 in Israel, 6.9 : 1 in Mexico and 8 : 1 in Japan [5–8]. In our study, the demographic characteristics, early clinical symptoms and the course of the disease were consistent with the previously published data indicating that TA strikes at young age [6–12].

Headache, hypertension (systolic blood pressure of 140 mmHg and/or diastolic blood pressure of 90 mmHg and above) were

**Table 3.** Arterial damage in the patients with TA (the present study)

Arteries involved	<i>n</i>
Subclavian	101 (55%)
Carotid	98 (53%)
Vertebral	16 (9%)
Axillary	11 (6%)
Brachial	12 (6.5%)
Pulmonary	6 (3%)
Coronary	31 (17%)
Celiac	42 (23%)
Superior mesenteric	45 (25%)
Renal	77 (42%)
Femoral	25 (14%)
Iliac	33 (18%)
Aortic arch	39 (21%)
Ascending thoracic aorta	15 (8%)
Descending thoracic aorta	9 (5%)
Abdominal aorta	52 (28.4%)
Lesion types	<i>n</i>
Stenosis	94 (51%)
Stenosis + occlusion	55 (30%)
Occlusion / Aneurysm	2 (1%)
Stenosis / aneurysm / occlusion	7 (4%)
Occlusion	8 (4%)
Stenosis + coarctation	3 (2%)
Stenosis + aneurysm	14 (7.6%)

Table 4. Surgical interventions performed in the patients with TA

Surgery type	Patients (n = 66)
Renal artery bypass with autogenous vein	4 (6%)
Carotid-subclavian bypass grafting	4 (6%)
Brachial artery bypass with autogenous vein	1 (1.5%)
Autogenous vein patch reconstruction of the brachial artery	1 (1.5%)
Renal artery stenting	13 (20%)
Descending thoracic aorto-bifemoral bypass grafting	3 (4.5%)
Thoracoabdominal bypass grafting	2 (3%)
Celiac trunk and superior mesenteric artery bypass grafting	3 (4.5%)
Abdominal aorta thrombectomy	2 (3%)
AFBG	7 (11%)
Renal artery angioplasty	11 (17%)
Carotid artery stenting	1 (1.5%)
Subclavian artery angioplasty	1 (1.5%)
Subclavian artery stenting	1 (1.5%)
Thrombectomy for thrombosis of a femoropopliteal bypass graft	1 (1.5%)
AFBG + SFA bypass grafting on the right side. Thrombosis of the aorto-femoral bypass graft/ graft thrombectomy in both branches. SFA and DFA angioplasty on the left, formation of a single ostium, profundoplasty on the right side	1 (1.5%)
Right renal artery dilatation	2 (3%)
Kidney autotransplantation	1 (1.5%)
Nephrectomy	4 (6%)
Renal artery thrombectomy	2 (3%)
BCA bypass grafting	2 (3%)
Left renal artery endarterectomy	1 (1.5%)
Subclavian-carotid anastomosis	2 (3%)
Celiac artery endarterectomy	1 (1.5%)
Brachial artery thrombectomy	1 (1.5%)
SFA thrombectomy on the right side	1 (1.5%)
Graft thrombectomy of the right branch	1 (1.5%)
Transfemoral amputation	2 (3%)
Abdominal revision for mesenteric thrombosis	1 (1.5%)
Infrarenal aorta bypass grafting	1 (1.5%)
Resection and end-to-end anastomosis of the small bowel following acute mesenteric thrombosis	1 (1.5%)
Resection of aneurysm in the brachiocephalic trunk	2 (3%)
Bifurcation alloplastic grafting of the aorta, carotid and brachiocephalic arteries	3 (4.5%)
Carotid artery thrombectomy	2 (3%)
Abdominal cavity and renal artery revision	2 (3%)
Resection of the right part of the large bowel and the terminal ileum + jejunotransverse anastomosis following acute mesenteric thrombosis	1 (1.5%)
Iliofemoral thrombectomy	1 (1.5%)
Implantation of arteriovenous graft in the left forearm	1 (1.5%)
Aorto-bicarotid bypass grafting	3 (4.5%)
Thoracoabdominal replacement following aortic coarctation	1 (1.5%)
Aneurysm resection in the abdominal aorta	1 (1.5%)
Aortic stenting following coarctation	1 (1.5%)
Resection of proximal anastomotic aneurysm in the subclavian artery	1 (1.5%)
Carotid-subclavian bypass grafting	1 (1.5%)
Autogenous vein repair of the subclavian artery	1 (1.5%)
Brachial artery dilatation	1 (1.5%)
Iliofemoral bypass grafting	1 (1.5%)
Coronary artery stenting	5 (7.5%)
AMCB	1 (1.5%)
DFA stenting on the right	1 (1.5%)
Linear iliofemoral bypass on the right side	1 (1.5%)

**Note:** AFBG — aorto-femoral bypass grafting; AMCB — aorto- and mammary coronary bypass; BCA — brachiocephalic artery; SFA — superficial femoral artery; DFA — deep femoral artery.

**Table 5.** Medication therapy received by the patients with Takayasu arteriitis

Medication therapy	Patients (n = 183)
Glucocorticoids	96 (52%)
Glucocorticoids + immunosuppressive agents (cyclophosphamide, azathioprine, hydroxychloroquine, methotrexate)	43 (23%)
No immunosuppressive therapy received or no exhaustive information about immunosuppressive therapy available in the medical records	40 (21%)
Genetically engineered drugs	0 (0%)
Antiplatelet agents	116 (63%)
Statins	27 (15%)
Nonsteroidal anti-inflammatory drugs	42 (23%)
Plasmapheresis	31 (17%)

**Table 6.** Causes of death in the patients with TA

Cause of death	Patients (n = 31)
Multiple cerebral infarctions resulting from progressive cerebral ischemia	1 (3%)
Cerebral infarction due to thrombosis of the internal carotid artery	1 (3%)
Bronchopneumonia	1 (3%)
Decompensated heart failure resulting from aortic regurgitation	2 (6%)
Massive bleeding due to anastomotic suture line failure following autogenous vein replacement of the renal artery	1 (3%)
Bronchopneumonia complicated by abscess after aorto-bicarotid bypass grafting, cerebral reperfusion injury and postoperative coma following implantation of a cardiac pacemaker	1 (3%)
Cerebral infarction + encephalopathy after cerebral reperfusion injury and postoperative cerebral coma after aorto-bicarotid bypass grafting	1 (3%)
Postoperative sepsis caused by suppurative mediastinitis after performing subclavian-carotid anastomosis	1 (3%)
Cerebral infarction due to thromboembolism following resection of brachiocephalic aneurysm	1 (3%)
Cerebral infarctions in the presence of progressive cerebral ischemia after bifurcation aorto-carotid bypass grafting	1 (3%)
Small bowel gangrene in the presence of intestinal ischemia after bifurcation aorto-femoral bypass grafting	1 (3%)
Postoperative peritonitis due to anastomotic suture line failure following small bowel resection for mesenteric thrombosis	2 (6%)
Intracerebral hemorrhage due to hypertension	2 (6%)
Pulmonary embolism caused by deep vein thrombosis of the lower extremities	1 (3%)
Pulmonary embolism caused by multiple arterial and venous thrombosis of the internal organs	1 (3%)
Cerebral infarction of the common carotid artery	1 (3%)
Massive bleeding due to the rupture of dissecting aortic arch aneurysm	1 (3%)
Massive bleeding due to the rupture of dissecting abdominal aortic aneurysm	2 (6%)
Acute renal failure caused by abdominal aorta thrombosis	1 (3%)
Peritonitis due to acute mesenteric thrombosis	1 (3%)
Myocardial infarction	2 (6%)
Hepatic cancer	1 (3%)
Myocardial insufficiency (ischemic stroke)	1 (3%)
Poisoning	2 (6%)
Unknown	2 (6%)

**Note:** PE — pulmonary embolism.

similarly frequent in all studies including our cohort of patients [9–14] (Table 8).

The most commonly involved vessels were the subclavian, carotid and renal arteries. Stenosis was the most common lesion type. The most prevalent (43%) TA type was type V (according to Moriwaki's classification). The carotid and subclavian arteries suffered the same types of lesions in all analyzed studies, including ours. Similar to other cohorts, the Ural sample demonstrated rare involvement of the vertebral, pulmonary and iliac arteries. Interestingly, damage to the ascending aorta and coronary arteries was very frequent in the Korean population [9,15–18] (Table 9).

There are reports that the brachiocephalic artery is affected in 85% of Russian patients with TA, whereas damage to the renal artery is observed in 23% cases [19, 20] (Table 10).

Except for the Serbian study, all other research works indicate that type V of arterial involvement is the most frequent, while type III is the most rare. The Serbian sample is characterized by a high frequency of types I and IIa damage. Type IIb prevails in the Korean population. Type IV is relatively widespread in India and Brazil. Both genetic and environmental factors can contribute to the clinical manifestations of TA (Table 11) [15–17, 21–24].

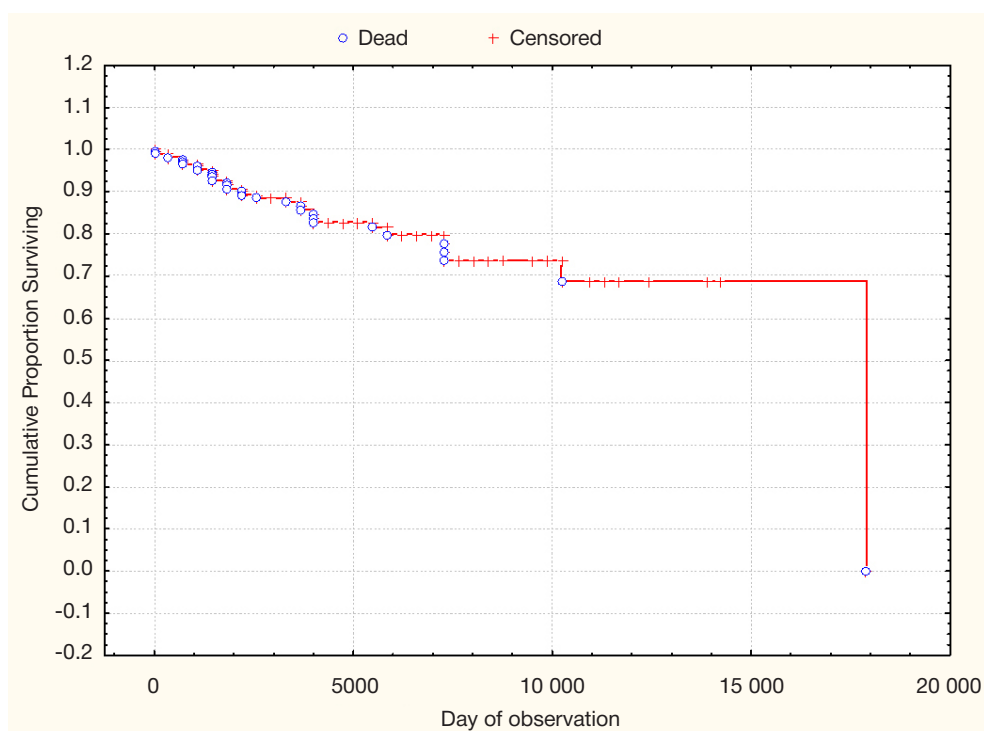


Fig. 1. Survival of the patients with TA

Table 7. Cardiovascular complications in patients with TA

	Patients with MACE ( <i>n</i> = 72)
Myocardial infarction	14 (20%)
Ischemic stroke	24 (35%)
Transient ischemic attack	3 (3%)
Hemorrhagic stroke	4 (6%)
Thrombosis of the renal artery	5 (7%)
Thrombosis of the brachial artery	2 (3%)
Mesenteric thrombosis	4 (6%)
Thrombosis of the radial artery	1 (1.4%)
Thrombosis of the brachiocephalic trunk	1 (1.4%)
Thrombosis of the dorsalis pedis artery	2 (3%)
Thrombosis of the axillary artery	1 (1.4%)
Thrombosis of the infrarenal aorta	1 (1.4%)
Thrombosis of the abdominal artery	2 (3%)
Thrombosis of the carotid artery	3 (3%)
Thrombosis of the subclavian artery	3 (3%)
Celiac thrombosis	1 (1.4%)
Aneurysm rupture in the thoracic aorta	2 (3%)
Aneurysm rupture in the abdominal aorta	1 (1.4%)
Thrombosis of the aorto-femoral bypass graft	6 (8%)
PE	3 (3%)
Thrombosis of the jugular vein	2 (3%)
Cerebral venous sinus thrombosis	1 (1.4%)
Thrombosis of the sural veins	1 (1.4%)
Thrombosis of the small saphenous vein	1 (1.4%)
Thrombophlebitis of the tibial veins	1 (1.4%)
Thrombophlebitis of the aorto-venous bypass graft of the renal artery	1 (1.4%)

**Table 8.** Clinical symptoms of TA in different geographical regions

	This study (n = 183), %	Italy (n = 67), % [9]	India (n = 106), % [10]	Brazil (n = 73), % [11]	South Africa (n = 272), % [12]	Japan (n = 84), % [13]	Russia (n = 215), % [14]
Malaise	47.5	n/a	n/a	n/a	10	n/a	50
Weight loss	24	12	9.4	28	n/a	5	9
Fever	35.5	39	16	26	10	20	n/a
Headache	47	33	47	45	n/a	n/a	50
Dizziness	22	27	n/a	29	n/a	n/a	n/a
Pain, weakness, numbness of the upper extremities	49	52	59	58	12	54	50
Hypertension (systolic pressure of 140 mmHg and diastolic pressure of 90 mmHg)	53	46	52	36	77	52	68
Pulse asymmetry in the upper extremities	49	73	59	85	12	54	50
Blood pressure difference > 10 mmHg	20	72	59	85	12	54	50

**Table 9.** Arteries affected by the pathology in patients with TA residing in different geographical regions

Arteries	This study (n = 183), %	China (n = 411), % [15]	Korea (n = 20), % [16]	USA (n = 126), % [17]	Italy (n = 104), % [9]	France (n = 82), % [18]
Subclavian	53	79.8	67.1	6.3	65.6	68.3
Carotid	55	79.1	72.1	50.9	44.3	59.8
Vertebral	9	28.7	n/a	18.5	13	28.0
Pulmonary	3	68.9	13.4	33.3	n/a	n/a
Coronary	17	35.7	63.3	22.2	n/a	n/a
Mesenteric	25	29.7	22.8	24.7	31.6	n/a
Renal	42	48.9	32.2	18.7	34.4	14.6
Iliac	18	27.2	13.3	13.5	19.7	18.3
Ascending aorta	8	9.5	47.8	9.1	n/a	n/a

**Table 10.** Damage to the arteries in patients with TA representing the Russian population

Arteries	This study (n = 183)	Central Russian regions [19]	North European Russia [20]
Subclavian	55	85%	n/a
Carotid	53		n/a
Vertebral	9		n/a
Pulmonary	3	n/a	n/a
Coronary	17	n/a	n/a
Mesenteric	25	n/a	n/a
Renal	42	n/a	23%
Iliac	18	n/a	n/a
Ascending aorta	5	n/a	n/a

**Table 11.** Angiographic characteristics of TA in different regions across the world

	This study	China [15]	Korea [16]	USA[17]	India [21]	Mexico [22]	Serbia [23]	Brazil [24]
Type I, %	33	22.1	11.1	20	6.9	19	50	11.9
Type IIa, %	5	3.9	8.6	6	1	3	19	6
Type IIb, %	0,5	3.9	14.1	7	5.9	4	0	1
Type III, %	2	2.9	4.0	5	2.9	4	0	9
Type IV, %	17	6.3	7.6	5	28.4	2	0	27
Type V, %	43	60.8	54.5	57	54.9	69	31	18

In our cohort of patients, survival rates were similar to those reported in previous publications [17, 25–27]. However, there are reports of different 5- and 10-year survival rates (69 and 36%, respectively) [28]. In the Arab population, the 5-year survival rate is as low as 50% [29]. The record-breaking 100% survival rate is reported in Japan [30].

A national TA registry is needed to estimate the prevalence of the disease in different ethnic groups. It will provide valuable information about TA presentation and clinical course necessary to establish the timely diagnosis. The actual prevalence of TA can be higher than suggested in the literature. Timely diagnosis and treatment will help to improve patient outcomes.

The main limitation of the present study is its retrospective design. Besides, the study was conducted in inpatients only. In different time periods, the diagnostic procedures used in the patients were different, which also complicates data interpretation.

## CONCLUSIONS

The clinical presentations of TA are diverse. Timely diagnosis can be a challenge when a patient presenting with general inflammation has a healthy pulse pattern, develops collateral circulation and demonstrates no specific symptoms of arterial damage. Patients with TA should be warned against a high risk of cardiovascular complications and advised to monitor and control their blood pressure, lipid counts and blood coagulability. Hemodynamically significant stenosis, occlusion or thrombosis of damaged arteries can be corrected surgically, contributing to antihypertensive therapy, helping to eliminate the symptoms of ischemia and prevent new vascular complications. The majority of patients in our cohort had Moriwaki's type V of arterial damage. High survival rates can be explained by a young age and a capacity to develop collateral circulation.

## References

- Nasonov EL, Nasonova VA. Rheumatology. National guidelines. Moscow, 2010; 539–67.
- Volosnyakov D, Glazyrina G, Serebryakova E, et al. Nonspecific aortoarteritis (Takayasu arteritis) in children and adolescents: literature review and clinical case. *Difficult patient*. 2015; 1 (13): 36–9.
- Arend W, Michel B, Bloch D, et al. The American College of Rheumatology 1990 criteria for the classification of Takayasu arteritis. *Arthritis Rheum*. 1990; (33): 1129–34.
- Moriwaki R, Noda M, Yajima M, et al. Clinical manifestations of Takayasu arteritis in India and Japan new classification of angiographic findings. *Angiology*. 1997; (48): 369–79.
- Asri A, Tazi-Mezalek Z, Aouni M, et al. Takayasu's disease in Morocco. Report of 47 cases. *Rev Med Interne*. 2002; (23): 9–20.
- Ishikawa K, Maetani S. Long-term outcome for 120 Japanese patients with Takayasu's disease. Clinical and statistical analyses of related prognostic factors. *Circulation*. 1994; (90): 1855–60.
- Toshihiko N. Current status of large and small vessel vasculitis in Japan. *Int J Cardiol*. 1996; (54): 91–8.
- Zheng DY, Liu LS, Fan DJ. Clinical studies in 500 patients with aortoarteritis. *Chin Med J*. 1990; (103): 536–40.
- Vanoli M, Bacchiani G, Origgi L, et al. Takayasu's arteritis: a changing disease. *J Nephrol*. 2001; (14): 497–505.
- Jain S, Kumari S, Ganguly N, et al. Current status of Takayasu arteritis in India. *Int J Cardiol*. 1996; (54): 111–6.
- Sato EL, Hatta FS, Levy-Neto M, et al. Demographic, clinical, and angiographic data of patients with Takayasu arteritis in Brazil. *Int J Cardiol*. 1998; (66): 67–70.
- Mwipatayi B, Jaffeij P. Takayasu arteritis: clinical features and management: report of 272 cases. *ANZ J Surg*. 2005; (75): 110–7.
- Nakao K, Ikeda M, et al. Takayasu's arteritis: Clinical Report of Eighty-four Cases and Immunological Studies of Seven Cases. *Circulation*. 1967; (35): 1141–55.
- Arabidze G, Abugova SP, et al. Clinical aspects of Takayasu syndrome (215 cases). *Ter Arkh*. 1980; 52 (5): 124–9.
- Jing Li, Fei Sun, et al. The clinical characteristics of Chinese TAayasu's arteritis patients: a retrospective study of 411 patients over 24 years. *Arthritis Res Ther*. 2017; (19): 107. DOI: 10.1186/s13075-017-1307-z.
- Lee GY, Jang SY, Ko SM, et al. Cardiovascular manifestations of TAayasu arteritis and their relationship to the disease activity: analysis of 204 Korean patients at a single center. *Int J Cardiol*. 2012; 159 (1): 14–20.
- Schmidt J, Kermani TA, Bacani AK, et al. Diagnostic features, treatment, and outcomes of Takayasu arteritis in a US cohort of 126 patients. *Mayo Clin Proc*. 2013; 88 (2): 821–30.
- Arnaud L, Haroche J, Toledano D, et al. Cluster analysis of arterial involvement in Takayasu arteritis reveals symmetric extension of the lesions in paired arterial beds. *Arthritis Rheum*. 2011; 63 (4): 1136–40.
- Pokrovskij AV, Zotikov AE, Yudin VI. Nespecificeskij aortoarterit (bolezni' Takayasu). M.: IRIS, 2002.
- Chikhladze NM. Arterial hypertension in patients with non-specific aortoarteritis. *Systemic Hypertension*. 2018; 15 (2): 43–48. DOI: 10.26442/2075-082X\_2018.2.43-48.
- Moriwaki R, Noda M, Yajima M, et al. Clinical manifestations of Takayasu arteritis in India and Japan—new classification of angiographic findings. *Angiology*. 1997; 48 (5): 369–79.
- Soto ME, Espinola N, Flores-Suarez LF, et al. Takayasu arteritis: clinical features in 110 Mexican Mestizo patients and cardiovascular impact on survival and prognosis. *Clin Exp Rheumatol*. 2008; 26 (3 Suppl 49): 9–15.
- Petrovic-Rackov L, Pejnovic N, Jevtic M, et al. Longitudinal study of 16 patients with Takayasu's arteritis: clinical features and therapeutic management. *Clin Rheumatol*. 2009 Feb; 28 (2): 179–85. DOI: 10.1007/s10067-008-1009-7.
- Clemente Maria, et al. Brazilian multicenter study of 71 patients with juvenile-onset TAayasu's arteritis: clinical and angiographic features. *Rev Brasil Reumatol*. 2016 Mar; 56 (2): 145–51.
- Phillip R, Luqmani R. Mortality in systemic vasculitis: a systemic review. *Clin Exp Rheumatol*. 2008; 26 (5): 94–104.
- Balakrishnan KG, Subramanyan R, Joy J. Natural history of aortoarteritis (Takayasu's disease). *Circulation*. 1989; 80 (3): 429–37.
- Hall S, Barr W, Lie JT, Stanson AW, Kazmier FJ, Hunder GG. Takayasu arteritis. A study of 32 North American patients. *Medicine (Baltimore)*. 1985; 64 (2): 89–99.
- Park MC, Lee SW, Park YB, Chung NS. Clinical characteristics and outcomes of Takayasu's arteritis: analysis of 108 patients using standardized criteria for diagnosis, activity assessment and angiographic classification. *Lee Scand J Rheumatol*. 2005; 34 (4): 284–92.
- Mustafa K. Takayasu's arteritis in Arabs. *Clin Rheumatol*. 2014 Dec; 33 (12): 1777–83. DOI: 10.1007/s10067-014-2633-z.
- Ishihara T, Haraguchi G, Kamiishi T, Tezuka D, Inagaki H, Isobe M. Sensitive assessment of activity of Takayasu's arteritis by pentraxin3, a new biomarker. *J Am Coll Cardiol*. 2011; 57 (16): 1712–3.

## Литература

- Насонов Е. Л. Ревматология: российские клинические рекомендации. М.: ГЕОТАР-Медиа, 2010; 331 с.
- Волосников Д. К., Глазырина Г. А., Серебрякова Е. Н. Неспецифический аортоартериит (артериит Такаюсу) у детей и подростков: обзор литературы и описание случая. Трудный пациент. 2015; 1 (13): 36–9.
- Arend W, Michel B, Bloch D, et al. The American College of Rheumatology 1990 criteria for the classification of Takayasu arteritis. *Arthritis Rheum.* 1990; (33): 1129–34.
- Moriwaki R, Noda M, Yajima M, et al. Clinical manifestations of Takayasu arteritis in India and Japan new classification of angiographic findings. *Angiology.* 1997; (48): 369–79.
- Asri A, Tazi-Mezalek Z, Aouni M, et al. Takayasu's disease in Morocco. Report of 47 cases. *Rev Med Interne.* 2002; (23): 9–20.
- Ishikawa K, Maetani S. Long-term outcome for 120 Japanese patients with Takayasu's disease. Clinical and statistical analyses of related prognostic factors. *Circulation.* 1994; (90): 1855–60.
- Toshihiko N. Current status of large and small vessel vasculitis in Japan. *Int J Cardiol.* 1996; (54): 91–8.
- Zheng DY, Liu LS, Fan DJ. Clinical studies in 500 patients with aortoarteritis. *Chin Med J.* 1990; (103): 536–40.
- Vanoli M, Bacchiani G, Origgi L, et al. Takayasu's arteritis: a changing disease. *J Nephrol.* 2001; (14): 497–505.
- Jain S, Kumari S, Ganguly N, et al. Current status of Takayasu arteritis in India. *Int J Cardiol.* 1996; (54): 111–6.
- Sato EL, Hatta FS, Levy-Neto M, et al. Demographic, clinical, and angiographic data of patients with Takayasu arteritis in Brazil. *Int J Cardiol.* 1998; (66): 67–70.
- Mwipatayi B, Jeffey P. Takayasu arteritis: clinical features and management: report of 272 cases. *ANZ J Surg.* 2005; (75): 110–7.
- Nakao K, Ikeda M, et al. Takayasu's arteritis: Clinical Report of Eighty-four Cases and Immunological Studies of Seven Cases. *Circulation.* 1967; (35): 1141–55.
- Арабидзе Г. Г., Абугова С. П., Матвеева Л. С. Клинические аспекты болезни Такаюсу (215 наблюдений). *Тер. архив.* 1980; (5): 124–9.
- Jing Li, Fei Sun, et al. The clinical characteristics of Chinese TAayasu's arteritis patients: a retrospective study of 411 patients over 24 years. *Arthritis Res Ther.* 2017; (19): 107. DOI: 10.1186/s13075-017-1307-z
- Lee GY, Jang SY, Ko SM, et al. Cardiovascular manifestations of TAayasu arteritis and their relationship to the disease activity: analysis of 204 Korean patients at a single center. *Int J Cardiol.* 2012; 159 (1): 14–20.
- Schmidt J, Kermani TA, Bacani AK, et al. Diagnostic features, treatment, and outcomes of Takayasu arteritis in a US cohort of 126 patients. *Mayo Clin Proc.* 2013; 88 (2): 821–30.
- Arnaud L, Haroche J, Toledano D, et al. Cluster analysis of arterial involvement in Takayasu arteritis reveals symmetric extension of the lesions in paired arterial beds. *Arthritis Rheum.* 2011; 63 (4): 1136–40.
- Покровский А. В., Зотиков А. Е., Юдин В. И. Неспецифический аортоартериит (болезнь Такаюсу). М.: ИРСИСЪ, 2002.
- Чихладзе Н. М. Артериальная гипертензия у больных с неспецифическим аортоартериитом. Системные гипертензии. 2018; 15 (2): 43–8.
- Moriwaki R, Noda M, Yajima M, et al. Clinical manifestations of Takayasu arteritis in India and Japan — new classification of angiographic findings. *Angiology.* 1997; 48 (5): 369–79.
- Soto ME, Espinola N, Flores-Suarez LF, et al. Takayasu arteritis: clinical features in 110 Mexican Mestizo patients and cardiovascular impact on survival and prognosis. *Clin Exp Rheumatol.* 2008; 26 (3 Suppl 49): 9–15.
- Petrovic-Rackov L, Pejnovic N, Jevtic M, et al. Longitudinal study of 16 patients with Takayasu's arteritis: clinical features and therapeutic management. *Clin Rheumatol.* 2009 Feb; 28 (2): 179–85. DOI: 10.1007/s10067-008-1009-7.
- Clemente Maria, et al. Brazilian multicenter study of 71 patients with juvenile-onset TAayasu's arteritis: clinical and angiographic features. *Rev Brasil Reumatol.* 2016 Mar; 56 (2): 145–51.
- Phillip R, Luqmani R. Mortality in systemic vasculitis: a systemic review. *Clin Exp Rheumatol.* 2008; 26 (5): 94–104.
- Balakrishnan KG, Subramanyan R, Joy J. Natural history of aortoarteritis (Takayasu's disease). *Circulation.* 1989; 80 (3): 429–37.
- Hall S, Barr W, Lie JT, Stanson AW, Kazmier FJ, Hunder GG. Takayasu arteritis. A study of 32 North American patients. *Medicine (Baltimore).* 1985; 64 (2): 89–99.
- Park MC, Lee SW, Park YB, Chung NS. Clinical characteristics and outcomes of Takayasu's arteritis: analysis of 108 patients using standardized criteria for diagnosis, activity assessment and angiographic classification. *Lee Scand J Rheumatol.* 2005; 34 (4): 284–92.
- Mustafa K. Takayasu's arteritis in Arabs. *Clin Rheumatol.* 2014 Dec; 33 (12): 1777–83. DOI: 10.1007/s10067-014-2633-z.
- Ishihara T, Haraguchi G, Kamiishi T, Tezuka D, Inagaki H, Isoobe M. Sensitive assessment of activity of Takayasu's arteritis by pentraxin3, a new biomarker. *J Am Coll Cardiol.* 2011; 57 (16): 1712–3.

## FREQUENCY OF CARBOHYDRATE METABOLISM DISORDERS IN DAY-CARE PATIENTS WITH BORDERLINE FASTING BLOOD SUGAR LEVELS AND AT LEAST ONE RISK FACTOR FOR DIABETES MELLITUS

Boeva VV<sup>1</sup> ✉, Boeva TA<sup>2</sup>, Zavyalov AN<sup>3</sup>

<sup>1</sup> Federal Clinical Centre of High Medical Technologies, Moscow Region, Novogorsk, Russia

<sup>2</sup> Tambov Central Regional Hospital, Pokrovo Prigorodnoe Rural Settlement, Russia

<sup>3</sup> Pirogov Russian National Research Medical University, Moscow, Russia

In order to assess the diagnosis of carbohydrate metabolism disorders, day care patients from Tambov central regional hospital were investigated. The study was conducted during 6 months in 2018. The study included 91 patients and allowed the diagnosis of type 2 diabetes mellitus (DM) in 31 (34.0%) cases, 6 (6.5%) impaired fasting glucose and 22 (24.1%) impaired glucose tolerance. This survey highlighted the necessity to expand the screening populations at risk for developing type 2 diabetes. The rationale for the 75-gram oral glucose tolerance test for all individuals with fasting plasma glucose  $\geq 5.6 \leq 6.0$  mmol/l and having one or more risk factors for developing type 2 diabetes and / or metabolic syndrome is shown. Among these categories diabetes was detected in 4.3%, and prediabetes in 14.4% of cases.

**Keywords:** diabetes mellitus type 2, impaired fasting glucose, impaired glucose tolerance, screening, fasting venous plasma glucose, prediabetes

**Author contribution:** all authors participated in conceiving and planning the study, collected and analyzing the data. Boeva VV prepared the study for publication.

**Compliance with ethical standards:** the study was approved by the Ethics Committee of Pirogov Russian Medical Research Medical University (Protocol 176 dated June 25, 2018). All patients gave informed consent to participate.

✉ **Correspondence should be addressed:** Valentina V. Boeva  
Ivanovskaya 3, Novogorsk, Moscow region, 141435; BoevaVV@yandex.ru

**Received:** 20.01.2019 **Accepted:** 12.03.2019 **Published online:** 15.03.2019

**DOI:** 10.24075/brsmu.2019.014

## ЧАСТОТА НАРУШЕНИЙ УГЛЕВОДНОГО ОБМЕНА У ПАЦИЕНТОВ ДНЕВНОГО СТАЦИОНАРА С ПОГРАНИЧНЫМИ ЗНАЧЕНИЯМИ ГЛИКЕМИИ НАТОЩАК И ХОТЯ БЫ ОДНИМ ФАКТОРОМ РИСКА РАЗВИТИЯ САХАРНОГО ДИАБЕТА

В. В. Боева<sup>1</sup> ✉, Т. А. Боева<sup>2</sup>, А. Н. Завьялов<sup>3</sup>

<sup>1</sup> Федеральный клинический центр высоких медицинских технологий Федерального медико-биологического агентства России, Московская область, городской округ Химки, микрорайон Новогорск, Россия

<sup>2</sup> Тамбовское областное государственное бюджетное учреждение здравоохранения «Тамбовская Центральная районная больница», Тамбовская область, Тамбовский район, с. Покрово-Пригородное, Россия

<sup>3</sup> Российский национальный исследовательский медицинский университет имени Н. И. Пирогова, Москва, Россия

С целью оценки диагностики нарушений углеводного обмена проведено обследование пациентов, поступивших в дневной стационар Тамбовского областного государственного бюджетного учреждения здравоохранения (ТОГ БУЗ) «Тамбовская Центральная районная больница» в период 6 месяцев 2018 г. Проведенное в рамках дневного стационара обследование 91 человека позволило выявить у 31 (34,0%) человека сахарный диабет 2-го типа (СД), у 6 (6,5%) нарушенную гликемию натощак и у 22 (24,1%) нарушенную толерантность к глюкозе. Данное обследование показало необходимость расширения популяции скрининга в группах риска по развитию сахарного диабета 2 типа. Дано обоснование проведения перорального теста толерантности с 75 г глюкозы всем лицам с глюкозой венозной плазмы натощак  $\geq 5,6 \leq 6,0$  ммоль/л, имеющим один или более факторы риска развития СД 2 типа и/или метаболический синдром: среди данной категории СД был выявлен в 4,3%, а предиабет — в 14,4% случаев.

**Ключевые слова:** сахарный диабет 2 типа, нарушенная гликемия натощак, нарушенная толерантность к глюкозе, скрининг, глюкоза венозной плазмы натощак, предиабет

**Информация о вкладе авторов:** В. В. Боева — анализ литературы, планирование исследования, анализ и интерпретация данных; Т. А. Боева — анализ литературы, планирование исследования, анализ и сбор данных; А. Н. Завьялов — анализ литературы, анализ и интерпретация данных.

**Соблюдение этических стандартов:** этический комитет ФГБОУ ВО РНИМУ им. Н. И. Пирогова Минздрава России; №176 от 25 июня 2018 г.

✉ **Для корреспонденции:** Валентина Владимировна Боева  
ул. Ивановская, д. 3, Новогорск, Московская обл., 141435; BoevaVV@yandex.ru

**Статья получена:** 20.01.2019 **Статья принята к печати:** 12.03.2019 **Опубликована онлайн:** 15.03.2019

**DOI:** 10.24075/vrgmu.2019.014

Diabetes mellitus (DM) is a major public health concern that has serious social implications. By the end of 2017, type 2 DM had been diagnosed in 425 million of the world population. By 2045, this number will have reached 629 million. It is estimated that 212.4 million people worldwide do not know that they have type 2 DM [1]. In January 2018, the National Diabetes Registry reported that of 4.6 million Russian citizens diagnosed with DM, 4.1 million had type 2 DM [2]. Extrapolated results of the NATION cross-sectional study conducted in Russia suggest that about 20.7 million Russian residents are prediabetic and another 4.2 million do not know that they already have type 2

DM. Thus, the actual prevalence of type 2 DM in Russia is at least 5.5% (8 million people); 19.3% of Russians are prediabetic. The current situation with diabetes poses a serious threat to public health: at least 50% of the population do not know they are ill, do not receive any treatment and, therefore, are at high risk for complications [3, 4].

Between 2007 and 2012, the number of Russian patients with DM was increasing steadily by 6.23% (or 173,640) a year [5].

According to the report of the Federal Diabetes Mellitus Registry published on January 17, 2018, the prevalence of type 2 DM in Tambov region was 4,044.3 per 100,000 population,

ranking second among 85 Russian regions [2]. Therefore, Tambov region could be a good location for a pilot study of type 2 DM epidemiologic trends in Russia. The analysis of type 2 DM in the adult population of Tambov region demonstrates that its prevalence was increasing gradually between 2011 and 2018, from 1600,6 and 2477,0 per 100,000 population. In the first place, this trend is associated with increased primary incidence of type 2 DM that had risen from 208.1 to 242.6 by 2018 [6].

Obviously, prevention and timely diagnosis of type 2 DM is becoming a nationwide concern. The prevalence of the disease remains high; it also tends to grow over time. At present, screening for DM in the groups at risk is not as effective as it should be. A systemic population approach is needed that will, among other things, seek to expand screening programs both locally and statewide.

As part of the Federal Targeted Program on the *Prevention and Control of Major Diseases*, the Diabetes Mellitus Project was being implemented in Russia from 2007 to 2012. The project aimed at improving life expectancy and reducing complications in patients with DM, i. e. it focused on secondary prevention. There are no statewide programs for primary prevention of type 2 DM launched to stop progression of prediabetes into diabetes.

The term “prediabetes” was proposed by the World Health Organization in 1965. Since 1999, the terms “prediabetes” and “carbohydrate metabolism disorder” have been used to describe the two health conditions preceding DM: impaired fasting glucose (IFG) and impaired glucose tolerance (IGT), as well as the combination of the two, highlighting a high risk for type 2 DM in the affected patients (4–9% cases a year) [3, 7].

Because at least 50% of patients with type 2 DM do not know they have it, we could be facing a situation when the criteria for patient eligibility for DM screening are not sufficiently sensitive.

The prevalence of metabolic syndrome (MS) varies from 14 to 24% in the general population [8]. The symptoms of this condition are observed in 20–50% of the working population of

the developed countries [9]. In Russia, MS is diagnosed in 30% of adults over 30, and the number of such patients is growing steadily [10]. In 90% of cases, type 2 DM is accompanied by abdominal obesity and is a clinical outcome of MS.

Timely diagnosis of type 2 DM is still a challenge. In spite of the increasing availability of diagnostic techniques, the diagnosis is often delayed until the time when complications have already cropped up, which typically occurs within several years after the actual onset of the disease. Timely diagnosis of carbohydrate metabolism disorders could curb the incidence of type 2 DM, prevent complications or disabilities, and reduce the financial burden on the public healthcare system. Therefore, further research into DM is a matter of paramount importance.

## METHODS

This cross-sectional noninterventive observational cohort study was conducted in 91 individuals (24 males and 67 females) aged 32 to 79 years. The participants were selected from 840 patients of Tambov Central District Hospital who had presented at the day-care unit over the period of 6 months in 2018. The following inclusion criteria were applied:

1. Fasting plasma glucose (FPG) of at least 5.6 mmol/L;
  2. At least one risk factor (RF) for type 2 DM [1], including:
    - age over 45 years;
    - excess weight or obesity (BMI  $\geq 25$  kg/m<sup>2</sup>);
    - abdominal obesity (waist circumference  $> 94$  cm in men and  $> 80$  cm in women);
    - elevated blood pressure  $\geq 140/90$  mmHg or antihypertensive medication therapy in progress;
    - hypercholesterolemia (LDP  $\geq 1.8$  mmol/L);
    - cardiovascular disorders;
    - previously detected impaired fasting glucose or impaired glucose tolerance;
    - family history of DM.
- All patients gave written informed consent to participate.

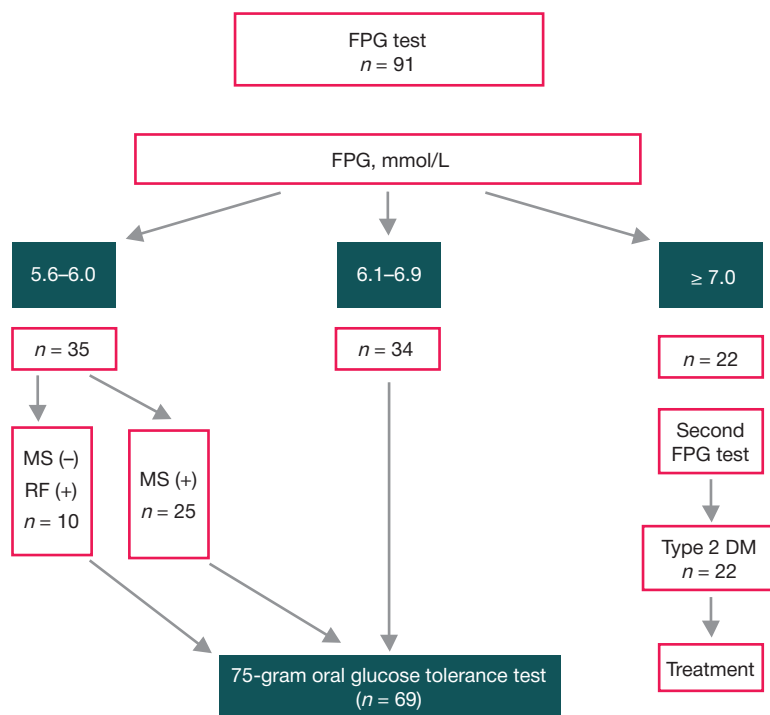


**Fig. 1.** The study included 91 patients, who were then distributed into 3 groups depending on their blood sugar levels. Patients with FPG  $\geq 7.0$  mmol/L (measured in two repeated tests) were diagnosed with type 2 DM and prescribed adequate treatment. Patients with FPG between 6.1 and 6.9 mmol/L underwent an oral glucose tolerance test (OGTT). Patients with FPG between 5.6 and 6.0 mmol/L who were at risk for developing type 2 DM and metabolic syndrome also underwent OGTT. FPG — fasting plasma glucose

The following exclusion criteria were applied: type 2 DM; type 1 DM; an exacerbation of any chronic disease; inflammation; a severe comorbidity; FPG < 5.6 mmol/L.

The patients were examined for the symptoms of metabolic syndrome and assessed for the risk of developing type 2 DM. According to IDF (2005), the main clinical manifestations of MS in Caucasian patients include abdominal obesity (waist circumference > 94 cm in men and > 80 cm in women) and two or more factors listed below [11]:

1) elevated triglycerides > 1.7 mmol/L or lipid-lowering therapy in progress;

2) low HDL (< 1.03 mmol/L in men and < 1.29 mmol/L in women) or lipid-lowering therapy in progress;

3) elevated blood pressure  $\geq$  130/85 mmHg or antihypertensive therapy in progress;

4) fasting blood sugar  $\geq$  5.6 mmol/L or previously diagnosed type 2 diabetes.

All patients with FPG falling in the range between 5.6 and 6.0, MS or at least one risk factor for type 2 DM underwent a 75-gram oral glucose tolerance test (OGTT). The schematic representation of the study is provided in Fig. 1.

The obtained data were processed in Statistica ver 6.1 (StatSoft; Russia). Because the Kolmogorov–Smirnov normality test revealed non-normal distribution, the nonparametric Mann–Whitney U-test was applied.

## RESULTS

Of 91 patients included in the analysis, 22 (24.2%) had presented with complaints of fatigue, dry mouth, increased thirst, frequent urination, itchy skin, weight gain, or unstable blood pressure. Type 2 DM was confirmed in 22 patients (4 men and 18 women) aged 34 to 69 years whose FPG was  $\geq$  7.0 mmol/L in two repeated tests.

Thirty-five patients (38.4%) had FPG in the range from 5.6 to 6.0 mmol/L, metabolic syndrome and at least one risk factor for developing type 2 DM. In 34 patients (37.3%), FPG ranged from 6.1 to 6.9 mmol/L; 97.0% of such patients (or 33 out of 34) had symptoms of metabolic syndrome. An oral glucose tolerance test was ordered for all those patients.

Carbohydrate metabolism disorders were observed in 64.8% ( $n = 59$ ) of the patients with borderline fasting blood sugar and at least one risk factor for type 2 DM; 34.0% ( $n = 31$ ) of those individuals had never been diagnosed with type 2 DM before, and 30.7% ( $n = 28$ ) were prediabetic. Twenty-two (24.1%) prediabetic patients had IGT.

All patients with new-onset type 2 DM ( $n = 31$ ) had signs of metabolic syndrome. In 9 patients, type 2 DM was diagnosed based on OGTT.

Figure 3 shows the distribution of the patients depending on the severity of carbohydrate metabolism disorders revealed by OGTT in the group of 35 individuals with initial FPG between 5.6 and 6.0 mmol/L.

Figure 4 shows the distribution of the patients depending on the severity of carbohydrate metabolism disorders revealed by OGTT in the group of 34 patients with initial FPG between 6.1 and 6.9 mmol/L.

Clinical and demographic characteristics of the patients grouped by the severity of carbohydrate metabolism disorders ( $n = 91$ ) are shown in Table 1.

OGTT conducted in 69 participants revealed that 13.0% (9 patients) had type 2 DM, 31.8% (22 patients) had IGT, and 8.7% (6 patients) had IFG. Normal fasting blood sugar levels were observed in 46.3% (32) of the participants (Table 2). Interestingly, the frequency of IFG cases was low.

Of 9 patients with new-onset type 2 DM, 3 had FPG between 5.6 and 6.0 mmol/L and 6 had FPG between 6.1 and 6.9 mmol/L.

The distribution of the patients depending on the severity of carbohydrate metabolism disorders (OGTT) in the groups with initial IFG levels ranging from 5.6 to 6.0 mmol/L ( $n = 35$ ) and from 6.1 to 6.9 mmol/L ( $n = 34$ ) is shown in Table 2.

OGTT demonstrated that 2.8% of the participants from the group with initial FPG between 5.6 and 6.0 mmol/L had IFG; the frequencies of IGT and type 2 DM cases were 11.5% and 4.3%, respectively. Thus, there were 14.4% prediabetic patients in the studied cohort.

Glucose tolerance was significantly less prevalent in the patients with FPG ranging from 6.1 to 6.9 mmol/L.

Most patients were over 45 years of age. This was true for 100% of the patients in the IFG and IGT groups and for 84.3% and 90.3% of the patients in the groups with normal carbohydrate metabolism and new-onset type 2 DM, respectively. All groups were dominated by overweight or obese patients. All patients had increased waist circumference. No significant differences were observed in the number of patients with a family history of type 2 DM (Table 1).

The number of patients with elevated blood pressure was significantly higher in the group with normal carbohydrate metabolism and prediabetes in comparison with the group with new-onset type 2 DM ( $p < 0.05$ ).

No significant differences were detected between the groups in terms of lipid counts, chronic pancreatitis or the history of cardiovascular diseases ( $p > 0.05$ ).

It should be noted that there were more patients with a history of elevated glucose levels in the group with new-onset DM ( $p > 0.05$ ). Of 8 patients, only 2 had had their carbohydrate metabolism disorder and impaired glucose tolerance verified. Those patients had been receiving metformin for no longer than one year before the study and terminated the drug without consulting their physician. No diagnostic tests had been previously performed in the rest of the patients to assess their metabolic status.

Among 4 patients with IGT who had been diagnosed with elevated blood sugar between 2013 and 2018, one woman had been taking metformin for 6 years continuously (500 mg per day). This allowed her to stay at the prediabetic stage

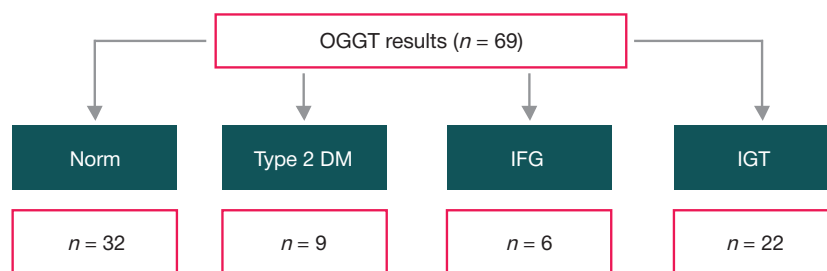


Fig. 2. The overall distribution of the patients depending on the severity of carbohydrate metabolism disorders revealed by OGTT. IFG — impaired fasting glucose; IGT — impaired glucose tolerance; OGTT — oral glucose tolerance test

without progressing to diabetes. No patients from our cohort had been recommended to undergo a 75-gram oral glucose tolerance test before.

Two patients with IFG had been diagnosed with elevated blood sugar (up to 6.5 mmol/L) within a year preceding this study, but had chosen not to consult an endocrinologist. The oral glucose tolerance test was conducted when those patients presented at the day-care unit with unstable blood pressure.

All patients with carbohydrate metabolism disorder were examined by an endocrinologist. The patients with new-onset type 2 DM were prescribed glucose-lowering therapy.

The patients with IFG and IGT were prescribed metformin at a starting dose of 500 mg before bed to prevent type 2 DM and given recommendation on maintaining blood sugar levels. The patients with normal blood sugar were recommended to undergo a control test in a year and to consult an endocrinologist if their glucose levels should rise.

The patients with normal glucose tolerance were given dietary and weight loss recommendations. They were also recommended an antihypertensive therapy and statins for treating dyslipidemia.

Summing up, OGTT should be ordered for the patients with FPG in the range between 5.6 and 6.0 mmol/L who are at risk for developing DM and/or metabolic syndrome.

## DISCUSSION

The incidence of type 2 DM in 91 study participants who had borderline fasting glucose levels and at least one risk factor for this condition was 34.0% ( $n = 31$ ). IFG was diagnosed in 6.5% ( $n = 6$ ) of patients and IGT, in 24.1% patients ( $n = 22$ ). Thirty-two participants (35.1%) had normal glucose tolerance.

According to the NATION study, about 21 million Russian residents aged 20 to 79 years are prediabetic; another 4.2 million do not know they have type 2 DM [3]. In this study, a glycosylated hemoglobin test was used as a diagnostic criterium. This approach is an alternative to [12]; it has its advantages (higher specificity for type 2 DM) and drawbacks (lower specificity for prediabetic conditions) [13, 14].

Because at least 50% of patients with type 2 DM do not know they have it, we could be facing a situation when the criteria for patient eligibility for DM screening are not sufficiently sensitive. Depending on the country, different criteria are applied to identify groups at risk for type 2 DM. The Canadian Diabetes Association highlights the necessity of conducting screening for type 2 DM in all patients older than 40 regardless of the presence of specific risk factors [15]. The criteria proposed by the American Diabetes Association (ADA) include age over 45 years (regardless of the risk factors present) or

**Table 1.** Clinical and demographic characteristics of patients

Parameters	Norm ( $n = 32$ )	IFG ( $n = 6$ )	IGT ( $n = 22$ )	Type 2 DM ( $n = 31$ )
Men	10 (31.2%)	3 (50.0%)	5 (22.7%)	6 (19.3%)
Women	22 (68.7%)	3 (50.0%)	17 (77.2%)	25 (80.6%)
Age $\geq 45$ years	27 (84.3%)	6 (100%)	22 (100%)	28 (90.3%)
Family history of type 2 DM	2 (6.2%)	1 (16.6%)	6 (27.2%)	7 (22.5%)
BMI $\geq 25$	30 (93.7%)	6 (100%)	21 (95.4%)	31 (100%)
WC > 80 cm (women)	22 (100%)	3 (100%)	17 (100%)	25 (100%)
WC > 94 cm (men)	10 (100%)	3 (100%)	5 (100%)	6 (100%)
Hypertension	32 (100%)*	6 (100%)	22 (100%)*	25 (80.6%)
Hypercholesterolemia	21 (65.6%)	6 (100%)	15 (68.1%)	18 (58.0%)
Chronic pancreatitis	3 (9.3%)	1 (16.6%)	3 (13.6%)	5 (16.1%)
Cardiovascular diseases	9 (28.1%)	2 (33.3%)	4 (18.1%)	8 (25.8%)
AMI	3 (9.3%)	1 (16.6%)	2 (9.0%)	3 (9.6%)
ACE	3 (9.3%)	0 (0%)	1 (4.5%)	0 (0%)
TIA	1 (3.1%)	0 (0%)	0 (0%)	2 (6.4%)
Peripheral artery disease	2 (6.2%)	1 (16.6%)	1 (4.5%)	3 (9.6%)
History of hyperglycemia	3 (9.3%)	2 (33.3%)	4 (18.1%)	8 (25.8%)

**Note:** \*— differences are significant,  $p < 0.05$ ; BMI — body mass index; IFG — impaired fasting glucose; IGT— impaired glucose tolerance; AMI — acute myocardial infarction; ACE — acute cerebrovascular event; WC — waist circumference; OGTT— oral glucose tolerance test; DM — diabetes mellitus; TIA — transient ischemic attack.

**Table 2.** The distribution of the patients depending on the severity of carbohydrate metabolism disorders (OGTT)

Carbohydrate metabolism	$n = 69$		X <sup>2</sup> / $\phi$	$p$
	FPG 5.6–6.0	FPG 6.1–6.9		
Normal	22 (31.8%)	10 (14.4%)	6.5	0.011*
IFG	2 (2.8%)	4 (5.7%)	0.43	> 0.05
IGT	8 (11.5%)	14 (20.2%)	1.9	0.17
DM	3 (4.3%)	6 (8.6%)	0.3	> 0.05

**Note:** \*— differences are significant,  $p < 0.05$ ; FPG — fasting plasma glucose; IFG — impaired fasting glucose; IGT— impaired glucose tolerance; OGTT— oral glucose tolerance test; DM — diabetes mellitus. In the subgroup of patients with FPG levels ranging from 5.6 to 6.0 mmol/L, there were 2.8% cases of IFG, 11.5% cases of IGT and 4.3% cases of type 2 DM (based on OGTT results). Thus, the frequency of prediabetic conditions in the subgroup was 14.4%. The frequency of IGT was significantly lower in the subgroup with FPG between 6.1 and 6.9 mmol/L.

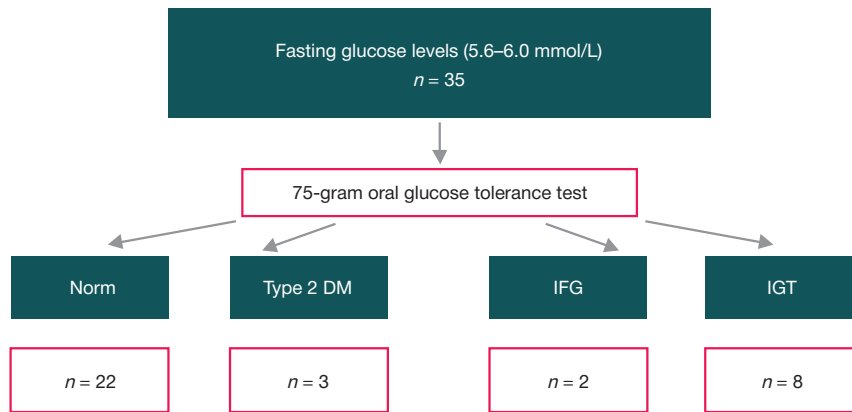


**Fig. 3.** The distribution of the patients depending on the severity of carbohydrate metabolism disorders revealed by OGTT in the group of 35 individuals with initial FPG between 5.6 and 6.0 mmol/L. IFG — impaired fasting glucose; IGT — impaired glucose tolerance; OGTT — oral glucose tolerance test

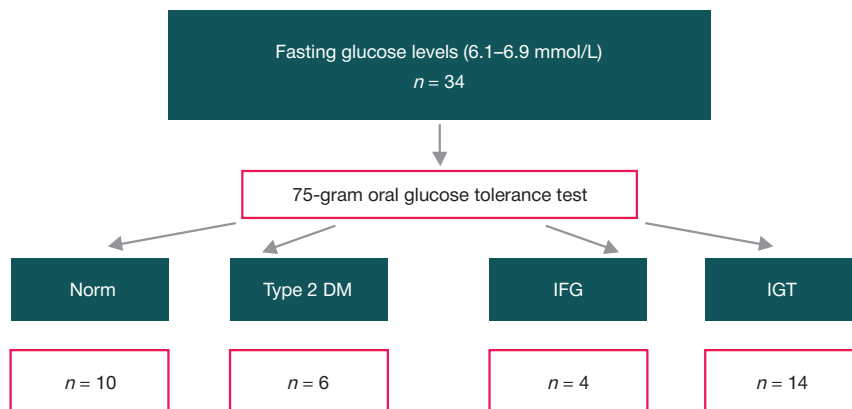


**Fig. 4.** The distribution of the patients depending on the severity of carbohydrate metabolism disorders revealed by OGTT in the group of 34 individuals with initial FPG between 6.1 and 6.9 mmol/L. IFG — impaired fasting glucose; IGT — impaired glucose tolerance; OGTT — oral glucose tolerance test

age younger than 45 years + the presence of the risk factors [16]. European clinical guidelines suggest using a questionnaire to assess the risk for type 2 DM and then conduct screening in the populations at moderate and high risk for the disease [17]. Such differences in the criteria for patient eligibility have economic and epidemiological causes.

Our study has demonstrated the need for covering broader populations in the groups at risk for type 2 DM. We have provided a rationale for performing a 75-gram oral glucose tolerance test in all individuals with FPG between 5.6 and 6.0 mmol/L who have at least one risk factor for type 2 DM and/or metabolic syndrome. In our study, DM was diagnosed in 4.3% of such patients; another 14.4% were prediabetic. Early diagnosis of carbohydrate metabolism disorders and timely medication therapy would help to prevent development of

DM 2 in prediabetic patients. Timely diagnosis and treatment of type 2 DM could prevent possible complications.

## CONCLUSIONS

- 1) Screening for carbohydrate metabolism disorders in patients with borderline fasting glucose has revealed that the actual prevalence of type 2 DM is three times higher than reported.
- 2) Screening should be performed in patients at risk for type 2 DM using a FPG test even in the absence of clinical manifestations of diabetes in such patients.
- 3) A 75-gram oral glucose tolerance test should be performed in all patients with metabolic syndrome and/or one or more risk factors for type 2 DM with FPG between 6.1 and 6.9 mmol/L, as well as those who have FPG ranging from 5.6 to 6.0 mmol/L.

## References

1. International Diabetes Federation. Diabetes Atlas, 8<sup>th</sup> ed, 2017.
2. State Diabetes Register. Professional All-Russian Resource on Diabetes Nosology under the auspices of Endocrinology Research Center/ <http://diaregistry.ru/content/o-proekte.html#content> Verified on May 28, 2018.
3. Dedov II, Shestakova MV, editors. Algorithms of Specialized Medical Care for Diabetes Mellitus Patients. 8-th Edition. Moscow, 2017.
4. Dedov II, Shestakova MV, Galstyan GR. Prevalence of Type 2 Diabetes Mellitus in Adult Russian Population (NATION study). Diabetes Mellitus. 2016; 19 (2): 104–112.
5. Results of implementation of the subprogramme «Diabetes Mellitus» of the Federal Target Program «Prevention and Control of Socially Significant Diseases in 2007–2012». Edited by Dedov II., Shestakova MV. Diabetes Mellitus. 2013; Special edition 2S: 2–48.
6. Tambov Regional State Budgetary Establishment «Technical and Material Support Center of Healthcare Institutions Activities». Form No. 12. Order of the Federal State Statistics Service: On form approval dated 2016 July 21; 355.
7. Starodubova AV., Chervyakova YuV., Kopelev AA., Alieva AM. Possibilities of Drug Correction of Metabolic Disorders and Prevention of Diabetes Mellitus in Case of Carbohydrate

8. van Vliet-Ostapchouk J, Nuotio M, Slagter S, Doiron D, Fischer K, Foco L, et al. The prevalence of metabolic syndrome and metabolically healthy obesity in Europe: a collaborative analysis of ten large cohort studies. *BMC Endocrine Disorders*. 2014; 14 (1): 9.
9. Simonenko VB, Medvedev IM, Tolmachev VV. Патогенетические аспекты артериальной гипертонии при метаболическом синдроме/ *Klinich. medicina*. 2011; 89 (1): 49–51.
10. Ivashkin VT, Drapkina OM, Korneeva ON. Клинические варианты метаболического синдрома. М: Медицинское информационное агентство. 2011; 220.
11. International Diabetes Federation (IDF): Consensus on the Criteria of Metabolic Syndrome. *Obesity and Metabolism*. 2005; (3): 47–9.
12. Khetan A, Rajagopalan S, Prediabetes, *Can J Cardiol*. 2018 May; 34(5): 615–23.
13. Yan S, et al. Diagnostic accuracy of HbA1c in diabetes between Eastern and Western. *Eur J Clin Invest*. 2013 Jul; 43(7): 716–26.
14. Barry E. Efficacy and effectiveness of screen and treat policies in prevention of type 2 diabetes: systematic review and meta-analysis of screening tests and interventions. *BMJ*. 2017 Jan; 4; 356: i6538.
15. Goldenberg R, Punthakee Z. Canadian Diabetes Association 2013 clinical practice guidelines for the prevention and management of diabetes in Canada: definition, classification and diagnosis of diabetes, prediabetes and metabolic syndrome. *Can J Diabetes*. 2013; 37.
16. Classification and diagnosis of diabetes. *Diabetes Care*. 2017; (40): 11–24.
17. ESC Guidelines on diabetes, pre-diabetes, and cardiovascular diseases developed in collaboration with the EASD: the task force on diabetes, pre-diabetes, and cardiovascular diseases of the European Society Of Cardiology (ESC) and Developed in Collaboration With The European Association For The Study Of Diabetes (EASD). *Eur Heart J*. 2013; (34): 3035–87.

### Литература

1. International Diabetes Federation. *Diabetes Atlas*, 8<sup>th</sup> ed, 2017.
2. Государственный регистр сахарного диабета. Профессиональный всероссийский ресурс по нозологиям диабета под эгидой Эндокринологического Научного Центра. Доступно по ссылке: <http://diaregistry.ru/content/o-proekte.html#content>. Проверено 28.11.18.
3. Дедов И. И., Шестакова М. В., редакторы. Алгоритмы специализированной медицинской помощи больным сахарным диабетом. 8-е издание. М., 2017.
4. Дедов И. И., Шестакова М. В., Галстян Г. Р. Распространенность сахарного диабета 2 типа у взрослого населения России (исследование NATION). *Сахарный диабет*. 2016; 19 (2): 104–12.
5. Результаты реализации подпрограммы «Сахарный диабет» Федеральной целевой программы «Предупреждение и борьба с социально значимыми заболеваниями 2007–2012 гг». Под ред. Дедова И. И., Шестаковой М. В. *Сахарный диабет*. 2013; Спецвыпуск 2S: 2–48.
6. Тамбовское областное государственное бюджетное учреждение «Центр материально-технического обеспечения деятельности учреждений здравоохранения». Форма №12. Приказ Росстата: Об утверждении формы от 21.07.2016; № 355.
7. Стародубова А. В., Червякова Ю. В., Копелев А. А., Алиева А. М. Возможности медикаментозной коррекции метаболических нарушений и профилактики сахарного диабета при нарушениях углеводного обмена. *Лечебное дело*. 2015; (3): 59–65.
8. van Vliet-Ostapchouk J, Nuotio M, Slagter S, Doiron D, Fischer K, Foco L, et al. The prevalence of metabolic syndrome and metabolically healthy obesity in Europe: a collaborative analysis of ten large cohort studies. *BMC Endocrine Disorders*. 2014; 14 (1), 9.
9. Симоненко В. Б., Медведев И. М., Толмачев В. В. Патогенетические аспекты артериальной гипертонии при метаболическом синдроме. *Клиническая медицина*. 2011; 89 (1): 49–51.
10. Ивашкин В. Т., Драпкина О. М., Корнеева О. Н. Клинические варианты метаболического синдрома. М.: Медицинское информационное агентство, 2011; с. 220.
11. Международная Федерация диабета (IDF): консенсус по критериям метаболического синдрома. *Ожирение и метаболизм*. 2005; (3): 47–9.
12. Khetan A, Rajagopalan S, Prediabetes. *Can J Cardiol*. 2018 May; 34 (5): 615–23.
13. Yan S. et al. Diagnostic accuracy of HbA1c in diabetes between Eastern and Western. *Eur J Clin Invest*. 2013 Jul; 43 (7): 716–26.
14. Barry E. Efficacy and effectiveness of screen and treat policies in prevention of type 2 diabetes: systematic review and meta-analysis of screening tests and interventions. *BMJ*. 2017 Jan; 4; 356: i6538.
15. Goldenberg R, Punthakee Z. Canadian Diabetes Association 2013 clinical practice guidelines for the prevention and management of diabetes in Canada: definition, classification and diagnosis of diabetes, prediabetes and metabolic syndrome. *Can J Diabetes*. 2013; 37.
16. Classification and diagnosis of diabetes. *Diabetes Care* 2017; (40): 11–24.
17. ESC Guidelines on diabetes, pre-diabetes, and cardiovascular diseases developed in collaboration with the EASD: the task force on diabetes, pre-diabetes, and cardiovascular diseases of the European Society Of Cardiology (ESC) and Developed in Collaboration With The European Association For The Study Of Diabetes (EASD). *Eur Heart J*. 2013; (34): 3035–87.

In issue 4 (July–August 2018) of the Bulletin of RSMU a few errors were made:

**THE PROPER STRUCTURE OF A BIOSAFETY SYSTEM AS A WAY OF REDUCING THE VULNERABILITY OF A SOCIETY, ECONOMY OR STATE IN THE FACE OF A BIOGENIC THREAT**

Gushchin VA, Manuilov VA, Makarov VV, Tkachuk AP

✉ **Correspondence should be addressed:** Vladimir A. Gushchin  
Gamalei 18, Moscow, 123098; wowaniada@gmail.com

**Received:** 30.09.2018 **Accepted:** 14.10.2018

**DOI:** 10.24075/brsmu.2018.054

The following corrections should be applied:

	Published text:	Correction:
p. 5, item «Funding»	This work was supported by the Ministry of Health of the Russian Federation as part of the project The National System for Chemical and Biological Security of the Russian Federation (2015–2020) and by the Ministry of Education and Science as part of the project RFMEFI60117X0018.	This work was supported by the Ministry of Education and Science within the framework of the project RFMEFI60117X0018.
p. 5, item «Финансирование»	Статья подготовлена при поддержке Министерства здравоохранения Российской Федерации в рамках программы «Национальная система химической и биологической безопасности 2015–2020» и Министерства образования и науки РФ в рамках проекта RFMEFI60117X0018.	Статья подготовлена при поддержке Министерства образования и науки РФ в рамках проекта RFMEFI60117X0018.

In issue 4 (July–August 2018) of the Bulletin of RSMU a few errors were made:

### HIGH-PERFORMANCE AEROSOL SAMPLER WITH LIQUID PHASE RECIRCULATION AND PRE-CONCENTRATION OF PARTICLES

Akmalov AE, Kotkovskii GE, Stolyarov SV, Verdiev BI, Ovchinnikov RS, Pochtovyy AA, Tkachuk AP, Chistyakov AA

✉ **Correspondence should be addressed:** Gennadii E. Kotkovskii  
Kashirskoe shosse, 31, Moscow, 115409; geko@mail.ru

**Received:** 27.07.2018 **Accepted:** 23.08.2018

**DOI:** 10.24075/brsmu.2018.049

The following corrections should be applied:

	Published text:	Correction:
p. 25, item «Funding»	This work was supported by the Federal Target Program The National System for Chemical and Biological Security of the Russian Federation (2015-2020), the state contract No. K-27-НИР/148-2 signed by the Ministry of Healthcare of the Russian Federation and the National Research Nuclear University MEPhI.	This work was supported by the Ministry of Education and Science within the framework of the project RFMEFI60117X0018.
p. 25, item «Финансирование»	Федеральная целевая программа «Национальная система химической и биологической безопасности Российской Федерации (2015–2020 г.)», государственный контракт №К-27-НИР/148-2 между Министерством здравоохранения Российской Федерации и Национальным исследовательским ядерным университетом «МИФИ»	Статья подготовлена при поддержке Министерства образования и науки РФ в рамках проекта RFMEFI60117X0018.

In issue 4 (July–August 2018) of the Bulletin of RSMU a few errors were made:

### PERFORMANCE OF THE ORIGINAL WORKSTATION FOR AEROSOL TESTS UNDER CONTROLLED CONDITIONS

Kleymenov DA, Verdiev BI, Enenko AA, Gushchin VA, Tkachuk AP

✉ **Correspondence should be addressed:** Denis A. Kleymenov  
Gamalei 18, Moscow, 123098; 10000let@rambler.ru, denis.a.kleymenov@gamaleya.org

**Received:** 06.08.2018 **Accepted:** 31.08.2018

**DOI:** 10.24075/brsmu.2018.053

The following corrections should be applied:

	Published text:	Correction:
p. 32, item «Funding»	This work was supported by the Ministry of Health of the Russian Federation as part of the project The National System for Chemical and Biological Security of the Russian Federation (2015–2020) and by the Ministry of Education and Science as part of the project RFMEFI60117X0018.	This work was supported by the Ministry of Education and Science within the framework of the project RFMEFI60117X0018.
p. 32, item «Финансирование»	Статья подготовлена при поддержке Министерства здравоохранения Российской Федерации в рамках программы «Национальная система химической и биологической безопасности 2015–2020» и Министерства образования и науки РФ в рамках проекта RFMEFI60117X0018.	Статья подготовлена при поддержке Министерства образования и науки РФ в рамках проекта RFMEFI60117X0018.